PLANNING FOR AUTONOMY AND ELECTRIFICATION IN FUTURE TRANSPORTATION SYSTEMS

By

Harprinderjot Singh

A DISSERTATION

Submitted to
Michigan State University
in partial fulfillment of the requirements
for the degree of

Civil Engineering—Doctor of Philosophy

2022

ABSTRACT

PLANNING FOR AUTONOMY AND ELECTRIFICATION IN FUTURE TRANSPORTATION SYSTEMS

By

Harprinderjot Singh

Autonomous vehicles (AVs) and electric vehicles (EVs) will improve safety, mobility, roadway capacity and provide efficient driving, efficient use of travel time, and reduced emissions. However, these technologies affect vehicle miles traveled (VMT), travel time, ownership cost, and electric grid network. Shared mobility systems can ameliorate the high price of these technologies. However, the shared mobility system poses additional problems such as users' waiting time, inconvenience, and increased VMT. Further, the impact of these emerging technologies varies on different groups of users (different values of travel time (VOTT). Another hurdle to the adoption of EVs is the limited range and scarcity of charging infrastructure. A well-established network of charging infrastructure, especially the direct current fast chargers (DCFC), can alleviate this challenge. However, the widespread adoption of EVs and the growing network of DCFC stations will increase the electric energy demand affecting the electric grid stability, demand-supply imbalance, overloading, and degradation of the electric grid components. Distributed energy resources (DER) such as solar panels and energy storage systems (ESS) can support the EV demand and reduce the load on the electric grid. This study develops modeling frameworks for the optimal adoption of AVs and EVs, considering their effect on transportation systems, the environment, and the electric grid network. Further, it suggests different scenarios that would promote the adoption of these technologies and provide a sustainable and resilient system.

This study proposes a multi-objective mathematical model to estimate the optimal fleet configuration in a system of private manual-driven vehicles (PMVs), private AVs (PAVs), and

shared AVs (SAVs) while minimizing the purchase and operating costs, time (travel and waiting time), and emission production. SAVs can be the optimal solution with the efficient use of travel time or the purchase price below a certain relative threshold. PAVs can be the optimal solution only if the onboard amenities are improved, lifetime mileage is increased, AV technology is installed in luxurious cars, and adopted by people with high VOTT. The framework is extended to consider different combinations of EVs, AVs, and conventional human-driven vehicles in a private and shared mobility system. The metaheuristics based on genetic and simulated annealing algorithms are developed to solve the large-scale NP-hard nonlinear optimization problem. The model is implemented for the network of Ann Arbor, Michigan. The results suggest that EVs are optimal for the system due to low operating costs and zero tailpipe emissions. Shared autonomous electric vehicles (SAEVs) are the best option for users with low VOTT. Private autonomous electric vehicles (PAEVs) would favor the system if the travel time savings are at least 20% or the price of AV technology is less than one-third of the vehicle price.

The study then investigates the optimum investment technology to support the rising energy demand at the DCFC stations and reduce the load on the electric grid network. The different investments include purchasing and installing various ESS (new batteries (NB), second-life batteries (SLB), flywheels), solar panels, electric grid upgrades, and the cost of buying/selling electricity from/to the electric grid. The model is implemented for the DCFC stations supporting the future needs of EV charging demand for urban trips in the major cities of Michigan in 2030. The combination of SLBs and solar panels provides maximum benefits. The total annual and electricity savings are $25,000-$165,000 and $40,000-$300,000 per city.

Dedicated to my *Parents*-- their hard work, resilience, and enduring compassion for all living beings continues to inspire me.

ACKNOWLEDGMENTS

I am most thankful to my Ph.D. advisor, Dr. Mehrnaz Ghamami, for her untiring patience in guiding me through every step of the PhD and sharing her time and knowledge so generously. I have been inspired not only by her scientific fervor and diligence but also her kindness and thoughtfulness that makes her an excellent advisor as well as a wonderful friend and colleague. Her commitment and assistance were limitless, and I will treasure these qualities throughout my life. It has been a great learning and rewarding experience working with her. She has been a constant source of inspiration.

I feel immensely fortunate and thankful to Dr. Ali Zockaie, Dr. Peter Savolainen, Dr. Timothy Gates, and Dr. Tongbin Qu for providing their co-operation, feedback, and support during my research work. They have been very supportive not only during my PhD work but also guiding, and supporting me for the success in my career.

It has been an honor to be a part of this rich intellectual community and I am thankful to all the faculty in the Department of Civil and Environmental Engineering who have trained or guided me in one form or the other. A big thank you to Laura Post (current grad secretary) and Bailey Weber for being there, helping out and making my life easier as a graduate assistant all throughout my PhD program.

I made several beautiful friendships during the last five years at MSU for which I am forever grateful. Mohammad, Fatemeh, Anshu, Meghna, Amirali- you made the rough patches less burdensome and the fun times more memorable. It was a memorable experience working with you all, collaborating, helping each other, discussing about our diverse cultures, and food. Thank you

and much love to companions whom I met much before I joined MSU- Dinesh, Alok, Gopal, Himanshu, Roopak, Dharamveer - how lucky am I to have friends who are like family!

I am thankful from the bottom of my heart to my family, my father, Mr. Major Singh, my mother, Mrs. Renu Ravinder Kaur, my brother, Mr. Harmanjot Singh, my sister, Mrs. Amrinder Kaur, who instilled in me a love for knowledge and a knack for discipline, and have stood by my side patiently through all my struggles and victories.

Funding acknowledgement: This material is based, in part, upon work supported by the Department of Energy and Energy Services under Award Number EE008653. The author also appreciates the assistance of the Bureau of Transportation Planning staff at the Michigan Department of Transportation (MDOT) in making data available to the study, especially Bradley Sharlow and Jesse Frankovich. The author naturally remains solely responsible for all contents of the dissertation.

TABLE OF CONTENTS

LIST OF TABLES

LIST OF FIGURES

CHAPTER 1 INTRODUCTION

1.1 Overview and Objectives

Cars started as environmental saviors (Kars4Kids, 2017; Keim, 2013; Levitt and Dubner, 2009), clearing the streets from horse manure (Carlisle, 2016; Hayden, 2016; Keim, 2013; Levitt and Dubner, 2009; Milsom, 2019; Nikiforuk, 2013; Private Fleet, 2010), possible fleas (Carlisle, 2016; Nikiforuk, 2013), and even carcasses (Hayden, 2016; Nikiforuk, 2013). The shift from horses to cars was a significant change in the transportation industry. The benefits of cars include but are not limited to increased speed, longer travel distance, and high carrying capacity (Private Fleet, 2010). However, in today's world, cars have turned into one of the significant environmental challenges. Transportation is the leading contributor of greenhouse gas emissions in the US, with light-duty vehicles accounting for about 60% of production in this sector (EPA, 2020). The transportation system faces another significant change moving towards autonomous vehicles (AV) and electric vehicles (EV) technology. These technologies will trigger disruptive changes to transportation systems, infrastructure, users' travel behavior, environment, and electric grid network. Inspite of myriad potential benefits like improved safety and mobility, reduced emission, efficient use of travel time; these technologies might affect vehicle miles traveled (VMT), travel time, and ownership cost (Brown et al., 2014; Chen et al., 2016; Cokyasar et al., 2020; de Looff et al., 2018; Dias et al., 2020; Eberhard and Tarpenning, 2006; Fagnant and Kockelman, 2015; FastCompany, 2014; Gai et al., 2019; Ghamami et al., 2020a; Gruel and Stanford, 2016; Gucwa, 2014; Harper et al., 2016; Hidrue et al., 2011; Kröger et al., 2019; LeVine Steve, 2017; Moore et al., 2020; NHTSA, 2016; Y. (Marco) Nie et al., 2016; Romm, 2006; Saleh and Hatzopoulou, 2020; Samaras and Meisterling, 2008; Singh et al., 2021; Soteropoulos et al., 2019; Stogios et al., 2019; Tomás et al., 2020; Vasebi and Hayeri, 2020; Wadud et al., 2016; Zhang et al., 2018; Zhong et al.,

2020). There are also studies indicating that AVs can promote the adoption of EVs (Annema, 2020; Brown and Dodder, 2019; Weiss et al., 2017). The AVs can enhance the battery performance and battery life of EVs by optimizing the driving cycles and energy recovery during regenerative braking (Annema, 2020), which will ameliorate some of the limitations of EVs. On the other hand, EVs can resolve the issues of increased emissions (Wang et al., 2018) and operating costs (Weiss et al., 2017) associated with increased VMT due to AVs. EVs can also reduce the total ownership cost of autonomous EVs (AEV) due to their low operating cost (Weiss et al., 2017). However, these technologies might not be affordable to the users with the added cost of AV technology and battery price, increasing the purchase price of these vehicles (FastCompany, 2014; Hidrue et al., 2011; LeVine Steve, 2017; Singh et al., 2021). Then, it might be reasonable to adopt these technologies as a shared mobility system where users are not required to buy these vehicles. Instead, these will be owned by transportation network companies (TNC). The shared mobility would also reduce the vehicle ownership and fleet size requirements (Chen et al., 2016; Fagnant et al., 2016; Fagnant and Kockelman, 2014; Golbabaei et al., 2020; Singh et al., 2021; Soteropoulos et al., 2019; Spieser et al., 2016; Zhang et al., 2015) parking demand (Yan et al., 2020; Zhang et al., 2015), labor costs (Liu et al., 2020), and the cold start emissions (Fagnant and Kockelman, 2014; Singh et al., 2021). However, this system poses additional problems such as the waiting time and the emanated inconvenience (Fagnant and Kockelman, 2014; Singh et al., 2021), increased VMT (Burns et al., 2013; Fagnant and Kockelman, 2014; Oh et al., 2020; Singh et al., 2021; Yan et al., 2020), and increased congestion (Oh et al., 2020; Overtoom et al., 2020) due to empty miles generation. Another paramount concern that arises due to the growth of EVs which will be further promoted with the growth of AVs, is the rise in the electric energy demand that can effect the electric grid stability, supply-demand imbalance, and overloading of the electric grid distribution

system (Khalid et al., 2019). The provision of distributed energy resources (DER) such as energy storage system (ESS), and solar panels, at the EV charging station can reduce the electric grid upgrade cost and support EV charging demand (Rafi and Bauman, 2021). In light of all of the above promoting and demoting factors, it is crucial to develop an optimal approach to adopt these technologies considering their effect on environment, transportation systems, and the electric grid network.

The purpose of this study is threefold. First, it develops a framework to estimate the optimal fleet configuration of private human-driven vehicles (PHDV), private AV (PAV), and shared AV (SAV) that will minimize the total system cost comprising of emission production, user's time, and total cost of ownership. The study captures the trade-off between the benefits of increased mobility, efficient use of travel time (reduction in Value of Travel Time (VOTT)), efficient driving, and the negative impacts of increased VMT and the higher ownership cost of AVs. Second, the study considers the EV and AV in private and shared mobility systems to estimate the optimal combination of these technologies to minimize the system cost. It also captures competing factors like improved safety, roadway capacity, driver productivity, increased congestion, increased VMT, zero tailpipe emissions, low operating cost, limited charging infrastructure, and the limited range of EVs. Third, it proposes an optimal investment technology at the direct current fast charging (DCFC) stations to support the EV charging demand in urban areas and reduce the load on the electric grid. The study captures the time-dependent existing energy demand and EV charging demand, capacity constraints of the electric grid, different types of DER (solar panels, ESS), and the cost of purchasing electricity from the electric grid.

1.2 Knowledge Gap and Research Motivation

Autonomous-electric technologies will improve the future of mobility while exacerbating some aspects of the transportation system. These technologies will also affect the environment and the electric grid network. Further, adopting these technologies as private or shared mobility systems will have different implications. The various trade-offs involved have been studied to estimate the generalized transportation cost, which analyzed the different effects of AV and EV technologies. Some studies captured the effect of reduced VOTT (Correia and van Arem, 2016), empty miles generation (Correia and van Arem, 2016; Singh et al., 2021; Zhang et al., 2018), changes in parking cost (Correia and van Arem, 2016), improvement in roadway capacity (Childress et al., 2015) by the adoption of private AVs (PAVs), while others considered SAVs and their effects on emissions (Fagnant and Kockelman, 2014; Singh et al., 2021) and VMT (Burns et al., 2013; Fagnant and Kockelman, 2014; Singh et al., 2021). Other studies estimate optimal incentive policies (Y. Nie et al., 2016) and find charging station locations (Chen et al., 2020; Ghamami et al., 2020a; Kavianipour et al., 2021b; Yang et al., 2017) for the adoption of EVs. However, the prior research is focused on considering the limited number of factors influencing the adoption of AV and EV technologies. It is essential to capture trade-offs among all the influential factors to estimate the overall impact and favorable conditions for adopting these technologies in the transportations system. For instance, the emissions can increase significantly due to increased VMT with the adoption of PAVs/SAVs. However, the efficient driving pattern and reduced number of cold-starts in these vehicles may result in an overall reduction of emissions. An increase in VMT also increases the operating and maintenance cost of the vehicle (AAA, 2017), which may reduce due to the efficient driving pattern. Further, the emissions and operating costs can be substantially reduced if the vehicles are electric.

The travel behavior of the users will also change with the adoption of AVs. The different advantages of AVs, such as efficient use of travel time and roadway, and reduced parking cost, will encourage users to travel more, which will increase VMT in the system. These self-driving vehicles will allow non-drivers, physically disabled, and the elderly to travel independently on their own, encouraging them to travel more, which will again increase VMT in the system. The AVs can efficiently relocate on their own for the next scheduled trip. The relocating ability of AVs not only allows to serve multiple trips in a shared system, but it also allows serving multiple family trips by the same AV in a private system, as opposed to having two or more human-driven vehicles. Vehicle sharing reduces vehicle ownership, which will generate additional empty miles (with no passengers) in the system. These different factors will affect the VMT in the system. It is essential to consider all of these competing factors (changes in travel behavior, family dynamics, reduction in vehicle ownership, empty miles generated) for the increase in VMT due to AVs to better understand the effects of the adoption of AVs. Further, the high cost of AV technology and the battery may be compensated by the reduced maintenance cost of EVs and efficient driving behavior of AVs. The increased travel time cost due to changes in travel behavior with AVs and the reduction in VOTT, and improvement in roadway capacity is another aspect that has not been thoroughly studied in the literature. Thus, this study develops frameworks that will consider all the contradicting and corroborating factors mentioned above in a system of emerging technologies capturing their implications in both private and shared mobility systems.

Finally, the growing EV market share, enhanced by the AV technology, will mandate the EV DCFC stations network deployment. This network of DCFC stations would reduce the charging time and concerns related to the limited range of these vehicles. However, the widespread network of the DCFC stations and rising EV charging demand will increase the load on the electric

grid. Therefore, it might be required to provide DER at the charging station to support the EV charging demand and reduce the load on the electric grid. Thus, it is essential to propose an optimal design of DER by capturing the existing load on the electric grid, increasing EV charging demand, and the capacity constraints of the electric grid network. Further, it is crucial to consider the electric grid upgrade costs and compare them with the investment cost of DER. In addition, it is crucial to consider different DER to propose the best DER for various conditions. This is the primary motivation in developing a modeling framework to estimate the optimal investment technology to support the fast charging demand of EVs considering the electric grid upgrade costs, investment in different DER (solar panels, ESS), and cost of energy (electricity). The results can also provide electricity discounted pricing scenarios.

1.3 Research Significance and Contributions

The main objective of this study is to provide modeling frameworks for the optimal adoption of AVs and EVs by considering their effect on the transportation systems, the environment, and the electric grid network. The study aims to address the following research questions:

- What are the different influential factors involved with the adoption of AVs and EVs, and what are their impacts on mobility, the environment, and the electric grid network?
- How to model these factors and capture the trade-offs among various promoting/demoting factors?
- What are the scenarios or range of different influential factors that will reduce the negative impacts of the new technologies and promote their adoption?

- What will be the impact of EVs on the electric grid network, and how can this impact be managed to reduce the load on the electric grid?

The main contributions of this study are as follows:

- Simultaneously capturing several influential factors, including changes in travel behavior, driving behavior, increase in VMT, travel time, operating costs, and ownership costs, and the variety of trade-offs among these contributing factors, that will govern the adoption of AV and EV technologies.
- Estimating and calibrating functions for the various contributing factors, using the limited available data on AVs, mainly focusing on simulation data.
- Developing a mathematical model for optimizing the adoption of AVs in private and shared mobility systems to minimize emissions, time (travel and waiting), and the total cost of ownership.
- Analyzing various scenarios to capture different stakeholders' perspectives, including but not limited to car companies, system planners, and policymakers, to promote the adoption of AV and EV technologies.
- Developing a mathematical model to find the best DER to support the rising energy demand at the EV fast charging (DCFC) stations while minimizing the investment cost and the cost of purchasing electricity from the electric grid. The investment includes purchasing and installing ESS and solar panels and electric grid upgrades.
- Developing a time-dependent energy demand model at the DCFC stations considering the electric grid network details, capacity constraints of the electric grid components, and seasonal variation in solar energy, electricity rates, and energy demand.

1.4 Research Methods and Dissertation Outline

The dissertation consists of six chapters. The first chapter describes the overview of the problem and the objective of the study. The second chapter includes a comprehensive review of the literature related to the dissertation topic.

Chapter 3 presents a multi-objective framework for optimum fleet configuration of human-driven and autonomous vehicles in a shared or privately-owned mobility system to minimize the purchase and operating costs, time spent, and emission production. The proposed model captures the trade-off between the benefits of increased mobility, reduction in the VOTT, efficient driving pattern, and the negative impacts of increased VMT and ownership cost by adopting PAVs/SAVs. The proposed framework assists with the development of simplified adoption models that can be used by policymakers and/or investors.

Chapter 4 develops a modeling framework to estimate the optimal fleet configuration considering AV and EV technologies in a private and shared mobility system. The different mobility options positively and negatively influence the transportation system. The study captures the trade-offs embedded among different mobility options to determine the optimum combinations of these technologies for a sustainable transportation system. A nonlinear fleet optimization model is developed to minimize the system cost considering a multiclass user problem. The small-scale problem is solved using commercial solvers. However, commercial solvers cannot solve the large-scale nonlinear optimization problem. Hence, a metaheuristic is developed based on a modified parallel genetic algorithm (GA). The proposed framework provides the optimal conditions that favor emerging technologies in private and shared mobility systems. The outcomes of this research can be used to develop policies/incentives that will promote the adoption of AVs and EVs.

Chapter 5 presents an optimization model to estimate the optimal investment technology to support the electric grid hosting a network of DCFC stations. The objective is to minimize the system cost, including purchasing and installing the different ESS and solar panels, the cost of electric grid upgrades, and purchasing electricity from the electric grid. The study captures the time-dependent EV fast-charging demand, existing energy demand, capacity constraints of the electric grid network, seasonal variation in solar energy, electricity rates to propose the optimal investment technology. The proposed framework finds the optimal strategy to reduce the load on the electric grid and support the rising energy demand with the increased market penetration rate of EVs, exacerbated by introductions of AVs and SAVs.

Chapter 6 provides concluding remarks and future research directions.

CHAPTER 2 STATE OF ART OVERVIEW

2.1 Overview

Numerous studies capture the effects of AVs and EVs on the transportation system, environment, and electric grid network. A comprehensive review of the literature is presented in the following subsections. Section 2.2 discusses the studies related to AVs and their implications. Section 2.3 discusses the research related to EVs. Section 2.4 discusses the synergies between these two technologies and how these can promote the adoption of each other. Then, the adoption of these technologies as shared mobility systems is discussed in section 2.5. Section 2.6 and 2.7 present the studies capturing the effect of rising EV charging demand on the electric grid, scope, and implementation of DER at these charging stations.

2.2 Autonomous Vehicles

Automated Vehicle Technology has been the subject of interest to many researchers recently (Chehri and Mouftah, 2019; Fagnant et al., 2016; Greenblatt and Shaheen, 2015; Gruel and Stanford, 2016; Levin and Boyles, 2015; Wadud et al., 2016; Wang et al., 2018; Zhang et al., 2015). This technology has the potential to improve the transportation system in numerous aspects, such as safety (Fagnant and Kockelman, 2015; Harper et al., 2016; NHTSA, 2016; Wadud et al., 2016), mobility (Brown et al., 2014; Harper et al., 2016), driver productivity (de Looff et al., 2018; Gucwa, 2014; van den Berg and Verhoef, 2016), congestion mitigation (Center for Sustainable Systems, 2017; Fagnant and Kockelman, 2015; Wadud et al., 2016), road capacity (Childress et al., 2015; Gucwa, 2014) and energy savings (Brown et al., 2014; Chehri and Mouftah, 2019; Fagnant and Kockelman, 2015; Folsom, 2012; Greenblatt and Saxena, 2015; Morrow et al., 2014). However, the AVs can significantly increase VMT in the system due to empty miles generated

(Fagnant and Kockelman, 2014), improved mobility of non-drivers (Harper et al., 2016), roadway capacity (Childress et al., 2015; Gucwa, 2014), reduced VOTT (Childress et al., 2015; Gucwa, 2014) and reduced parking cost (Childress et al., 2015), etc. The increase in VMT will also increase emissions and operating costs. Further, these vehicles have high ownership costs (FastCompany, 2014; LeVine Steve, 2017) due to the added value of AV technology. However, no studies currently capture all the listed interconnections and trade-offs. Hence, it is essential to understand the overall impact of AVs on the transportation system and determine the conditions favorable to the adoption of these vehicles. This section reviews all studies considering the advantages and disadvantages of AVs.

2.2.1 Advantages of Autonomy

Researchers found that AVs can reduce energy use by mitigating congestion (Center for Sustainable Systems, 2017; Wadud et al., 2016), altering the size (Center for Sustainable Systems, 2017; Morrow et al., 2014; Wadud et al., 2016), and weight (Brown et al., 2014; Greenblatt and Shaheen, 2015; Morrow et al., 2014). The AVs can be programmed to follow efficient driving practices or eco-driving, potentially reducing fuel consumption and energy usage (Brown et al., 2014; Center for Sustainable Systems, 2017; Wadud et al., 2016). The platooning effect in connected AVs, which involves a group of vehicles traveling closely together, can provide potential energy savings (Brown et al., 2014; Center for Sustainable Systems, 2017; Greenblatt and Shaheen, 2015; Morrow et al., 2014; Wadud et al., 2016). One of the studies estimates that AVs can improve fuel efficiency by up to 90% (Brown et al., 2014). The studies estimate that AVs can potentially reduce energy use up to nearly 80% due to platooning, right-sizing and weighting, automated vehicle sharing, efficient traffic flow, and parking (Greenblatt and Shaheen, 2015; Morrow et al., 2014). The estimated reduction in energy consumption due to eco-driving behavior

and platooning of AVs can be up to 25% and 3%-25%, respectively (Center for Sustainable Systems, 2017; Wadud et al., 2016). Thus, the adoption pattern of AVs has been an interest to researchers (Jiang, Zhang, Wang, & Wang, 2019; Menon, Barbour, Zhang, Pinjari, & Mannering, 2019; Sheela & Mannering, 2020).

AVs can be shared by multiple travelers traveling at different times to and from various locations (Fagnant and Kockelman, 2015). This system, known as Shared Autonomous Vehicle (SAV) system, can replace a significant number of private human-driven (conventional) vehicles (PHDV) (Bischoff and Maciejewski, 2016; Fagnant et al., 2016; Fagnant and Kockelman, 2018, 2014). Estimates have shown that a single SAV can replace 12 personal vehicles in a grid network (Fagnant and Kockelman, 2014). Another study reports a replacement rate of 9.3 personal vehicles per SAV in the regional network system of Austin, Texas (Fagnant et al., 2016). The smaller fleet size of the SAV system, compared to the system of PMV, results in continuous repositioning of each SAV to pick up another traveler, making each SAV busy (Fagnant and Kockelman, 2014). As a result, the amount of cold-start emissions reduces significantly with SAVs compared to PMVs (Fagnant and Kockelman, 2014). The cold-start emissions produce CO, NO_x and VOC, etc. (Chester and Horvath, 2008). The adoption of SAVs can significantly reduce VOC, CO, and NO_x production (49%, 34%, and 18%, respectively) due to the decreased number of cold-starts (Fagnant and Kockelman, 2014). The smaller fleet size requirements and continuous repositioning of SAV will also substantially reduce parking demand (Zhang et al., 2015).

The introduction of AVs increases the attractiveness of traveling by car and willingness to drive longer distances and allows efficient use of travel time by drivers in the vehicle (de Looff et al., 2018; Gruel and Stanford, 2016; Gucwa, 2014). The efficient use of travel time reduces the VOTT significantly (de Looff et al., 2018). VOTT is interpreted as an individual's willingness to

pay to avoid another travel time unit (de Looff et al., 2018). A study using the Netherlands as the case study applies discrete choice models to the data obtained from a stated preference survey, estimating VOTT for an AV with office interior to be 6.26€/h as compared to 8.37€/h for a human-driven car (de Looff et al., 2018).

2.2.2 Disadvantages of Autonomy

Private AVs (PAVs) and SAVs have the potential to improve the transportation system in different ways, as mentioned above. However, these vehicles can also worsen some aspects of the transportation system, such as increased VMT, causing increased emissions and operating costs, high ownership costs, and waiting time (if SAVs are considered a substitute to PMV). PAVs and SAVs are expected to increase vehicle miles significantly traveled (VMT) (Brown et al., 2014; Chehri and Mouftah, 2019; Childress et al., 2015; Gucwa, 2014; Harper et al., 2016; Wang et al., 2018). AVs will increase the mobility of the non-drivers, elderly, and people with travel restrictions due to medical conditions, causing an increase in VMT by up to 14% (Harper et al., 2016). Based on the 2009 NHTS (National Household Travel Survey) data, VMT can increase by up to 40% (Brown et al., 2014). A study estimated a 20% increase in VMT, considering the effect of increased road capacity (30%), reduction in VOTT (35%), and reduction in parking cost (50%) (Childress et al., 2015). Gucwa (2014) estimated a 4-8% increase in VMT in San Francisco, Bay Area, due to the simultaneous increase in roadway capacity and reduction in VOTT (Gucwa, 2014).

Adoption of AVs can significantly reduce vehicle ownership resulting in empty miles generation and a consequent increase in VMT in the system (Zhang et al., 2018). Zhang et al. (2018) estimated a 9.5% decrease in vehicle ownership and a 13.3% increase in VMT in the system due to the adoption of PAVs in the Atlanta Metropolitan area (Zhang et al., 2018). Further, the use

of SAVs also results in empty miles generation, which depends upon the fleet size and trip density (Burns et al., 2013; Fagnant and Kockelman, 2014). It has been estimated that SAVs can increase VMT by 11% due to empty repositioning (Fagnant and Kockelman, 2014).

The high ownership cost is another critical factor affecting the adoption of PAVs and SAVs. The expected purchase price of AVs is estimated to be more than $250,000 (FastCompany, 2014; LeVine Steve, 2017). Fagnant et al. (2018) assume that the cost of adding AV technology to the existing vehicle would be $50,000 (Fagnant and Kockelman, 2018). However, some studies show that the cost of adding AV technology to the vehicle will come down to $3,000-$10,000 in the future (Fagnant and Kockelman, 2015; IHS, 2014). The high ownership cost of AV, combined with increased running emissions and operating costs due to increased VMT, can significantly affect the adoption of these vehicles. Hence, it is essential to consider this factor while estimating system effects due to AV adoption.

2.3 Electric Vehicles

EVs are becoming popular because of their higher energy efficiency (Annema, 2020; Eberhard and Tarpenning, 2006; Romm, 2006) compared to gasoline vehicles. Recent growth in the adoption of EVs has a significant impact on greenhouse gas emissions(Chen et al., 2016; Crist, 2012; Gai et al., 2019; Kavianipour et al., 2020; Nie and Ghamami, 2013; Samaras and Meisterling, 2008; Stogios et al., 2019)**,** and energy usage (Chen et al., 2016). However, the limited driving range (Ghamami et al., 2020a; Hidrue et al., 2011), the high purchase price (Hidrue et al., 2011), and the low density of charging infrastructure (Ghamami et al., 2020a; Hidrue et al., 2011) has impeded the adoption of EVs. Some of the current EV models have a range greater than 300 miles per charge. However, it is still lower as compared to conventional gasoline vehicles. The limited range of EVs makes the customers concerned about EV running out of charge with no

charge stations nearby, called range anxiety (Tate et al., 2008). These limitations also make the shared mobility services using EVs challenging. Studies have shown that investing in charging infrastructure, rather than providing purchase subsidies, further improves the adoption of EVs (Y. (Marco) Nie et al., 2016). There is also a trade-off in investing the available funds on battery or charging infrastructure technological advancement (Nie and Ghamami, 2013). A study suggests that the smaller batteries with denser charging infrastructure might be more cost-effective than building long-ranged plug-in EVs (Ghamami et al., 2016). As infrastructure is one of the main challenges in the adoption of EVs, the optimal location of EV charging stations has been an interest to many researchers (Chen et al., 2020; Dashora et al., 2010; Frade et al., 2011; Ghamami et al., 2020a, 2016; Kavianipour et al., 2021b; Sweda and Klabjan, 2011; Yang et al., 2017). Some studies have obtained driving pattern information of EV users through travel surveys to estimate the optimal location of charging infrastructure (Andrews et al., 2012; Avci et al., 2015; Sweda and Klabjan, 2011). Other studies have utilized taxi GPS data to estimate optimal charging station locations for shared EVs (Shahraki et al., 2015; Tu et al., 2016). Some studies used traffic simulation data based on origin and destination of trips to capture travel information of private EVs. These studies either considered fixed-route choice (Lim and Kuby, 2010; Xie et al., 2016; Zockaie et al., 2016) or interaction between traffic assignment problems and charging stations locations (Fakhrmoosavi et al., 2021; Ghamami et al., 2020a; He et al., 2018; Kavianipour et al., 2021a, 2021b). Another critical factor in the adoption of EVs is their performance reliability under adverse weather conditions as the fuel efficiency of EVs and charging efficiency decreases significantly in cold weather conditions (Hawkins, 2019). Studies suggest that battery performance reduces by 25-30% in cold weather conditions (EERE, 2021). One of the studies estimates that the battery performance is more crucial as compared to rising charging demand in summer for optimal

deployment of DCFC stations (Fakhrmoosavi et al., 2021). The AV technology can reduce some of the limitations of EVs, which will promote their adoption.

2.4 Synergies and combined implications of autonomous-electric vehicles technology

As discussed above, AVs and EVs can have various impacts on the transportation system. However, the synergy between AV and EV technology can ameliorate and enhance some of these impacts and influence the adoption of both technologies. Some of AV technology features might require a battery (Brown and Dodder, 2019), which will further promote EV adoption. EVs' zero tailpipe emission can partially attenuate the environmental consequences of increased VMT by adopting AVs(Wang et al., 2018). The EVs can reduce the operating cost induced due to an increase in travel of users with the adoption of AVs, which can also offset the higher purchase price of autonomous EVs (AEV) (Weiss et al., 2017). The induced travel demand by the adoption of AVs may increase gasoline fuel prices, promoting the adoption of alternative-fuel vehicles such as EVs (Brown and Dodder, 2019). On the other hand, AV technology can implement efficient algorithms promoting a smoother drive cycle and maximizing energy recovery with regenerative braking (Annema, 2020). AEVs can be programmed to choose energy-efficient routes, considering congestion, number of stops, etc. (Annema, 2020), improving battery efficiency. Improved battery efficiency and driving range, as a result, will mitigate range anxiety and enhance the battery life of AEV. AVs are more compatible with vehicle-to-grid (V2G) technology by synchronizing the operating, charging, and discharging algorithms (Lam et al., 2016). This allows AEV owners to receive compensation for delivering energy to the electric grid during peak hours(Annema, 2020) and will encourage users to adopt AEVs.

However, the AVs and EVs have higher purchase prices due to the additive cost of LIDAR technology and batteries, respectively. Tesla’s “full self-driving” option, featuring automatic car

parking and lane changing, costs around $10,000 (Porter, 2020). Other studies predicted the AV technology cost would be around $2000-$10,000 (Fagnant and Kockelman, 2015; IHS, 2014; Ritchie, 2019). EVs are also more expensive than gasoline vehicles, as a significant portion of the cost is the cost of their batteries. Studies show that the price of Lithium-Ion batteries has reduced by 85% from 2010 to 2018 (BloombergNEF, 2019). However, the unit battery cost is still $176/kWh in 2018 (BloombergNEF, 2019). The high purchase price of these technologies questions the affordability of these vehicles as private modes. However, the adoption of these technologies as a shared mobility system might overcome these challenges.

2.5 Shared mobility with autonomous-electric vehicles

The AV technology facilitates the dynamic ridesharing system (Krueger et al., 2016), reducing fleet size, emissions, congestion, and parking demand (Golbabaei et al., 2020). The shared AVs provide guaranteed compliance to real-time changes in demand compared to human-driven taxis (Hyland and Mahmassani, 2018). A well-planned and demand-responsive system will decrease the fleet size requirement and users' waiting time compared to a conventional taxi system (Spieser et al., 2016). The replacement rate is defined as the number of private human-driven vehicles (PMV) a single SAV or shared autonomous electric vehicle (SAEV) can replace while serving the same equivalent demand due to its ability to travel independently. This replacement is larger for SAVs than SAEVs due to the long charging time and low range of the EV batteries (Chen et al., 2016; Fagnant et al., 2016; Fagnant and Kockelman, 2014; Zhang et al., 2015). AVs have the potential to partially overcome the limitation of EVs, especially in a shared mobility system, by automating the charging process and managing the range, considering the location of the charging station and real-time demand (Chen et al., 2016). SAEV provides a driver-free method to efficiently relocate based on real-time demand and charging infrastructure availability (Chen et

al., 2016). SAEVs not only allows for a reduction of labor costs (Bösch et al., 2018; Hyland and Mahmassani, 2018; Liu et al., 2020) but also reduce energy costs (Chen et al., 2016; Eberhard and Tarpenning, 2006; Romm, 2006) of transportation network companies (TNC) providing shared mobility services. The electrification of SAVs and renewable energy charging can enhance environmental benefits (Golbabaei et al., 2020). The AV technology increases the vehicle utilization rate in the shared mobility system (Weiss et al., 2017), increasing the miles traveled and the associated operating and emission cost. This promotes the electrification of the fleet with substantial savings in operating costs (Weiss et al., 2017) and zero tailpipe emissions. Some studies find that the AV technology will reduce the charging cost of shared EVs, allowing the vehicles to charge when the electricity price is low (Iacobucci et al., 2019, 2018). The reduction in cold-start emissions (Fagnant and Kockelman, 2014; Singh et al., 2021), parking demand (Yan et al., 2020; Zhang et al., 2015), and driver cost (Liu et al., 2020) are some of the other advantages of SAVs.

The shared mobility system increases users' waiting time (Fagnant and Kockelman, 2014; Singh et al., 2021) VMT (due to empty miles generation) (Burns et al., 2013; Fagnant and Kockelman, 2014; Oh et al., 2020; Singh et al., 2021; Yan et al., 2020), and the total travel time in the system (Oh et al., 2020; Overtoom et al., 2020). The high replacement rate of SAVs or smaller fleet size exponentially increases the users' waiting time and empty miles generation (Singh et al., 2021). The limited charging infrastructure is another potential barrier to the adoption of SAEVs. The studies have assessed the effect of charging infrastructure on the operation and performance of the SAEV fleet (Chen et al., 2016; Loeb et al., 2018; Vosooghi et al., 2020; Zhang et al., 2020). Further, the high charging time and limited battery size can affect service usage and increase waiting time for SAEVs (Vosooghi et al., 2020). The faster-charging infrastructure such as super-chargers or battery swapping might be required to improve the service performance of

SAEVs to be comparable to that of SAVs (Vosooghi et al., 2020). The widespread network of these fast chargers will reduce the charging time and ease the concerns related to the limited range of EVs. Hence, it will enhance the growth of EVs. However, this will increase the electricity demand and overload the electric grid. The provision of DER at these charging stations would reduce the load on the electric grid and support the EV fast-charging demand.

2.6 Effect of growth in EV charging demand and requirement of Distributed Energy Resources

The EV and the associated industries have grown rapidly in recent years (Ma, 2019). In 2019, electric car sales hit a record high of 2.1 million globally, increasing by 40% from the previous year (IEA, 2020). The rapid growth of the EV market will necessitate the development of proper electric vehicle charging infrastructure to serve the electric energy demand(Ma, 2019; Negarestani et al., 2016). There are three standard EV charging levels (Morrow et al., 2008). The charging level 1 and level 2 are based on AC voltage with charging power of 1.44 kW and 3.3 kW, respectively(Morrow et al., 2008). The charging level 3 is a direct current fast charging (DCFC) which can have a charging power of up to 150 kW, allowing EV to charge in 10-25 minutes (Negarestani et al., 2016). While the level 1 and level 2 chargers are typically used for overnight charging at home supporting intra-city trips (Negarestani et al., 2016), the DCFC chargers are used for public applications similar to gasoline service stations (Morrow et al., 2008; Yilmaz and Krein, 2013). The DCFC chargers have gained much attention due to the short charging time (Negarestani et al., 2016). The survey shows that the charging time and the charging infrastructure are the primary concerns of EV customers, with the majority of the customers placing significant importance on fast charging(Chakraborty et al., 2019). The deployment of DCFC chargers is mandatory for the widespread adoption of EVs (Chakraborty et al., 2019). The comprehensive

network of DCFC chargers will reduce the range anxiety and charging time, allowing users to travel freely, even for long-distance intercity trips (Rafi and Bauman, 2021).

However, the widespread usage and rise in the EV charging demand will affect the electric grid (Negarestani et al., 2016; Rafi and Bauman, 2021). The EV charging stations can affect the electric grid stability, supply-demand imbalance, overloading and degradation of the distribution system, voltage fluctuations, and power system losses (Khalid et al., 2019). One of the studies tested the IEEE 3-bus system and showed that its stability deteriorates with the addition of EV load(Onar and Khaligh, 2010). Another study showed that the stability margin lowers if the EV power load is constant compared to the constant impedance load (Das and Aliprantis, 2008). McCarthy and Wolfs, 2010 mention that the peak demand increases due to the uncontrolled charging demand of EVs (McCarthy and Wolfs, 2010). A UK-based study indicates that the demand increases by 18 % with a 10% increase in EV load (Mahalik et al., 2010; Putrus et al., 2009). The rise in EV load also increases power losses in the electric grid system, which can be about 40% during off-peak charging at an EV load penetration rate of 62% (Bradley et al., 1981). The high penetration of EV load causes significant overloading of distribution transformers, thereby reducing the performance and the life (Masoum et al., 2010). The distribution system might have to be reinforced to support EV charging demand during peak periods(Pieltain Fernandez et al., 2011). Further, the DCFC chargers will impose an unpredictably large load on the electric grid (Gallinaro, 2020; Knupfer et al., 2018; Richard and Petit, 2018a). Also, the majority of DCFC charging stations should be located along the highways outside the cities to support long-distance trips (Rafi and Bauman, 2021). However, these locations would be in rural areas with weak electric grid connections far away from the main distribution electric grid (Baatar et al., 2021; Rafi and Bauman, 2021). This would require the electric grid upgrades and high

installation cost for the DCFC charging stations at these locations (INL, 2015). Electric grid upgrades might be necessary even in urban areas (with strong electric grid connections) at locations with high peak demand and multiple fast charging ports (Rafi and Bauman, 2021). Expanding the DCFC charging network would require more upgrades of distribution lines and transformers than that of the substation, transmission lines, and power plants (Rafi and Bauman, 2021). The increase in demand can be as high as 1.2 MW with a typical Electrify America installation of two 350 kW chargers and four 150 kW chargers along the highways (Nicholas and Hall, 2018). One of the studies shows that the electric grid reinforcement cost could be $1.6 billion in Norway, to support the uncontrolled charging of large EV load by 2040 (Molnar, 2019). In light of the above, the provision of ESS at the charging stations can play a vital role to mitigate the electric grid upgrade cost (Rafi and Bauman, 2021), reduce the peak electricity demand i.e. peak shaving (Gallinaro, 2020; Knupfer et al., 2018), prevent overloading of the electric grid (Nicholas and Hall, 2018) as well as supporting the fast charging EV demand.

The provision of ESS can minimize or eliminate the upgrades of the electric grid (Rafi and Bauman, 2021). One of the studies shows that the battery energy storage system can save up to $157,000 annually for six 350 kW chargers at the DCFC charging station (Francfort et al., 2017). Even in remote areas, the ESS can be less costly than electric grid reinforcement (EASE, 2019). Further, the use of renewable energy sources along with ESS can be advantageous as ESS can efficiently store intermittent renewable energy (e.g., solar energy) to support EV demand (Rafi and Bauman, 2021). These ESS can be charged at low electricity demand and prices, charge EVs with higher power suitable for the DCFC chargers, substantially reduce the electric grid's load, reduce the operating cost, and monthly electricity demand charges from the electric grid (Rafi and Bauman, 2021).

2.7 Distributed Energy Resources supporting EV charging demand

The literature consists of numerous studies considering DER like solar panels, and batteries to support EV charging demand. One of the studies, considered energy loss, charging demand, and life cycle to optimize the size of ESS supporting fast-charging stations (Negarestani et al., 2016). M.Gjelaj et al. perform a cost-benefit analysis to minimize the operating cost of DCFC stations considering connection costs, installation costs, and ESS life cycle costs (Gjelaj et al., 2017c). Another study optimizes the size of ESS considering mixed-integer linear programming (Salapic et al., 2018). The studies have assessed the integration of bidirectional DCFC station with ESS into the low voltage electric grid (Gjelaj et al., 2017a) and optimal size of ESS to ameliorate the adverse effect on the electric grid (Gjelaj et al., 2017b). One of the studies develops a modeling framework considering the ESS degradation, trade-offs between the power rating of EV charging station, and size of the ESS (Richard and Petit, 2018b). Another study compared second life batteries (SLB) with new batteries (NB) of lithium-ion (Li-ion) to support EV fast-charging demand and reduce the electric grid load (Kamath et al., 2020). The study concluded that the levelized cost of electricity reduces by 12-41% when using SLB instead of new batteries. A comparison of different storage technologies proposed flywheel storage systems to minimize the energy cost and storage cost at the fast charging station (Negarestani et al., 2016). However, technological advancements have changed the cost of different ESS (especially the Li-ion batteries).

The studies have also considered renewable energy (RE) to support EV charging stations. These can assist in peak-shaving and reduce electric grid power losses (Ma, 2019). Further, the provision of ESS can improve or completely remove the power fluctuations of RE power generators(Ma, 2019). One of the studies estimated the impact of variation in the number of DCFC

stations, load profiles, electricity price, geographic locations on the economic and energy performance of DCFC stations with solar panels and ESS (Yang and Ribberink, 2019). The system provides energy savings, and the economic viability is promising, considering the unit price of DER in the year 2021-2026, with a payback period of 12-16 years (Yang and Ribberink, 2019). A study optimizes the annual cost of energy to estimate the location and size of level 2 charging stations, distributed ESS, and solar panels/wind turbines (Kandil et al., 2018) over the grid network. The cost includes the investment cost of technologies, energy consumption, and renewable energy savings. The study estimated that to support existing and EV demand; the solar panels can provide savings of around 70-75% instead of distributed ESS, which can provide only approximately 15-20% savings. Li et al., 2019 develop an optimization framework to minimize the electricity cost and the number of charge/discharge cycles of ESS for the solar panel-assisted EV charging station (Li et al., 2019). The study showed that optimum coordination between the energy resources and EVs could maintain stable power system operations and reduce the charging cost. Another study proposed a solar panel and lithium ferro phosphate battery as the optimal solution out of three ESSs, including lead-acid and lithium nickel cobalt aluminum oxide batteries (Nizam and Wicaksono, 2019). The optimization minimizes the initial capital and operating cost of the off-grid charging station in rural areas (Nizam and Wicaksono, 2019). Ugirumurera and Haas, 2017 estimated the optimum number of solar panels and size of ESS to support the EV charging system with energy generation exclusively by the solar farm. The optimum number of solar panels decreases with an increase in the average delay of EV users and the power rating of each charging station (Ugirumurera and Haas, 2017). One of the studies implemented GA and Monte-Carlo method to optimize the location and capacity of solar panels and ESS to support charging stations considering uncertainties in EV demand, solar panel power, electricity price

(Khanghah et al., 2017). The study showed that the ESS and solar panels could reduce the system's operating cost, power losses, and voltage sags. Hilton et al., 2019 develop an optimization framework to maximize the profit and minimize the electric grid connection cost and associated energy cost for a solar panel-ESS charging station (Hilton et al., 2019). The study showed that the solar farm and ESS reduce grid energy use and can provide savings, especially if the grid connection cost is high.

CHAPTER 3 OPTIMAL ADOPTION OF AV IN PRIVATE AND SHARED MOBILITY SYSTEMS

3.1 Overview

The AVs may impose positive or negative externalities on the transportation system and environment. Numerous studies are capturing the trade-offs among different influential factors that govern the adoption of AVs. However, it is important to consider all the competing factors and capture the trade-offs between these factors so as to estimate the overall impact of AVs on the transportation system, and environment. Further, the implications of AVs would be different in private and shared mobility systems. This study develops a modeling framework to estimate the impacts of PAVs and SAVs on the environment and the transportation system, considering the changes in travel behavior, VMT, emission production, driving behavior, travel time, operating costs, and cost of ownership. A multi-objective framework is developed to find the best vehicle fleet (PMV, PAV, or SAV) that will result in minimum emissions, minimum time spent, and minimum total cost of ownership. It is worth noting that this study estimates and calibrates functions for the various contributing factors, using the limited available data on AVs, mainly focusing on simulation data.

The remainder of this study is as follows. Section 3.2 discusses the problem statement and objective of the study, followed by the methodology in section 3.3. The case study, numerical results, and the summary are presented in sections 3.4, 3.5, and, 3.6, respectively.

3.2 Problem Statement

This study aims to capture the trade-off between the benefits of increased mobility, efficient use of travel time (reduced VOTT), efficient driving, and the negative impacts of

increased VMT, as well as the higher ownership cost as a result of the adoption of AVs. This study aims to minimize emission production, users' time, and total cost of ownership (purchase price and operating cost) by proposing a multi-objective optimization framework. This framework finds the best configuration of different vehicle types (PMVs, PAVs, or SAVs) for urban trips, under different circumstances. The different circumstances may vary over time or regions and affect the listed trade-offs. It is important to note that this study considers fully autonomous vehicles (Level 5 autonomy) which do not require human drivers.

The contradicting and complementary factors listed above are functions of a variety of parameters. Thus, each function needs to be defined and calibrated. The emission produced is derived from the superposition of four factors; VMT (Moore et al., 2010), number of cold-starts (Chester and Horvath, 2008; EPA, 1994; Reiter and Kockelman, 2016), and speed and acceleration rate (Int Panis et al., 2006; Qi et al., 2004). The categories of emissions considered are running emissions and cold-start emissions. The running emissions are the function of speed, acceleration, and VMT. The cold-start emissions are a function of the number of trips, emission per cold-start, and the number of cold-starts per person-trip. The operating cost of the vehicle includes the fuel and maintenance cost, which are functions of VMT generated, cost of fuel, fuel efficiency, and maintenance cost per mile. The total VMT generated in the system is estimated considering changes in users' travel behavior, changes in family dynamics, reduction in vehicle ownership, and empty miles generated due to the adoption of PAVs/SAVs. The travel time cost is a function of occupied VMT, VOTT, and the reduction factor for VOTT (RVOTT) due to the adoption of PAVs/SAVs. The total waiting time cost in the system, which applies exclusively to SAVs, depends on the waiting time cost per unit time, fleet size, and trip density in the system. The

ownership cost is a function of the purchase price, average miles driven per year, and total miles traveled by vehicle during its lifetime.

3.3 Modeling Framework

The methodology has two main steps. First, the definition and calibration of the travel pattern, emission production and cost functions, pre and post-adoption of the AVs. Second, defining a multi-objective optimization problem to find the optimum market for these vehicles, considering the changes in travel patterns, emission production, and costs.

As discussed above, the introduction of PAVs/SAVs affects the travel pattern of users. There are a variety of underlying reasons that cause this change. These reasons and their effects are carefully studied and discussed in the subsections below. The changes in travel pattern and driving pattern affects emission production. The adoption of SAVs reduces cold-start emissions in the system. Adopting PAVs/SAVs also affects users' travel time cost and SAVs come with possible waiting times. It is worth noting that the purchase price and operating costs of AVs are different from that of PMVs. The objective of the study is to find the optimum vehicle fleet and vehicle type, under different underlying conditions, and the best way to use these vehicles to minimize the emissions, total time spent by the users in the system, and the total cost of owning the vehicles (purchase cost and operating costs), including changes in VMT, emissions, waiting time, operating cost and ownership cost. The study also does a comparative analysis of the results while minimizing emission cost (focusing on environmental concerns) to that of minimizing all the different system costs (emissions, total time, and total cost of owning vehicles). The multi-objective model is reduced to a Linear Programming (LP) problem, with the market share of each vehicle type (PMV, PAV, or SAV), defined as the number of vehicles of that type, being the decision variable.

The factors affecting VMT are discussed in section 3.3.1. The emission estimation is presented in 3.3.2. Section 3.3.3 explains how ownership cost and operating cost are estimated. The system travel time cost and waiting time cost (due to SAVs) are discussed in sections 3.3.4 and 3.3.5, respectively. Further, the Linear Programming problem and its analytical solution are presented in sections 3.3.6 and 3.3.7, respectively.

3.3.1 Factors affecting VMT

The adoption of autonomous vehicles affects the average VMT due to the changes in travel behavior, family dynamics, vehicle ownership, housing locations, and trip chaining. The detailed influence of these factors are explained below:

Changes in the travel behavior: The efficient utilization of roadway, reduction in the VOTT, and parking costs due to the adoption of PAVs/SAVs will encourage the users to travel more which will increase the VMT in the system. The reduction in VOTT is the result of the efficient use of travel time in these vehicles. The self-drive and self-park capability of these vehicles provides them with a variety of less expensive parking options. The parking cost is further reduced due to better utilization of the space by these vehicles (as no room is required for the driver to get out). The computer-controlled vehicles will use the road more efficiently which will increase the roadway capacity. All these factors will change users' travel behavior, encouraging them to travel more, which will increase VMT in the system. This effect has been considered by (Childress et al., 2015) and the presents study captures it through the parameter α_j^{rc} .

Changes in family dynamics: The ability of the AVs to drive on their own will increase independence and encourage non-drivers, elderly, and physically disabled to travel more. The

increase in VMT due to the above-mentioned factor has been quantified by (Harper et al., 2016) and captured by the parameter α_j^{nd}, in this study.

Reduction in vehicle ownership: The same PAV can be used by different family members if the schedule of their trips allows. The vehicle can travel on its own picking up and dropping off family members. Similarly, a single SAV can serve multiple trips within the city. This will reduce the number of vehicles and vehicle ownership, which will not only increase VMT per vehicle but, will also generate additional empty miles (with no passenger) between drop-off (current trip) and pick-up (next trip) locations. These effects are quantified by VMT per vehicle (α_j^{rnv}) and empty mile generation (α_j^{emp}) factors.

The other factors which might affect VMT are the land-use changes and trip chaining. The adoption of SAVs is expected to reduce urban sprawl (Meyer et al., 2017; Zhang, 2017). However, as accessibility in rural areas increases some population groups might consider moving to remote locations (Meyer et al., 2017; Zhang, 2017). Studies have shown that in the US Atlantic region, with the introduction of SAVs elderly are expected to move closer to city centers (by 2-7%), while younger people are expected to move further away (by 7-10%) (Zhang, 2017). Another study for Australia reported 3-4% of the population moving to suburbs with the adoption of PAVs, considering 50% reduction in VOTT (Thakur et al., 2016). There are also studies that predict AVs to have no effect on the housing location (Zmud and Sener, 2017). Thus, the true effect of self-driving vehicles on housing location is still unclear which will not only be region-specific but will also depend upon the demographics. Hence, it is difficult to quantify this effect and it is not considered in this study. Another factor that can affect VMT is the trip chaining dynamics. The adoption of PAVs/SAVs might reduce total travel costs due to efficient use of the roadway, reduced VOTT, and the reduction in parking, fuel and insurance cost and efficient use of vehicles,

causing users to engage less in trip chaining (Rodier, 2018). Due to insufficient data, it is difficult to quantify this effect and therefore not considered in this study. However, the effect on VMT due to the efficient use of the roadway capacity, reduced VOTT, and reduction in parking cost has been captured by the parameter α_j^{rc} which partially captures the effect of reduced trip chaining.

Equation 1 represents miles per vehicle m_j^{pv} for each vehicle type j (PMV, PAV, and SAV), in the given system for the duration of study T, considering different factors for VMT increase.

$$m_j^{pv} = \alpha_j^{rc}\alpha_j^{nd}\alpha_j^{emp}\alpha_j^{rnv}m_{pmv}^{pv} \quad 1$$

In which, the term m_{phdv}^{pv} is the average VMT per PMV for the duration of the study T. Each of the other parameters represents one of the main factors affecting average VMT due to the adoption of AVs, as explained above. The factor α_j^{emp} is a function of the replacement rate γ_j for vehicle type j (PAV or SAV), as presented in Equations 2 and 3. The replacement rate is defined as the number of PMVs replaced by each PAV or SAV, as a result of carsharing. The increase in empty miles is also a function of the increase in the number of trips (η_{sav}) due to the adoption of SAVs. The larger the density of the area and larger the number of trips, it is more likely that the consecutive trips are closer together location-wise. This means while the empty miles generated increases with an increase in the replacement rate, it decreases with an increase in the number of trips in a given system, exclusively for SAVs. The detailed functions are presented in section 3.4.

$$\alpha_{pav}^{emp} = f(\gamma_{pav}) \quad 2$$

$$\alpha_{sav}^{emp} = f(\gamma_{sav}, \eta_{sav}) \quad 3$$

The factor α_j^{rnv} is equal to the replacement rate γ_j. This is based on the conclusion that the reduction in the number of vehicles will result in an equivalent increase in miles per vehicle to serve the same trips. The increase in VMT due to changes in travel behavior and family dynamics with the adoption of AVs are captured by α_j^{rc} and α_j^{nd}. Note that, all of the factors representing an increase in VMT are equal to 1 for PMV.

3.3.2 Emission Estimation

This section presents the estimation of the amount of emission produced by each of the PMVs, PAVs, and SAVs. The pollutants considered for emission estimation are CO_2, CO, and NO_X. The CO emissions are estimated from the cold-starts of the vehicle (Chester and Horvath, 2008). The amount of CO_2, which is the main component of running emissions, is estimated using the trip trajectory of the vehicle (Int Panis et al., 2006). NO_X is estimated for both running emissions (Int Panis et al., 2006) and cold-start emissions (Chester and Horvath, 2008).

3.3.2.1 Running Emissions

The running emission is a function of the speed and acceleration of the vehicle:

$$\hat{e}(t)_{ij}^{re} = f_i\left[v_j(t), a_j(t)\right] \quad \forall i, j \qquad 4$$

Here, $\hat{e}(t)_{ij}^{re}$ is the instantaneous running emission for emission type i (CO_2 and NO_X) and vehicle type j (PMV, PAV, or SAV). The term $v_j(t)$ and $a_j(t)$ are the instantaneous speed and acceleration of the vehicle type j. These are determined using the trip trajectory of the vehicle type j. The trajectories are obtained considering efficient driving (for PAVs and SAVs) and nonefficient-driving (for PMVs) behaviors. Efficient driving is defined as the smooth driving pattern without any sudden changes in acceleration/deceleration rate causing a reduction in

emission production and fuel consumption. Further, Equation 5 is used to estimate running emissions per mile (e_{ij}^{re}) for emission type i by vehicle type j.

$$e_{ij}^{re} = \frac{\int_0^{T_s} \hat{e}(t)_{ij}^{re} dt}{L} \quad 5$$

In which, L is the length of the stretch considered and T_s is the time required to drive through that stretch. The total running emission (E_{ij}^{RE}) per vehicle type j for the emission type i is as follows:

$$E_{ij}^{RE} = e_{ij}^{re} m_j^{pv} \quad 6$$

3.3.2.2 Cold-start Emissions

In general, a cold-start is defined as any start that occurs after one hour of the end of the preceding trip (EPA, 1994; Reiter and Kockelman, 2016). A significant amount of CO and NOx are produced in each cold-start. The cold-start emission is a function of the number of trips. The amount of cold-start emission produced by PAVs is comparable to that of PMVs. However, the cold-start emissions produced by SAVs are considerably less than that of PMVs (Fagnant and Kockelman, 2014). This is due to the reduction in the number of cold-starts per person trip because of the continuous repositioning of the vehicle with the engine being turned off less frequently. The number of cold-starts (N_{sav}^{cs}) per person-trip decreases with the increase in the replacement rate and the increase in the number of trips due to the adoption of SAVs. Hence, a factor accounting for the reduction in number of cold-starts (β_j^{rcs}) is considered in the model (Equation 7). The term N_{phdv}^{cs} is the original number of cold-starts per person-trip in the PMV system. The number of cold-starts per person-trip in a system comprising of SAVs (N_{sav}^{cs}) is the function of replacement rate of SAVs (γ_{sav}) and increase in the trips due to the adoption of SAVs (η_{sav}). The detailed

function for N_{sav}^{cs} is presented in the section 3.4. The number of cold-starts per person-trip in a system comprising of PAVs (N_{pav}^{cs}) is assumed to be equal to that of PMV (N_{pmv}^{cs}). Hence, the factor β_j^{rcs} is equal to 1 for PMVs and PAVs.

$$\beta_j^{rcs} = \frac{N_j^{cs}}{N_{pmv}^{cs}} \quad 7$$

The total cold-start emission (E_i^{CS}) per vehicle type j for the emission type i is as follows:

$$E_{ij}^{CS} = e_i^{cs}\eta_j\alpha_j^{rnv}\beta_j^{rcs}m_{pmv}^{pv} \quad 8$$

In which, e_i^{cs} is the cold-start emissions (CO and NOx) per mile for emission type i by PMVs. Note that CO_2 is a negligible factor in cold-start emissions. The term η_j represents the increase in the total number of trips generated due to the adoption of PAVs and SAVs. The value of η_j is given by Equation 9.

$$\eta_j = \beta_j^{nd}\beta_j^{rc} \quad 9$$

The term β_j^{nd} represents the increase in the number of trips as a result of the improved mobility of non-drivers, due to the adoption of PAVs and SAVs. The term β_j^{rc} represents the increase in trips due to the efficient use of roadway capacity, reduction in VOTT, and parking cost. The value of η_j and α_j^{rnv} for PMV is equal to 1

3.3.3 Purchase and Operating Costs

The purchase price of PAVs and SAVs is expected to be higher than that of PMVs, considering the cost of LIDAR technology, other radar systems, and the variety of sensors installed in the vehicle. This study also includes operating costs (maintenance cost and fuel cost) to estimate

optimal fleet configuration. The purchase price, fuel, maintenance, and operating cost over the duration of the study T for a vehicle type j are presented in Equations 10 to 13, respectively.

$$C_j^{oc} = \left(\frac{C_j^o}{S_j}\right) T \quad 10$$

$$C_j^f = \left(\frac{C_f}{m_{pg}}\right) R_j^f \, m_j^{pv} \quad 11$$

$$C_j^m = C_m m_j^{pv} \quad 12$$

$$C_j^{op} = C_j^f + C_j^m = \left[\left(\frac{C_f}{m_{pg}}\right) R_j^f + C_m\right] m_j^{pv} \quad 13$$

In which, the terms C_j^o and S_j represent purchase price and average service life (in years) of vehicle type j, respectively. The term R_j^f denotes the reduction factor for fuel consumption as the result of efficient driving patterns of autonomous vehicles. Thus, the factor will be equal to 1 for PMVs. The factors C_f and m_{pg} are the average fuel cost per gallon and the fuel efficiency of the PMVs (average miles per gallon of fuel), respectively. The factor C_m is the average maintenance cost per mile. The average service life of the vehicle type j is given as follows:

$$S_j = \frac{M_j^T}{m_j^{py}} \quad 14$$

In which, M_j^T and m_j^{py} are the total lifetime mileage of the vehicle (total miles traveled by the vehicle during its lifespan) and total miles traveled in a year by vehicle type j, respectively. The term m_j^{py} is obtained considering different factors causing an increase in VMT due to the adoption of PAVs and SAVs. The detailed calibrated function is presented in section 3.4.

3.3.4 Travel Time

The travel time in the given system, estimated based on the average speed and miles traveled by the vehicle, is presented as follows:

$$TT_j = \frac{m_{phdv}^{pv} \alpha_j^{rc} \alpha_j^{nd} \alpha_j^{rnv}}{v_j} \quad 15$$

In which, TT_j and v_j are the total travel time per vehicle (in the study period T) and the average speed for the vehicle type j.

3.3.5 Waiting Time

Similar to other shared-mobility systems, the use of SAVs might result in users' waiting time. The reduced number of vehicles in the shared system increases the likelihood of waiting for an available ride. On the other hand, the increase in trip density of the system increases the likelihood of finding the next departure location close to the current or arrival location of SAV, resulting in an overall reduction in the average waiting time. Thus, the average waiting time (w_{sav}^{pt}) is a function of the replacement rate of SAV (γ_{sav}) and the increase in the number of trips (η_{sav}) due to the adoption of SAVs (Equation 16). The average waiting time increases with an increase in the replacement rate and decreases with an increase in the number of trips in a given system.

$$w_{sav}^{pt} = f(\gamma_{sav}, \eta_{sav}) \quad 16$$

The waiting time per vehicle W_{sav}^{wt} for the duration of the study T, is given as follows:

$$W_{sav}^{wt} = w_{sav}^{pt} T_{ps} \quad 17$$

In which, T_{ps} is the number of trips generated per SAV for the duration of the study, given as follows:

$$T_{ps} = \gamma_{sav} T_p \eta_{sav} \quad (18)$$

Here, T_p represents the original number of trips generated per PMV (in time T), when PAVs and SAVs are not present in the system. The total waiting time per vehicle is equal to zero for PMVs and PAVs.

3.3.6 Optimization problem

The objective of this study is to find the best vehicle type under different underlying conditions that will minimize emissions, time (waiting and travel time), and cost of ownership (purchase price and operating costs) of the vehicles. The problem is formulated as a multi-objective optimization problem with an aim to minimize societal costs, user costs, and investor costs. The societal costs include emission (running and cold-start). Ownership and operating costs are user and/or investor costs, depending on the SAVs operation agreements. The travel time and waiting time are user costs. The multi-objective optimization problem is defined as follows:

$$\min Z_1 = \sum_j \sum_i \left(E_{ij}^{CS} + E_{ij}^{RE}\right) N_j) \quad (19)$$

$$\min Z_2 = \sum_j \left(TT_j + W_j^{wt}\right) N_j \quad (20)$$

$$\min Z_3 = \sum_j \left(C_j^{oc} + C_j^{op}\right) N_j \quad (21)$$

s.t.:

$$\sum_j \left(\gamma_j N_j\right) \geq N_0 \quad (22)$$

$$N_j \geq 0 \qquad \forall j \tag{23}$$

In which, the objective functions, Z_1, Z_2 and Z_3, are minimizing the emissions, time (travel and waiting time), and ownership cost (purchase price and operating cost), respectively. The term N_j represents the number of vehicles of type j (PMV, PAV, or SAV) in the system. The term γ_j is the replacement rate (number of PMVs replaced by each vehicle) of vehicle type j. This term captures the effect of the reduced number of vehicles and vehicle ownership in the system due to the adoption of PAVs/SAVs, as they can replace multiple PMVs. The term N_0 is the number of PMVs originally present in the system. Equation 22 ensures that the new fleet of vehicles (PMV, PAV, and SAV), after accounting for replacement rate, is equivalent to the former fleet of PMV. This ensures that all the trips currently available in the system are served. The constraint has been set as greater than/equal to so as to reduce the computational complexity. The objective to minimize the cost function will eventually treat the constraint as an equality constraint. Equation 23 is a feasibility constraint.

The above problem is a multi-objective optimization problem with three objectives. The problem is converted to a single-objective optimization problem by converting the total emissions and total time in the equivalent monetary values, considering cost per unit emissions and value of time. The modified total emissions (Z_1') and total time (Z_2') cost objective functions are as follows:

$$Z_1' = \sum_j \sum_i c_i \left(E_{ij}^{CS} + E_{ij}^{RE}\right) N_j \tag{24}$$

$$Z_2' = \sum_j \left(V_{phdv}^{tt} R_j^{tt} TT_j + C_w W_j^{wt}\right) N_j \tag{25}$$

In which, c_i is the societal cost of producing one unit of emission type i (CO_2, CO, and NO_X). The term V_{phdv}^{tt} and R_j^{tt} are the VOTT for PMVs and the reduction factor for VOTT (RVOTT) due to the adoption of PAVs and SAVs, respectively. The RVOTT considers the effect of increased driver productivity in AVs. A value of 0.8, means the VOTT is reduced to 80% of its original value. The value of R_j^{tt} is equal to 1 for PMVs. The term C_w denotes the average cost of waiting per unit time. The modified single objective optimization problem is defined as follows:

$$\text{Min } Z = Z_1' + Z_2' + Z_3 \qquad 26$$

s.t.:

$$\sum_j (\gamma_j N_j) \geq N_0 \qquad 27$$

$$N_j \geq 0 \qquad \forall j \qquad 28$$

This is a linear programming problem (LP), solved analytically as well as by a dual-simplex algorithm. The dual-simplex algorithm is well known for solving linear minimization problems with linear constraints and non-negative decision variables (Koberstein, 2008; Nocedal and Wright, 2006; Padberg, 1999). In every successive iteration, this algorithm improves the solution and has a method to identify when the optimal solution is reached and terminates immediately. These properties make this algorithm efficient and suitable to solve the proposed optimization problem.

3.3.7 Analytical Solution

To solve the linear programming problem analytically, first Lagrangian relaxation is used to incorporate the major constraint into the objective function. Then the Karush–Kuhn–Tucker

(KKT) conditions are applied, which are necessary but not sufficient conditions for optimality for the given optimization problem. Finally, different conditions for optimality are investigated.

3.3.7.1 Lagrangian Relaxation

As there is only one main constraint in the proposed optimization problem given by Equation 27, the optimization problem is solved analytically using Lagrangian relaxation by introducing a Lagrangian multiplier (μ). The new optimization problem in the expanded form is as follows:

$$\begin{aligned}\text{Min } L = {} & C_{phdv}N_{phdv} + C_{pav}N_{pav} + C_{sav}N_{sav} \\ & - \mu\left(N_{phdv} + \gamma_{pav}N_{pav} + \gamma_{sav}N_{sav} - N_0\right)\end{aligned} \tag{29}$$

Subject to Constraints:

$$N_{phdv}, N_{pav}, N_{sav}, \mu \geq 0 \tag{30}$$

Where, C_{phdv}, C_{pav} and C_{sav} are the parameter representing the total cost per vehicle for PMV, PAV, and SAV, respectively. These include all the costs defined in previous sections of the methodology. The above problem is solved using KKT conditions as explained in the following subsection.

3.3.7.2 KKT Conditions

The KKT conditions are applied to solve the above Linear Programming Problem. These conditions are listed below:

$$N_{phdv}\left(\frac{\partial L}{\partial N_{phdv}}\right) = 0\ ;\ \ \frac{\partial L}{\partial N_{phdv}} \geq 0; \tag{31}$$

$$N_{pav}\left(\frac{\partial L}{\partial N_{pav}}\right) = 0; \qquad \frac{\partial L}{\partial N_{pav}} \geq 0; \tag{32}$$

$$N_{sav}\left(\frac{\partial L}{\partial N_{sav}}\right) = 0; \qquad \frac{\partial L}{\partial N_{sav}} \geq 0; \tag{33}$$

$$\mu\left(\frac{\partial L}{\partial \mu}\right) = 0\ ; \qquad \frac{\partial L}{\partial \mu} \geq 0; \tag{34}$$

Condition 31 implies that

$$N_{phdv}\left(C_{phdv} - \mu\right) = 0 \rightarrow N_{phdv} = 0\ or\ \mu = C_{phdv} \tag{35}$$

$$And \qquad \frac{\partial L}{\partial N_{phdv}} = C_{phdv} - \mu \geq 0 \tag{36}$$

Condition 32 implies that

$$N_{pav}\left(C_{pav} - \gamma_{pav}\mu\right) = 0; N_{pav} = 0\ or\ \gamma_{pav}\mu = C_{pav} \tag{37}$$

$$And \qquad \frac{\partial L}{\partial N_{pav}} = C_{pav} - \gamma_{pav}\mu \geq 0 \tag{38}$$

Condition 33 implies that

$$N_{sav}(C_{sav} - \gamma_{sav}\mu) = 0; N_{sav} = 0\ or\ \gamma_{sav}\mu = C_{sav} \tag{39}$$

$$And \qquad \frac{\partial L}{\partial N_{sav}} = C_{sav} - \gamma_{sav}\mu \geq 0 \tag{40}$$

Condition 34 implies that

$$\mu = 0\ or\ \left(\ N_{phdv} + \gamma_{pav}N_{pav} + \gamma_{sav}N_{sav} - N_0\right) = 0 \tag{41}$$

$$And \qquad \frac{\partial L}{\partial \mu} = N_{phdv} + \gamma_{pav} N_{pav} + \gamma_{sav} N_{sav} - N_0 \geq 0 \qquad 42$$

Now we have four equations (35,37,39, and 41) with four unknown variables ($N_{phdv}, N_{pav}, N_{sav}\ and\ \mu$), subject to four inequality constraints (36,38,40, and 42). Hence, we can solve for the unknown variables using the above set of equations which is explained in detail in the following subsection.

3.3.7.3 A solution to the optimization problem

From Equation 41, if $\mu = 0$, as $C_{phdv}, C_{pav}, C_{sav} \neq 0$ in our case, from Equations 35,37, and 39, $N_{phdv}, N_{pav}, N_{sav} = 0$. Then, from Equation 42, $N_0 \leq 0$, which is only possible in a system with no vehicles. Therefore,

$$N_{phdv} + \gamma_{pav} N_{pav} + \gamma_{sav} N_{sav} - N_0 = 0 \qquad \& \quad \mu > 0 \qquad 43$$

From, Equations 35,37,39, and 41, there are seven possible cases as listed below:

$$\mu = C_{phdv} = \frac{C_{pav}}{\gamma_{pav}} = \frac{C_{sav}}{\gamma_{sav}}; \qquad N_{phdv} + \gamma_{pav} N_{pav} + \gamma_{sav} N_{sav} = N_0 \qquad 44$$

$$\mu = C_{phdv} \neq \frac{C_{pav}}{\gamma_{pav}} \neq \frac{C_{sav}}{\gamma_{sav}}; \qquad N_{pav} = N_{sav} = 0\ ; \quad N_{phdv} = N_0 \qquad 45$$

$$\mu = C_{phdv} = \frac{C_{pav}}{\gamma_{pav}} \neq \frac{C_{sav}}{\gamma_{sav}}; \qquad N_{sav} = 0; \quad N_{phdv} + \gamma_{pav} N_{pav} = N_0 \qquad 46$$

$$\mu = C_{phdv} = \frac{C_{sav}}{\gamma_{sav}} \neq \frac{C_{pav}}{\gamma_{pav}}; \qquad N_{pav} = 0; \quad N_{phdv} + \gamma_{sav} N_{sav} = N_0 \qquad 47$$

$$\mu = \frac{C_{pav}}{\gamma_{pav}} \neq \frac{C_{sav}}{\gamma_{sav}} \neq C_{phdv}; \qquad N_{phdv} = N_{sav} = 0\ ; \quad N_{pav} = \frac{N_0}{\gamma_{pav}} \qquad 48$$

$$\mu = \frac{C_{pav}}{\gamma_{pav}} = \frac{C_{sav}}{\gamma_{sav}} \neq C_{phdv}; \qquad N_{phdv} = 0; \;\; N_{pav} + \gamma_{sav} N_{sav} = N_0 \tag{49}$$

$$\mu = \frac{C_{sav}}{\gamma_{sav}} \neq \frac{C_{pav}}{\gamma_{pav}} \neq C_{phdv}; \qquad N_{phdv} = N_{pav} = 0 \; ; \;\; N_{sav} = \frac{N_0}{\gamma_{sav}} \tag{50}$$

The solution to the optimization problem can be any one of the above cases, depending upon the value of different parameters assumed in the study. However, to check the uniqueness of the solution we must check other conditions as explained in the following subsection.

3.3.7.4 The uniqueness of the optimal solution

For the solution to be unique, both of the following conditions should be met: -

- The objective function should be strictly convex near the optimal solution and it should be an overall convex function.
- The set of unknown variables should be a convex feasible set.

For checking the condition first, we estimate the Hessian Matrix (H) for the objective function (Equation 26), which is given below:

$$H = \begin{bmatrix} \frac{\partial^2 Z}{\partial N_{phdv}^2} & \frac{\partial^2 Z}{\partial N_{phdv} \partial N_{pav}} & \frac{\partial^2 Z}{\partial N_{phdv} \partial N_{sav}} \\ \frac{\partial^2 Z}{\partial N_{pav} \partial N_{phdv}} & \frac{\partial^2 Z}{\partial N_{pav}^2} & \frac{\partial^2 Z}{\partial N_{pav} \partial N_{sav}} \\ \frac{\partial^2 Z}{\partial N_{sav} \partial N_{phdv}} & \frac{\partial^2 Z}{\partial N_{sav} \partial N_{pav}} & \frac{\partial^2 Z}{\partial N_{sav}^2} \end{bmatrix} = \begin{bmatrix} 0 & 0 & 0 \\ 0 & 0 & 0 \\ 0 & 0 & 0 \end{bmatrix} \tag{51}$$

In order to satisfy the condition first, all of the Eigenvalues for the Hessian Matrix should be greater than zero. Therefore, we estimate Eigenvalues for the Hessian Matrix which is given by the following equation.

$$|H - \lambda I| = 0 \rightarrow \lambda^3 = 0 \rightarrow \lambda = 0 \quad (52)$$

All the three Eigenvalues for the Hessian Matrix equal to zero. Hence, it is a convex function but not strictly convex. Further, the constraints of the objective function (Equations 27 and 28) represent the area above the plane (given by Equation 53) in the positive quadrant, which is always a convex feasible set.

$$N_{phdv} + \gamma_{pav} N_{pav} + \gamma_{sav} N_{sav} = N_0 \quad (53)$$

As the objective function is not strictly convex. Hence, the uniqueness of the optimal solution can not be proved for this optimization problem.

It is important to note that the current multi-objective problem is a linear programming (LP) problem that has a convex pareto front. As the pareto front is convex, for every pareto optimal solution there exist positive values of weights such that the pareto optimal solution is the optimal solution for the corresponding single-objective optimization (Deb, 2001). Hence, every point on the pareto optimal front can be obtained by selecting the appropriate weights for the single-objective optimization problem. The dual-simplex algorithm is a quick way to solve the LP problem providing the exact optimal solution on the pareto front for the selected weights. Further, this study also does sensitivity analysis with respect to these weights (VOTT and unit cost of emissions) to obtain the optimal solution. The value of these weights and the corresponding optimal solution can be decided based on the discussion with policymakers for the specific applications of the model. The weighted sum method is being used in this study considering the fact that the problem is an LP problem (convex pareto front).

3.4 Case study

This study assumes a hypothetical transportation system with signalized arterial roads in a small or mid-sized urban area of the United States. The trips within this transportation system can be served with PMVs, PAVs, or SAVs. As SAVs are not suitable to serve long-distance trips, only internal trips within the system boundaries are considered. The duration of the study T is assumed to be 1 year. The number of PMVs originally present in the system (N_0) is estimated as follows:

$$N_0 = T_{pt} \times \frac{365}{T_p} \quad 54$$

In which, T_{pt} is the total number of trips per day in the system. The value of T_p (number of trips per PMV per year) is given as follows:

$$T_p = N_{tdl} \times \frac{365}{N_{vpl}} \quad 55$$

Here, N_{tdl} and N_{vpl} are the number of trips per day per licensed driver and the number of vehicles per licensed driver. These values are assumed to be 3.02 and 0.99, respectively (Santos et al., 2011).

3.4.1 VMT Variation Parameters

The average urban VMT for each light-duty PMV (m_{pmv}^{pv}) is assumed to be 6334 miles/year (FHWA, 2017). The calibrated functions representing variation in VMT, derived and/or calibrated using different studies, are listed in Table 3.1.

The value of the parameter $\beta_{pav/sav}^{nd}$, which represents the increase in the trip generation due to the improved mobility of non-drivers, with the adoption of PAVs and SAVs, is assumed to be equal to the total mile increase factor ($\alpha_{pav/sav}^{nd}$). This factor ($\beta_{pav/sav}^{nd}$) is estimated considering

the average trip length remains the same. The changes in average trip length due to the adoption of PAVs/SAVs is captured by parameter $\alpha_{pav/sav}^{rc}$. The value of the parameter $\beta_{pav/sav}^{rc}$, which represents the increase in the number of trips as a result of the improved roadway capacity, reduction in VOTT, and reduction in parking cost, is assumed to be 1.049 (Childress et al., 2015). These parameters can be used to estimate the value of η_j, using Equation 9.

3.4.2 Emission Estimation Parameters

The unit societal cost of CO_2, CO, and NO_x (Table 3.2) emissions are used along with emission production functions to calculate the total emission cost.

3.4.2.1 Running Emissions

This study adopts an instantaneous emission model (Int Panis et al., 2006) to estimate the running emissions (CO_2 and NO_X). The trajectories for efficient-driving (PAVs/SAVs) and nonefficient-driving (PMVs) profile at a signalized arterial corridor are obtained using the study, He et al. (2015). The speed and acceleration profiles are obtained for these trajectories which are incorporated in the calibrated emission model to estimate instantaneous running emissions. Further, the running emission per mile (e_{ij}^{re}) is estimated using Equation 5.

3.4.2.2 Cold-start Emissions

The function for the number of cold-starts per person-trip when only SAVs are in the system (Table 3.1), is calibrated based on the data available from the sensitivity analysis of the number of cold-starts with respect to the replacement rate and the trips generated (Fagnant and Kockelman, 2014).

3.4.3 Ownership and Operating Costs Parameters

The average purchase price of PMVs is assumed to be $30,000 (NADA, 2012). The costs of PAVs and SAVs are assumed to be $10,000 higher than that of PMVs. It is based on the assumption that AV technology will add up to $7000-$10,000 to the existing purchase price of PMVs by the end of 2025 (IHS, 2014). The average annual miles traveled per SAV (m_{sav}^{py}) is assumed to be equal to that traveled within the urban area (m_{sav}^{pv}). It is based on the assumption that SAVs behave similar to a taxi system and do not travel outside the given urban boundaries. The average annual miles traveled per PAV (m_{pav}^{py}) is estimated, assuming that if the trip is outside the given urban system, the PAV will not return empty to the system, (due to the long travel distance) (Table 3.1). The total lifetime mileage of PMV (M_{pmv}^{T}) is as follows:

$$M_{pmv}^{T} = m_{pmv}^{py} \times S_{pmv} \quad 56$$

The total lifetime mileage of PAV(M_{pav}^{T}) is assumed to be equal to that of PMVs. However, the total lifetime mileage for SAVs (M_{sav}^{T}) is assumed to be comparable to that of a regular taxi, which is equal to 250,000 miles (Fagnant and Kockelman, 2018).

The reduction factor for fuel consumption as the result of efficient driving patterns of PAVs/SAVs ($R_{pav/sav}^{f}$), is assumed to be 0.75. This value is based on the conclusion that eco-driving is expected to reduce fuel consumption by 25% (Center for Sustainable Systems, 2017; Wadud et al., 2016).

3.4.4 Travel Time Cost Parameters

The average speed is obtained from the speed profile of efficient driving (for PAVs/SAVs) and nonefficient driving behavior (for PMVs) (He et al., 2015). The VOTT is assumed to be

$18.82/hr (van den Berg and Verhoef, 2016). The reduction factor for VOTT (RVOTT) is assumed to be 0.8, which means the users can use their travel time 20 percent more efficiently when riding in an autonomous vehicle (van den Berg and Verhoef, 2016).

3.4.5 Waiting Time Cost Parameters

The function of the average waiting time (W_{sav}^{pt}) per trip (in minutes) as given in Table 3.1 Functions and their Definitions, is calibrated based on the data available from the sensitivity analysis of waiting time per trip with respect to the replacement rate and trip generation (Fagnant and Kockelman, 2014), and is set to maintain a positive value.

The waiting time cost per unit time (C_w) is assumed to be 70% of the wage rate (Fagnant and Kockelman, 2018). The average wage rate (W_r) in the US is estimated as $22.59/hr (Tradingeconomics.com, 2018) in May 2018.

A summary of the different functions for vehicle type j and different parameters assumed in the study are listed in Table 3.1 and Table 3.2, respectively. The functions listed below are estimated/calibrated using the data from the studies listed in the last column. It is important to note that as the AVs are not operational on the road, the calibration of the different factors is based on the simulation data conducted by the different studies. These calibrated functions might be different in practical applications depending upon the urban area or network chosen and also when AVs are actually on the road. However, we believe that the nature of dependency of these dependent factors to that of independent factors would remain the same. Considering the limited data, the current study aims to capture this dependency of the dependent factors rather than proposing the exact function to consider the effect of the adoption of PAVs and SAVs.

3.4.6 Scenarios considered for Optimization

The study estimates the optimal solution under two scenarios as explained below:-

- The optimum vehicle fleet that will result in a minimum total system cost. The weight factors for this model are:

$$\psi_l = 1 \qquad \forall\, l \tag{57}$$

- The optimum vehicle fleet that will result in minimum emission cost. The weight factors for this model are:

$$\psi_{RE} = \psi_{CS} = 1 \tag{58}$$

$$\& \qquad \psi_{oc} = \psi_{op} = \psi_{tt} = \psi_{wt} = 0 \tag{59}$$

Table 3.1 Functions and their Definitions

Parameter	Definition	Function	Source/ Justification
γ_j	Replacement rate	$\begin{cases} 1 & \mathrm{j} = \mathrm{PMV} \\ 1.105 & \mathrm{j} = \mathrm{PAV} \\ 12 & \mathrm{j} = \mathrm{SAV} \end{cases}$	(Zhang et al., 2018) (Fagnant and Kockelman, 2014)
α_j^{nd}	Factored VMT increase due to improved mobility of non-drivers	$\begin{cases} 1 & \mathrm{j} = \mathrm{PMV} \\ 1.14 & \mathrm{j} \in \{\mathrm{PAV}, \mathrm{SAV}\} \end{cases}$	(Harper et al., 2016)
α_j^{rc}	Factored VMT increase due to the	$\begin{cases} 1 & \mathrm{j} = \mathrm{PMV} \\ 1.2 & \mathrm{j} \in \{\mathrm{PAV}, \mathrm{SAV}\} \end{cases}$	(Childress et al., 2015)

Table 3.1 (cont'd)

	reduction in VOTT, parking cost, and efficient use of the roadway			
α_j^{rnv}	Factored VMT increase per vehicle due to the reduction in the number of vehicles	$\begin{cases} 1 & \text{j} = \text{PMV} \\ \gamma_{pav} & \text{j} = \text{PAV} \\ \gamma_{sav} & \text{j} = \text{SAV} \end{cases}$		Reducing the number of vehicles results in an equivalent increase in VMT per vehicle
α_j^{emp}	Factored VMT increase due to the empty repositioning of autonomous vehicles	$\begin{cases} 1 & \text{j} = \text{PMV} \\ \max\left[\left(1.34\, log_e\, \gamma_{pav} + 1.001\right), 1\right] & \text{j} = \text{PAV} \\ \max[(0.98 \exp(0.008\gamma_{sav}) - 0.04 \log_e \eta_{sav} + 0.02\ ), 1] & \text{j} = \text{SAV} \end{cases}$		Calibrated based on (Zhang et al., 2018) Calibrated based on (Burns et al., 2013)
β_j^{nd}	Factored increase in the trip generation due to the improved mobility of non-drivers	$\begin{cases} 1 & \text{j} = \text{PMV} \\ \alpha_j^{nd} & \text{j} \in \{\text{PAV}, \text{SAV}\} \end{cases}$		Assuming average trip length remains the same
β_j^{rc}	Factored increase in trip generation due to the reduction in VOTT and parking	$\begin{cases} 1 & \text{j} = \text{PMV} \\ 1.049 & \text{j} \in \{\text{PAV}, \text{SAV}\} \end{cases}$		(Childress et al., 2015)

Table 3.1 (cont'd)

	cost and efficient use of the roadway		
N_j^{cs}	Number of cold-starts per person trip when only vehicle type j is present in the system	$\begin{cases} 0.64 & \text{j} \in \{\text{PMV}, \text{PAV}\} \\ \max[(0.645\gamma_{sav}^{-1.022} - 0.011\eta_{sav}^3 + 0.047\eta_{sav}^2 - 0.062\eta_{sav} + 0.027), 0] & \text{j} = \text{SAV} \end{cases}$	(Fagnant and Kockelman, 2014; Kang and Recker, 2009) Calibrates based on (Fagnant and Kockelman, 2014) Assuming PAV trips outside the system does not generate empty ride and SAVs travels only within urban boundaries Assuming SAVs behave similarly to a taxi system (Fagnant and Kockelman, 2018) Calibrated based on (Fagnant and
m_j^{py}	Average annual miles traveled per vehicle j	$\begin{cases} m_{pmv}^{py} & \text{j} = \text{PMV} \\ \left[\left(m_{pmv}^{py} - m_{pmv}^{pv}\right) + m_{pmv}^{pv}\alpha_j^{emp}\right]\alpha_{pav}^{rc}\alpha_{pav}^{nd}\alpha_{pav}^{rnv} & \text{j} = \text{PAV} \\ m_{sav}^{pv} & \text{j} = \text{SAV} \end{cases}$	
M_j^T	Total miles traveled during the lifespan of the vehicle j	$\begin{cases} m_{pmv}^{py} S_{pmv} & \text{j} = \text{PMV} \\ M_{pmv}^T & \text{j} = \text{PAV} \\ 250{,}000\ miles & \text{j} = \text{SAV} \end{cases}$	
W_{sav}^{pt}	The average waiting time (minutes) per	$\max[(0.0003\exp(0.575\gamma_{sav}) - 0.551\eta_{sav}^3 + 2.177\eta_{sav}^2 - 2.832\eta_{sav} + 1.206), 0]$	

Table 3.1 (cont'd)

	trip, exclusively for SAVs	Kockelman, 2014).

Table 3.2 Definition and Value of Different Parameters

Parameter	Definition	Values assumed in the deterministic model
T_{pt}	Number of daily trips in the system (Burns et al., 2013)	528,000 trips/day
T	Study period	1 year
N_{tdl}	Number of daily trips per licensed driver (Santos et al., 2011)	3.02 trips/licensed driver
N_{vpl}	Number of vehicles per licensed driver (Santos et al., 2011)	0.99 veh./licensed driver
m_{pmv}^{pv}	Average VMT per PMV in the given urban system during T (FHWA, 2017)	6334 miles/year
c_{co_2}	The societal cost of producing one unit of CO_2 (US DOT, 2015)	\$49/metric ton
c_{co}	The societal cost of producing one unit of CO (assumed 2. 813 times than that of CO_2(Shindell, 2015))	\$137.84/metric ton
c_{NO_x}	The societal cost of producing one unit of NO_X (US DOT, 2015)	\$7877/metric ton
$e_{co_2,pmv}^{re}$	Running emission (CO_2) per mile for each PMV (obtained using the instantaneous emission model by (Int Panis et al., 2006) for nonefficient-driving profile (He et al., 2015))	337.81 gm/mile/vehicle
$e_{co_2,pav/sav}^{re}$	Running emission (CO_2) per mile for each PAV/SAV (obtained using instantaneous emission model by (Int Panis et al., 2006) for efficient-driving profile (He et al., 2015))	260.40 gm/mile/vehicle
$e_{no_x,pmv}^{re}$	Running emission (NO_x) per mile for each PMV (obtained using the instantaneous emission model by (Int Panis et al., 2006) for nonefficient-driving profile (He et al., 2015))	0.148 gm/mile/vehicle

Table 3.2 (cont'd)

$e^{re}_{no_x,pav/sav}$	Running emission (NO_x) per mile for each PAV/SAV (obtained using instantaneous emission model by (Int Panis et al., 2006) for efficient-driving profile (He et al., 2015))	0.118 gm/mile/vehicle
e^{cs}_{co}	Cold-start emission (CO) per mile for each PMV (Chester and Horvath, 2008)	7.3 gm/mile/vehicle
$e^{cs}_{no_x}$	Cold-start emission (NO_X) per mile for each PMV (Chester and Horvath, 2008)	0.17 gm/mile/vehicle
C^{o}_{pmv}	Average purchase price of PMV (NADA, 2012)	$30,000
$C^{o}_{pav/sav}$	Purchase Price of PAV/SAV ($10K higher than that of PMV (IHS, 2014))	C^{o}_{phdv}+$10,000
S_{pmv}	The average service life of PMV (IHS Markit, 2016)	11.6 years
m^{py}_{pmv}	Total miles that one PMV travels in a year (FHWA, 2017)	11,370 miles/yr.
C_f	Fuel cost (AAA, 2017)	$2.329/gallon
m_{pg}	Fuel efficiency (FHWA, 2017)	24 miles/gallon
$R^{f}_{pav/sav}$	Reduction factor for fuel consumption due to efficient driving of PAV/SAV (Center for Sustainable Systems, 2017; Wadud et al., 2016)	0.75
C_m	Maintenance cost (AAA, 2017)	$.0794/mile
v_{pmv}	The average speed of PMV (estimated from nonefficient-driving profile (He et al., 2015))	31.68 mph
$v_{pav/sav}$	The average speed of PAV/SAV (estimated from efficient-driving profile (He et al., 2015))	27.91 mph
V^{tt}_{pmv}	Value of Travel Time (VOTT) for PMV (van den Berg and Verhoef, 2016)	$18.82/hr.
$R^{tt}_{pav/sav}$	Reduction Factor for VOTT (RVOTT) due to efficient use of travel time in PAV/SAV (van den Berg and Verhoef, 2016)	0.8

Table 3.2 (cont'd)

C_w	Cost of waiting time (assumed to be 70% of the wage rate (Fagnant and Kockelman, 2018). The average wage rate (W_r) of the US is $22.59/hr (Tradingeconomics.com, 2018) in May 2018.)	$15.813/hr.

3.5 Numerical Experiments

The proposed optimization problem is a linear programming problem with linear constraints. The model aims to minimize the total system cost by finding the best fleet configuration under different circumstances. The system cost consists of the user, investor, and societal costs (environmental cost).

3.5.1 Base Scenario

The solution to the optimization problem for the base scenario (considering values of parameters reported in Table 3.1 and Table 3.2), calculated using analytical methods as well as dual simplex algorithm, is presented in the following subsections.

3.5.1.1 Analytical solution for the base case

The assumed value of different parameters (Table 3.1 and Table 3.2) for the case study are used to obtain different costs type per vehicle (C_j^l) in the optimization problem (given by Equation 26-28). The total cost per vehicle (C_j) for vehicle type j, assuming a uniform weight ($\psi_l = 1 \ \forall l$), is obtained using Equation 60. The corresponding values obtained are given in Equation 61 and 62.

$$C_j = \sum_l \psi_l C_j^l \qquad \forall j \tag{60}$$

$$C_{phdv} = 7{,}593.67;\ C_{pav} = 12{,}589.08;\ C_{sav} = 94{,}552.69; \tag{61}$$

$$\gamma_{pav} = 1.105;\ \gamma_{sav} = 12;\ N_0 = 173{,}086 \tag{62}$$

Comparing these values, with all the possible solutions (Equations 44 to 50). We have

$$C_{phdv} = 7{,}593.67; \quad \frac{C_{pav}}{\gamma_{pav}} = 11{,}392.83; \quad \frac{C_{sav}}{\gamma_{sav}} = 7{,}879.391 \tag{63}$$

Which implies:

$$C_{phdv} \neq \frac{C_{pav}}{\gamma_{pav}} \neq \frac{C_{sav}}{\gamma_{sav}} \tag{64}$$

Therefore, the only three possible cases would be:

1. $$\mu = \frac{C_{pav}}{\gamma_{pav}} \neq \frac{C_{sav}}{\gamma_{sav}} \neq C_{phdv}; \quad N_{phdv} = N_{sav} = 0\ ; \quad N_{pav} = \frac{N_0}{\gamma_{pav}}; \tag{65}$$

2. $$\mu = \frac{C_{sav}}{\gamma_{sav}} \neq C_{phdv} \neq \frac{C_{pav}}{\gamma_{pav}}; \quad N_{phdv} = N_{pav} = 0\ ; \quad N_{sav} = \frac{N_0}{\gamma_{sav}}; \tag{66}$$

3. $$\mu = C_{phdv} \neq \frac{C_{pav}}{\gamma_{pav}} \neq \frac{C_{sav}}{\gamma_{sav}}; \quad N_{pav} = N_{sav} = 0\ ; \quad N_{phdv} = N_0; \tag{67}$$

For case 1, we have,

$$\mu = \frac{C_{pav}}{\gamma_{pav}} = 11{,}392.83 \tag{68}$$

Now from Equation 36, we have,

$$C_{phdv} - \mu \geq 0 \tag{69}$$

In the base case presented in this study, $C_{phdv} - \mu = 7{,}593.67 - 11{,}392.83 = -3799.16 < 0$.

Thus, it does not satisfy Equation 36. Hence, this case is rejected.

For case 2, we have,

$$\mu = \frac{C_{sav}}{\gamma_{sav}} = 7{,}879.391 \qquad 70$$

Again comparing it with Equation 36 of section 3.3.7.2, we have $C_{phdv} - \mu = 7{,}593.67 - 7{,}879.391 = -285.72 < 0$. Thus, it also does not satisfy Equation 36 in section 3.3.7.2. Hence, this case is also rejected.

Therefore, the only case would be 3:

$$N_{phdv} = N_0 \; and \;\; N_{pav} = N_{sav} = 0 \qquad 71$$

This solution satisfies all of the inequalities mentioned in section 3.3.7.2 (Equations 36,38,40, and 42). Hence, this is our solution to the optimization problem while minimizing the system cost. Therefore, using the base parameter values, the system cost would be minimum if only PMVs are present in the system.

3.5.1.2 Solution for the base case using a dual-simplex algorithm

The solution to the proposed model is obtained in MATLAB using the 'dual-simplex' algorithm. The algorithm applies the simplex algorithm to obtain the solution to the dual problem. The algorithm involves two phases. In the first phase, the algorithm estimates the initial basic feasible solution. In the second phase, the algorithm performs iterations to reduce the infeasibility of the primal problem while maintaining the feasibility of the dual problem. The algorithm tests the optimality of the solution in every iteration and stops once the optimality is reached or both primal and dual problem becomes feasible. The results obtained using a dual-simplex algorithm are found to be consistent with that of the analytical solution. In the base scenario, using the parameter values listed in Table 3.1 and Table 3.2, the optimal solution suggests PMVs as the best

type of vehicle. The travel time and ownership cost are the major costs, contributing 50% and 34% to the total system cost in the PMV system, respectively (Figure 3.1). The fuel consumption, maintenance, and emissions contribute to 8%, 7%, and 2% of the total system cost, respectively. The increased VMT due to the adoption of PAVs and SAVs results in higher total travel time in the system, higher fuel and maintenance costs for users while increasing the societal cost of emissions. Thus, these vehicles under the current situation, in the base scenario, do not appear in the optimum fleet configuration. The number of cold-starts and associated emissions (CO and NO_x) in the SAV system is less than that of the PMV system. However, the running emissions (CO_2 and NO_x), due to increased VMT, are significantly higher in the SAV system. The cost of ownership of the vehicular fleet for the SAV system as a whole is smaller than the PMV system due to the higher total lifetime mileage of SAVs. But it is not small enough to cover for the costs increased due to an increase in VMT in the system.

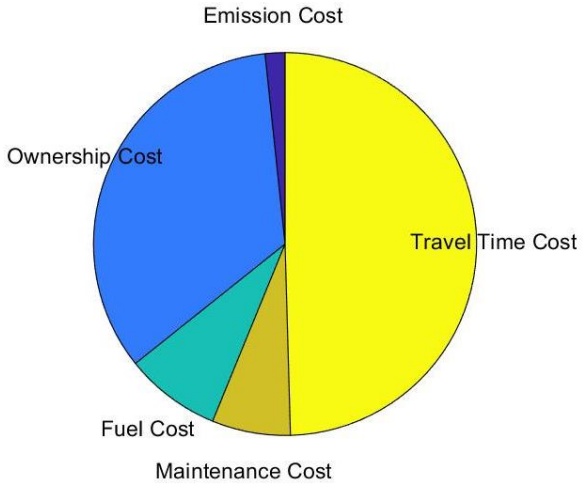

Figure 3.1 The different components of the objective function at the optimal solution for the base scenario

3.5.2 System Analysis with Private and Shared Mobility

In different regions and over time, the parameters such as VMT variations, VOTT, RVOTT, etc. may change. Various studies predict the above-mentioned factors and their influence on AV adoption. However, as the AVs are not operational on the road, the exact values of these factors are still a question. Hence, this study does sensitivity analysis with respect to the main factors and proposes suitable values of these factors that will promote the adoption of PAVs/SAVs. It should be noted that the sensitivity analysis is done based on discrete values of parameters rather than a continuous variation to reduce the computational time.

3.5.2.1 Sensitivity to user and system-related parameters

The VOTT and RVOTT represent user characteristics and are among the most important factors affecting the optimal solution. The configuration of the system, which in part is presented by the user to vehicle ratio, affects the optimal solution. A larger reduction in VOTT (lower RVOTT), or more efficient use of travel time makes SAVs the most promising option (Figure 3.2). However, if the replacement rate of SAVs is very high (e.g. ≥ 16 PMVs per SAV, at RVOTT=0.7), then there is an exponential increase in the empty miles generation and users' waiting time. Hence, at higher replacement rates, SAVs are not the optimal solution. Further, at such a high replacement rate, with efficient use of travel time ($\text{RVOTT} \leq 0.4$), the travel time cost for PAVs becomes very low, resulting in PAVs entering the optimal solution (Figure 3.2). However, the VOTT of users adopting PAVs should be high (at least \$18/hr). It is important to note that the increase in the empty miles results in each SAV traveling a larger amount of miles in a year. Hence, it reduces the lifetime of the vehicle. As a result, the ownership cost per year increases for SAVs with an increase in the empty miles traveled.

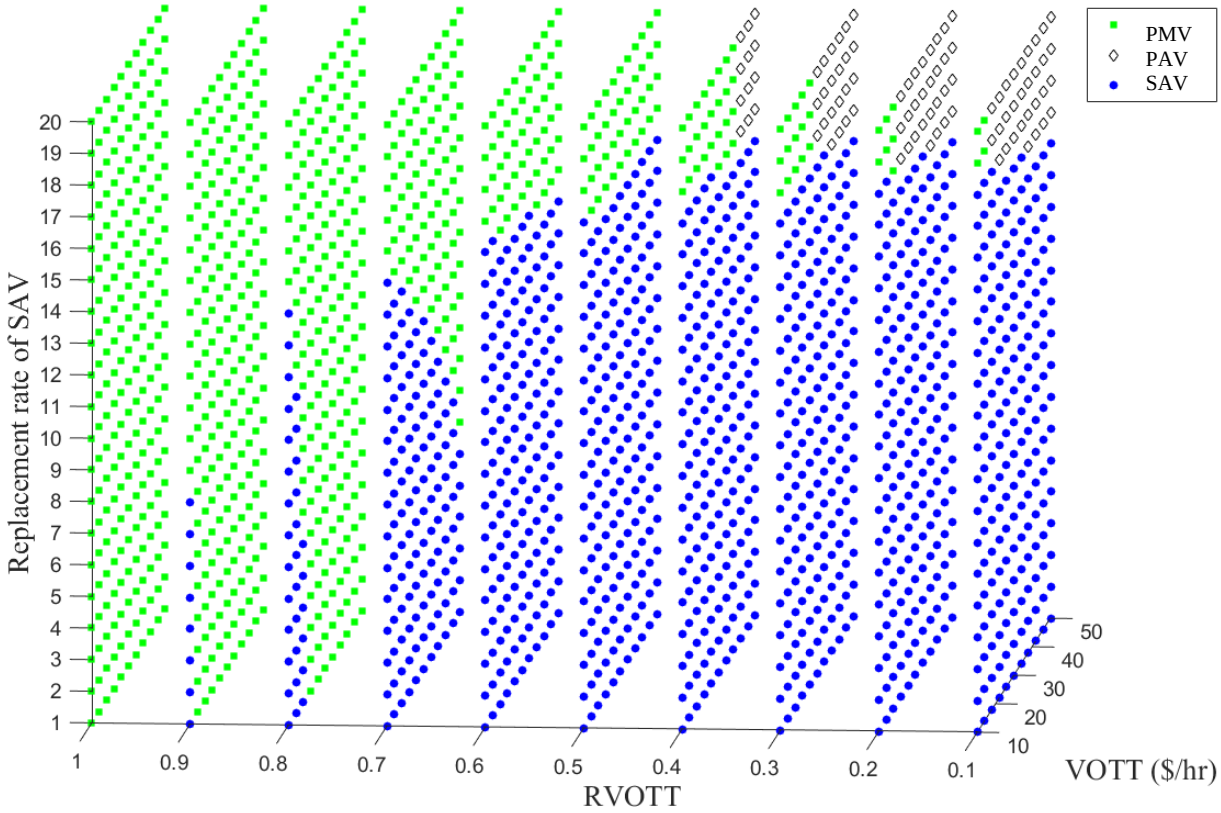

Figure 3.2 Optimal vehicle type (PMV, PAV, and SAV) considering variations in VOTT, Reduction Factor for VOTT (RVOTT), and replacement rate of SAV.

It is important to note that the RVOTT, as an incentive in the adoption of autonomous vehicles, is only effective if there is a significant reduction (RVOTT$\leq$ 0.6). If RVOTT is higher, then the increased VOTT of users switches the optimal solution to PMVs. The reason is that the increased mobility of the users with the adoption of PAV/SAV, increases the total travel time and the total system cost, hence a significant reduction in VOTT is required to make these vehicles competitive in the market (for system planners). With a significant improvement in the efficient use of travel time, this study confirms the findings of the recent studies (Fagnant et al., 2016; Fagnant and Kockelman, 2014). Even with less efficient use of travel time (higher RVOTT), SAVs can appear in the optimal solution, if there is a larger fleet of SAVs (lower replacement rate) supporting the trips of the users. It can be concluded that efficient use of travel time is a significant

factor in the adoption of PAVs/SAVs. This can be a function of the different features of autonomous vehicles that provide a working or recreational environment inside the vehicle. It is worth noting that even though reducing the fleet size of SAVs reduces the upfront cost of the system, it increases the emission, waiting time, operating and maintenance cost, thus the appropriate fleet size is reported in this study.

3.5.2.2 Sensitivity to vehicle specifications

This study estimates the optimal solution by assuming the average current purchase price for PMVs and the cost of AV technology to estimate the purchase price of PAVs/SAVs. However, the price of PMVs and PAVs/SAVs can vary significantly depending on various factors. This study finds the optimal solution under the different purchase prices of vehicles (Figure 3.3). The analysis shows that among other factors the optimum fleet configuration is a function of the relative cost of PMVs and PAVs/SAVs. The adoption of SAVs can be the optimal solution if the purchase price of SAVs is below a certain relative threshold than that of PMVs. For example, if the purchase price of PMVs is $60,000, then the purchase price of SAVs should be less than or equal to $100,000 for SAVs to be the optimal solution. The PMV-PAV/SAV cost function of the optimum market can be used for planning purposes (Figure 3.3).

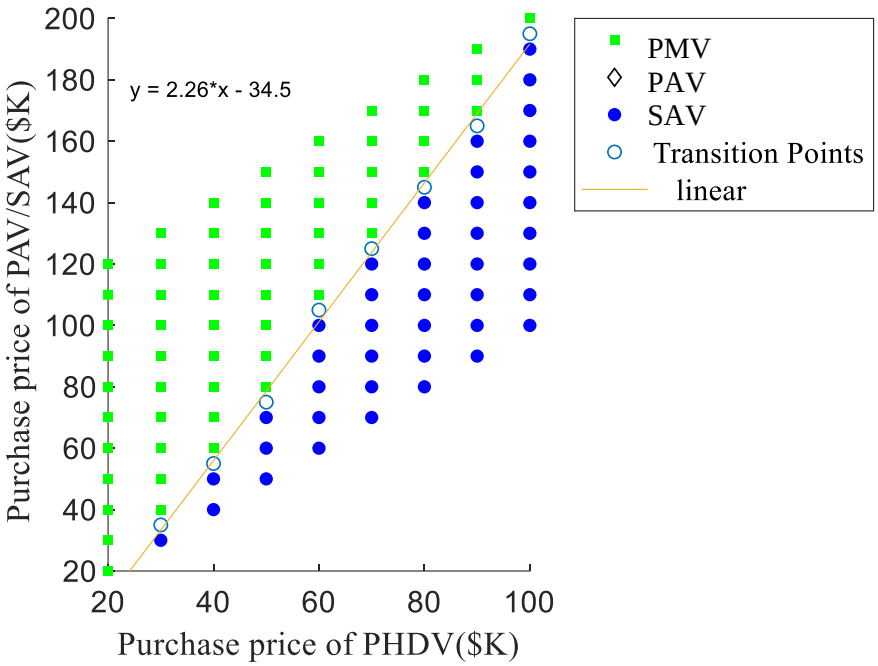

Figure 3.3 Sensitivity to purchase price

3.5.3 System Analysis without Shared-Mobility

The shared-mobility systems are shown to be the optimum answer in many scenarios tested in the previous section, while the adoption of PAVs appeared as the least favorable option. In this section, the study analyses different scenarios in which shared mobility is not an option.

First, the model is analyzed with respect to the purchase price and the total lifetime mileage of PAVs. The total lifetime mileage of PMVs on average is equal to 131,892 miles, which is obtained from Equation 56. The adoption of PAVs will be the optimal solution, if the total lifetime mileage of PAV is increased (at least to 240,000 miles) (Figure 3.4). For PAVs to be a part of the optimum market, these vehicles should be able to travel long distances during their lifespan. This can be achieved by following an efficient driving pattern and scheduled maintenance. The computer-controlled vehicles can be programmed to follow the maintenance schedule on their

own, without any inconvenience to their owners. Further, in addition to the higher total lifetime mileage of PAVs, the purchase price of PMVs should also be sufficiently high (preferably ≥ $40,000) for PAVs to appear in the market. The higher purchase price of PMVs reduces the fraction of additional cost required to install AV technology, for a given cost of AV technology. Thus, it increases the range of acceptable purchase price of PAVs, for PAVs to be the optimal solution. In other words, the PAVs would be the optimal solution, if the AV technology is installed in luxurious cars.

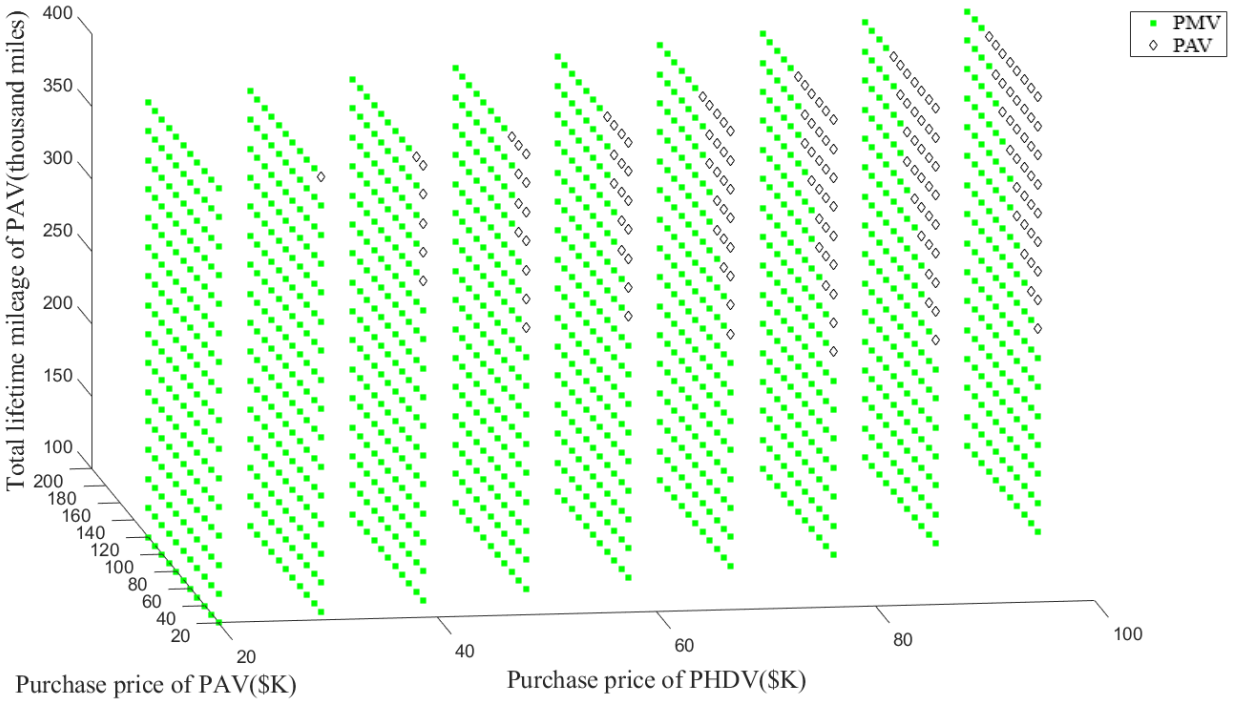

Figure 3.4 Sensitivity analysis considering the purchase price of PMV and PAV, and total lifetime mileage of PAV

The analysis results with respect to VOTT, RVOTT, and total lifetime mileage of PAVs are presented in Figure 3.5. The PAV adoption would be the optimal solution if RVOTT is below a certain threshold, which increases with an increase in the total lifetime mileage of PAV or VOTT (Figure 3.5). For example, if the total lifetime mileage of PAVs is 200,000 miles and the VOTT of users is $26/hr, the RVOTT should be less than or equal to 0.5, for PAVs to be the optimal

solution. Reducing VOTT by improving amenities on-board, advancing the total lifetime mileage of PAVs, and the adoption of PAVs by users with high VOTT, are the ways to make these vehicles an optimum option in the fleet.

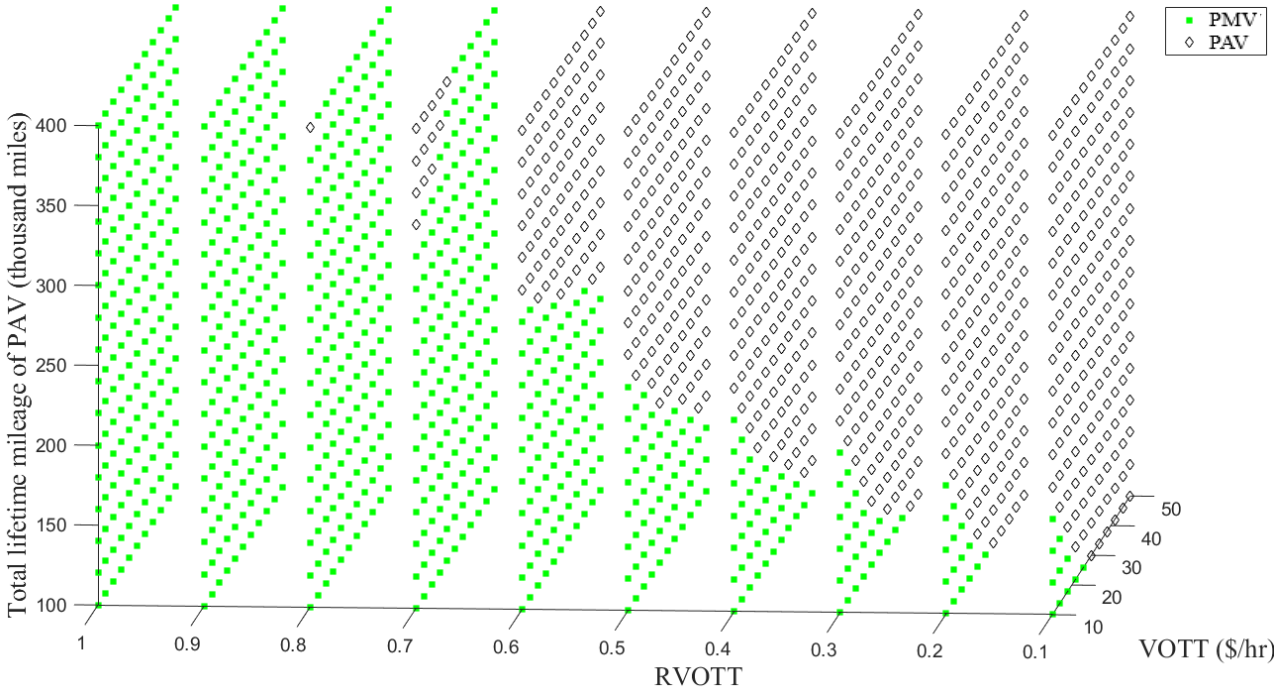

Figure 3.5 Optimal vehicle type (PMV and PAV), in absence of shared mobility, considering variations in VOTT, Reduction Factor for VOTT (RVOTT) and Total lifetime mileage of PAV

3.5.4 Emission Production in Different Scenarios

The emission produced in the system may vary due to the changes in parameters such as VMT, driving behavior, replacement rate, number of cold-starts, emission per cold-start, number of trips. These parameters may vary across different regions. Also, the societal cost of producing one unit of emission, for different emissions (CO_2, CO, and NO_x) may vary with time, depending upon their effect on the environment. The sensitivity analysis of the emission production and the associated cost, with respect to these parameters, is presented in the following sub-sections.

3.5.4.1 Emission Production while optimizing total system cost

The replacement rate and societal cost per unit of different emissions are the two most important factors affecting the optimal solution and the amount of emission produced. The lower replacement rate or CO_2 Cost, or higher CO Cost, make SAVs the optimal solution (Figure 3.6). The running emissions (CO_2) are higher (Figure 3.6 a and c), but the cold-start emissions (CO) are lower (Figure 3.6 b and d), in the SAV system than that in the PMV system. The reason is that each SAV keeps on empty repositioning itself to serve the trips with the engine being turned off less frequently, which increases the VMT but decreases the number of cold-starts. Further, the higher replacement rate reduces the number of cold-starts and associated cold-start emissions in an SAV system (Figure 3.6b). The higher replacement rate also causes an exponential increase in empty miles generated resulting in an increase in VMT and associated costs such as running emissions (Figure 3.6a), Thus, SAVs are not the optimal solution at a higher replacement rate. However, if the societal cost of CO is significantly high, then SAVs can be the optimal solution even at a higher replacement rate. For example, the SAVs are the optimal solution if the societal cost of CO is at least \$7000/tonne, at a replacement rate of 12 PMVs per SAV (Figure 3.6 a and b). At a low replacement rate ($\gamma_{sav} = 4$), the empty miles generated, and the average waiting time is negligible. Thus, SAVs would always be the optimal solution, under different CO Costs (Figure 3.6 a and b). Considering the cost of CO_2, the optimal solution is invariably the adoption of PMVs at higher replacement rates ($\gamma_{sav} = 8\ or\ 12$) (Figure 3.6 c and d). It is due to the higher system cost in the SAV system, which further increases with an increase in CO_2 cost. However, at significantly low replacement rates ($\gamma_{sav} = 4$), the negligible empty miles generation and waiting time, can make SAVs the optimal solution if CO_2 cost is below a certain threshold (< \$100/tonne) (Figure 3.6 c and d). The PAVs do not appear in the market because of the significant increase in

VMT and trip generation, resulting in higher emissions, operating costs, ownership costs, and travel time costs.

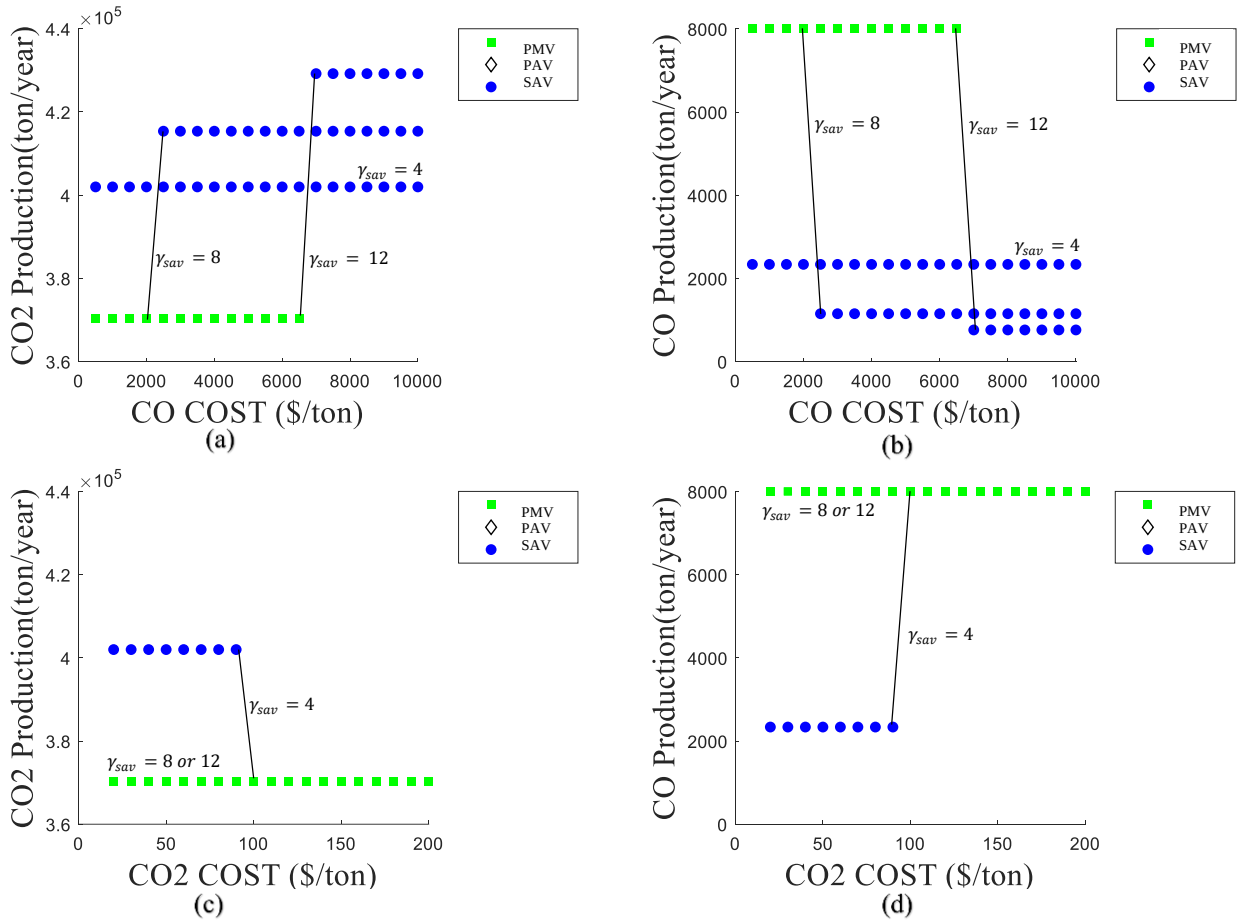

Figure 3.6 Sensitivity to Emission Cost

3.5.4.2 Sensitivity to Emission Cost while Minimizing Emission Cost

This section represents the emission produced and the optimum vehicle type with an objective to minimize the emission cost. The higher replacement rate favors PMVs as the optimal solution, similar to what was observed while minimizing the system cost (Figure 3.7). However, the optimum market switches to SAVs at lower CO costs, while minimizing only the emission cost

(Figure 3.7 a and b). This is due to the smaller share of the emission cost in the total system cost estimated. The reason is that the higher replacement rate is only increasing running emissions rather than other costs while minimizing emission costs. Further, the cost of CO_2 should be below a certain threshold (e.g. \$50/tonne at $\gamma_{sav} = 4$) for SAVs to be the optimal solution (Figure 3.7 c and d). This threshold increases with a decrease in the replacement rate because of the reduction in running emissions (CO_2) in the SAV system (Figure 3.7 c and d). The adoption of PAVs increases the total miles traveled and the number of cold-starts in the system, due to the generation of empty miles, improved mobility, and increased number of trips. Hence, the adoption of these vehicles would result in higher emission production than that of PMVs/SAVs.

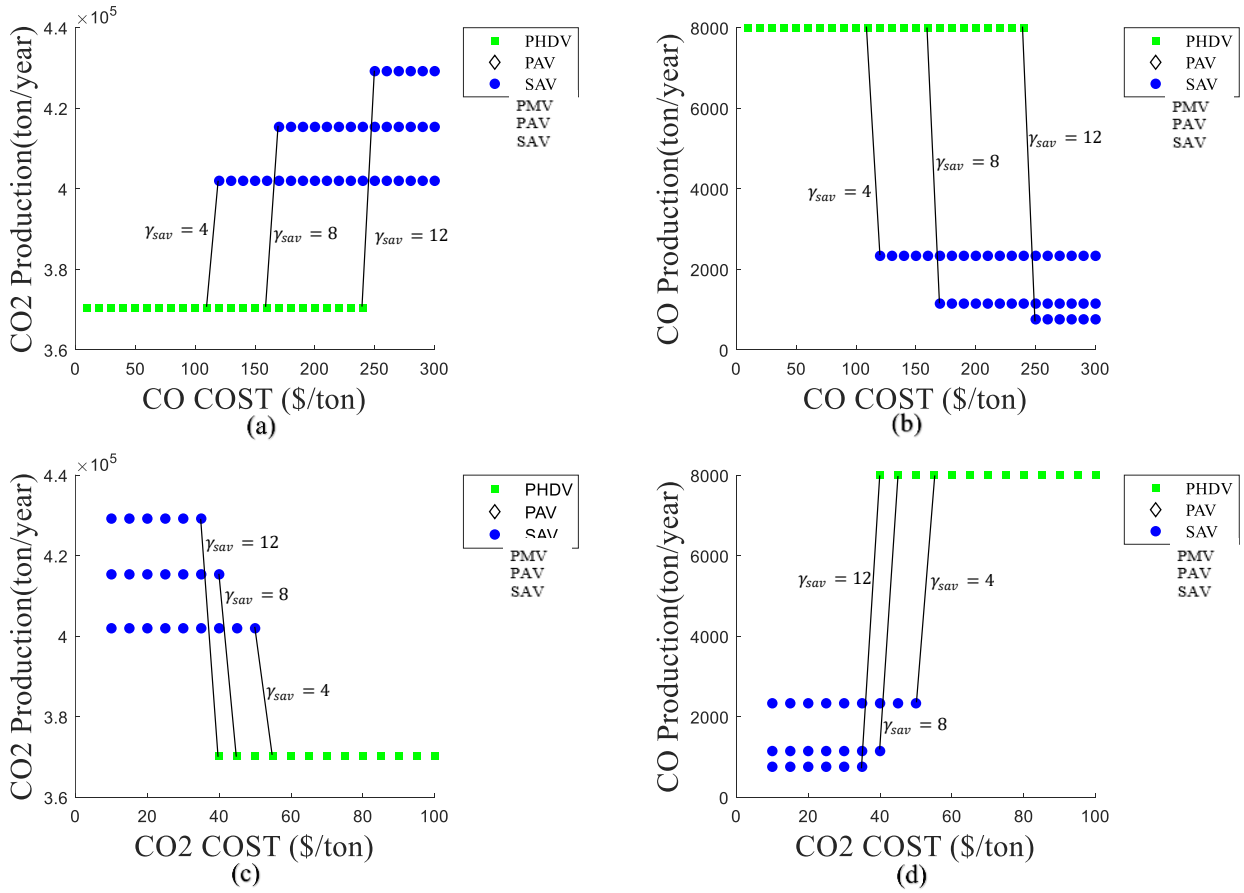

Figure 3.7 Sensitivity to Emission Cost while Minimizing Emission Costs

3.5.5 Analysis results for the real-world scenarios

The analysis and results in the aforementioned sections are based on parameter estimations for mid-sized urban areas in the US. This section considers and compares two cities of San Francisco, CA, and Hammond, LA. These two cities are selected based on their distinct characteristics. San Francisco, CA is one of the largest cities in the US with a high wage rate, high fuel prices, and a large number of trips. Hammond, LA is one of the small cities with low wage rates, low fuel prices, and a smaller number of trips. The characteristics of these cities are presented in Table 3.3.

Table 3.3 Characteristics of the cities

Parameter	Definition	San Francisco, CA	Hammond, LA
T_{pt}	Number of daily trips in the system in 2017 (NHTS, 2017)	1155288.1 trips/day	19292.76 trips/day
VMT	VMT in the city in 2017 (NHTS, 2017)	9226712 miles/day	128428.4 miles/day
τ	Number of daily vehicle trips per household (Mcguckin and Fucci, 2018)	5.11 trips/hh	5.11 trips/hh
μ	Number of vehicles per household (Mcguckin and Fucci, 2018)	1.88 veh./hh	1.88 veh./hh
λ	Trips per vehicle	$\frac{\tau}{\mu}$	$\frac{\tau}{\mu}$
N_0	Number of vehicles required	$\frac{T_{pt}}{\lambda}$	$\frac{T_{pt}}{\lambda}$
m_{pmv}^{pv}	Average VMT per PMV	$\frac{VMT}{N_0} \times 365$	$\frac{VMT}{N_0} \times 365$

Table 3.3 (cont'd)

m_{pmv}^{py}	Total annual miles of each PMV in 2017 (FHWA, 2019)	11,467miles/yr.	11,467miles/yr.
C_f	Fuel cost in 2017 (EIA, 2020a, 2020b)	$ 3.142/gallon	$ 2.295/gallon
V_b^{tt}	Value of Travel Time (VOTT) for PMV for USA (van den Berg and Verhoef, 2016)	$18.82/hr.	$18.82/hr.
W^b	The average wage rate of the US in 2017 (Tradingeconomics.com, 2020).	$22.05/hr	$22.05/hr
W^r	The average wage rate for the city in 2017 (BLS, 2018a, 2018b)	$33.51/hr	$18.02/hr
V_{pmv}^{tt}	VOTT for PMV for the city	$\frac{V_b^{tt} \times W^r}{W^b}$	$\frac{V_b^{tt} \times W^r}{W^b}$

The analysis results for the two cities under the current scenario suggest PMVs as the optimal solution. However, the sensitivity results regarding various parameters, such as the purchase price of PMVs/SAVs, replacement rate, and RVOTT show the variation in the optimal solution (Figure 3.8). It can be observed that the relative threshold (slope and intercept) of the purchase price of PAV/SAV, below which SAVs are the optimal solution, is higher for the city of Hammond as compared to San Francisco (Figure 3.8a). This is because the waiting time cost associated with SAVs is higher in San Francisco due to the higher wage rate and higher cost of waiting compared to the users in Hammond. Hence, the adoption of SAVs would be more favorable in the city of Hammond. The PAVs are not the optimal solution due to their high normalized ownership cost.

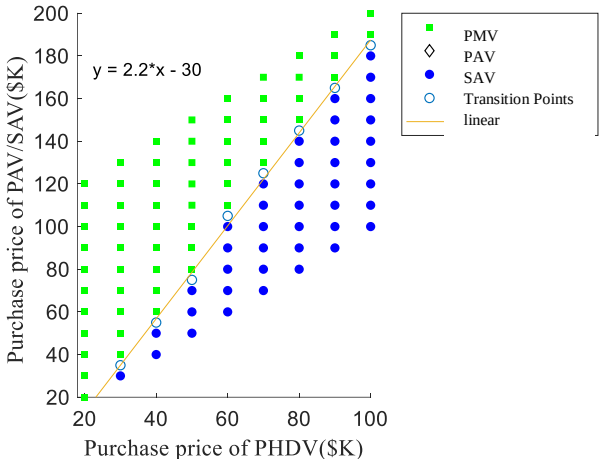

i) Hammond, LA

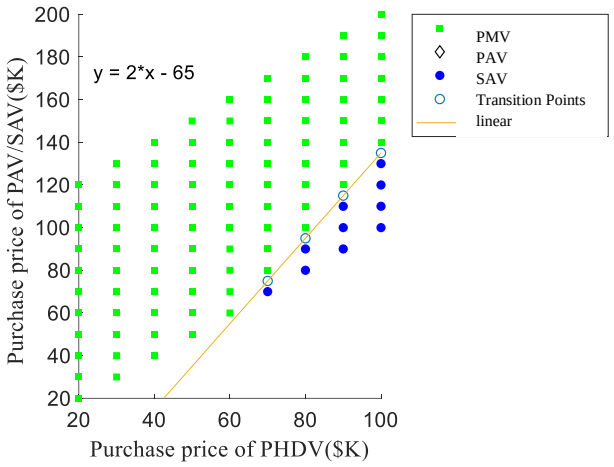

ii) San Francisco, CA

a) Sensitivity to the purchase price of vehicles

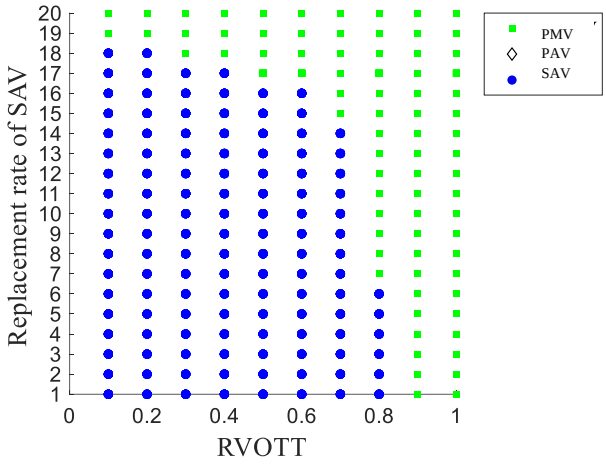

i) Hammond, LA

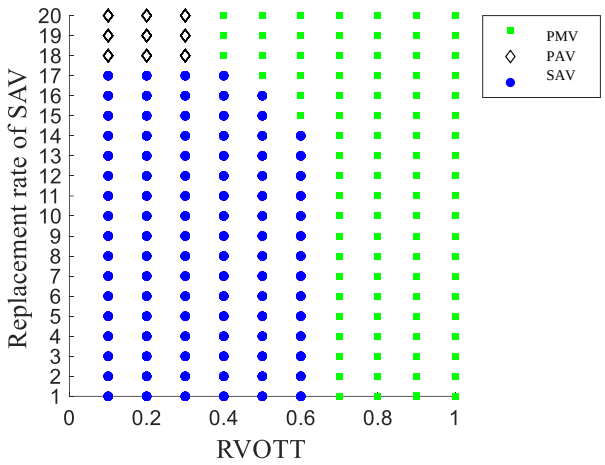

ii) San Francisco, CA

b) Sensitivity to the replacement rate of SAVs and RVOTT

Figure 3.8 Sensitivity analysis results for the city of Hammond, LA, and San Francisco, CA

The base values for the replacement rate and RVOTT for SAVs are 12 PMVs per SAV and 0.8, respectively. However, the optimum choice is sensitive to these two parameters, as observed in Figure 3.8b. The replacement rate has to be below a certain threshold for SAVs to be the optimal solution so that the waiting time of the users, empty miles generated, and the associated costs are

reduced. This threshold decreases with an increase in RVOTT as the driver productivity decreases in AVs, which increases the travel time cost for PAV/SAVs. The higher threshold for the replacement rate of SAVs in the city of Hammond as compared to that of San Francisco makes Hammond to be more favorable for the adoption of SAVs. Another conclusion is that PAVs can be the optimal solution in San Francisco if the reduction in VOTT is relatively high (RVOTT $\leq$ 0.3) and fewer SAVs are available (replacement rate of SAVs is greater than 17 PMVs per SAV). This significantly reduces the travel time cost associated with PAV/SAVs. However, the waiting time, empty miles, and the associated cost for the SAV system are significantly high due to the high replacement rate making them a non-optimal choice. A similar observation can not be made for Hammond as the overall cost for PMV is still lower than PAVs even at low RVOTT due to the lower VOTT of users and the higher purchase price of PAVs. Thus, the effect of high ownership costs of PAVs dominates over the impact of the high travel time cost of PMVs.

3.6 Summary

Autonomous Vehicles and Shared Autonomous Vehicles claim to have significant benefits to the transportation system, such as improved safety, road capacity, mobility, and reduction in emission (due to the efficient driving pattern). However, these vehicles will also increase VMT in the system, which may increase the emissions, travel time, and operating cost of the vehicle. Further, the purchase price of these vehicles would be higher than that of Human-driven Vehicles. To gain insight regarding how PAVs and SAVs will affect the environment and transportation system, the travel pattern, emission, and cost functions for these vehicles are developed and calibrated. Then, to minimize the negative impacts and maximize the benefits of these vehicles in a transportation system, a multi-objective optimization model is proposed to find the optimum fleet configuration by minimizing the overall cost of the system. The system cost consists of

emissions (running and cold start), travel time, waiting time, operating, and ownership cost. The objective of this study is to determine the optimum vehicle type (PMV, PAV, or SAV) and fleet size resulting in the reduction of emissions or overall system cost.

Some of the findings of this study are intuitive, which are used to confirm the barebone of the study. However, this study also has some major findings that are unique and valuable to expand the current line of research. These are separated in the summary section for clarification purposes.

Intuitive findings

- The adoption of PAVs/SAVs is affected not only by the high ownership cost and waiting time but **mainly** by the increased VMT, which increases operating costs.
- The higher running emission cost of autonomous vehicles (due to increased VMT) is more than the savings in cold-start emissions by SAVs.
- The lower replacement rate, or lower CO_2 cost, or higher CO cost favor SAVs as the optimal solution for emission cost minimization.
- The adoption of PAVs would always result in higher emissions costs as compared to that of PMV/SAV due to an increase in VMT and trip generation. Hence, these vehicles do not appear in the market while minimizing the emission cost.

Contributory findings

- This study finds a threshold for the required reduction in the value of travel time. In other words, the required improvements for efficient use of travel time to overcome the other high costs of adoption of autonomous vehicles. This can be done by improving on-board amenities and maybe even the drivetrain, which is valuable information for car companies and their investment policy.

- SAVs are often selected as the optimal choice compared to PAVs. This study derives simplified adoption models for this choice. The simplified adoption models have the ability to get peripheral conditions as an input and find the following factors that make SAVs the optimum choice:
    - Relative purchase price function for SAVs and PMVs.
    - The replacement rate of SAVs (significantly lower than current suggested/expected practice)
    - Reduced value of travel time for SAVs (substantially reduced)
    - The unit cost of different types of emission (CO_2 and CO)(using appropriate policies)

  These simplified models can be adopted by policymakers and/or investors.
- The adoption of SAVs is more favorable for Hammond, LA, as compared to San Francisco, CA. The main reason is the lower wage rate in Hammond, which reduces the waiting cost.
- In the absence of shared mobility, PAVs can be the optimal solution, under the conditions suggested by the simplified adoption models derived in this study. The simplified adoption models can be adopted by policymakers and/or investors to meet the following requirements:
    - On-board amenities improvement
    - Improved total lifetime mileage of PAVs
    - The target group for adoption of PAVs (Adopted by users with a high value of travel time)
- PAVs are only the optimal solution when the AV technology is installed in luxurious cars and in the absence of shared mobility.

CHAPTER 4 OPTIMUM ADOPTION OF AV AND EV IN PRIVATE AND SHARED MOBILITY SYSTEMS

4.1 Overview

The AV and EV technology have synergies. These two technologies enhance and ameliorate the effects of one another and promote their adoption. Hence, it is essential to capture the combined effect of these two technologies on the environment and the transportation system. A modeling framework is developed to capture the trade-offs among the competing factors that govern the overall impact of EVs and AVs on the transportation system and environment. A fleet optimization problem considers the different combinations of these technologies in private and shared mobility systems in a network of multiclass users with different VOTT. The objective is to minimize the system cost, which is a combination of total time, emissions, ownership cost, driver cost, and crash cost.

The remainder of this study is as follows. Section 4.2 discusses the problem statement and objective of the study, followed by the problem formulation in section 4.3. The solution method, numerical results, and the summary are presented in sections 4.4, 4.5, and, 4.6, respectively.

4.2 Problem Statement

While the autonomous and electric vehicle technology might improve the transportation system in different aspects, there are certain other aspects that might worse off due to implementation of such technologies. Further, these technologies will have different effects on the private and shared mobility systems. It is important to note that the shared mobility system considered in this study is like a taxi system or other carpooling services provided by transportation network companies (TNC), which can serve multiple trips and users, and also allow users to

carpool in the same vehicle. In contrast to the private mobility system, the vehicles in the shared mobility system have high utilization rate (serving multiple trips) and high lifetime mileage. These mobility options have different positive and negative influence on the performance of transportation systems. The different combinations of these technologies will govern the overall impact on the transportation system. However, the variety of trade-offs (Figure 4.1) embedded in these options makes it challenging to determine the optimum combinations of these technologies required to provide a sustainable transportation system. This optimization and cost-benefit analysis are necessary for policy makers to implement and invest in the best incentive policies.

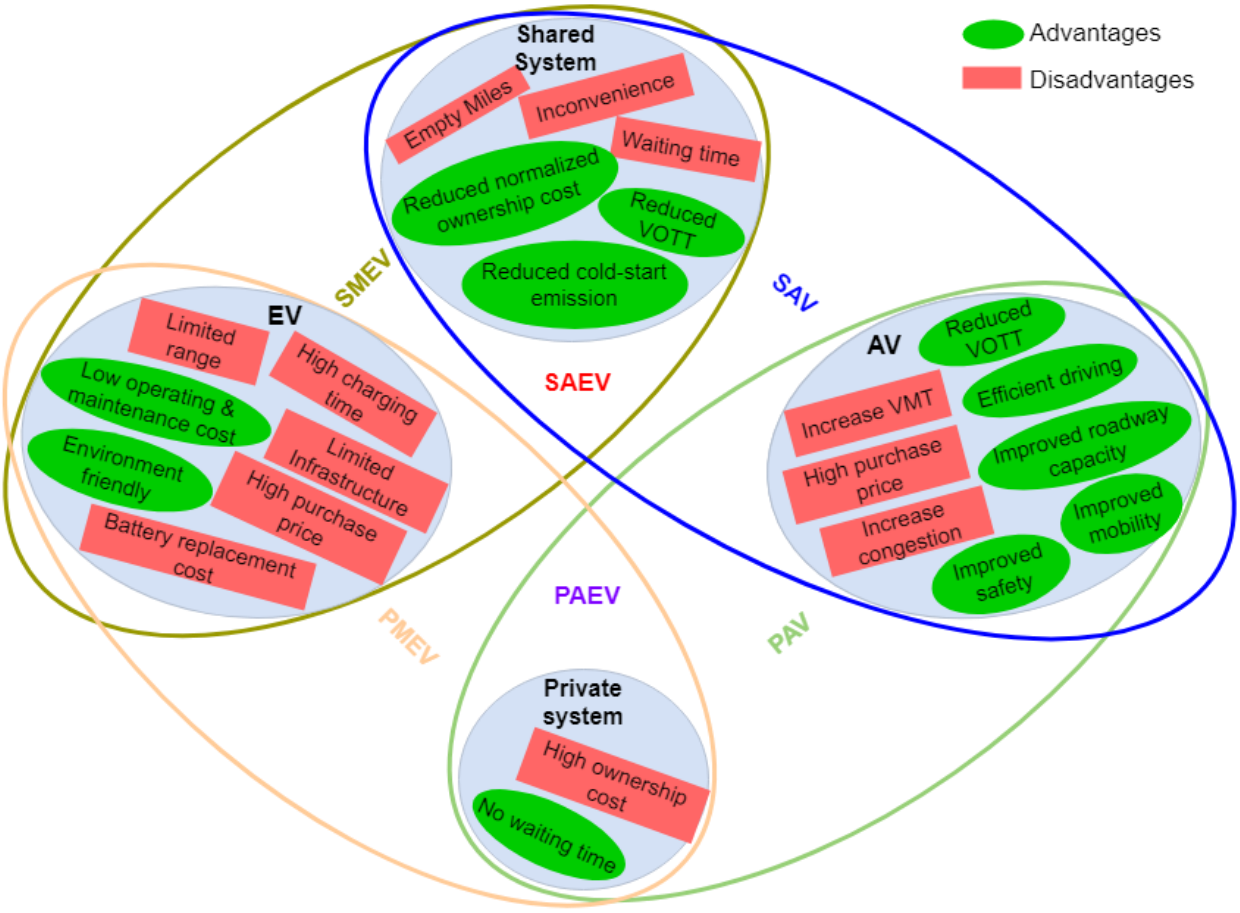

Figure 4.1 Trade-offs associated with different mobility options

This study aims to estimate the optimal fleet configuration considering AV and EV technologies in a private and/or shared mobility system to minimize the total system cost. This configuration is defined by the number of vehicles of each type and the number of PMVs each vehicle type replaces to ensure all trips' feasibility. The vehicle types considered here are PMVs, private manual-driven electric vehicles (PMEVs), private autonomous vehicles (PAVs), and private autonomous electric vehicles (PAEVs). Similarly, these vehicles are considered in a shared capacity (Shared manual-driven vehicle (SMV), shared manual-driven electric vehicle (SMEV), shared autonomous vehicle (SAV), shared autonomous electric vehicle (SAEV)). These vehicle types are shown in Figure 4.2. Another important factor considered in the study is the replacement rate of each vehicle type. The replacement rate is defined as the number of PMVs replaced by one vehicle of type j, serving equivalent trips. One shared vehicle or an AV can serve multiple trips by continuous repositioning to different pickup locations. Hence, these vehicles can replace multiple PMVs, which reduces the number of vehicles in the system. However, a higher replacement rate increases the waiting time, empty miles, and inconvenience of users. A nonlinear optimization model is developed to minimize the total system cost, with the number of vehicles of each type, the replacement rate of each vehicle type, and the number of interzonal trips of the different user classes served by each vehicle type as decision variables. The system cost includes the following cost terms in the monetary unit: travel time (tt), waiting time (wt), emissions (running emission (re) and cold-start emission (cs)), operating (op), normalized ownership (noc), driver (dr), and crash (cr). These costs are estimated considering different factors as shown in Figure 4.3. The notations used in the study are presented in Table 4.1.

It is important to note that this study considers multiclass users with different VOTT. Further, the study considers fully autonomous vehicles (Level 5 Autonomy) that do not require any driver assistance.

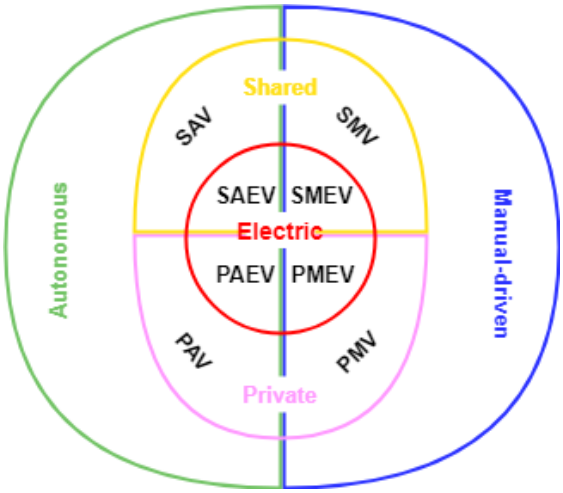

PMV: Private Manual-driven Vehicle
PMEV: Private Manual-driven Electric Vehicle
PAV: Private Autonomous Vehicle
PAEV: Private Autonomous Electric Vehicle
SMV: Shared Manual-driven Vehicle
SMEV: Shared Manual-driven Electric Vehicle
SAV: Shared Autonomous Vehicle
SAEV: Shared Autonomous Electric Vehicle

Figure 4.2 The vehicle type considered in this study based on different technologies/systems

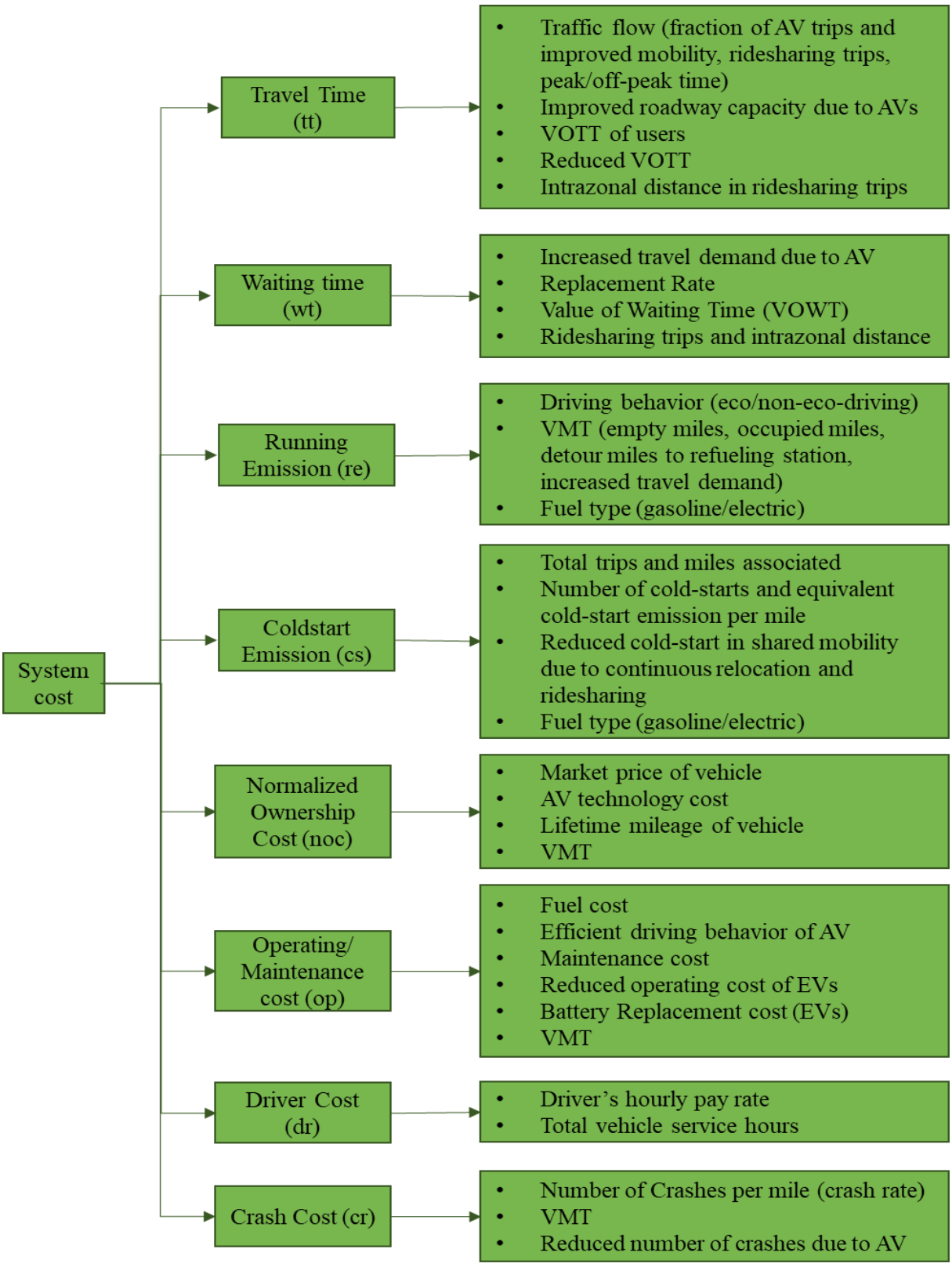

Figure 4.3 Diagram of different cost terms in the objective function and influencing factors

Table 4.1 Nomenclature

Sets	Definition
$o, d, z \in Z$	Set of different zones (o= origin zone, d=destination zone, z=zone)
$k \in K$	Set of different user class
$i \in I$	Set of different emissions considered $\{CO_2, NO_x, VOC, PM\}$
$j \in J$	Set of different vehicle types considered {PMV, PMEV, PAV, PAEV, SMV, SMEV, SAV, SAEV}
$g \in \mathrm{G}$	Set of different cost types $\begin{cases} Running\ Emissions\ cost(re), Cold\ Start\ Emissions\ cost(cs), \\ Normalized\ Ownership\ cost(noc), Operating\ cost(op) \\ Travel\ Time\ cost(tt), Waiting\ time\ cost\ (wt) \\ Driver\ cost\ (dr), Crash\ Cost\ (cr) \end{cases}$
$b \in B$	{peak hour, off-peak hour}
Decision variable	**Definition**
N_j	The number of vehicles of vehicle type j
γ_j	Replacement rate (equals to 1 for PMV, PMEV)
f_{jkod}	The fraction of OD trips for user class k served by vehicle j
State variables	**Definition**
A_j	The average number of times the one vehicle needs to be refueled in time t_0 for vehicle type j
C_j^g	Total cost of type g for vehicle type j
E_{ij}^{CS}	Cold-start emission normalized per mile
$m_j^{'}$	The total interzonal miles per vehicle j in the time t_0
$m_j^{''}$	The total detour miles traveled to refueling station per vehicle j in the time t_0

Table 4.1 (cont'd)

m_j'''	The total intrazonal miles per vehicle j to pickup/drop off different riders in carpooling trips for the shared mobility
m_j	The total miles traveled per vehicle j in the study time period t_0
t_j	The total time spent by one vehicle of vehicle type j
TT_{odb}	The travel time from zone o to d during time period b(peak or off-peak)
U_j	Total number of vehicle trips in the original system (in the absence of EV/AV technology) that should be served by vehicle j
V_{jodb}	The average vehicle trips per hour during time period b (peak or off-peak), along the path between zone o and d by vehicle j, respectively
W_j'	The average interzonal waiting time per person trip
α_j	Factored VMT increase due to the empty rides for repositioning of autonomous vehicles

Parameter	Definition	Function/Values	Source
$E_{CO_2,j}^{RE}$	Running emission (CO_2) considering efficient-driving profile for AVs and nonefficient-driving profile for non-AVs	$\begin{cases} 338\ \text{g/mile} & j \in \{PMV, SMV\} \\ 260\ \text{g/mile} & j \in \{PAV, SAV\} \\ 0 & \text{otherwise} \end{cases}$	(He et al., 2015; Int Panis et al., 2006; Singh et al., 2021)
$E_{NO_x,j}^{RE}$	Running emission (NO_x-)considering efficient-driving profile for AVs and nonefficient-driving profile for non-AVs	$\begin{cases} 148\ \text{mg/mile} & j \in \{PMV, SMV\} \\ 118\ \text{mg/mile} & j \in \{PAV, SAV\} \\ 0 & \text{otherwise} \end{cases}$	(He et al., 2015; Int Panis et al., 2006; Singh et al., 2021)
$E_{VOC,j}^{RE}$	Running emission (VOC) considering efficient-driving profile for AVs and	$\begin{cases} 491\ \text{mg/mile} & j \in \{PMV, SMV\} \\ 589\ \text{mg/mile} & j \in \{PAV, SAV\} \\ 0 & \text{otherwise} \end{cases}$	(He et al., 2015; Int Panis et al., 2006; Singh et al., 2021)

Table 4.1 (cont'd)

	nonefficient-driving profile for non-AVs		
$E_{PM,j}^{RE}$	Running emission (PM)considering efficient-driving profile for AVs and nonefficient-driving profile for non-AVs	$\begin{cases} 8747\ \mu g/mile & j \in \{PMV, SMV\} \\ 6378\ \mu g/mile & j \in \{PAV, SAV\} \\ 0 & \text{otherwise} \end{cases}$	(He et al., 2015; Int Panis et al., 2006; Singh et al., 2021)
h_j	Hourly pay rate for a driver ($/hr)	$\begin{cases} \$12/hr & j \in \{SMV, SMEV\} \\ 0 & \text{otherwise} \end{cases}$	(PayScale, 2019)
$l_j^{'}$	The average detour distance traveled per refueling/recharging		
l_{od}	The interzonal distance between the zones o and d ($\forall\ o \neq d$)		
Q_{kodb}	Number of trips from zone o to zone d ($\forall\ o \neq d$) during period b for the user class k		
R_j	Range (in miles) for the vehicle type j	$\begin{cases} 300\ miles & j \in \{PMV, PAV, SMV, SAV\} \\ 150\ miles & j \in \{PMEV, PAEV, SMEV, SAEV\} \end{cases}$	
s_j	The average speed of the vehicle	30 miles/hr	(Singh et al., 2021)
t_0	Duration of study		
$t_j^{'}$	The average time required per refueling	$\begin{cases} 1.5\ min & j \in \{PMV, PAV, SMV, SAV\} \\ 1\ hr & j \in \{PMEV, PAEV, SMEV, SAEV\} \end{cases}$	
$t_j^{''}$	The average inconvenience time at the refueling station	3 minutes	

Table 4.1 (cont'd)

x_j	Crashes per million (10^6) VMT for vehicle type j	$\begin{cases} 5 & j \in \{PMV, PMEV, SMV, SMEV\} \\ 2.5 & j \in \{PAV, PAEV, SAV, SAEV\} \end{cases}$	(Cicchino, 2017; Tefft, 2017)
y	Equivalent cost per crash	\$26,745 per crash	(Fletcher, 2019; Tefft, 2017)
χ_z	The average intrazonal distance between different locations at zone z for users carpooling.		
λ_j	Average car occupancy		
τ_b	The time during time period b		
Λ_{jod}	Capacity (veh/hr) of the roadway along the link from zone o to zone d in a system of vehicle type j		(Childress et al., 2015)
μ_{jod}	The fraction of person trips carpooling from zone o to zone d served by vehicle j	$\begin{cases} N/A & j \in \{PMV, PMEV, PAV, PAEV\} \\ 0.2 & j \in \{SMV, SMEV, SAV, SAEV\} \end{cases}$	
η_j	Factored increased in the number of trips due to the improved mobility with the adoption of vehicle j	$\begin{cases} 1 & j \in \{PMV, PMEV\} \\ 1.14 & j \in \{SMV, SMEV\} \\ 1.20 & j \in \{PAV, PAEV, SAV, SAEV\} \end{cases}$	(Singh et al., 2021)
β_i	Equivalent cold-start emission per mile in a PMV system	$\begin{cases} 14 \text{ g/mile} & i = CO_2 \\ 80 \text{ mg/mile} & i = NO_x \\ 1{,}963 \text{ mg/mile} & i = VOC \\ 11 \text{ mg/mile} & i = PM \end{cases}$	(He et al., 2015; Int Panis et al., 2006; Reiter and Kockelman, 2016; Singh et al., 2021)

Table 4.1 (cont'd)

ω_k	Value of travel time (VOTT) for user class k	$\begin{cases} \$20/\text{hr} & k = 1 \\ \$50/\text{hr} & k = 2 \\ \$100/\text{hr} & k = 3 \end{cases}$	
Δ_j	Reduction factor for VOTT (RVOTT) due to the adoption of vehicle *j*	$\begin{cases} 1 & j \in \{PMV, PMEV\} \\ 0.8 & j \in \{PAV, PAEV\} \\ 0.9 & j \in \{SMV, SMEV, SAV, SAEV\} \end{cases}$	(Singh et al., 2021) Assumed
ϖ_k	Value of waiting time (VOWT) for user class k		(Singh et al., 2021)
π_i	The societal cost of producing one unit of emission i	$\begin{cases} \$50/\text{metric ton} & i = CO_2 \\ \$7{,}900/\text{metric ton} & i = NO_x \\ \$2{,}000/\text{metric ton} & i = VOC \\ \$360{,}383/\text{metric ton} & i = PM \end{cases}$	(US DOT, 2015)
ρ_j	Average purchase price of the vehicle type *j*	$\begin{cases} \$30{,}000 & j \in \{PMV, SMV\} \\ 4 \times (\rho_{PMV})^{0.87} & j \in \{PMEV, SMEV\} \\ \rho_{PMV} + \$10{,}000 & j \in \{PAV, SAV\} \\ 4 \times (\rho_{pav})^{0.87} & j \in \{PAEV, SAEV\} \end{cases}$	(EnergySage, 2019; IHS, 2014; NADA, 2012)
δ_j	Total lifetime mileage of the vehicle j	$\begin{cases} 130{,}000 \text{ miles} & j \in \{PMV, PMEV, PAV, PAEV\} \\ 250{,}000 \text{ miles} & j \in \{SMV, SMEV, SAV, SAEV\} \end{cases}$	(Singh et al., 2021) (Singh et al., 2021)
Ω	Life of EV battery	100,000 miles	(Union of Concerned Scientists, 2019)
ϑ	The total price of the battery	\$9,600	(BloombergNEF, 2020; Ghamami et al., 2019)
φ_j	Average fuel cost per mile	$\begin{cases} \$0.10/\text{mile} & j \in \{PMV, SMV\} \\ \$0.04/\text{mile} & j \in \{PMEV, SMEV\} \\ \$0.07/\text{mile} & j \in \{PAV, SAV\} \\ \$0.03/\text{mile} & j \in \{PAEV, SAEV\} \end{cases}$	(AAA, 2017; ChooseEnergy, 2019; FHWA,

Table 4.1 (cont'd)

			2017; Ghamami et al., 2019; Wadud et al., 2016)
σ_j	Maintenance cost per mile	$\begin{cases} \$0.08/\text{mile} & j \in \{PMV, PAV, SMV, SAV\} \\ \$0.04/\text{mile} & j \in \{PMEV, PAEV, SMEV, SAEV\} \end{cases}$	(AAA, 2017; Berman, 2016)
ζ	Average trips per PMV per day		(Santos et al., 2011)

4.3 Problem Formulation

This study aims to capture the effects of different technologies (electrification and automation) on the transportation system. The adoption of these technologies has a variety of impacts on users' convenience, travel behavior, travel cost, and travel time. These technologies will also impact the traffic flow dynamics, safety, and emission in transportation systems. The cost of owning and operating these vehicles is different than those of PMVs. Thus, an optimization framework is proposed to find the optimum fleet configuration in a private and shared mobility system. The study considers eight different vehicle types, four in private mode (PMV, PEV, PAV, PAEV) and four in the shared system (SHDV, SEV, SAV, SAEV). The modeling framework, cost components, and factors influencing the adoption of different technologies are explained in the following subsections. The notations used in this study are listed in Table 4.1. The superscripts are used to define the cost types such as tt for travel time, re for running emissions, cs for cold-start emissions, etc. The subscripts are used for indices in the sets such as j and k for vehicle type and user class, respectively.

4.3.1 Optimization Problem

The trade-offs associated with different technologies and systems have specific effects on various cost types. However, finding the adoption strategy with the minimum overall cost to the transportation system is essential. The objective of the study is to estimate the optimum fleet configuration that will result in minimum transportation cost, including time (travel time cost, waiting time cost), emission (running and cold start), ownership, operating, driver cost, and crash cost (Equation 72). The decision variables are the number of vehicles (N_j) of each vehicle type j, the replacement rate (γ_j) for each type, and the fraction of OD trips for user class k served by vehicle j (f_{jkod}). The parameters C_j^g are the costs associated with the adoption of vehicle j ($j \in \{PMV, PMEV, PAV, PAEV, SMV, SMEV, SAV, SAEV\}$) for the cost type g. The optimization framework proposed is as follows:

$$\min Z = \sum_j \sum_g C_j^g \qquad 72$$

s.t.:

$$\sum_j f_{jkod} = 1 \qquad \forall k, \forall o, \forall d, o \neq d \qquad 73$$

$$t_j \leq t_0 \qquad \forall j \qquad 74$$

$$\gamma_j N_j = \frac{U_j}{\zeta} \qquad \forall j \qquad 75$$

$$N_j \geq 0 \qquad \forall j \qquad 76$$

$$\gamma_j = 1 \qquad j \in \{PHDV, PEV, PAV, PAEV\} \qquad 77$$

$$\gamma_j \geq 2 \qquad j \in \{SHDV, SEV, SAV, SAEV\} \qquad 78$$

$$f_{jkod} \geq 0 \qquad \forall j, \forall k, \forall o, \forall d, \ o \neq d \qquad 79$$

Equation 73 ensures that all the trips of all the user classes are being served. Equation 74 ensures that the total time spent, which includes interzonal time (travel and waiting time), intrazonal time (travel and waiting time), the detour time to the refueling station, the refueling time, and the inconvenience time at refueling stations, is less than the total time available (t_0). This constraint provides enough backup vehicles in the system to cover incidentals. Equation 75 certifies that the trips assigned to a specific vehicle type are served by providing the equivalent number of vehicles considering the estimated replacement rate ($\gamma_j N_j$). The term U_j is the total number of vehicle trips in the original system (in the absence of EV/AV technology) that should be served by vehicle j. The term ζ is the number of vehicle trips per vehicle in the original system when there are only human-driven vehicles. Equations 76 to 79 are the feasibility constraints. The number of vehicles should be positive. The replacement rate for private modes are set as 1. The replacement rate for shared mode is set to a lower bound of 2 to operate as a shared mobility system (Equation 78). The fraction (f_{jkod}) should be greater than zero. The term U_j is defined as follows:

$$U_j = \sum_o \sum_d \sum_b \left(\left\lceil \frac{\mu_{jod} \sum_k f_{jkod} Q_{kodb}}{\lambda_j} \right\rceil + (1 - \mu_{jod}) \sum_k f_{jkod} Q_{kodb} \right) \qquad 80$$

Where, μ_{jod} represents the fraction of users willing to carpool and is set as zero for private modes. The λ_j is the average car occupancy. The term Q_{kodb} is the total person trips in the original system between origin o and destination d, for the user class k, during the time-period b (peak or off-peak hour). The different cost functions considered in the study are developed in the following subsections.

4.3.2 Travel time cost

The sketch network is modeled as a complete graph with zone centroids as demand generation and attraction points. The vehicles are assumed to follow user equilibrium, minimizing their travel time. The average number of vehicle trips V_{jodb} per hour for each vehicle type j, on the path between zones o and d, during the peak/off-peak hour is expressed as follows:

$$V_{jodb} = \left(\left\lceil \frac{\mu_{jod} \eta_j \sum_k f_{jkod} Q_{kodb}}{\lambda_j} \right\rceil + (1 - \mu_{jod}) \eta_j \sum_k f_{jkod} Q_{kodb} \right) \left(\frac{1}{\tau_b} \right) \quad (81)$$

Where, the term τ_b represents the time duration of period b. The η_j captures the increased number of trips due to improved mobility with the adoption of AVs. Adoption of AVs leads to efficient use of the roadway, hence improving the roadway capacity. These vehicles also allow users to use their travel time more efficiently, consequently reducing the in-vehicle VOTT. AVs are known to enhance the mobility of non-drivers and reduce the parking cost due to self-parking at cheaper locations and better utilization of parking space (as no room is required for the driver to access the vehicle). All these potential benefits change the travel behavior of the users and increase the total trips in the system, which is captured by parameter η_j. The f_{jkod} is the decision variable representing the fraction of the OD trips of user classes k assigned to vehicle type j. This study captures the effect of high demand during peak periods on the utilization rate of vehicles and refueling/recharging requirements. However, to reduce the complexity of the optimization problem, this study assumes that the optimal solution is identical for both the peak and off-peak periods.

The roadway capacity during peak/off-peak hour, along the path between zones o and d is estimated considering the fraction of different types of vehicles along the path, and the roadway

capacity (Λ_{jod}) in a system of vehicle type j. This study accounts for the improved roadway capacity due to the adoption of AVs. The computer-controlled AVs operate at shorter headways (due to the reduced reaction time) and keep traffic flow parameters steady, boosting the maximum throughput/capacity (Lu et al., 2020). Considering the above effect on traffic flow, the travel time during peak/off-peak hour (TT_{odb}) between zones o and d is obtained using BPR function as follows (Bureau of Public Roads, 1964):

$$TT_{odb} = TT_{od}^{0}\left[1 + \xi_1\left(\frac{\sum_j V_{jodb}}{\left(\frac{\sum_j V_{jodb}\,\Lambda_{jod}}{\sum_j V_{jodb}}\right)}\right)^{\xi_2}\right] \quad 82$$

Where, TT_{od}^{0} is the free-flow travel time between zones o and d.The terms, ξ_1 and ξ_2 are the calibrated parameters of the BPR function for different roadway conditions (Bureau of Public Roads, 1964).

The carpooling users might experience additional intrazonal travel time at the origin and destination for picking up and dropping off. This extra travel time tt_{jz} per person trip, experienced by the users already inside the vehicle, are obtained as follows:

$$tt_{jz} = \frac{\lambda_j - 1}{2}\left(\frac{\chi_z}{s_j}\right) \quad 83$$

Where, χ_z is the average intrazonal distance between pickup/drop-off locations at zone z. The s_j is the average speed of vehicle type j. The total travel time cost for vehicle j is defined as follows:

$$C_j^{tt} = \sum_{k\in K}\sum_{o\in Z}\sum_{d\in Z}\sum_{b\in B}\left[TT_{odb} + \mu_{jod}\left(tt_{jo} + tt_{jd}\right)\right] f_{jkod} Q_{kodb} \eta_j \Delta_j \omega_k \quad (84)$$

Where Z is the set of zones in the network.The ω_k and Δ_j are the VOTT for each user class k and reduction factor for VOTT (RVOTT) due to efficient use of travel time in vehicle type j. Unlike shared mobility systems and AVs, the users of private non-AVs cannot utilize their travel time to perform any other activity inside the car other than driving. Therefore, the RVOTT is set as 1 for private non-AVs (PMV, PEV). Further, the travel time savings in the shared mobility systems might be lesser than that in private AVs, due to the inconvenience to the users. Hence, the travel time savings in shared mobility systems is assumed to be half of that in private AVs.

4.3.3 Waiting Time Cost

The waiting time in a shared mobility system has two components. First, the time required for the empty vehicle to reach the origin of the first user (W_j'). Second, the average time required for the intrazonal trips (picking up the carpooling users in the same zone) (w_{jo}). The first component is a function of the replacement rate (γ_j) and the increased travel demand due to the adoption of AVs (η_j) (Singh et al., 2021). The higher replacement rate will reduce the number of vehicles resulting in an increased trip load on each vehicle. Consequently, this will increase the average waiting time (Singh et al., 2021). The increasing number of trips in a given system increases the likelihood of closer consecutive trips, reducing the average waiting time and travel distance (Singh et al., 2021). The factor $W_j^{'}$ for the shared mobility system is defined as follows (Singh et al., 2021):

$$W_j^{'} = max\left[\left(0.0003exp\left(0.575\gamma_j\right) - 0.551\eta_j^3 + 2.177\eta_j^2 - 2.832\eta_j + 1.206\right), 0\right] \quad (85)$$

The second component of the waiting time, defined as the average intrazonal time at the origin zone o, is defined as follows:

$$w_{jo} = \frac{\lambda_j - 1}{2}\left(\frac{\chi_o}{s_j}\right) \quad 86$$

Thus, the total cost of waiting time C_j^{wt} is as follows:

$$C_j^{wt} = \sum_{\mathrm{k}\in\mathrm{K}} \sum_{o\in Z} \sum_{d\in Z} \sum_{b\in B} \left(W_j' + \mu_{jod} w_{jo}\right) f_{jkod} Q_{kodb} \eta_j \varpi_k \quad 87$$

Where the term ϖ_k is the VOWT for the user class k.

4.3.4 Miles Traveled

The VMT in the system changes significantly with the adoption of different technologies. The AVs and shared mobility systems generate empty rides in the system, which increases VMT in the system. The improved mobility by the adoption of AVs further increases VMT in the system. Carpooling will reduce the interzonal miles, but it will add intrazonal miles to pickup/drop-off different users. EVs add extra detour miles for charging the vehicle due to the limited number of charging stations. To capture these effects, the total miles traveled is defined for each vehicle type. The total miles traveled include three categories: interzonal and intrazonal miles traveled, and detour miles traveled for refueling. The interzonal miles traveled per vehicle type j, include the occupied miles traveled and empty miles, as follows:

$$m_j' = \frac{\sum_{o\in Z} \sum_{d\in Z} \sum_{b\in B} V_{jodb} \tau_b l_{od}}{N_j} \alpha_j \quad 88$$

Where, l_{od} and N_j are the interzonal distance between zone o and d, and the number of vehicles of type j present in the system, respectively. The empty miles (α_j) is the function of the

replacement rate γ_j and the increased number of trips (η_j). The higher replacement rate increases the trip load on each vehicle, which increases the empty miles generated(Singh et al., 2021). The increased number of shared mobility trips increases the probability of consecutive trips closer, which reduces the overall empty miles (Singh et al., 2021). The empty mile function is given as follows (Singh et al., 2021):

$$\alpha_j = \begin{cases} 1 & j \in \{PHDV, PEV\} \\ \max\left[\left(1.34\, log_e\, \gamma_j + 1.001\right), 1\right] & j \in \{PAV, PAEV\} \\ \max[(0.98 \exp\left(0.008\gamma_j\right) - \ 0.04 \log_e \eta_j + 0.02\ ), 1] & j \in \{SHDV, SEV, SAV, SAEV\} \end{cases} \quad 89$$

The detour miles traveled (m_j'') to the refueling station, is critical for EVs considering the limited number of charging stations. It is a function of the density of refueling stations in the area (affecting average distance traveled per refueling (l_j')) and the total number of times (A_j) the vehicle needs to be refueled in a given time t_0, which is defined as follows:

$$m_j'' = A_j l_j' \quad 90$$

The number of times a vehicle needs to be refueled (A_j) is a function of total miles traveled (m_j) during time t_0, and the total miles a vehicle can drive on a full fuel tank or battery (known as the range (R_j) of the vehicle), which is defined as follows:

$$A_j = \frac{m_j}{R_j} \quad 91$$

The intrazonal miles are traveled within all the origin and destination zones to pick up and drop off users carpooling in the same vehicle. The total intrazonal miles traveled per vehicle (m_j''') is a function of the average car occupancy, the average distance between consecutive pickup and drop-off locations, and the total carpooling trips, which is defined as follows:

$$m_j''' = \frac{\sum_{o \in Z} \sum_{d \in Z} \sum_{b \in B} \frac{(\lambda_j - 1)}{\lambda_j} (\chi_o + \chi_d) \mu_{jod} \eta_j \sum_k f_{jkod} Q_{kodb}}{N_j} \quad 92$$

The overall total miles per vehicle (m_j) considering all the three components and using Equation 90 and 91, is as follows:

$$m_j = \begin{cases} \left(m_j' + m_j'''\right) \left(\frac{R_j}{R_j - l_j'}\right) & if\ N_j \neq 0 \\ 0 & otherwise \end{cases} \quad 93$$

4.3.5 Emissions

The emission cost is estimated considering major pollutants carbon dioxide (CO_2), nitrogen oxides (NO_x), volatile organic compounds (VOC) and particulate matter (PM) (Int Panis et al., 2006). The emission cost includes the societal cost of running and cold-start emissions in a system. The running emission cost (C_j^{re}) is a function of running emission per mile (E_{ij}^{re}) for emission type i, total miles per vehicle (m_j) and the number of vehicles of vehicle type j (N_j), which is estimated as:

$$C_j^{re} = \sum_i \pi_i E_{ij}^{re} m_j N_j \quad 94$$

The term π_i is the societal cost of producing a unit quantity of emission type. The term E_{ij}^{re} is derived considering instantaneous emissions (Int Panis et al., 2006) as the function of speed and acceleration of the vehicle type j, depending upon its driving behavior (eco-driving for AVs and non-eco-driving for other vehicles) (He et al., 2015; Singh et al., 2019).

The cold-start emission cost (C_j^{cs}) is a function of normalized cold-start emission per mile (E_{ij}^{CS}), and the occupied interzonal vehicle miles. It is important to note that the factor E_{ij}^{CS} accounts

for the reduction in cold-start in a shared mobility system. The number of cold-starts reduces with increased replacement rate (γ_j) and travel demand (η_j) in a shared mobility system, due to the continuous repositioning which reduces the frequency of engine shut-offs (Singh et al., 2019). The E_{ij}^{cs} for non electric shared mobility system, based on the study by Singh et al., is given as follows (Singh et al., 2019):

$$E_{ij}^{cs} = \max\left[\frac{\beta_i\left(0.645\gamma_j^{-1.022} - 0.011\eta_j^3 + 0.047\eta_j^2 - 0.062\eta_j + 0.027\right)}{0.64}, 0\right] \quad j \in \{SHDV, SAV\} \quad 95$$

The cold-start emission cost is defined as follows:

$$C_j^{cs} = \sum_i \pi_i E_{ij}^{cs} \sum_o \sum_d \sum_b V_{jodb}\tau_b l_{od} \quad 96$$

4.3.6 Ownership and Operation Costs

The normalized ownership cost (C_j^{noc}) over the study period (t_0) is a function of the purchase price (ρ_j), total lifetime mileage of the vehicle δ_j (total miles a vehicle can travel during its entire lifetime), and miles traveled per vehicle (m_j). It is important to note that the cost of adding AV technology is considered in the purchase price of AVs (ρ_j). The normalized ownership cost (C_j^{noc}) is as follows:

$$C_j^{noc} = \frac{\rho_j}{\delta_j} m_j N_j \quad 97$$

The operating cost (C_j^{op}) includes fuel and maintenance costs. It is a function of the fuel cost per mile (φ_j), the maintenance cost per mile (σ_j), the miles traveled per vehicle (m_j), the number of vehicles. For EVs, the battery might have to be replaced after its life is expired. Hence, the operating cost for EVs is also a function of the life of the battery (Ω), the battery price (ϑ),

and the total lifetime mileage of the vehicle (δ_j). It is important to note that the fuel cost per mile (φ_j) accounts for the reduction in fuel consumption due to the efficient driving behavior of AVs. The operating cost is defined as follows:

$$C_j^{op} = \begin{cases} \left(\varphi_j + \sigma_j\right) m_j N_j & if\ j \in \{PHDV, PAV, SHDV, SAV\} \\ \left(\varphi_j + \sigma_j + \left\lfloor \frac{\delta_j}{\Omega} \right\rfloor \frac{\vartheta}{\delta_j}\right) m_j N_j & if\ j \in \{PEV, PAEV, SEV, SAEV\} \end{cases} \quad 98$$

4.3.7 Driver Cost

The non-AV shared vehicles (SHDV, SEV) require human drivers. Thus, there would be a cost to support the salary of these drivers. The labor cost (C_j^{dr}) depends on the hourly salary of the driver (h_j), and the total service hours (t_j).

$$C_j^{dr} = h_j t_j N_j \quad 99$$

The total service hours can be divided into five components interzonal time (travel and waiting time), intrazonal time (travel and waiting time), the detour time to the refueling station, the refueling time, and the inconvenience time at a refueling station, which is defined as follows:

$$t_j = \frac{\sum_o \sum_d \sum_b \left(TT_{odb} + W_j'\right) V_{jodb} \tau_b}{N_j} + \frac{m_j'''}{s_j} + A_j \left(\frac{l_j'}{s_j} + t_j' + t_j''\right) \quad 100$$

Where, t_j' and t_j'' are the average refueling time and inconvenience time at the refueling station. The inconvenience time is the time to drive the vehicle in and out of the station, remove and put the nozzle back, and pay at the station.

4.3.8 Crash Cost

The adoption of AVs is known to reduce the number of crashes and the associated cost significantly. Hence, it is crucial to consider this cost to estimate the optimum vehicle fleet configuration. The cost estimated due to crashes C_j^{cr} for vehicle type j is as follows:

$$C_j^{cr} = yx_j m_j N_j \quad 101$$

Where, the term y is the average monetary value per crash. The term x_j is the crashes per VMT in a system of vehicle type j. This factor accounts for the reduction in crashes due to the adoption of AVs.

4.4 Solution Method

The optimization model is an NP-hard problem including nonlinear objective function with nonlinear constraints. It including various nonlinear functions (i.e., ceiling, exponential, and polynomial functions) for different variables. The small-scale hypothetical transportation problem is solved using nonlinear commercial solver 'Knitro'. Knitro is one of the most powerful and commonly used solver for complex nonlinear optimization problems (Artelys, 2019; Byrd et al., 2006; Ghamami et al., 2016). Therefore, the proposed model is implemented in AMPL and solved using Knitro. However, the current commercial solvers are unable to solve large-scale problems (i.e., a mid-size city in the US). Hence, the metaheuristic algorithms are developed based on the genetic algorithm (GA) and simulated annealing (SA) algorithm to solve large-scale problems. The developed metaheuristics are calibrated and validated using the small-scale network, and their performances are compared using a large-scale network in terms of solution quality and efficiency.

4.4.1 Genetic Algorithm (GA)

The initial input to the real-coded GA includes detailed network data, travel demand, vehicle types, user classes, cost types, and user-defined algorithm parameters (Figure 4.4). The algorithm is initialized by generating a population of n (population size) random solutions (labeled as parent population set (PPS)). The algorithm is then performed for the total number of generations (gen) or until the termination condition is met. In each iteration, the objective function value (OBJ), constraint violation (CV), and fitness value (FV) are estimated for the population of solution. The CV, estimated after normalizing the constraint, is defined as follows:

$$CV = \sum_{e} q_e(x) \tag{102}$$

In which, $q_e(x)$ is the non-negative constraint violation of the normalized e^{th} constraint. If the CV is zero, then the solution is feasible. To estimate FV the penalty-parameter-less approach is adopted, which is an efficient constraint handling method (Deb, 2012, 2000). The FV is defined as follows:

$$FV = \begin{cases} OBJ & if\ CV = 0 \\ OBJ_{max}^{feas} + CV & if\ CV \neq 0 \end{cases} \tag{103}$$

Where, OBJ_{max}^{feas} is the maximum OBJ among all the feasible solutions in a given population set. This method minimizes CV rather than OBJ if no feasible solution exists. Among two feasible solutions, the one with a smaller OBJ has a better fitness value (FV).

In the next step, the selection/reproduction of different solutions is performed based on binary tournament selection without replacement (Deb, 2012). The solution with a lower fitness value has a higher chance of getting selected. Further, this method selects exactly two (binary) copies of the best solution (lowest fitness). The crossover operation is performed on the new

population set (labeled as child population set (CPS)) generated after the selection procedure. This study performs a simulated binary crossover (SBX) operator using a distribution index Φ_c and crossover probability p_c. The SBX is an efficient crossover method for real-coded GA (Deb and Agrawal, 1995). The higher value of Φ_c generates the child solutions closer to the parent solutions. The crossover operation helps in searching the space close to the existing solutions.

Then the mutation operation is performed, which implements parameter-based mutation operation with polynomial distribution (distribution index Φ_m) (Deb, 2012, 2001). The mutation operation ensures that the algorithm avoids getting trapped in locally optimal solutions. The mutation probability (p_m) is limited to small values otherwise it might affect some of the good solutions.

Finally, the survivor selection is performed, which compares the new set of solutions (CPS) with the PPS and chooses the best population of the solution. This new set of best solutions is fed into the next iteration as PPS for the selection, crossover, and mutation process. The algorithm stops if the total number of generations is reached or the termination condition is met. Then, the solution with the lowest fitness is reported as the optimal solution. The flow-chart diagram of the proposed GA is as follows:

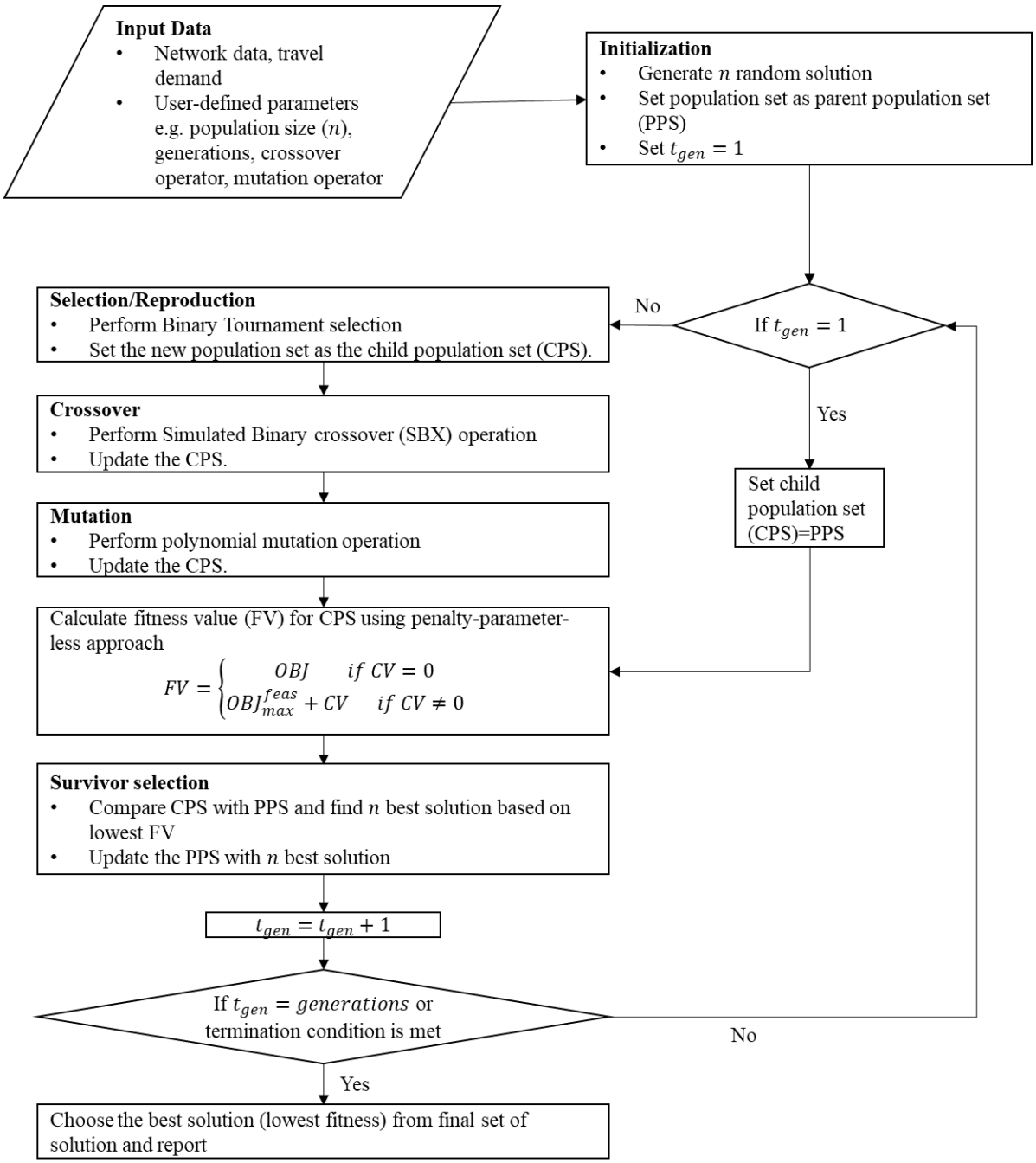

Figure 4.4 Flow chart diagram for Genetic Algorithm

This study proposes a metaheuristic algorithm based on the real-coded genetic algorithm (GA). However, due to the complexity of the proposed model, the GA algorithm takes a considerable amount of time to solve the model. Thus, certain modifications are made to improve

the performance of the metaheuristic algorithm. First, the set of solutions is generated in such a way that the equality constraint in Equation 73 is always satisfied. This is done by assuming a new integer variable $\emptyset_{kod}$ as follows:

$$1 \leq \emptyset_{kod} \leq J_n \tag{104}$$

Where, J_n is the number of vehicle types considered in the study. The algorithm is fed with the input variable $\emptyset_{kod}$ rather than f_{jkod} to optimize the objective function. The variable f_{jkod} is determined based on the estimated value of $\emptyset_{kod}$, as follows:

$$f_{jkod} = \begin{cases} 1 & if\ j = \emptyset_{kod}\ vehicle\ type\ in\ set\ J \\ 0 & otherwise \end{cases} \quad \forall k, \forall o, \forall d, o \neq d \tag{105}$$

Equations 104 and 105 ensures that the constraint in equation 73 is always satisfied. Further, the constraint in equation 75 is used to estimate N_j from the variable γ_j and f_{odjk}, thereby making it always satisfied. These modifications make it easier for GA to find a feasible solution and reduces the time in searching for the feasible set. To further improve the efficiency of the modified GA, a parallelization approach is adopted which involves multiple processors cores (using a cloud cluster of high-performance computers) to perform evaluation operations on the large population set. The algorithm is initialized by generating a population of n (population size) random solutions. These n solutions are equally divided into smaller subsets, which are fed into different computer cores (80-100 computer cores) in a cloud cluster for improving the algorithm speed. The above modifications substantially reduce the time and improve the performance of the GA.

4.4.2 Simulated Annealing (SA)

The SA solution method proposed in this study starts with an initial feasible solution and determines the objective function value for this solution (Figure 4.5). The algorithm includes two

iterative procedures. In the first iteration, a control parameter is reduced (similar to reducing the temperature as annealing in metallurgy) which reduces the probability of accepting worst solution. In the second iterative procedure, the algorithm perturbs the current solution by changing the value of decision variables to get a neighborhood solution. The objective function value of the neighborhood solution is compared with that of the current solution. If the objective function value of the neighborhood solution is better, then the current solution is replaced by the neighborhood solution deterministically. However, if the objective function of the neighborhood solution is worse, then it might replace the current solution probabilistically depending upon the difference in the objective function values. This allows algorithm to avoid getting trapped in local optima (Ghamami et al., 2020a). The current solution is updated based on the objective function value of neighboring solution and existing current solution. Then, in the next iteration another neighboring solution is generated randomly based on the current solution. The probability of accepting a worse solution decreases by adjusting the control parameter through the first iterative procedure to ensure convergence to the best solution. As, the problem is NP hard nonlinear problem, so to improve the performance and time of the SA algorithm, high-tech computers with substantially available RAM is utilized.

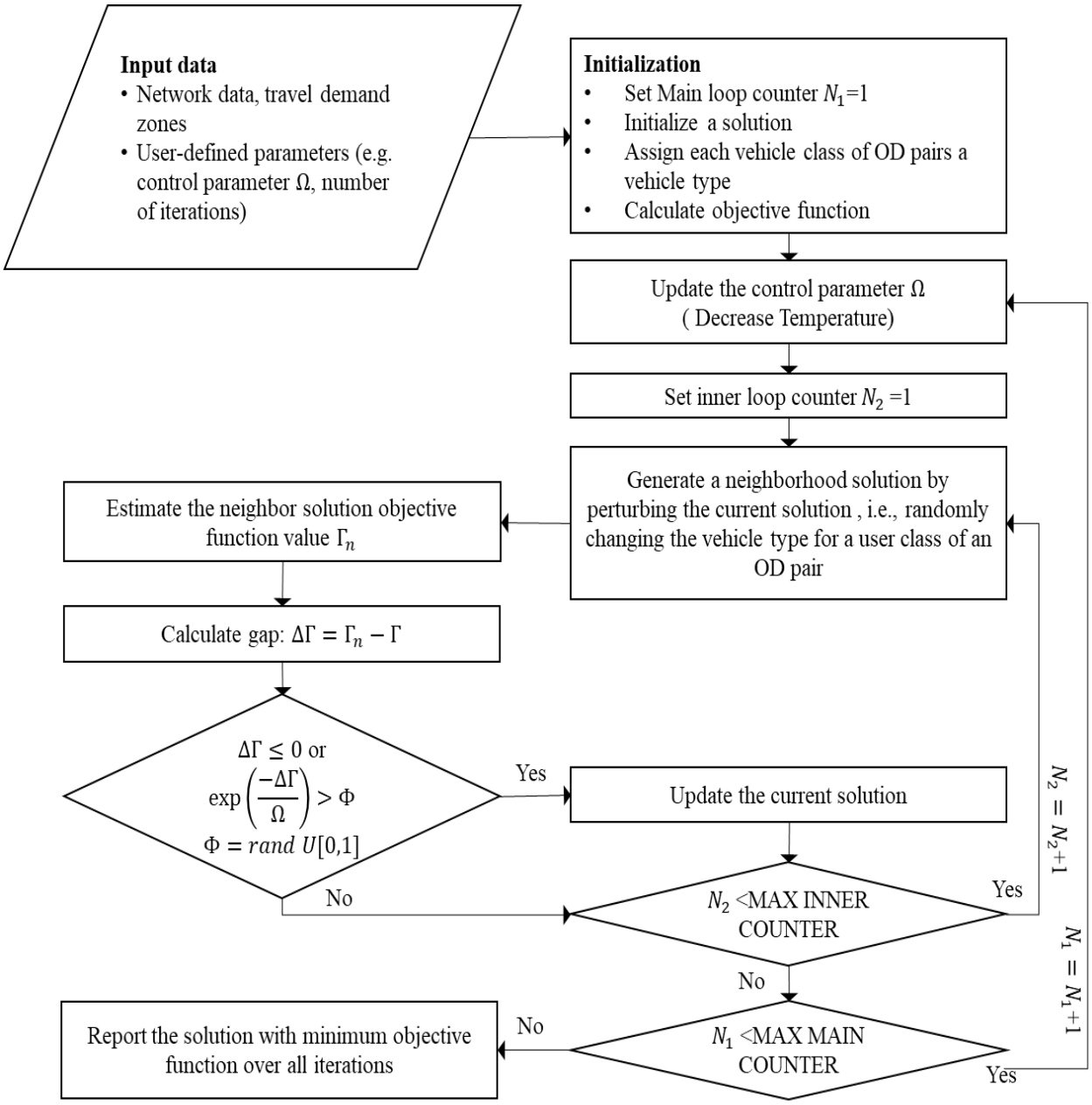

Figure 4.5 Flow chart of Simulated Annealing algorithm

4.5 Numerical Experiments

The modeling framework is implemented for a hypothetical case study and the real-world transportation network of Ann Arbor, Michigan. The values of different parameters for the "Base Scenario" are presented in Table 4.1. The hypothetical case study includes a transportation

network with four zones and three user classes in a mid-sized urban area of the US. These zones are assumed to be equidistant from one another (5 miles). A total of 30,000 trips per day are assumed to be equally distributed among each user class for each OD pair. The city of Ann Arbor consists of 36 Traffic Analysis zones (TAZ) and about 192,169 trips/day (Figure 4.6**)**. The distance between the zones varies from less than 5 miles to up to 23 miles. Further, the study considers three user classes differentiated based on their VOTT, as shown in Table 4.1. The study considers daily trips of a typical weekday in Ann Arbor, being equally distributed among the three user classes. The hypothetical problem is solved using the commercial solver 'Knitro.' However, the network of Ann Arbor cannot be solved using a commercial solver. Hence, metaheuristics are developed to solve the optimization problem for the network of Ann Arbor, Michigan. The metaheuristic algorithms are validated for the hypothetical problem. Finally, these metaheuristics are implemented to produce the results for the Ann Arbor case study network.

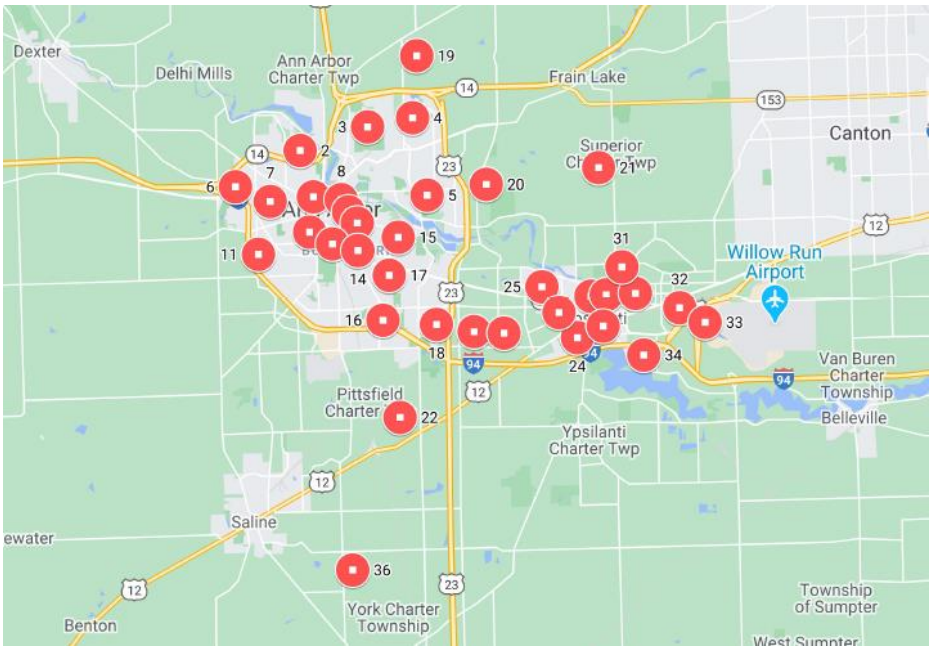

Figure 4.6 Traffic Analysis Zones (TAZ) Centroids in Ann Arbor, Michigan (Ghamami et al., 2019)

4.5.1 Algorithms Performance

The metaheuristic algorithms developed are based on GA and SA algorithms. The algorithms are compared with a commercial solver (Knitro). These algorithms are faster, and the solution is equal to that of the commercial solver for the hypothetical network (Table 4.2). It can be observed that as the size of the problem grows, the commercial solver is unable to solve the problem.

Table 4.2 Result and the Solution Time for different Optimization Techniques

	Case Study- Hypothetical Network		**Case Study- Ann Arbor, Michigan**	
	Objective function ($/day)	**Solution Time (min)**	**Objective function ($/day)**	**Solution Time (min)**
Knitro	294544	17.60	N/A	N/A
GA	294544	0.26	2059454	140.75
SA	294544	0.11	2059681	76.51

For Ann Arbor, the GA algorithm is parallelized using high-performance computers with multiple cores running in parallel (i.e., cloud computing). In contrast, the SA algorithm is implemented using high-tech computers with substantial available RAM. The SA algorithm converges faster (about 55%) than the parallel GA algorithm (Table 4.2 and Figure 4.7). The objective function value for the two algorithms is almost similar, with the value in GA slightly smaller. Thus, the SA algorithm should be used for the optimization problem that requires real-time output. However, to get more accurate results, GA should be used.

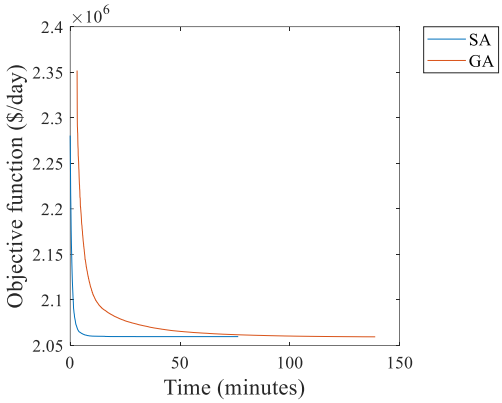

Figure 4.7 Comparison of SA and parallel GA algorithm for Ann Arbor, Michigan

The following subsection presents the results for the base scenario of the Ann Arbor network, followed by the sensitivity analysis for the same Ann Arbor network with respect to different parameters.

4.5.2 Base Scenario for Ann Arbor network

The optimum mode for the different user classes can vary with respect to trip length and depends upon the trade-offs between different factors such as operating costs, traffic congestion, travel time savings, etc. This subsection studies the base scenario considering the specifications and parameters listed in Table 4.1. The optimum mode by each user class for different distances for the base scenario is shown in Figure 4.8. The solution indicates the adoption of EVs (i.e., PMEVs, SAEVs, PAEVs) results in minimum system cost due to low operating costs, and zero tailpipe emissions. The non-electric modes (PMVs, PAVs, SAVs) are not the optimal solution as these result in significant emissions. Further, non-autonomous shared modes (SMVs, SMEVs) are not favorable as these modes pose higher crash costs and additional driver costs as compared to autonomous shared modes (SAEVs). Note that the total number of trips are higher if the adopted modes are autonomous or shared mode which is attributed to improved mobility of the users in these systems.

The lowest VOTT ($20/hr) users should predominantly adopt SAEVs to minimize the system cost (Figure 4.8a). These users can avail the benefits of travel time savings in SAEVs, and prefer waiting for these vehicles rather than incurring the high ownership cost of private modes. Note that, the VOWT is a function of the VOTT of the users. The optimal solution favors the adoption of PMEVs by the second user class (VOTT=$50/hr) over SAEVs, especially for short-distance trips (<10 miles), as the travel time savings are not significant to outweigh the waiting time experienced by users in SAEVs (Figure 4.8b). However, these travel time savings increases with an increase in the distance (>10 miles), making users shift to SAEVs. Further, the PAVs and PAEVs are not favorable for the second user class (Figure 4.8b) because the travel time savings are not significant enough to outweigh the high ownership cost of these vehicles. The optimal solution for the third user class (VOTT= $100/hr) is the adoption of private modes (PAEVs, PMEVs) to avoid the waiting time (Figure 4.8c). Further, the third user class (VOTT=$100/hr) should predominantly adopt PAEVs over PMEVs to avail the benefits of reduced crash cost and travel time savings in the short distance trips (<10 miles). The long-distance trips (>10 miles) of these users (VOTT=$100/hr) shifts to PMEVs over PAEVs because the increased number of trips (due to improved mobility by AVs) increases the operating cost and congestion, which outweighs the travel times savings, and crash reduction benefits in PAEVs (Figure 4.8c).

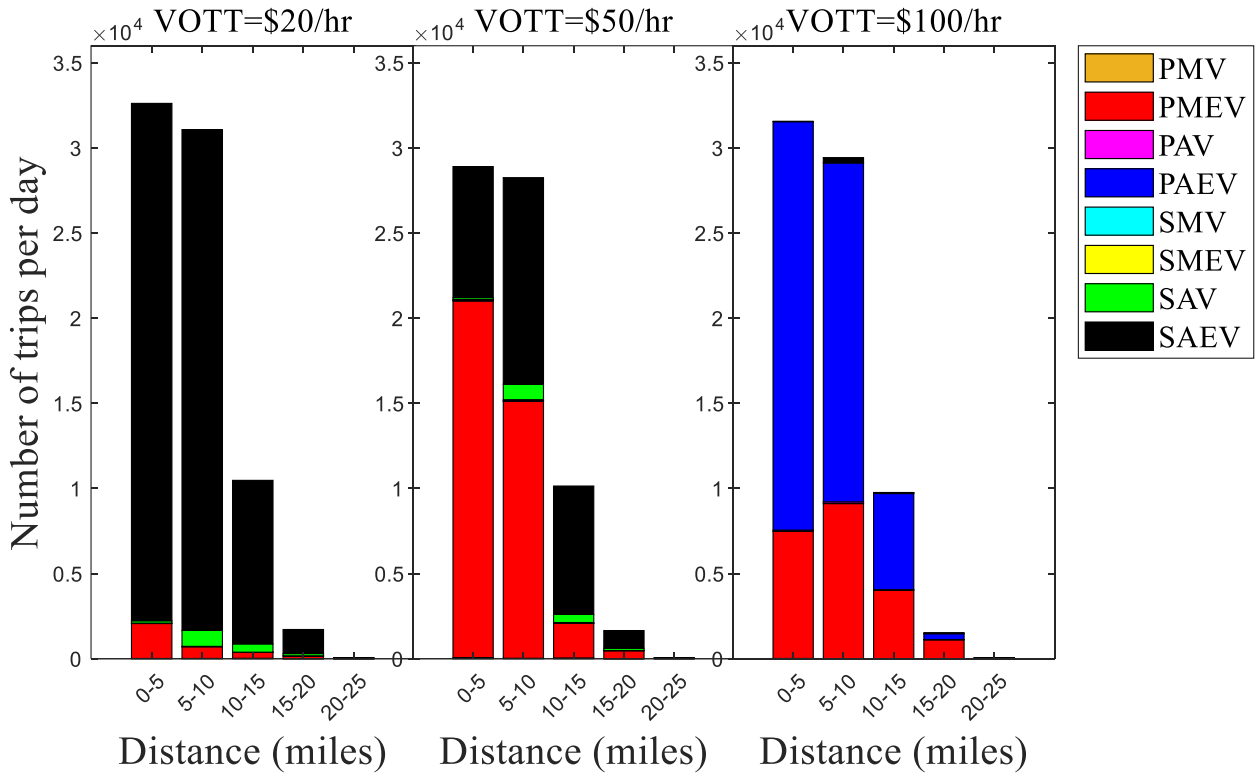

(a) (b) (c)

Figure 4.8 Optimum mode and vehicles type of different user classes for long and short distance commute trips for the base scenario in the Ann Arbor network

4.5.3 Sensitivity analysis of Ann Arbor network with respect to various parameters

The different parameters associated with the adoption of AV and EV will change with increase in market penetration rate of these vehicles. These factors, such as travel time savings, purchase price of vehicle and AV technology cost, would govern the fleet configuration in the system. Further, different stakeholders might be interested in optimum fleet under various scenarios. E.g. system planners would be interested in overall system costs, TNC might be interested in fleet size in carpooling and non carpooling scenario, users might be interested in the costs directly impacting them. The sensitivity analysis with respect to above-mentioned factors for the Ann Arbor, Michigan network are presented in this section.

4.5.3.1 Sensitivity to Reduction factor for VOTT (RVOTT)

The RVOTT represents the most critical factor that captures the ability of the autonomous or shared mobility system to allow users to efficiently use their travel time for other activities rather than driving. These travel time savings can offset the high ownership cost of AVs. The lower value of RVOTT implies greater travel time savings. Thus, the sensitivity of the results to variations of RVOTT, as the technology evolves, are presented in Figure 4.10 (the RVOTT for the base scenario is equal to 0.8 (Singh et al., 2021; van den Berg and Verhoef, 2016)). The dominant optimum vehicles are EVs. It can be observed that the solution shifts to PAEVs as the RVOTT is reduced, which is intuitive due to substantial travel time savings dominating over the high ownership cost and increased congestion (with increased VMT). Further, making these autonomous vehicles electric also reduces the operating costs and emissions in the system.

If there are no travel time savings (RVOTT=1) the optimal solution indicates PMEVs to be the optimal solution for users with high VOTT ($\geq$ 50/hr) due to high ownership cost of private autonomous vehicles (PAVs, PAEVs) and high waiting time cost in the shared mode (Figure 4.10a(ii, iii)). The users with the lowest VOTT ($20/hr) should predominantly adopt SAEVs as these users would not mind waiting (Figure 4.10a(i)). Further, the PMEVs are not dominant for users with low VOTT ($20/hr) because these vehicles have high ownership costs as opposed to the shared mode. Also, the crash cost is higher in PMEVs as opposed to SAEVs.

It is worth noting that the users with the lowest VOTT ($20/hr) should adopt SAEVs as long as the RVOTT is greater than 0.2 (travel time savings less than 80%) because the users with the lowest VOTT would prefer waiting for SAEVs rather than owning these costly vehicles as private modes (Figure 4.10a-d, (i)). The solution shifts to PAEVs at the lowest RVOTT (0.2) for

these users (VOTT=$20/hr) because the travel time savings are considerably high in PAEVs as opposed to SAEVs due to inconvenience caused in the shared mode (Figure 4.10e(i)).

The minimum system cost solution indicates users with VOTT of $50/hr adopting PAEVs over PMEVs only if travel time savings are substantial (RVOTT$\leq$0.6) to outweigh the high ownership cost of these vehicles (Figure 4.10c-e, (ii)). However, lesser travel time savings are required (RVOTT$\leq$0.8) in case of the users with highest VOTT of $100/hr, for the optimal solution to be PAEVs (Figure 4.10b-e, (iii)). Further, users with highest VOTT ($100/hr) may adopt PAEVs for long distance trips (> 10 miles), only if the travel time savings are 40% (RVOTT$\leq$ 0.6), otherwise these vehicles increases congestion and operating cost due to improved mobility in the system. The SAEVs are not the optimal solution for the users with high VOTT ($\geq$$50/hr), because these users would prefer private vehicles rather than waiting for the shared vehicle to pick them up.

Investment in promoting SAEVs is recommended even if there are no travel time savings, provided that the users have low VOTT. The PAEVs adoption will favor the system if there is at least 20% savings in the travel time with amenities onboard. These amenities can be the availability of charging ports, tables, computers, etc., to conduct meetings inside the vehicle or some collection of books, games, novels for recreational activities allowing users to make their travel time productive. The policies can be adopted to encourage the transportation network companies (TNC) to operate the fleet of SAEVs in the regions with denser populations of users with low VOTT or low incomes. Further, to promote the adoption of PAEVs the technology advancements are required to provide onboard amenities in the vehicle such that it provides ambiance to perform other activities e.g., organizing meetings, reading books, or other recreational activities.

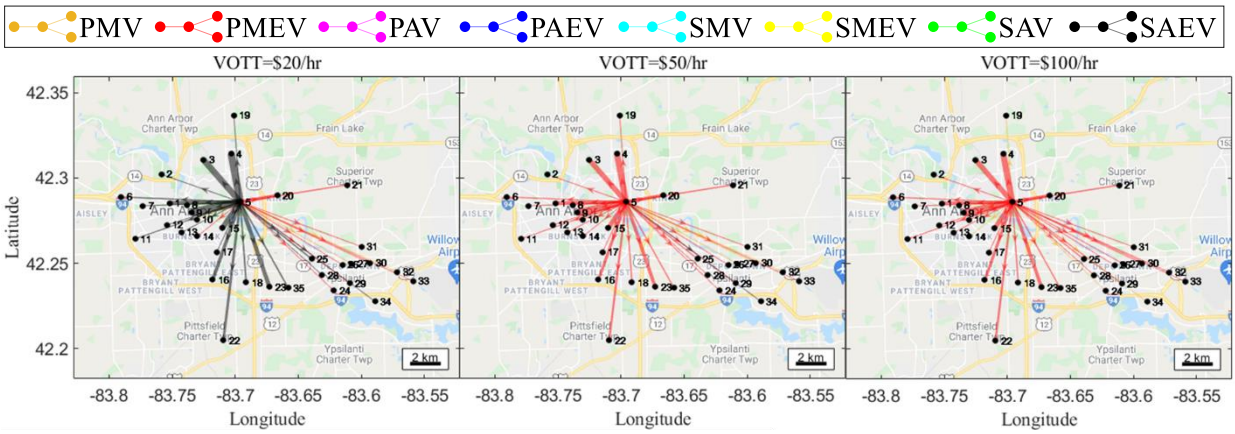

(i) (ii) (iii)

a) RVOTT=1

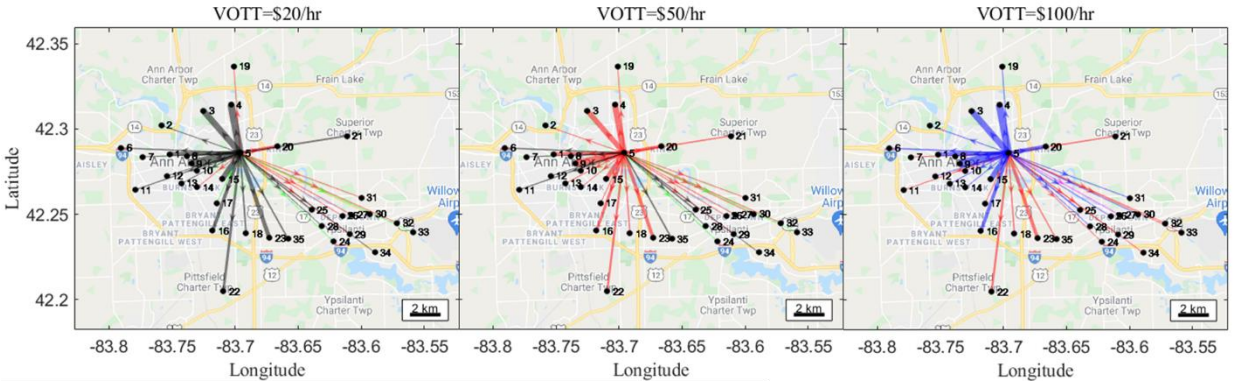

(i) (ii) (iii)

b) RVOTT=0.8

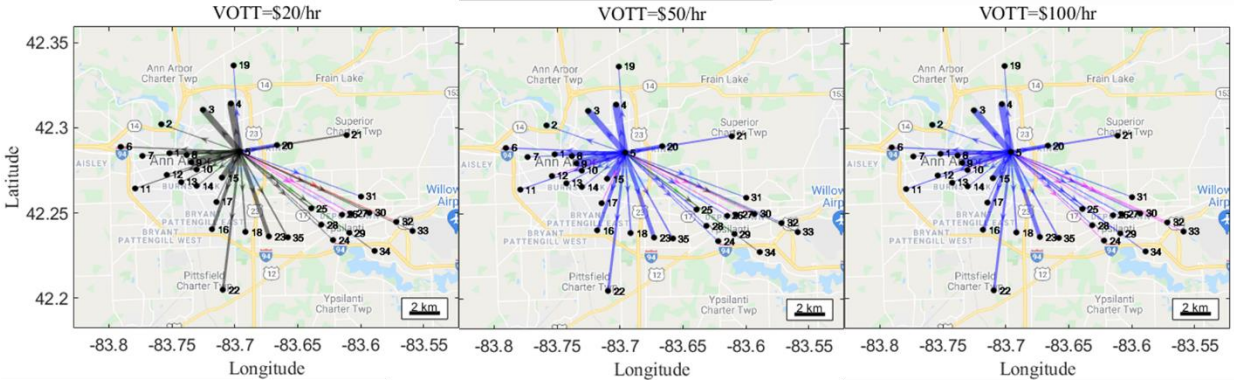

(i) (ii) (iii)

c) RVOTT=0.6

Figure 4.9 Sensitivity analysis of trips from zone 5 (origin) to all the zones for different user classes (i-iii) withwith respect to RVOTT (a-e), in Ann Arbor network

Figure 4.9 (cont'd)

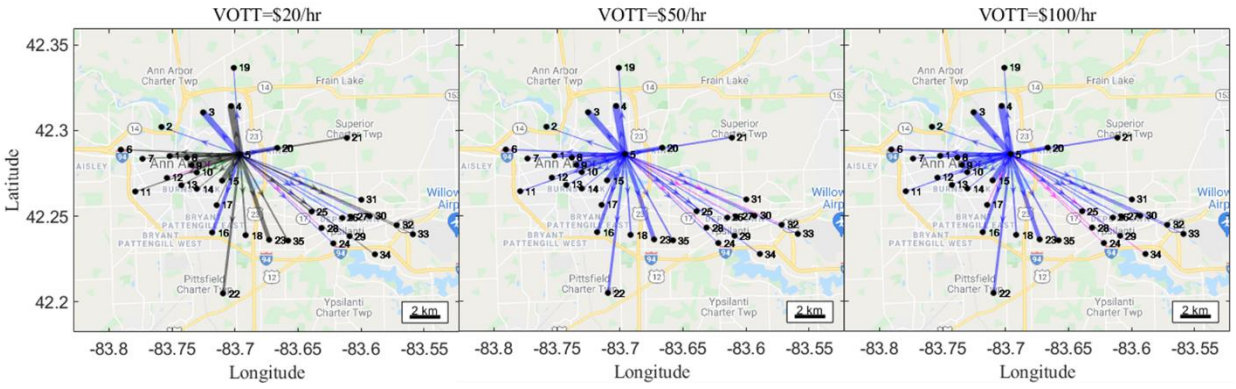

(i) (ii) (iii)

d) RVOTT=0.4

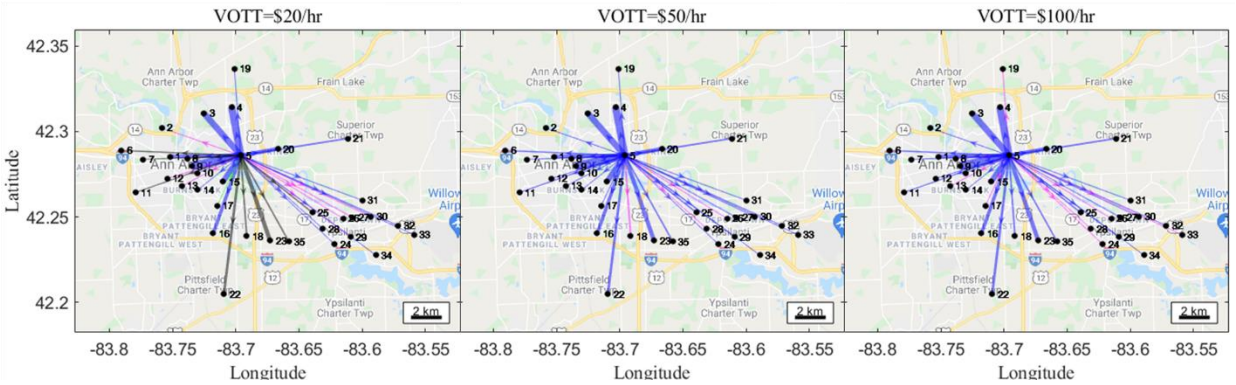

(i) (ii) (iii)

e) RVOTT=0.2

Figure 4.10 Sensitivity analysis of trips from zone 5 (origin) to all the zones for different user classes (i-iii) withwith respect to RVOTT (a-e), in Ann Arbor network

4.5.3.2 Sensitivity to cost of AV technology

The additional cost of AV technology is one of the significant factors governing these vehicles' adoption. The study considers two scenarios: adding AV technology to mid-priced cars ($30,000) that are affordable to most users. The second scenario is adding AV technology to luxurious cars ($80,000), affordable for high-income users. The AV technology cost varies from zero to half of the vehicle price, depending on the amenities provided.

In the scenario with mid-priced cars (Figure 4.11a), the users with the lowest VOTT ($20/hr) should predominantly adopt SAEVs, irrespective of the AV technology cost, due to travel time savings, smaller waiting cost, and reduced ownership cost in shared mode. The users with a VOTT of $50/hr should adopt a mix of SAEVs and PMEVs. The SAEVs would be optimal for

long-distance trips when the travel time savings outweighs the waiting time cost. However, for short-distance trips waiting time is a significant portion of total trip time and travel time savings are not enough in SAEVs making users (VOTT=$50/hr) switch to PMEVs. Further, the optimal solution for these users is PAEVs only if there is no additional cost of AV technology. The optimal solution for the third user class (VOTT=$100/hr) would predominantly be PAEVs until the price of the AV technology cost is greater than one-third of the vehicle price. At a higher cost (half of the vehicle price), the travel time savings do not outweigh the high ownership cost of PAEVs, and these users (VOTT=$100/hr) switch to PMEVs. Note that the PAEVs are the optimal solution at low AV technology cost even though PAEVs are more expensive than PAVs due to low operating costs and zero tailpipe emissions.

In the scenario with luxurious cars (Figure 4.11b), the system cost would be minimum if the fleet composition has SAEVs and PMEVs for the AV technology cost greater than zero. The users with high VOTT($100/hr) should adopt PMEVs to avoid waiting in the shared mode. The users with VOTT $\leq$ $50/hr should predominantly adopt SAEVs for the system cost to be minimum. The SAEVs provide benefits such as travel time savings, reduced ownership cost, the reduced crash cost that dominates the waiting time cost. Further, the PMEVs are expensive to afford due to high vehicle prices in addition to the added battery cost, which is significant in private mode. As the AV technology cost is reduced to zero, users with high VOTT ($100/hr) should shift to PAEVs due to substantial travel time savings.

The adoption of AV technology is recommended in shared electric mode for the users with low VOTT ($\leq$$50/hr) even if the price of AV is substantial (30-50% of the vehicle price). The users with the highest VOTT ($100/hr) should preferably adopt PAEVs unless the vehicle price and AV technology cost are substantial, making these users shift to PMEVs for minimum system

cost. The policies should be adopted to promote autonomous and electric vehicles together to ameliorate and enhance each other's effects. The low operating costs of EVs offset the high ownership cost of AVs. Further, the ownership cost can be further reduced if these vehicles are adopted as a shared mode, which can be utilized by low-income groups. The technology advancements are further needed to be improved in order to adopt these vehicles as private modes so that the cost of AV technology should come down to at least one-third of the vehicle prices. In the case of luxurious cars, the cost of AV technology should be negligible relative to the price of the vehicle to be adopted as private modes.

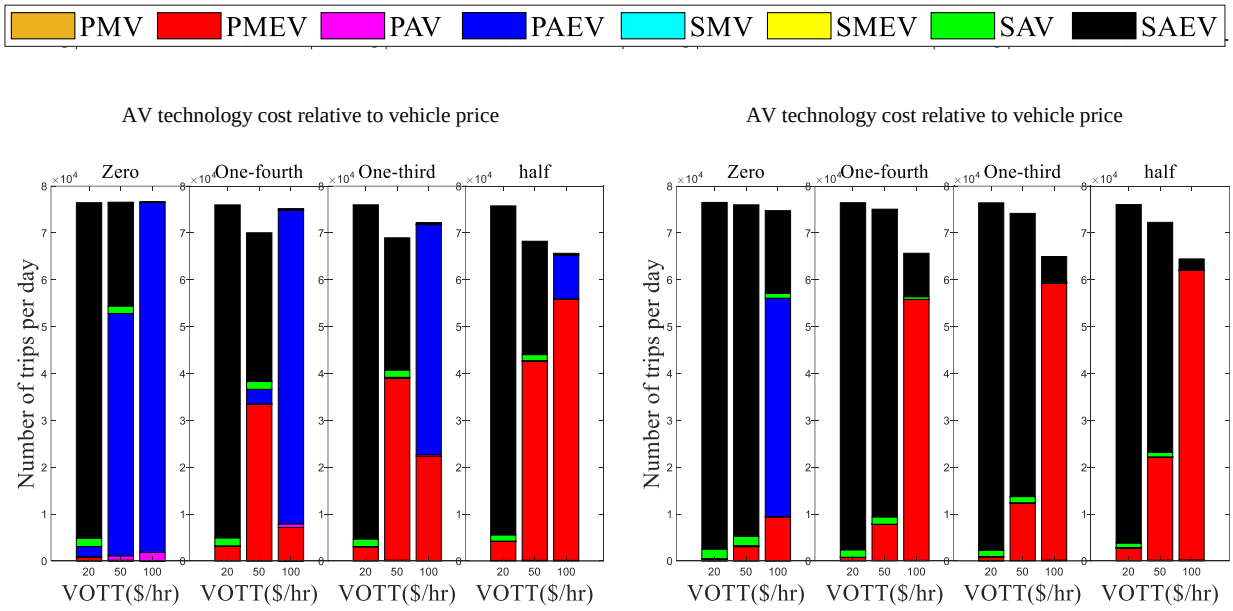

a) Mid-prices cars ($30,000) b) Luxurious cars ($80,000)

Figure 4.11 Sensitivity analysis of optimum vehicle type for different user classes with respect to AV technology cost for the mid-price car (a) and luxurious car (b), in Ann Arbor network

4.5.3.3 Sensitivity with respect to replacement rate and carpooling

The replacement rate of the shared modes is an essential factor that governs the fleet size requirement relative to the total number of trips. It affects the empty miles, users' waiting time, and cold-start emissions. In addition, carpooling reduces the fleet size requirement (increasing the

replacement rate) and reduces the empty miles, while increasing waiting time of users sharing the same ride. Hence, the sensitivity analysis with respect to replacement rate for carpooling and non-carpooling scenario is presented in this subsection. In the carpooling scenario 20% of the users are assumed to share the ride (base scenario) and in non-carpooling scenario it is assumed that no two users share the same ride.

The result shows that the SAEVs are less likely to be optimal solution with an increase in the replacement rate due to an exponential increase in the empty miles and users' waiting time (Figure 4.12). Hence, the fleet size should be provided as large as the number of vehicle trips in the system, resulting in replacement rate as low as possible. Further, if the replacement rate is lower (≤ 6), the trips served by SAEVs are lower in the carpooling scenario (Figure 4.12a) as compared to the non-carpooling scenario (Figure 4.12b). The user's waiting time increases with the carpooling due to extra time to pick up users sharing the same ride. However, at a higher replacement rate (≥ 9), the carpooling substantially reduces the empty miles generated, which dominates over extra waiting time added for carpooling. Thus, the number of trips served by SAEVs increases in the carpooling scenario (Figure 4.12a) relative to the non-carpooling scenario (Figure 4.12b) due to a reduction in the empty miles generated.

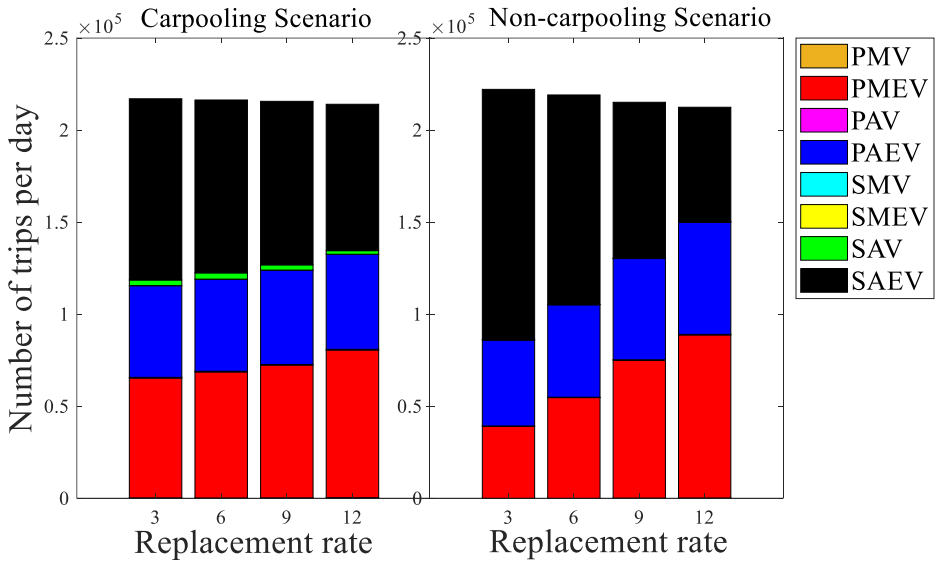

(a) (b)

Figure 4.12 Optimum vehicle type under different replacement rate (fleet size) for (a) carpooling and (b) non-carpooling scenario for the Ann Arbor network

Hence, the fleet size of the shared mode should be as large as the number of vehicle trips in the system. The larger fleet size or lower replacement rate reduces the users' waiting time as well as empty miles, which reduces the normalized ownership cost and the operating cost. Further, this larger fleet size is also favorable to TNCs because although the upfront cost would be higher but each of these vehicles would have less operating costs, which extends the effective life of these vehicles. A higher replacement rate or a reduced fleet size should preferably be adopted in the regions where users are more willing to share their rides. The TNC should deploy its fleet size considering the above factors. Note that the non-carpooling component of the replacement rate is the decision variable of the optimization problem. The optimal solution always sets this component to the lower bound value, which indicates that the cost associated with an exponential increase in empty miles and user's waiting time dominates the reduction in the cost associated with decrease in the cold-start emissions (or zero tailpipe emissions in EVs). Hence, the sensitivity results presented here are obtained by setting the lower bound of the replacement rate (decision variable)

to higher values. Further, the replacement rate in Figure 4.12 accounts for the reduction in the fleet size by both the non-carpooling and carpooling components.

4.5.3.4 Optimal solution without considering emissions

The EVs are favored to be included in the optimal solution due to their zero tailpipe emissions. In this subsection, we minimize the system cost without considering emissions to capture the shift in the optimal solution ignoring this societal cost.

Figure 4.13 indicates that the solution changes significantly if we do not consider emissions. Users with the lowest VOTT ($20/hr) should adopt SAVs to minimize the system cost as these users would not mind waiting for these vehicles and avail the benefits of travel time savings (Figure 4.13a). Further, the private and electric modes are not preferable due to the high ownership cost. Users with VOTT $50/hr should adopt a mix of SAVs, PMEVs, PMVs (Figure 4.13b). The SAVs should be adopted for long-distance trips to avail benefits of substantial travel time savings and insignificant waiting time. However, the travel time savings are not significant to outweigh waiting time cost for short-distance trips, and the users should switch to private modes. The PMEVs, PMVs should be adopted for short-distance trips by users with VOTT $50/hr, with most of the trips by PMEVs due to low operating costs compared to PMVs. The PAVs, PAEVs are not part of the optimal solution because of their high ownership cost. The users with high VOTT ($100/hr) predominantly adopt PAVs due to substantial travel time savings and reduced crash cost (as opposed to non-AVs), and no waiting time (as opposed to shared mode) (Figure 4.13c). Further, the PAEVs do not minimize the system cost as these contribute to additional battery costs, which increases the ownership costs.

In conclusion, the proper policies should be implemented to make users adopt environmental-friendly vehicles (EVs) to favor the system. This can be done by imposing carbon taxes, providing rebates over the purchase of EVs, developing adequate charging infrastructure, etc.

4.5.3.5 Optimal solutions considering costs directly impacting users

The users' main goal is to fulfill their trips with maximum benefits. Hence, it is crucial to estimate the optimal solution considering the costs directly impacting the users. These costs include travel time, waiting time, ownership, operating, and driver costs. The optimal solution is shown in Figure 4.14. The users with lowest VOTT ($20/hr) predominantly adopts SAVs due to low ownership cost, less waiting time, and travel time savings SAVs (Figure 4.14a). The users with high VOTT (≥ $50/hr) predominantly adopt PMEVs, which is attributed to low operating costs (as opposed to PMVs), low ownership cost (as opposed to PAVs, PAEVs), and no waiting time (as opposed to shared mode) (Figure 4.14b,c). The PAVs are adopted by some users with a high VOTT of $100/hr due to substantial travel time savings (Figure 4.14c). Further, some of the trips for the users with VOTT $50/hr are fulfilled by SAVs due to travel time savings, low ownership cost, and smaller waiting time costs (Figure 4.14b).

Hence, the users with low VOTT prefer to adopt SAVs availing the benefits of autonomy without owning these vehicles. Certain policies should be adopted to encourage TNCs to operate the fleet of SAVs in the regions with denser populations of users with low VOTTs or low incomes. Users with high VOTTs predominantly prefer PMEVs. Hence, the adoption of EVs should be promoted by providing adequate charging infrastructure and eliminating the human factors which are difficult to capture, such as range anxiety, and concerns for being stranded for long time at the charging stations.

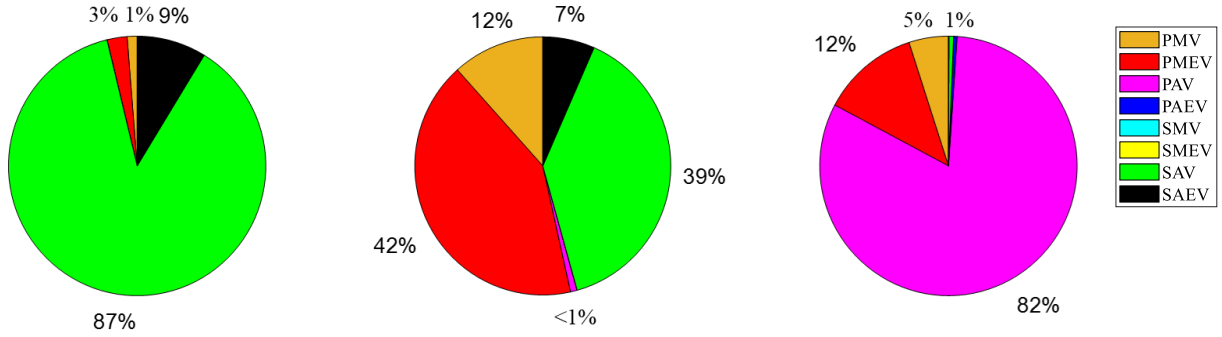

a) VOTT=$20/hr b) VOTT=$50/hr c) VOTT=$100/hr

Figure 4.13 Optimal solution for different user classes for scenario without considering emission costs in Ann Arbor, Michigan

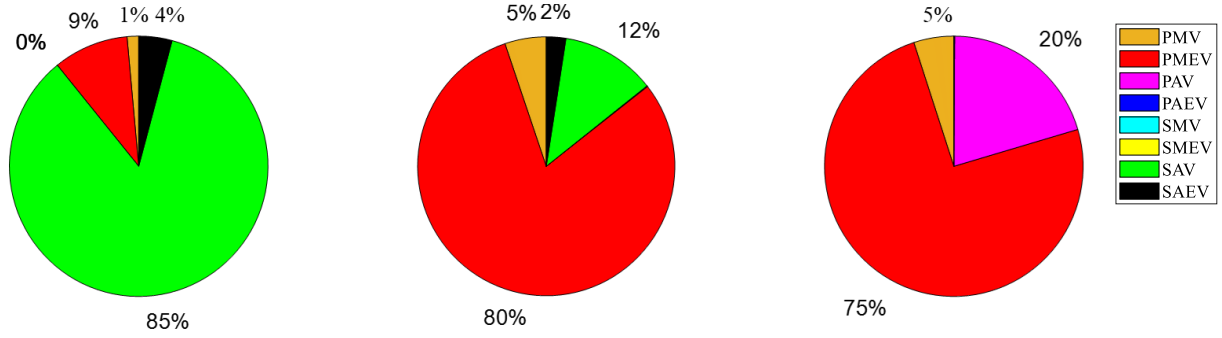

a) VOTT=$20/hr b) VOTT=$50/hr c) VOTT=$100/hr

Figure 4.14 Optimal solution for different user classes while minimizing the costs directly impacting users in Ann Arbor, Michigan

4.6 Summary

AV technology provides various potential benefits such as improved safety, mobility, roadway capacity, and driver productivity. One of the outcomes of these benefits is the increased VMT in the system, which will increase emissions and operating costs and affect the total system travel time. The cost of owning these vehicles is also high due to added cost of AV technology. The emissions and operating costs can be significantly reduced with the adoption of EVs. However, EVs have a limited range, higher battery price, and limited refueling infrastructure. In

light of these, AV and EV technology adoption in the shared mobility systems would be a promising solution. However, the shared mobility systems generate additional empty miles in the system and waiting time for users. Furthermore, the impact of these technologies would vary for different user classes defined based on their VOTT attributed to their income levels. This study builds a modeling framework to capture the trade-offs associated with emerging technologies/systems, and estimates the optimum fleet configuration of these technologies with the minimum total system cost, considering both private and shared mobility systems. A fleet optimization problem is developed in a multiclass user system to minimize the system cost, including emission, ownership, operating, travel time, waiting time, crash, and driver costs. The solution to the optimization problem provides fleet configuration of different vehicle types (PMV, PMEV, PAV, PAEV, SMV, SMEV, SAV, SAEV), which is also specific to various user classes having different VOTT or income levels. The developed metaheuristic algorithms based on GA and SA are validated using a hypothetical problem and then implemented to solve the NP-hard nonlinear real-world optimization problem (Ann Arbor, Michigan). The main findings from the research are as follows:

- The optimal solution is a combination of private and shared mobility and is sensitive to VOTT of the users, trip lengths, RVOTT, AV technology cost, ownership cost, replacement rate, emissions, and user-specific costs.
- The GA and SA algorithm both converge to a similar solution for smaller case studies. SA algorithm is twice faster than the GA. However, the GA provides a smaller objective function for larger case studies.
- The EVs are recommended as the optimal solution for the system due to their low operating costs, and zero tailpipe emissions. Hence, policies should be adopted to promote EV by

providing adequate charging infrastructure, rebates over the purchase of EVs, and imposing carbon taxes.

- Electrifying AVs would lower the operating cost that offsets their high ownership cost. Hence, policies should be adopted to promote vehicle automation and electrification together.
- SAEV adoption is recommended for users with low VOTT ($20/hr) even if there are no travel time savings or the price of AV technology is substantial. Hence, these should be deployed in regions with a denser population of low VOTT/low income groups.
- SAEVs are also recommended for users with VOTT of $50/hr, only if the trip length is greater than 10 miles.
- PMEVs are recommended for the short distance trips (<10 miles) of users with mid VOTT ($50/hr), and long distance trips (>10 miles) of users with high VOTT ($100/hr).
- PAEVs are recommended for short distance trips (<10 miles) of users with VOTT of $100/hr. In long distance trips (>10 miles) of these users (VOTT=$100/hr), the travel time savings of at least 40% ($RVOTT \leq 0.6$) is required for these trips to be PAEVs.
- Adoption of PAEVs may also be favorable for users with high VOTT ($100/hr) if the AV technology cost of a mid-priced car ($30,000) is reduced to at least one-third of the vehicle price. The AV technology deployment cost for luxurious cars ($80,000) is relatively negligible compared to the vehicle price, resulting PAEVs to be favorable to users with high VOTT ($100/hr).

- Technology advancements are required for promoting AVs as private mode so that the AV technology cost is reduced or the amenities onboard are improved, allowing efficient use of travel time through meetings, reading, or recreational activities.
- The fleet size of the shared mode should be as large as the number of vehicle trips in the system to avoid the exponential increase in empty miles generated, and the user's waiting time. Further, this large fleet size would also reduce operating cost and increase service life (in years) of each of the vehicles.
- The carpooling is favorable to the system if and only if the fleet size is such that the replacement rate is greater than 9, below which the extra waiting time in carpooling increase the system cost.
- Considering the costs directly impacting the users, the users with low VOTT or low incomes prefer SAVs. Users with high VOTT predominantly prefer PMEVs due to the low operating costs of EVs and no waiting time. Hence, the adoption of EVs should be promoted by eliminating uncaptured human factors, such as range anxiety and waiting at charging stations.

CHAPTER 5 DISTRIBUTED ENERGY RESOURCES TO SUPPORT EVS' FAST CHARGING STATIONS

5.1 Overview

The rapid growth in the market acceptance of EVs requires a well-developed network of DCFC stations. However, this network of DCFC stations along with the increased electric miles traveled will increase the electricity demand and affect the electric grid stability, supply-demand imbalance, and degradation of the electric grid distribution system. It is important to consider investment in technologies at these charging stations to support the EV charging demand and reduce the load on the electric grid. This study develops a framework to considers the capacity constraints of the electric grid network, the existing energy demand, the EV charging demand, and different types of DER to find the optimal investment technology at DCFC stations.

The remainder of this study is as follows. Section 5.2 discusses the problem statement and objective of the study, followed by the modeling framework in section 5.3. Section 5.4, 5.5, and 5.6 discusses the data collection, results of the numerical experiment, and the summary of the study.

5.2 Problem statement

The increasing market penetration rate of electric vehicles would necessitate the deployment of DCFC charging station network. This network of DCFC chargers will not only reduce the charging time but will also reduce/eliminate concerns related to the limited range of EVs. However, it will increase the load on the electric grid network causing supply-demand imbalance, and degradation of the electric grid system. The electric grid transmission and distribution system, which includes transmission lines, substations, feeder lines, segment etc.,

might need to be upgraded to support the rising EV charging demand. The investment cost to upgrade these can be substantial depending upon the location of DCFC stations and the arrival rate of EVs. However, the provision of DER such as ESS, solar panels, etc. can support the EV charging demand, reduce the load on the electric grid, and also reduce the electric cost. This study aims to estimate the optimum investment technology to support the rising EV charging demand. The study estimates the critical locations that would require the provision of DER which depends upon the EV charging demand, existing electricity demand, and the capacity constraints of the electric grid network. The study estimates the optimum type of DER for each of the DCFC locations depending upon the investment cost, electricity cost savings, and overall savings in the system cost. The study also captures the seasonal effect on the performance of these different types of DER. The detailed modeling framework to address the above-mentioned problem statement is presented in the following subsection.

5.3 Methodology

This study proposes an optimization modeling framework with an aim to find the optimal investment technology to support the fast charging demand of EVs. An optimization problem is developed to minimize the system cost which includes the project cost of NB/SLB Battery ESS (BESS), Flywheel ESS (FESS), and solar panels (if any), electric grid upgrade cost (i.e., cost of bringing electricity to the EV charging station, segment upgrades, feeder line upgrades, substation upgrades, and transmission upgrades), and the total cost of energy for refueling electric vehicles. It is worth noting that the project cost includes the cost of ESS (battery packs, flywheels, etc.), the balance of plant, inverter cost, construction cost, cost of solar panels, racking of solar panels, electrical balance of system, installation cost, etc. This study also considers the possibility of transmitting excess energy stored/generated (other than that required for EV charging) back to the

electric grid network, which reduces the overall electricity purchase cost as well as the system cost. The decision variables are the capacity of li-ion NB/SLB battery (BS^i), capacity of the flywheels (FS^i), area of the solar panels (A^i), additional feeder line capacity (AF^j), additional substation capacity (AS^k), additional subsegment/segment capacity (AG^i) to support EV charging demand at location i. The superscripts $i, j, k, and\ l$ represents segments/subsegments, feeder line, substation, and the transmission line, respectively. The study considers a discrete time-dependent energy model with a step size of τ. The EV charging demand depends upon the arrival rate of EVs throughout the day. The different notations used are presented in Table 5.1. The schematic diagram of the electric grid network is shown in Figure 5.1. The input data is fed into the optimization model to estimate the optimum investment technology with maximum cost savings.

The inputs and the outputs to the model are listed as below:

Inputs

1. Demand distribution over the entire electric grid network
    a. Spatiotemporal EV charging demand
    b. Spatiotemporal existing electricity demand
2. Electric grid network details of segment/subsegment, feeder line, substation, transmission line
    a. Spatial capacity
    b. Cost of upgrading
    c. Connections and locations
    d. Spatiotemporal time of use electricity rate
    e. Life of the grid components
3. Distributed energy resources (Li-ion NB BESS, Li-ion SLB BESS, FESS, solar panels)

a. Performance and charging/discharging rate

b. Unit cost of investment (includes installation, BOS, inverters etc.)

c. Life

Outputs

1. Distributed Energy Resources (Li-ion NB BESS, Li-ion SLB BESS, FESS, solar panels)
    a. Size
    b. Location
    c. Time dependent charge/discharge profile and power output
2. Electric grid network
    a. Additional capacity requirement of upgrading subsegment, feeder line, substation, transmission line
3. Investment cost & savings

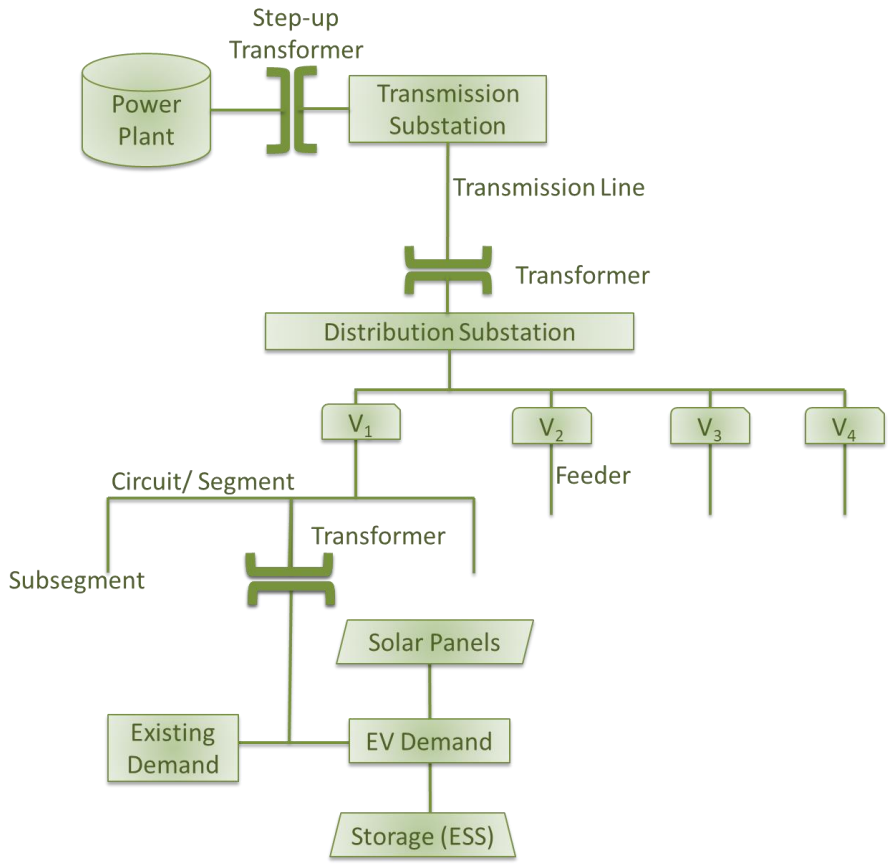

Figure 5.1 Flow chart diagram of electric grid network

Table 5.1 Nomenclature

Sets	**Definition**
$t \in \Gamma$	Set of time intervals
$i \in I$	Set of segments/subsegments
$j \in J$	Set of feeder lines
$k \in K$	Set of substation locations
$l \in L$	Set of transmission lines
$m \in M$	Set of seasons (summer, winter)
Decision variable	**Definition**

Table 5.1 (cont'd)

BS^i	Size of BESS at location *i* (kWh)
FS^i	Size of FESS at location *i* (kWh)
AG^i	Additional subsegment/segment capacity (kW)
AF^j	Additional feeder line capacity (kW)
AS^k	Additional substation capacity (kW)
AT^l	Additional transmission capacity (kW)
A^i	Area of the solar panel at location i (sq.m)

State variables	**Definition**
BE_t^{im}	Battery energy at time *t* and location i for the season *m* (kWh)
BP_t^{im}	Battery charging demand at time *t* +/- and location *i* for the season *m* (kW)
FE_t^{im}	Flywheel energy at time *t* and location i for the season *m* (kWh)
FP_t^{im}	Flywheel charging demand at time *t* +/- and location *i* for the season *m* (kW)
π_t^{im}	Power delivered to flywheel including self-discharge losses (kW)
Ψ^i	Maximum power of flywheel required (kW)
SP_t^{im}	Solar panel power at any time t and location *i* for the season *m*
EL_t^{im}	Net energy required/available from/to the electric grid by the EV charging station
α_t^{im}	Binary variable indicating if the energy is inflow (1) or outflow(0)
β_t^{im}	Binary variable indicating if the battery (1) or the flywheel (0) is selected
ω^i	Binary variable to ensure no power delivered to flywheel if it's not selected.

Table 5.1 (cont'd)

Parameters	Definition
CB	Unit project cost of battery ($/kWh)
CK	Unit project cost per kWh of FESS ($/kWh)
CL	Unit project cost per kW for FESS ($/kW)
CI	Unit project cost of solar panel ($/kW)
CG	Unit cost of subsegment/segment ($/kW)
CF	Unit cost of the feeder line ($/kW)
CS	Unit cost of substation ($/kW)
CT	Unit cost of transmission line ($/kW)
H	Life of the transmission line (years)
U	Life of substation (years)
V	Life of feeder line (years)
X	Life of segment (years)
Y	Life of solar panel (years)
Z	Life of BESS (years)
Q	Life of FESS (years)
R_t^{im}	Electricity rate at time t in the season m for location i ($/kWh)
O_t^{im}	Outflow rate at time t in the season m for location i ($/kWh)
FR^i	Fixed electricity rate for the base electricity provision cost
ED_t^{im}	EV charging demand (kW)
D_t^{im}	Demand at location i at time t in season m (kW)
G^i	Subsegment/segment capacity (kW)
F^j	Feeder line capacity (kW)

Table 5.1 (cont'd)

S^k	Substation capacity (kW)
T^l	Transmission capacity (kW)
CP	Maximum charging power of BESS (kW)
DP	Maximum discharging power of BESS (kW)
$A^{i,max}$	Maximum allowable size of solar panel based upon site conditions (sq.m)
$BS^{i,max}$	Maximum allowable size of BESS based upon site conditions (kWh)
$FS^{i,max}$	Maximum allowable size of flyhweel ESS based upon site conditions (kWh)
SR_t^{im}	The solar radiation intensity at location i and time t for the season m (kW/m^2)
w_t^{im}	Cloud coverage at any time t in season m for the location i
$q_n(w_t^{im})$	The calibrated parameters for solar radiation intensity dependent on w_t^{im}
μ^m	Length of the season m (days)
λ_t^{jm}	Self discharge loss in FESS(kW/hr)
η^j	Energy density of flywheel (kWh/m^3)
ϑ^j	Power density of flywheel (kW/m^3)
Λ	A very large number
Δ	Maximum state of charge of BESS
δ	Minimum state of charge of FESS
τ	Length of each time interval (hour)
θ^{ij}	Whether subsegment/segment *i* is on feeder line *j*
Ξ^{jk}	Whether feeder line *j* is connected to substation *k*

Table 5.1 (cont'd)

σ^{kl}	Whether transmission line *l* is connected to substation *k*
ρ^i	The efficiency of the solar panel at location i
ϕ_t^{im}	The sun's elevation angle at time t in season m for the location i

5.3.1 Optimization Model

The objective function includes the purchase cost of energy from the electric grid, and investment in DER technologies such as ESS (NB/SLB, flywheels), solar panels, and electric grid upgrades. The overall optimization problem is defined as follows:

$$\min \sum_{i\in I}\left(\beta^i \frac{CB\times BS^i}{Z} + \left(1-\beta^i\right)\frac{CK\times FS^i + CL\times \Psi^i}{Q}\right) + \sum_{i\in I}\frac{CI\times \rho^i A^i}{Y} +$$

$$\sum_i \frac{CG\times AG^i}{X} + \sum_{j\in J}\frac{CF\times AF^j}{V} + \sum_{k\in K}\frac{CS\times AS^k}{U} + \sum_{l\in L}\frac{CT\times AT^l}{H} + \quad (106)$$

$$\sum_{i\in I}\sum_m \mu^m \sum_{t\in\Gamma}\left(EL_t^{im}(\alpha_t^{im}R_t^{im} + (1-\alpha_t^{im})O_t^{im}) + FR^i\right)$$

s.t.

Supply-Demand constraints

$$G^i + AG^i + SP_t^{im} \geq D_t^{im} + ED_t^{im} + BP_t^{im} + \pi_t^{im} \qquad \forall t\in\Gamma, i\in I, m\in M \quad (107)$$

$$\sum_i\left(G^i + AG^i\right)\theta^{ij} \leq F^j + AF^j \qquad j\in J \quad (108)$$

$$\sum_j\left(F^j + AF^j\right)\Xi^{jk} \leq S^k + AS^k \qquad k\in K \quad (109)$$

$$\sum_k (S^k + AS^k)\sigma^{kl} \leq T^l + AT^l \qquad l\in L \quad (110)$$

$$\left(ED_t^{im} + BP_t^{im} + \pi_t^{im} - SP_t^{im}\right)\left(\alpha_t^{im} - 0.5\right) \geq 0 \qquad \forall t\in\Gamma, i\in I,\ m\in M \quad (111)$$

Battery storage constraints

$$BE_t^{im} = BE_{t-1}^{im} + BP_t^{im}\tau \qquad \forall t = 2,\dots,\Gamma,\ i\in I, m\in M \quad (112)$$

$$BE_1^{im} = BE_T^{im} + BP_1^{im}\tau \qquad \forall\, i \in I, m \in M \qquad 113$$

$$\delta \times BS^i \leq BE_t^{im} \leq \Delta \times BS^i \qquad \forall t \in \Gamma, i \in I, m \in M \qquad 114$$

$$-DP \leq BP_t^{im} \leq CP \qquad \forall t \in \Gamma, i \in I, m \in M \qquad 115$$

Flywheel storage constraints

$$FE_t^{im} = FE_{t-1}^{im} + FP_t^{im}\tau \qquad \forall t = 2, \dots, \Gamma,\ i \in I, m \in M \qquad 116$$

$$FE_1^{im} = FE_T^{im} + FP_1^{im}\tau \qquad i \in I,\ m \in M \qquad 117$$

$$0 \leq FE_t^{im} \leq FS^i \qquad \forall t \in \Gamma, i \in I,\ m \in M \qquad 118$$

$$-\Psi^i \leq FP_t^{im} \leq \Psi^i \qquad \forall t \in \Gamma, i \in I\ ,\ m \in M \qquad 119$$

$$\Psi^i \eta^i \leq FS^i \vartheta^i \qquad i \in I\ ,\ m \in M \qquad 120$$

$$FP_t^{im} = \pi_t^{im} - \omega^i \lambda_t^{im} \qquad \forall t \in \Gamma, i \in I,\ m \in M \qquad 121$$

$$FS^i\ \leq \Lambda \omega^i \qquad \forall t \in \Gamma, i \in I,\ m \in M \qquad 122$$

Solar panel power generation

$$0 \leq SP_t^{im} \leq \rho^i A^i SR_t^{im} \qquad \forall t \in \Gamma, i \in I, m \in M \qquad 123$$

Feasibility constraints

$$AG^i \geq 0 \qquad i \in I \qquad 124$$

$$AF^j \geq 0 \qquad j \in J \qquad 125$$

$$AS^k \geq 0 \qquad k \in K \qquad 126$$

$$AT^l \geq 0 \qquad l \in L \qquad (127)$$

$$BS^i, FS^i, \Psi^i \geq 0 \qquad i \in I \qquad (128)$$

$$0 \leq BS^i \leq BS^{i,max} \qquad i \in I \qquad (129)$$

$$0 \leq FS^i \leq FS^{i,max} \qquad i \in I \qquad (130)$$

$$0 \leq A^i \leq A^{i,max} \qquad i \in I \qquad (131)$$

$$\omega^i, \alpha_t^{im}, \beta^i \in \{0,1\} \qquad \forall t \in \Gamma, i \in I,\ m \in M \qquad (132)$$

The terms in the objective function represent the investment cost of BESS (NB/SLB), FESS, solar panels, segment upgrades, feeder line upgrades, substation upgrades, transmission line upgrades, and the cost of purchasing/selling the electricity from/to the electric grid, respectively. The terms $CB, CK, CL, CI, CG, CF, CS\ and\ CT$ are the unit project cost of BESS, project cost per FESS energy capacity, project cost per FESS power capacity, unit project cost of solar panel, and unit upgrade costs of segment, feeder line, substation, and transmission line, respectively. The β^i is a binary variable indicating either BESS or FESS is selected. The Ψ^i is the power capacity (maximum power) of the flywheel. The terms $Z, Q, Y, X, V, U, and\ H$ are the life (in years) of the BESS, FESS, solar panels, segment, feeder line, substation, and transmission line, respectively. The μ^m represents the number of days in season m in one year. The term EL_t^{im} is the net energy required/available from/to the electric grid by the DCFC station, and is defined as follows:

$$EL_t^{im} = \left(ED_t^{im} + BP_t^{im} + \pi_t^{jm} - SP_t^{im}\right)\tau \qquad \forall t \in \Gamma, i \in I, m \in M \qquad (133)$$

Where, the $ED_t^{im}, BP_t^{im}, \pi_t^{jm}\ and\ SP_t^{im}$ are the EV charging demand, battery charging demand, flywheel charging demand (including self-discharge losses) and the solar panel power generation at any time t of the day, in season m, respectively. The τ is the step size of the discrete time-dependent model. The $R_t^{im}, O_t^{im}\ and\ FR^i$ are the time-of-use rate for buying electricity from

grid, selling electricity to grid, and fixed monthly electricity purchase rates, respectively. The α_t^{im} is a binary variable indicating either energy is withdrawn or send back to the grid. The different constraints are explained in the following subsections.

5.3.2 Supply Demand Model

In order to ensure the feasibility of charging at a DCFC station, the available energy at any time t should be greater than the energy required. The energy required includes EV charging demand, existing electricity demand, and the energy required to charge the ESS. The available energy resources are the electric grid network and solar panel power generation. ESS is also used as a source of energy during parts of the day when it is discharging. The supply-demand model and the constraints are presented in Equations 107- 111. The $G^i, F^j, S^k, and\ T^l$ are the existing capacity of the segment, feeder line, substation, and transmission line, respectively. The $AG^i, AF^j, AS^k, and\ AT^l$ are the additional capacity of the segment, feeder line, substation, and the transmission line that might be required to support the EV charging demand, respectively. The $ED_t^{im}, BP_t^{im}, \pi_t^{im}, D_t^{im}\ and\ SP_t^{im}$ are the EV charging demand, BESS charging demand, FESS charging demand, existing demand, and the solar panel power generation at any time t of the day, in season m, respectively. The $\theta^{ij}, \Xi^{jk}, and\ \sigma^{kl}$ are the binary parameters capturing the network details of electric grid explaining whether, a segment i is connected to feeder line j, a feeder line j is connected to substation k, and a substation k is connected to transmission line l, respectively. Equation 107 ensures that the electric grid capacity at the segment level, and solar panel power generated is greater than the total electric power required at any time t. The equation 108, 109, 110, and 111 ensures that the electric grid capacity at feeder line level is greater than that at segment level, electric grid capacity at substation level is greater than the feeder line level, and the electric grid capacity at the transmission line level is greater than the substation level, respectively.

Equation 111 assigns the value 1 or 0 to the binary variable α_t^{im} depending upon if net energy is drawn from the electric grid or it is supplied back to the electric grid, respectively.

5.3.3 Energy Storage Model

The energy stored in the ESS at the end of any time t, is a function of charging/discharging power and the energy at the time $t-1$. The BESS model and FESS model are presented in Equations 112-115 and Equations 116-122, respectively. The BP_t^{im}, FP_t^{im} are the charging/discharging power of the BESS and FESS, respectively. The positive or negative values of BP_t^{im}, FP_t^{im} indicate that ESS is being charged or discharged, respectively. The BE_t^{im}, FE_t^{im} are the energy stored at the end of time t in the BESS and FESS, respectively. The BS^i, FS^i represents the size/capacity of the ESS. The Equations 112 and 116 update the energy stored in the ESS at end of time t, based on charging/discharging rate at time t, step size τ and energy stored at the end of time $t-1$. The Equations 113 and 117 updates the energy stored at the beginning of the time based on the energy stored at the end of time T. The BESS is allowed to charge to Δ and discharge to δ (20% of battery capacity) state of charge (SOC) to reduce the depth of discharge and protect the battery's health (equation 114). The BESS power is restricted by maximum allowable charging (CP) or discharging power (DP) as indicated in equation 115. The FESS energy cannot be greater than its energy capacity (Equation 118). The FESS power is restricted by maximum allowable power Ψ^i (equation 119). This maximum allowable power is restricted by size/energy capacity of FESS, energy density η^i, and power density ϑ^i of FESS (equation 120). Equation 121 updates the power delivered π_t^{im} to FESS based on FESS power FP_t^{im} and the self-discharge losses λ_t^{im}. Equation 121 and 122ensures that no power is delivered if the FESS is not selected through binary variable ω^i and a very large number Λ. As it is a minimization problem, this ω^i is zero if FS^i is zero, through Equation 121 and 122.

5.3.4 Solar Panel Power Generation Model

The maximum solar panel power generated depends upon the sun elevation angle ϕ_t^{im}, cloud coverage w_t^{im}, the efficiency of the solar panel ρ^i, and area of the solar panel A^i. The cloud coverage is measured in Oktas ranging from integer 0-8. The sky is divided into eight parts and the value indicates how much of that is covered by clouds (Jones, 1992). The value of 0 indicates completely clear weather conditions, and the value of 8 indicates complete overcast (Madsen et al., 1985). The solar panel power generation model at charging station location i is given in equation 123. The SP_t^{im} is the solar panel power at any time t which is limited by the maximum power that can be generated by solar panels at any time t. The solar radiation intensity $SR_t^{im}(W/m^2)$ is a function of cloud coverage w_t^{im}, and the sun elevation angle ϕ_t^{im} as given in Equation 134 (Ehnberg and Bollen, 2005; Nielsen et al., 1981; Ugirumurera and Haas, 2017).

$$SR_t^{im} = \frac{q_0(w_t^{im}) + q_1(w_t^{im}) \sin \phi_t^{im} + q_2(w_t^{im}) \sin^3 \phi_t^{im} - q_4(w_t^{im})}{q(w_t^i)} \qquad 134$$

The $q, q_0, q_1, q_2, and\ q_4$ are the calibrated parameters depending upon the cloud coverage, as given in the following table (Ehnberg and Bollen, 2005; Nielsen et al., 1981; Ugirumurera and Haas, 2017):

Table 5.2 The calibrated parameters for solar radiation intensity based on cloud coverage (Ehnberg and Bollen, 2005; Nielsen et al., 1981; Ugirumurera and Haas, 2017)

w_t^{im}	q_0 (W/m^2)	$q_1(W/m^2)$	$q_2(W/m^2)$	q	$q_4(W/m^2)$
0	-112.6	653.2	174	0.73	-95
1	-112.6	686.5	120.9	0.72	-89.2

Table 5.2 (cont'd)

2	-107.3	650.2	127.1	0.72	-78.2
3	-97.8	608.3	110.6	0.72	-67.4
4	-85.1	552	106.3	0.72	-57.1
5	-77.1	511.5	58.5	0.7	-45.7
6	-71.2	495.4	-37.9	0.7	-33.2
7	-31.8	287.5	94	0.69	-16.5
8	-13.7	154.2	64.9	0.69	-4.3

The bounds for variables are presented in Equations 124-132. The term $BS^{i,max}, FS^{i,max}$ and $A^{i,max}$ are the maximum allowable size of BESS, FESS, and solar panels depending upon the site conditions, respectively.

5.4 Data Collection

The input data includes the proposed and current EV fast charging (DCFC) station network, EV energy demand, existing energy demand (other than EV demand), electric grid network details and capacity constraints, ESS types, and characteristics, and solar panel characteristics and weather conditions. The details of obtaining each of these data sets are explained in this section.

5.4.1 DCFC locations and EV energy demand

The potential DCFC locations in Michigan are obtained from Phase-II of the "Electric Vehicle Charger Placement Optimization in Michigan" by our research team as Ghamami et al., 2020. These locations were estimated based on the simulated urban trips of EV users throughout the road network of different urban areas in Michigan, corresponding to the proposed EV market penetration rate (6%) in the year 2030 (Ghamami et al., 2020b; Kavianipour et al., 2021b) (Ghamami et al., 2020). Similarly, the time-dependent EV energy demand and power demand at

these DCFC locations are extracted based on the travel patterns. Note that the battery sizes of all EVs are assumed to be 70 kWh, and the charging power of DCFC chargers is assumed to be 50 kW.

5.4.2 Existing energy demand and electric grid network details

The existing energy demand, grid network details, and capacity constraints are obtained from the different utility companies, cooperatives, and municipalities. The companies provided data for the electric grid network and connections (i.e., substation, feeder line, segment, etc.) that will serve the proposed DCFC locations, existing energy demand, upgrade costs, and capacity constraints of the electric grid network. It is worth noting that the data was not available for some potential DCFC locations; thus, these locations are not considered for the analysis. A total of 75 DCFC locations were considered in the major cities of Michigan (i.e., Saginaw, Lansing, Flint, Grand Rapids, Kalamazoo, and Muskegon). The locations are presented below.

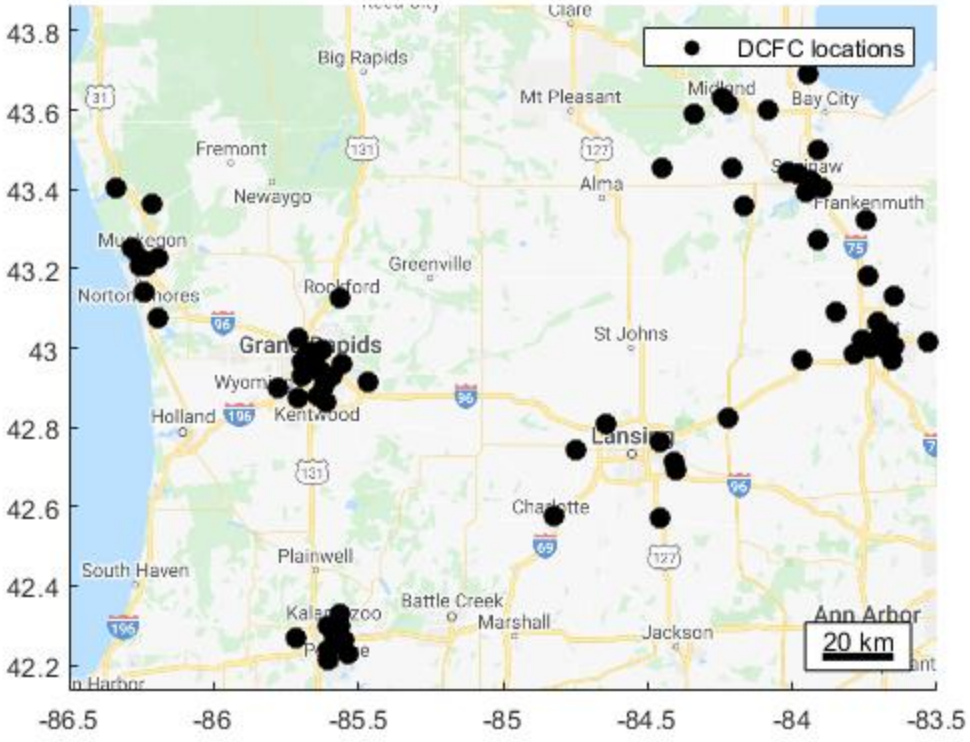

Figure 5.2 The proposed DCFC stations in Michigan in 2030 considered for DER analysis (Ghamami et al., 2020b; Kavianipour et al., 2021b).

5.4.3 Energy storage systems types and characteristics

The study considered different types of ESS technologies which include Li-ion battery, lead-acid, redox flow battery, sodium-sulfur, sodium metal halide, zinc-hybrid cathode, sodium-ion battery, flywheels (Beacon Power, 2021; Kane, 2021; Mongird et al., 2019; Patel, 2021; Rafi and Bauman, 2021). The Li-ion batteries are deployed across various industries due to high power density, high energy density, and performance (Mongird et al., 2019). The price of this ESS technology is consistently reducing due to major demand in EV industry (Mongird et al., 2019). These batteries are used in residential commercial buildings, distribution grids, renewable generation smoothing etc (EASE, 2022). Lead-acid batteries are also used for various applications such as load following, time shifting but these are not used for small portable systems (Mongird et al., 2019). Redox flow batteries consists of electrolyte solution in tanks acting as cathode and

anode (Mongird et al., 2019). The electrolyte is passed through a membrane to generate and store energy. This technology is currently in early phase of commercialization but it has long life, easy scalability, and operating at low temperature range (Mongird et al., 2019). Further, due to low energy density, large storage tanks are required (EASE, 2022). These are utilized for peak shaving, energy time shifting, etc (EASE, 2022). Sodium-sulfur battery is another electrochemical energy storage system which has high energy-density but it is highly corrosive, requires high operating temperatures ($300 - 350^0 C$), and consequent safety requirements (EASE, 2022; Mongird et al., 2019). Sodium Metal Halide (sodium nickel chloride) is used for various application such as residential buildings, EVs, renewable generation smoothing, etc (Mongird et al., 2019). These batteries have smaller range than other electrochemical storage, but has high performance, durability, and low sensitivity to ambient temperature (EASE, 2022; Mongird et al., 2019). Zinc-Hybrid Cathode batteries utilizes widely available material and can be supplied at low cost (Mongird et al., 2019). The Sodium-ion battery are in the development phase and are expected to replace Li-ion in the following years (especially in storage applications) as the cost of sodium is very low and it is available in abundance (EASE, 2022). Further, this technology is safer, operates on lower temperature, provides faster charging, and higher cycle life efficiency as compared to Li-ion batteries (Kane, 2021; Patel, 2021). However, the energy density of these batteries is currently lower than Li-ion batteries (Kane, 2021). Flywheels store energy in the form of electromechanical energy (Mongird et al., 2019). It consists of rotating cylinders which stores energy in the form of kinetic energy. Higher is the velocity, higher is the energy stored. The electric energy is withdrawn by slowing down the rotating cylinder. The flywheels have longer life cycle, and fast response time making them suitable for frequency regulations, and renewable smoothing (Mongird et al., 2019). The data related to different types of ESS, their characteristics, and their feasibility to serve

at the DCFC locations is obtained from different studies in the literature (Beacon Power, 2021; Cole et al., 2021; Kane, 2021; Mongird et al., 2019; Patel, 2021; Rafi and Bauman, 2021). The following table represents the characteristics, and project costs of different ESS:

Table 5.3 Different types of energy storage technologies (Beacon Power, 2021; EASE, 2022; Kane, 2021; Mongird et al., 2019; Patel, 2021; Rafi and Bauman, 2021)

ESS Type	Project Cost* ($/kWh)	Life (years)	Energy Density (Wh/L)	Power Density** (W/L)
Sodium- Sulfur	669	13.5	40	10
Li-Ion	362	10	90-130	23-33
Lead Acid	464	3	16	4
Sodium Metal Halide	669	12.5	65	16
Zinc-Hybrid Cathode	433	10	17	4
Redox Flow Battery	650	15	13	3
Flywheel	10,124	20	18	74
Sodium-ion (Current projection)	<Li-ion	>Li-ion	<Li-ion	>Li-ion

*The cost includes capital cost, power conversion system, the balance of plant, and construction cost

**Assuming Energy/Power=4 for batteries and 0.25 for flywheel

It can be observed that the Li-ion battery has the lowest project cost. Further, among the different battery technology, Li-ion batteries have the maximum energy density and power density. Thus, the Li-ion is the optimum choice among the batteries and is considered for analysis. The study also considers flywheels for the analysis due to the significantly high-power density, which might be useful during peak power demand of EV.

The study also considers SLB Li-ion batteries. The batteries are remanufactured after their end of life (EOL) to be used as SLB. The cost of remanufacturing SLB is around 30% of NB (Neubauer et al., 2012). The comparison of SLB with that of the NB Li-ion battery is as shown below:

Table 5.4 Comparison of second-life batteries (SLB) versus new lithium ion battery

	NB Li-ion battery	**SLB Li-ion battery**
Battery pack Cost	$137/kWh (BloombergNEF, 2020)	30% of new battery (Neubauer et al., 2012)
Battery Life	10 years (Kamath et al., 2020)	3-7 years (Kamath et al., 2020)
Battery Energy Capacity	Depend upon Size	70-80% of a new battery (Kamath et al., 2020)

The study also considered BESS with different storage durations. The storage duration is the time to charge/discharge the full battery at its power capacity. The smaller storage duration would mean that the battery can charge/discharge faster, which might be required, especially during peak hours. However, batteries with smaller storage durations are more expensive. The projected capital cost for different storage durations is as follows (Cole et al., 2021):

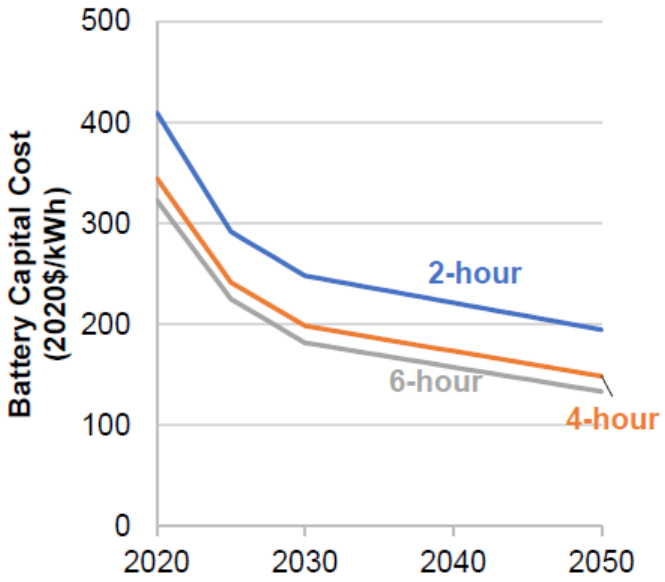

Figure 5.3 Projected BESS unit project cost with different storage durations (Cole et al., 2021)

This study considers the projected cost of the BESS system in 2050, including battery pack, balance of plant, inverter, construction cost, etc. Finally, the battery size is limited to 50 kWh per 50 kW charger due to area restrictions depending on site conditions (Gjelaj et al., 2020).

5.4.4 Solar panel characteristics and input data

The solar panels' output power depends upon the efficiency of the solar panels, sun elevation angle, and cloud coverage. The sun elevation angle throughout the year at different locations in Michigan is obtained from SunEarthTools, 2021 (Figure 5.4). The input data is fed into the optimization model to estimate the optimum investment technology with maximum cost savings. Note that these figures represents the sun elevation angle averaged over all the days in the given season (winter or summer). The cloud coverage data throughout the year is obtained from Weather Spark, 2022 (Figure 5.5). Note that the variation in sun elevation angle and cloud coverage is found to be similar in all urban areas of the Michigan. Hence, same variation is assumed for all the areas in Michigan.Finally, the solar panel efficiency of 19.5% (Feldman et al., 2021) and cost of $0.68/W (NREL, 2021) are considered in this study. . The cost of the solar panels

is the entire project cost, including inverters, structural balance of system (racking), electrical balance of system, installation cost, etc. The projected cost for the solar panels is considered to be for the year 2050 (NREL, 2021). It is important to note that the area of the solar panels is restricted to the maximum area based on the site conditions at each of the charging stations. Thus, the solar panel area is restricted to the charging/parking spot area per charger (Schmitt, 2016).

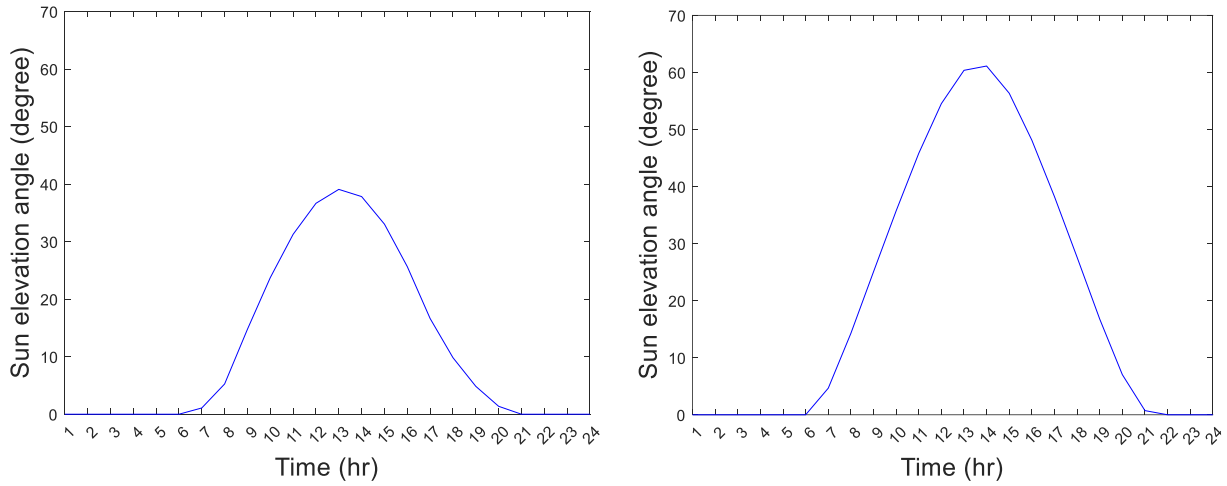

a) Winter season b) Summer season

Figure 5.4 Variation in sun elevation angle during the a) winter and b) summer season in Saginaw, Michigan (SunEarthTools, 2021)

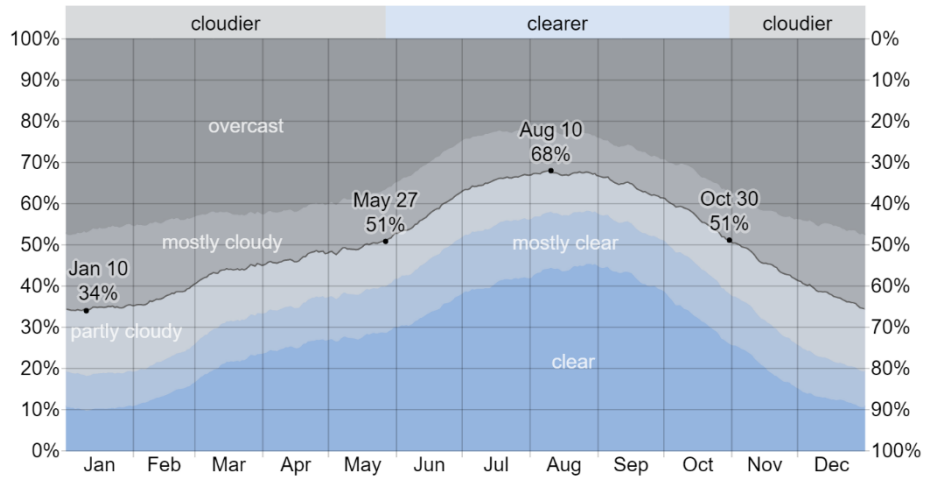

Figure 5.5 Variation in cloud coverage over the entire year in Saginaw, Michigan © WeatherSpark.com (Weather Spark, 2022)

5.5 Results

The model is applied to obtained the optimum size of DER, required grid upgrades, infrastructure cost and the savings. The results are obtained for the 75 DCFC locations at the six major cities (i.e., Saginaw, Lansing, Flint, Grand Rapids, Kalamazoo, and Muskegon) of Michigan. The study considers different scenarios for obtaining results which includes different combinations of DER (Li-ion NB BESS, Li-ion SLB BESS, FESS, solar panels), variation in EV charging demand, different storage duration of batteries, projected cost of the DER. These scenarios are listed as below:

- DERs
    - BESS, FESS, and solar panels
    - BESS, FESS only
- Battery cost, type, and storage duration
    - 2-hour storage duration
        - Li-ion NB $190/kWh
        - Li-ion SLB $145/kWh
    - 4-hour storage duration
        - Li-ion NB $150/kWh
        - Li-ion SLB $115/kWh
    - 6-hour storage duration
        - Li-ion NB $140/kWh
        - Li-ion SLB $105/kWh
- EV load factor (EV demand)
    - EV demand in the year 2030

- 1.5 times the EV demand in the year 2030
- 2 times the EV demand in the year 2030

The results are obtained for the 75 DCFC locations in the six major urban areas (i.e., Saginaw, Lansing, Flint, Grand Rapids, Kalamazoo, and Muskegon) of Michigan. The analysis has been done for the 2030 EV demand, 1.5 times the EV demand of 2030 (EV load factor of 1.5 means demand equivalent to 1.5 times the demand in the year 2030), and 2 times the EV demand of 2030, to predict future requirements of EV charging.

The suggested size of the battery (kWh) and the solar panels (square meter) for the various urban areas for 4-hour storage duration (Li-ion NB and SLB), are presented from Figure 5.6 to Figure 5.17. The optimum solution is the provision of solar panels at all the locations in all the cities. The size of these solar panels is the maximum area that can be provided depending upon the site area restrictions at each particular location. These solar panels provide savings in the electricity cost, charge the battery (especially during the summer and highest sun elevation angle), and supply extra energy to the electric grid (if any). The size of the battery depends upon the type and cost of battery (NB versus SLB), cost of upgrading the grid, and the EV load factor (EV load factor of 1.5 means demand equivalent to 1.5 times the demand in year 2030). When considering the NBs, numerous locations do not have batteries because of the high investment cost for the battery as compared to the cost of upgrading the grid. However, with SLBs all the locations have batteries, and the optimum size of these batteries is much larger than that of NBs. The investment cost for SLB is lower than upgrading the grid. Further, these batteries efficiently utilize the time of use electricity rates by charging during off-peak hours and discharging during peak hours. Note that the grid upgrading cost depends upon the capacity constraints of grid components at a given location. Substations might have to be upgraded (in the absence of DER), or a basic connection

can be the electricity provision costs. Note that flywheels are not the optimal solution as these have higher investment costs than batteries.

The temporal variation of demand/supply in summer for an EV load factor of 2 at one of the locations in Saginaw, Michigan, is shown in Figure 5.18 (at the Grid level) and Figure 5.19 (at DCFC station level). Figure 5.18 shows that the feeder capacity is less than the peak hour demand (existing demand plus EV demand). Solar panels and batteries are provided to support the extra demand and reduce the load on the grid. The Figure 5.18a and Figure 5.18b are the profile for the case of new battery and SLB, respectively. Figure 5.19 represents the detailed temporal demand/supply at DCFC level for battery, solar panel output, the EV demand and the electricity price at the charging station location. The SLB (Figure 5.19b) is able to utilize the time-of-use electricity rate more efficiently as compared to the NB (Figure 5.19a). The SLB (800 kWh) has larger size and can store more energy as compared to NB (575 kWh), during the off-peak hours (midnight and morning hours). It is evident from the figures (especially Figure 5.19b) that the battery charges from the midnight to morning when the electricity price as well as demand is low. The battery discharges during the morning peak hour when electricity price is higher. However, it again charges around the noon when the solar power output is maximum. Finally, it again discharges during the evening peak hour with increased electricity price.

The total cost breakdown for the different cities for the optimum scenario (SLB and solar panels) for 4-hour storage duration is shown in Table 5.5. It can be observed that the provision of DER provide substantial savings in the annual electricity cost ($40,000-$285,000) and the annual total cost ($25000-$165,000) for each of the major cities in Michigan. The maximum savings are in Grand Rapids, Michigan and the minimum savings are in Lansing, Michigan. The total savings are smaller because it includes additional investment costs for DER. Table 5.6 shows the same

cost breakdown considering NBs and solar panels for 4-hour storage duration. In this scenario, the annual electricity and annual total cost savings are around $25,000-$170,000 and $20,000-$145,000 respectively. The study also obtained results for other scenarios (No solar panels, 2-hour storage duration, 6-hour storage duration). However, the scenario with a 4-hour storage duration SLB and solar panels provides the maximum savings. SLBs are cheaper and offer an acceptable charging/discharging rate for the required power during peak hour demand. The cost breakdown for the 2-hour and 6-hour storage duration BESS are presented in appendix from Table A to Table A .

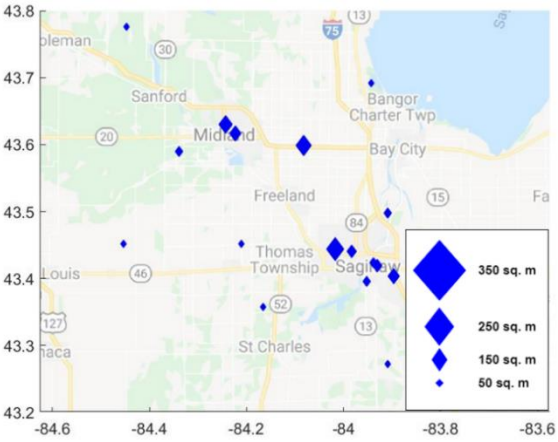

(i) Solar panel area (sq.m)

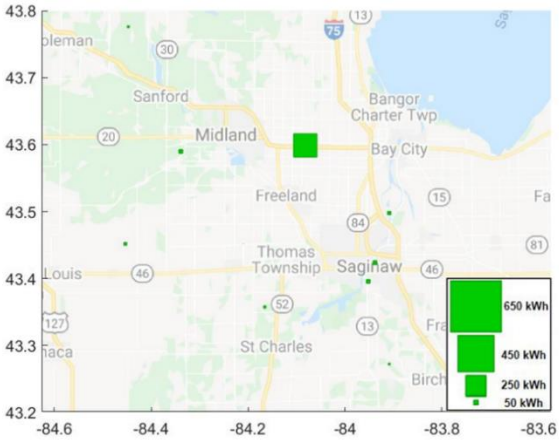

(ii) NB size (kWh)

a) EV load factor=1

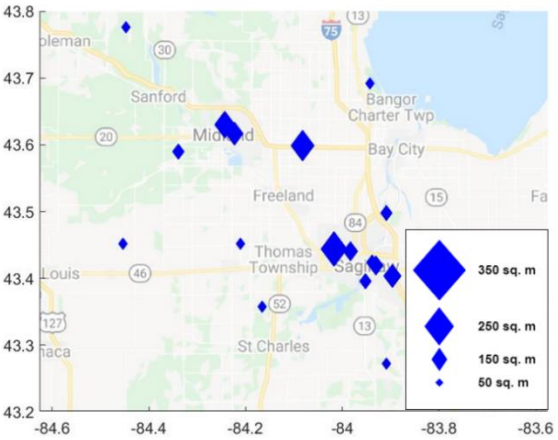

(i) Solar panel area (sq.m)

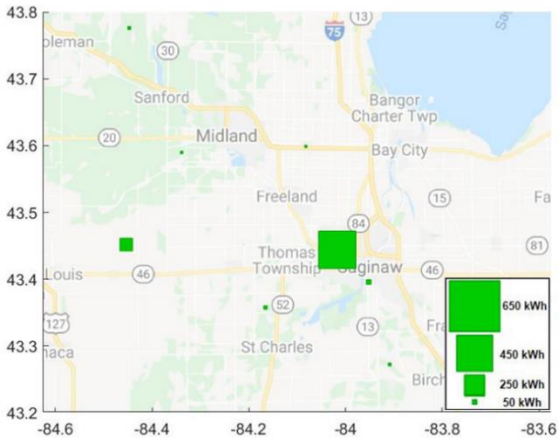

(ii) NB size (kWh)

b) EV load factor=1.5

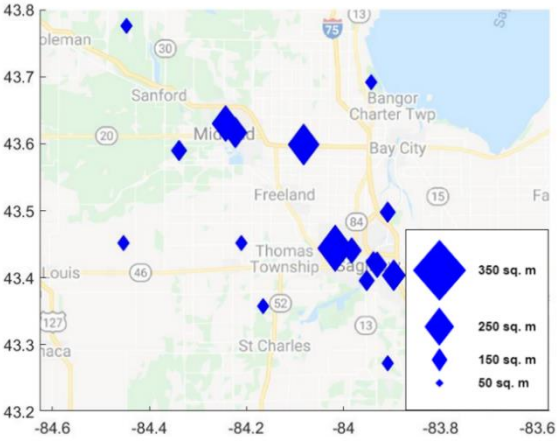

(i) Solar panel area (sq.m)

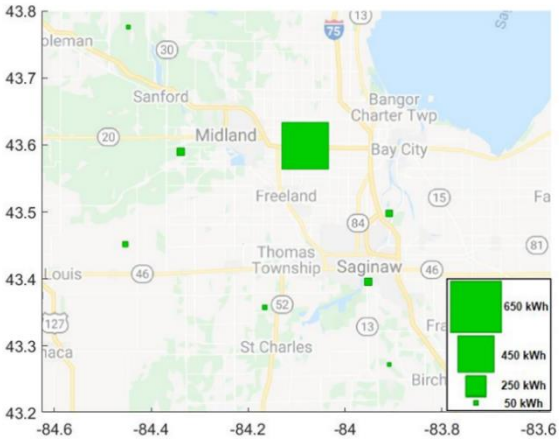

(ii) NB size (kWh)

c) EV load factor=2

Figure 5.6 Size of NB (4 hour storage duration) and solar panels for the city of Saginaw

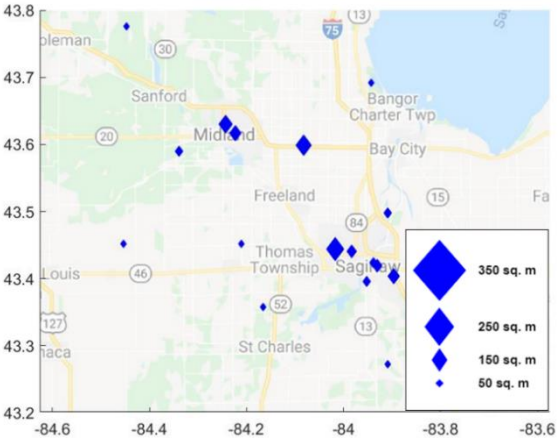

(i) Solar panel area (sq.m)

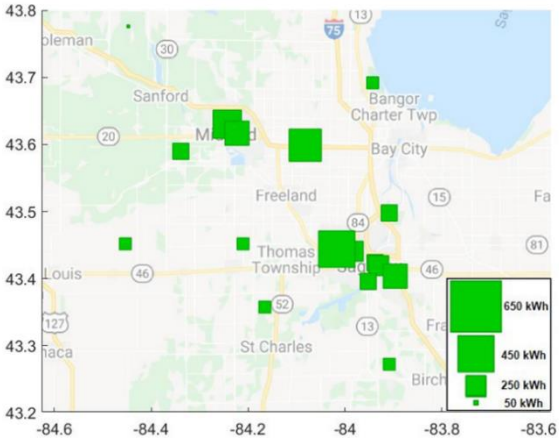

(ii) SLB size (kWh)

a) EV load factor=1

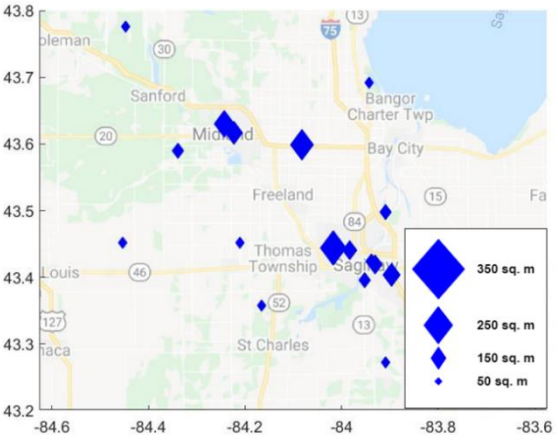

(i) Solar panel area (sq.m)

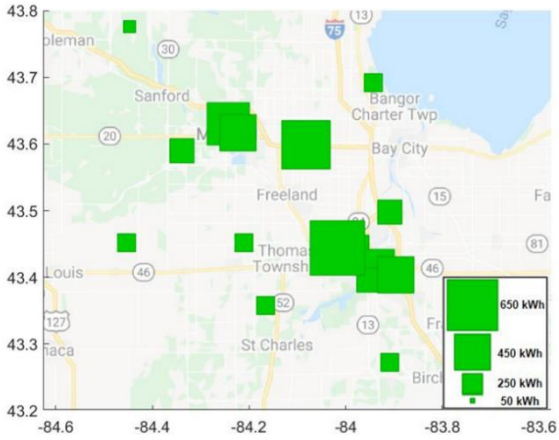

(ii) SLB size (kWh)

b) EV load factor=1.5

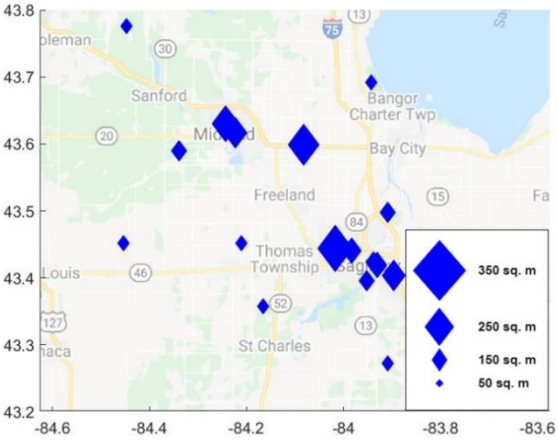

(i) Solar panel area (sq.m)

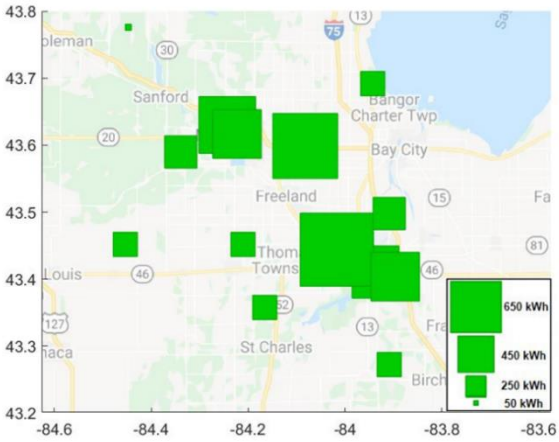

(ii) SLB size (kWh)

c) EV load factor=2

Figure 5.7 Size of SLB (4 hour storage duration) and solar panels for the city of Saginaw

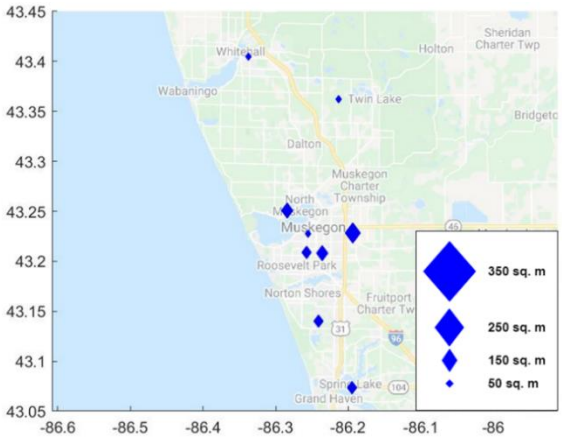

(i) Solar panel area (sq.m)

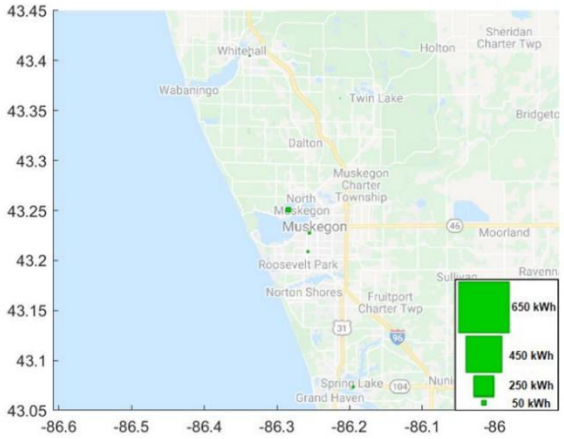

(ii) NB size (kWh)

a) EV load factor=1

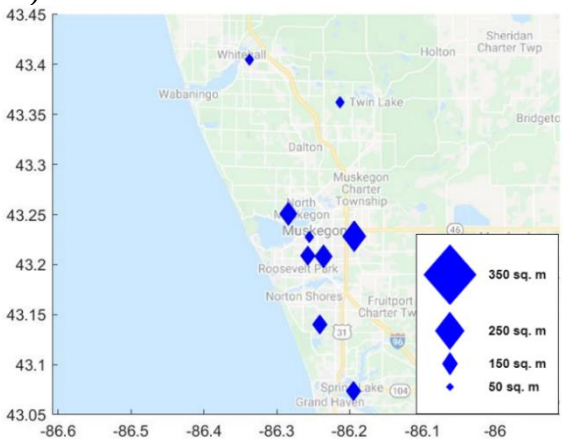

(i) Solar panel area (sq.m)

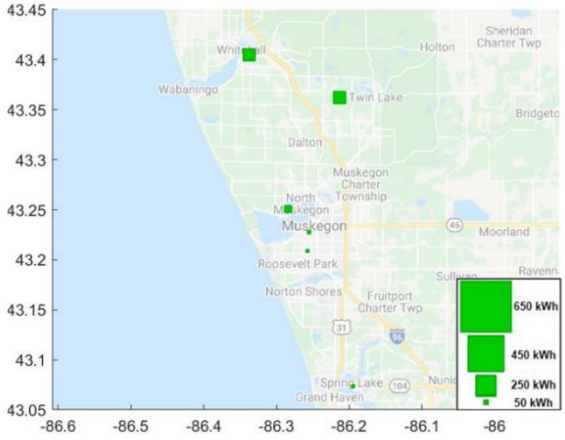

(ii) NB size (kWh)

b) EV load factor=1.5

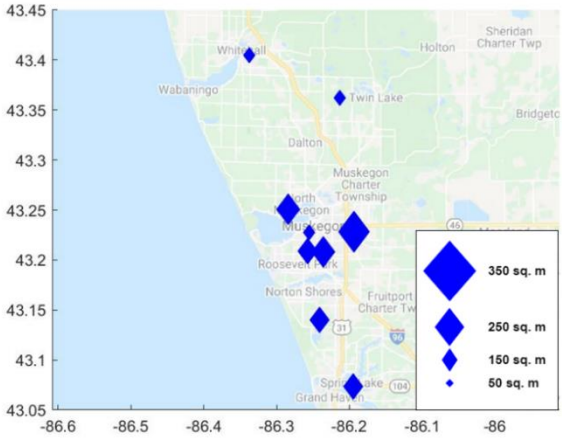

(i) Solar panel area (sq.m)

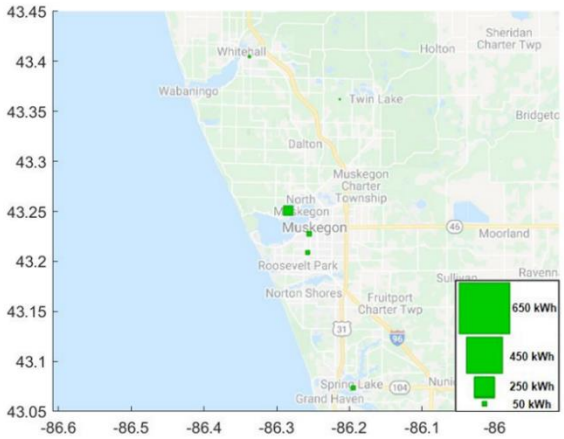

(ii) NB size (kWh)

c) EV load factor=2

Figure 5.8 Size of NB (4 hour storage duration) and solar panels for the city of Muskegon

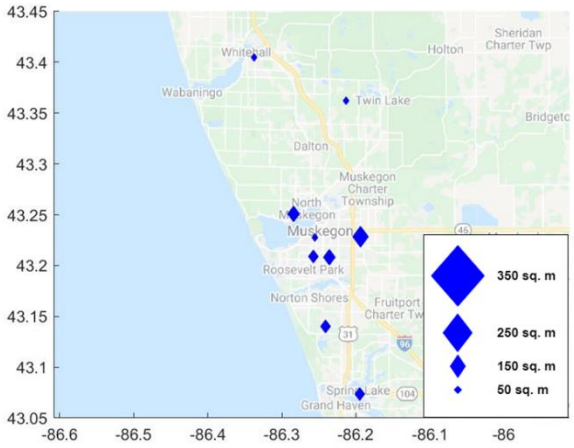

(i) Solar panel area (sq.m)

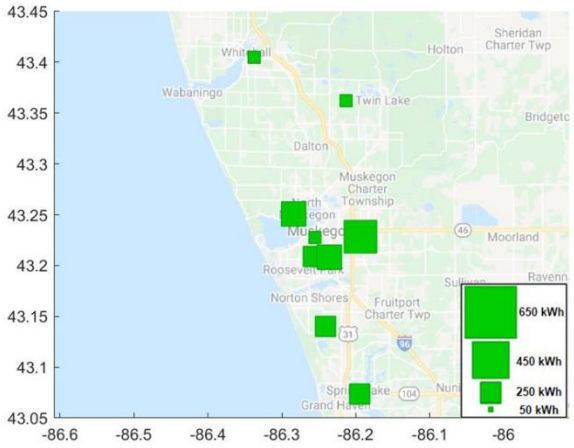

(ii) SLB size (kWh)

a) EV load factor=1

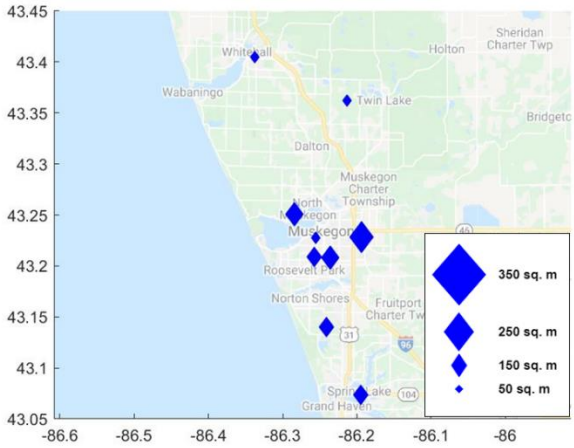

(i) Solar panel area (sq.m)

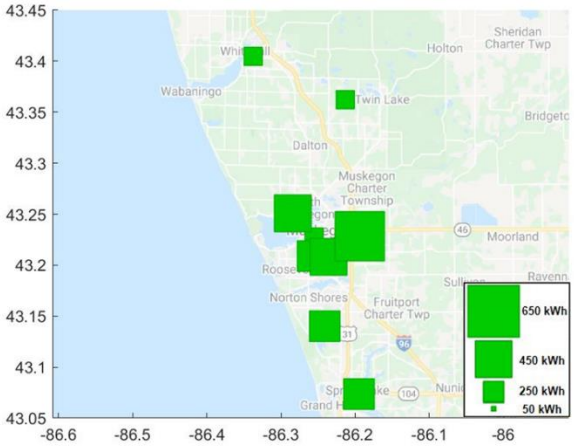

(ii) SLB size (kWh)

b) EV load factor=1.5

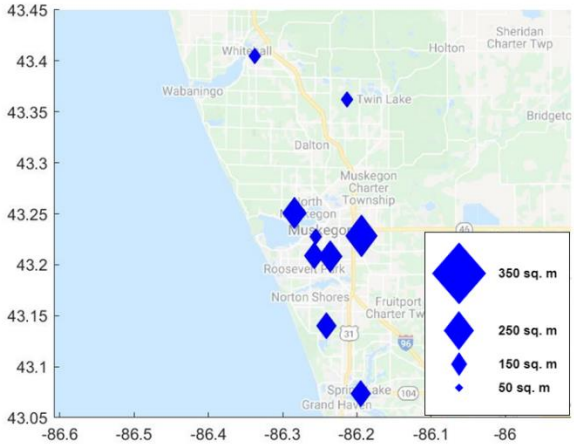

(i) Solar panel area (sq.m)

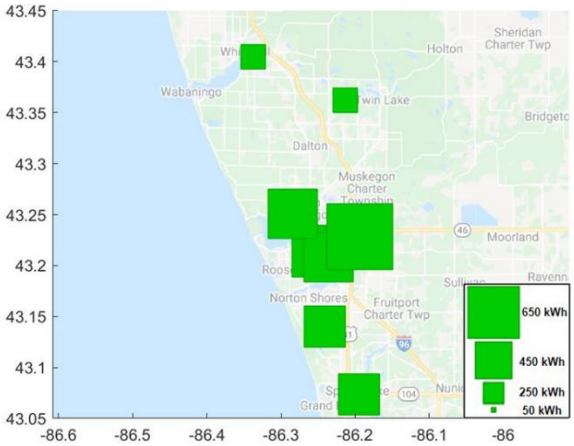

(ii) SLB size (kWh)

c) EV load factor=2

Figure 5.9 Size of SLB (4 hour storage duration) and solar panels for the city of Muskegon

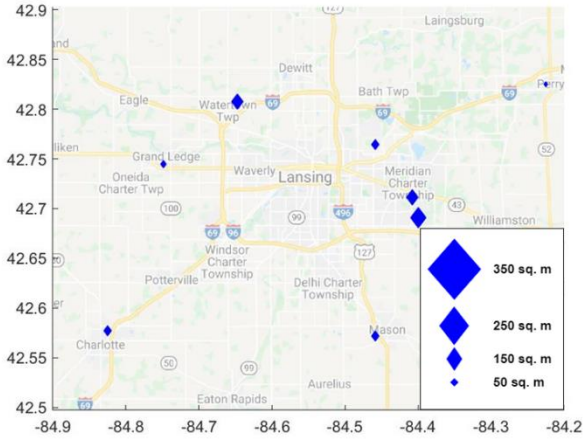

(i) Solar panel area (sq.m)

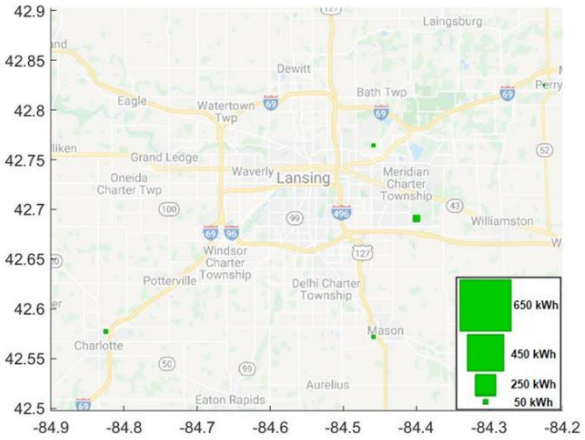

(ii) NB size (kWh)

a) EV load factor=1

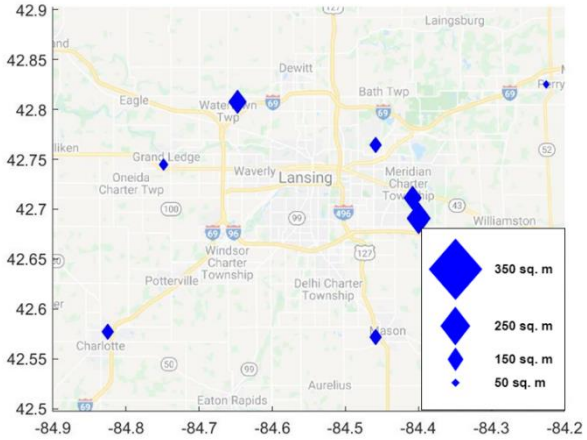

(i) Solar panel area (sq.m)

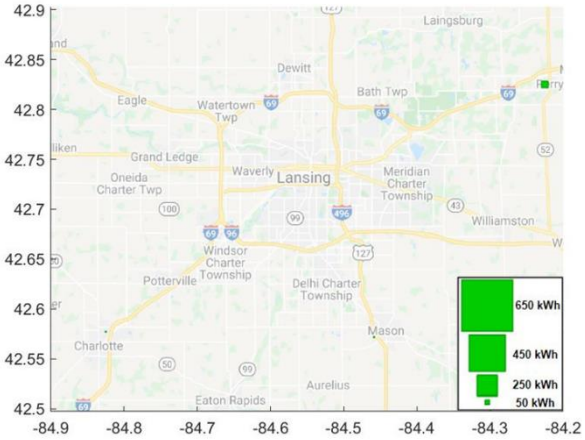

(ii) NB size (kWh)

b) EV load factor=1.5

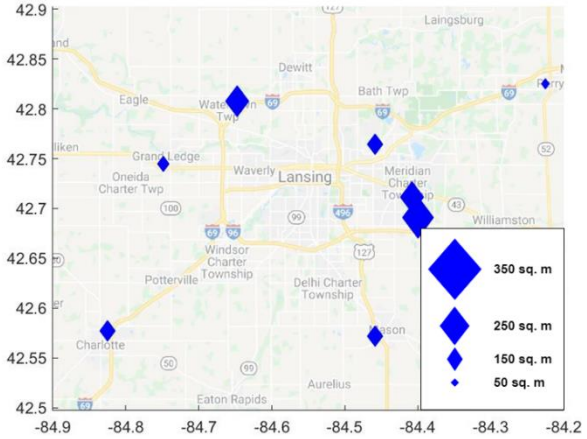

(i) Solar panel area (sq.m)

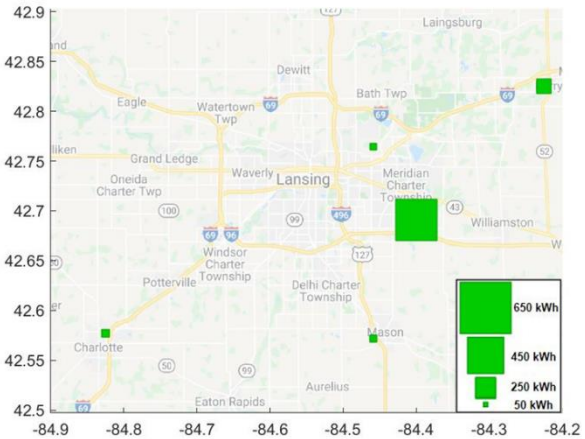

(ii) NB size (kWh)

c) EV load factor=2

Figure 5.10 Size of NB (4 hour storage duration) and solar panels for the city of Lansing

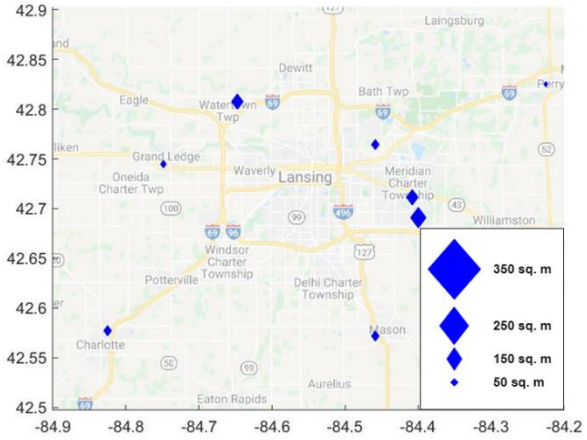

(i) Solar panel area (sq.m)

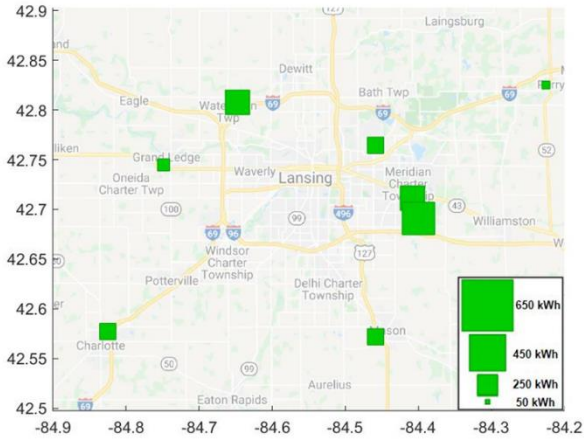

(ii) SLB size (kWh)

a) EV load factor=1

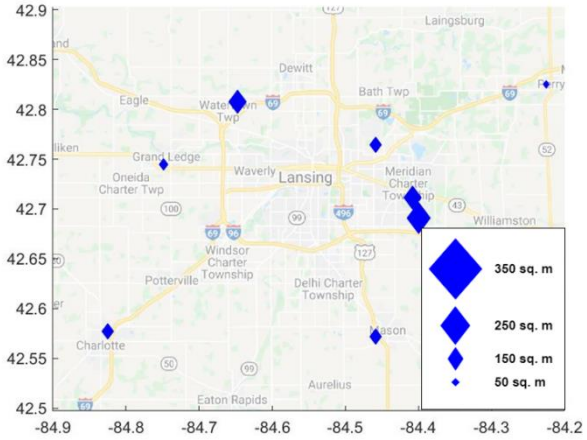

(i) Solar panel area (sq.m)

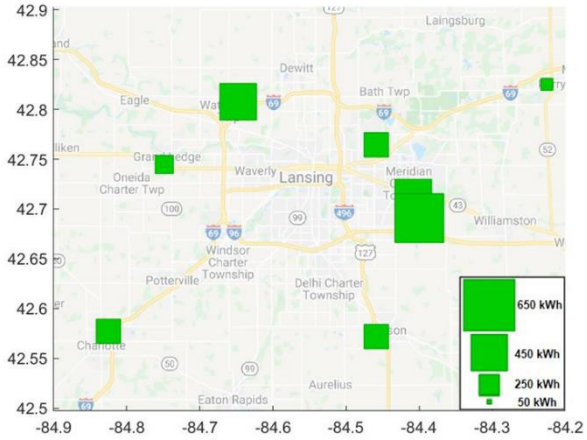

(ii) SLB size (kWh)

b) EV load factor=1.5

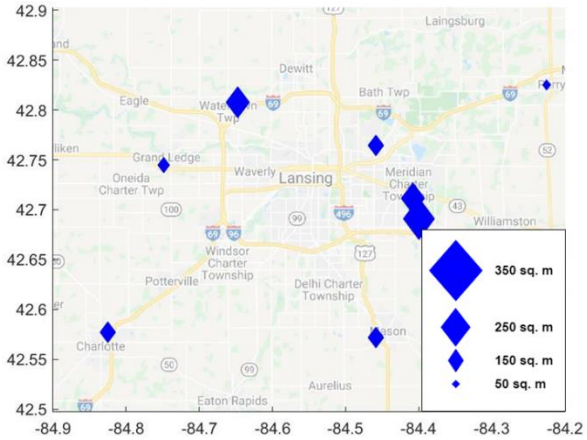

(i) Solar panel area (sq.m)

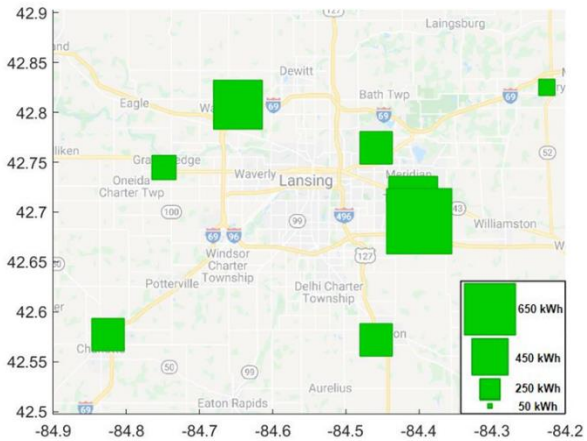

(ii) SLB size (kWh)

c) EV load factor=2

Figure 5.11 Size of SLB (4 hour storage duration) and solar panels for the city of Lansing

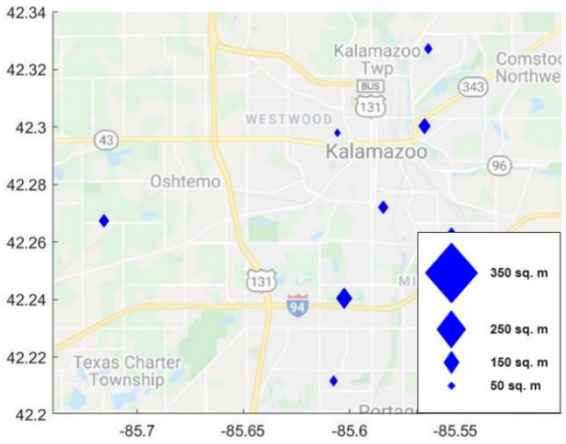

(i) Solar panel area (sq.m)

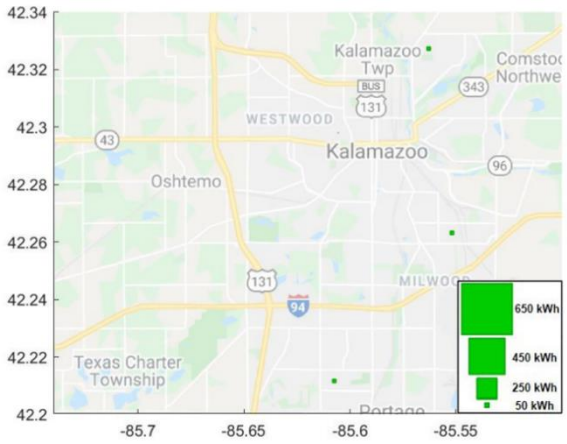

(ii) NB size (kWh)

a) EV load factor=1

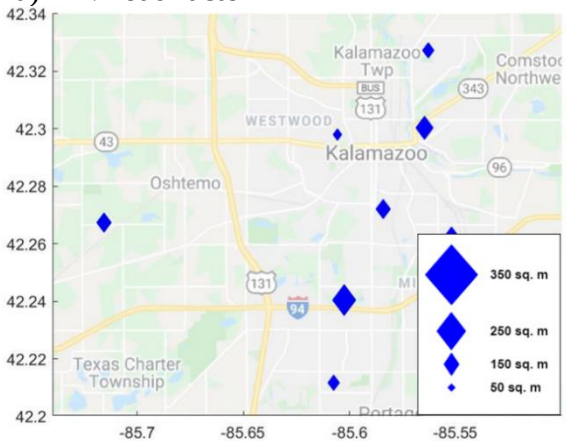

(i) Solar panel area (sq.m)

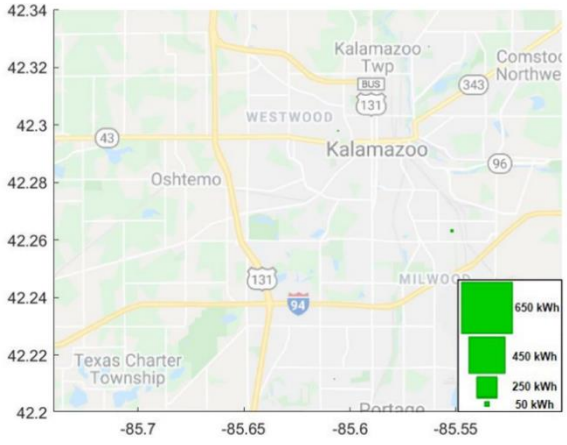

(ii) NB size (kWh)

b) EV load factor=1.5

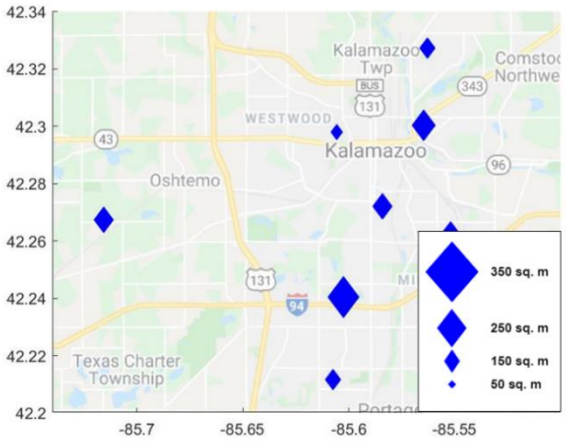

(i) Solar panel area (sq.m)

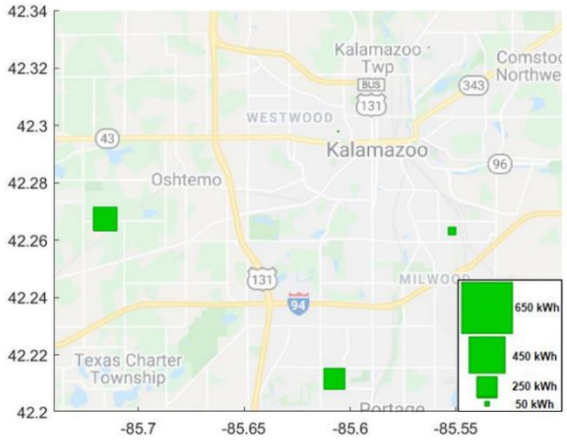

(ii) NB size (kWh)

c) EV load factor=2

Figure 5.12 Size of NB (4 hour storage duration) and solar panels for the city of Kalamazoo

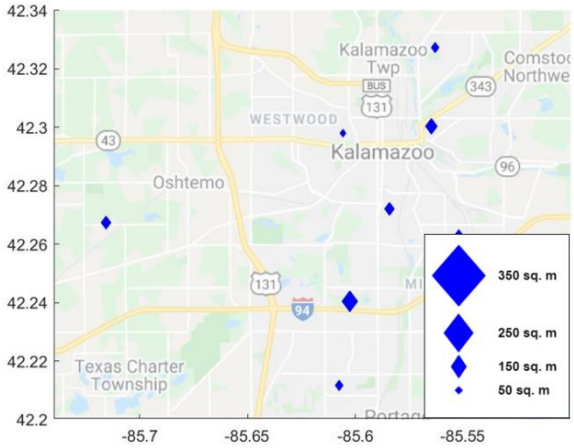

(i) Solar panel area (sq.m)

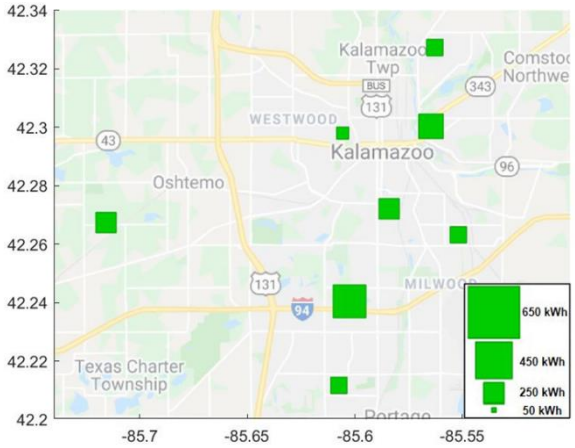

(ii) SLB size (kWh)

a) EV load factor=1

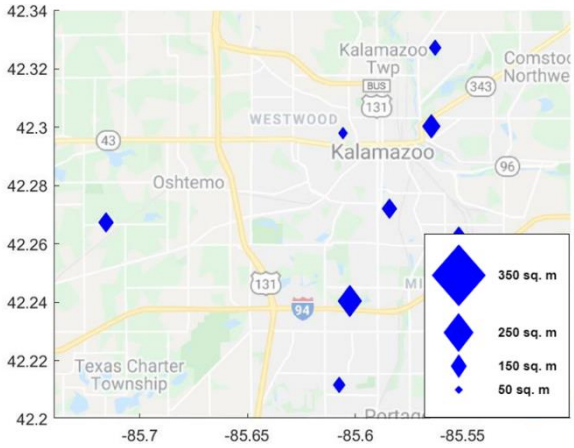

(i) Solar panel area (sq.m)

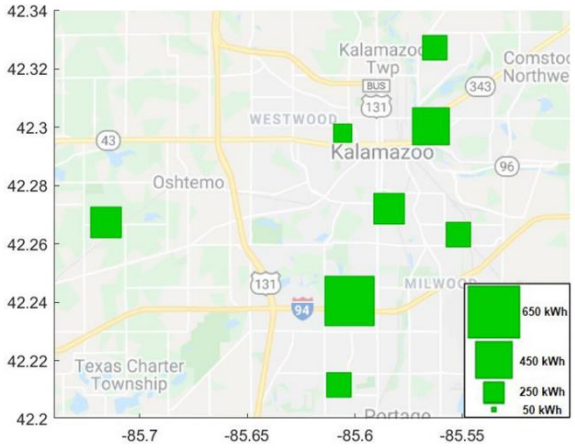

(ii) SLB size (kWh)

b) EV load factor=1.5

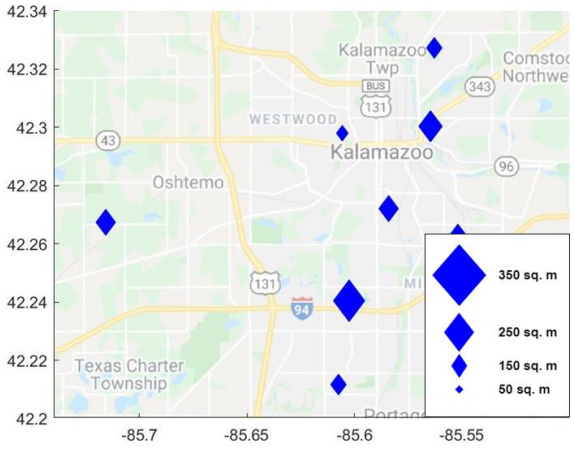

(i) Solar panel area (sq.m)

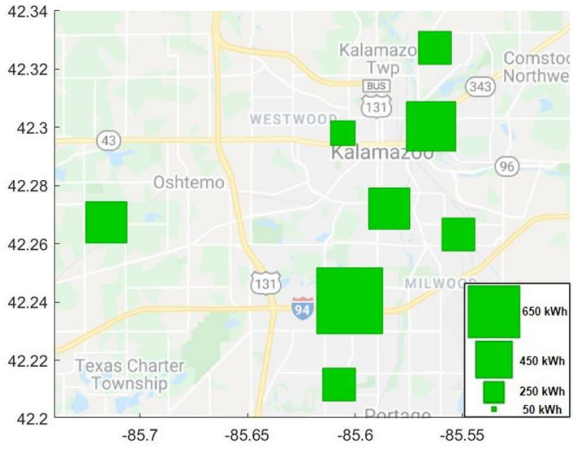

(ii) SLB size (kWh)

c) EV load factor=2

Figure 5.13 Size of SLB (4 hour storage duration) and solar panels for the city of Kalamazoo

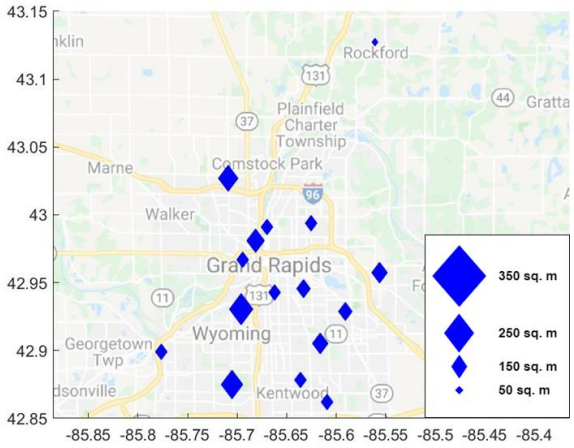

(i) Solar panel area (sq.m)

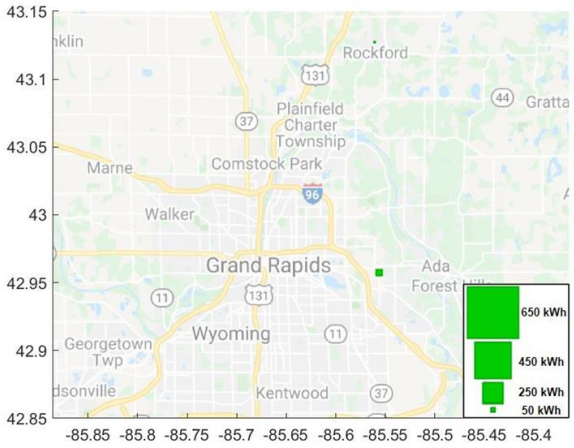

(ii) NB size (kWh)

a) EV load factor=1

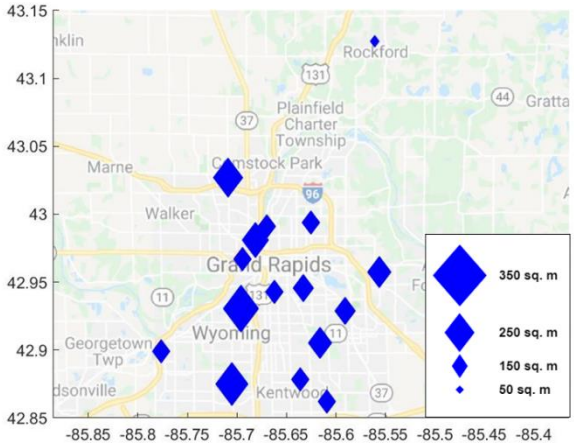

(i) Solar panel area (sq.m)

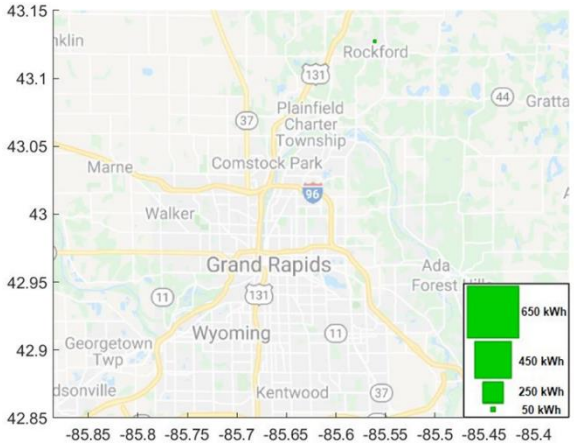

(ii) NB size (kWh)

b) EV load factor=1.5

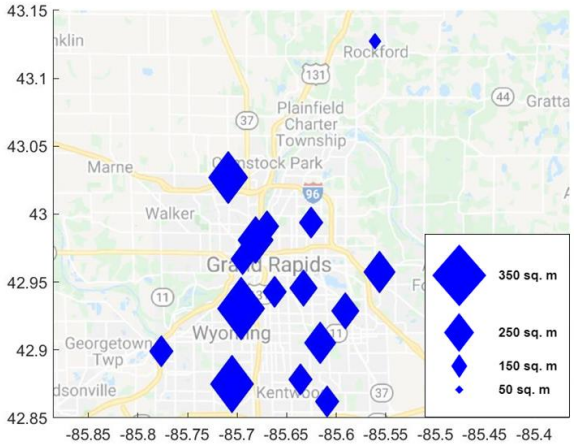

(i) Solar panel area (sq.m)

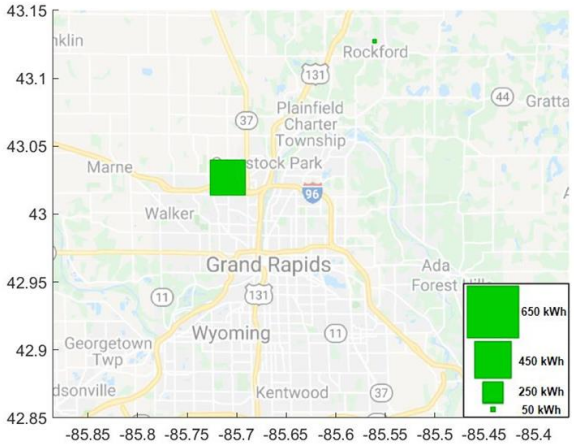

(ii) NB size (kWh)

c) EV load factor=2

Figure 5.14 Size of NB (4 hour storage duration) and solar panels for the city of Grand Rapids

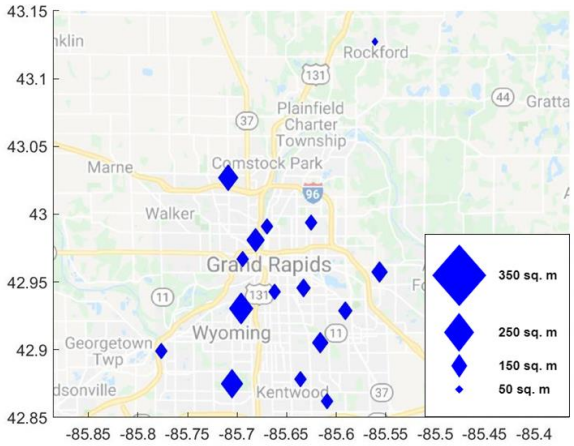

(i) Solar panel area (sq.m)

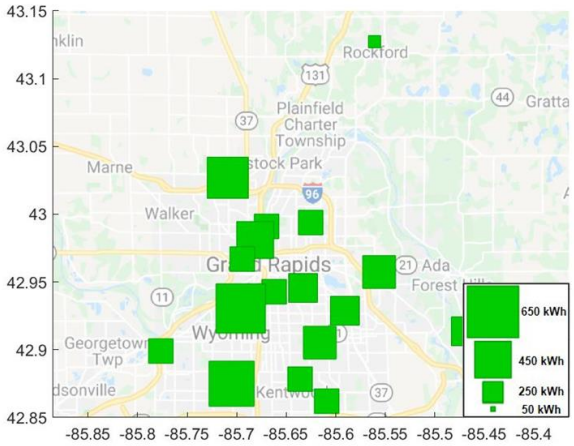

(ii) SLB size (kWh)

a) EV load factor=1

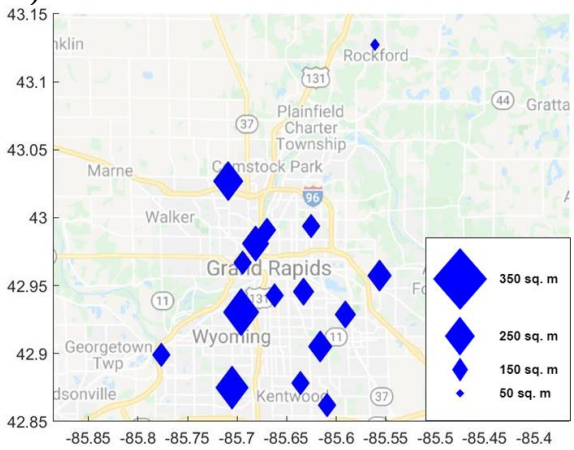

(i) Solar panel area (sq.m)

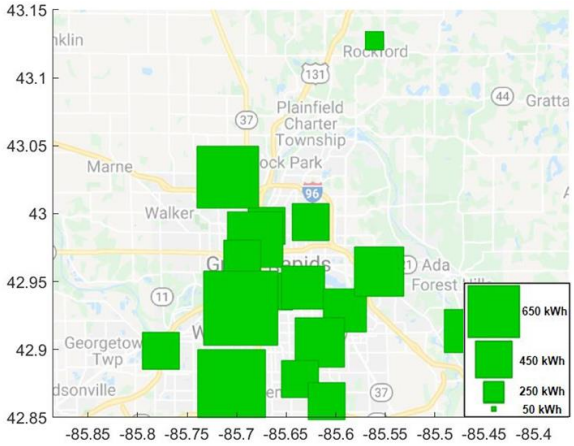

(ii) SLB size (kWh)

b) EV load factor=1.5

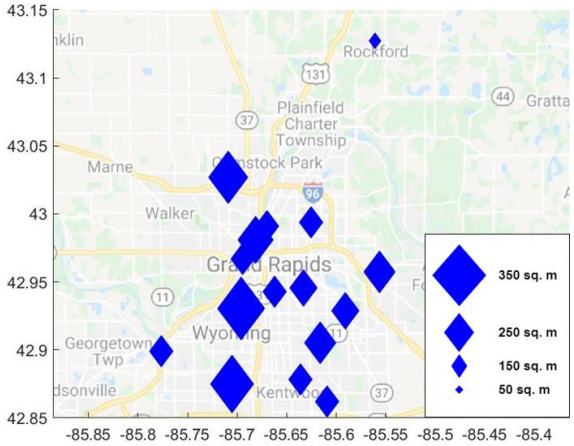

(i) Solar panel area (sq.m)

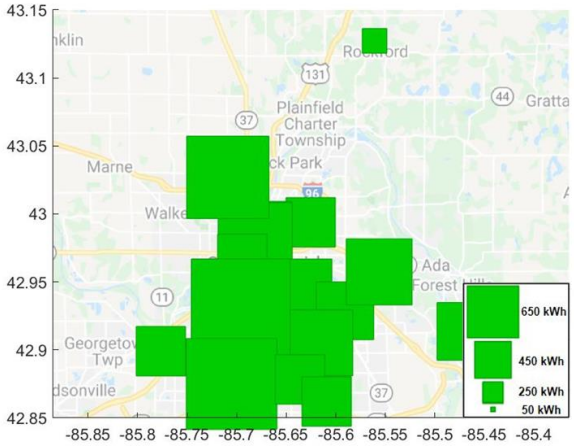

(ii) SLB size (kWh)

c) EV load factor=2

Figure 5.15 Size of SLB (4 hour storage duration) and solar panels for the city of Grand Rapids

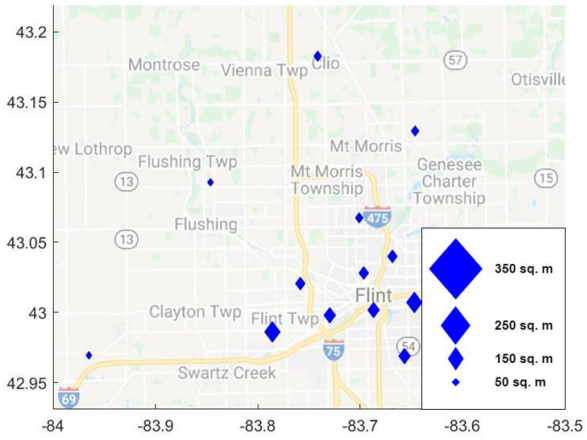

(i) Solar panel area (sq.m)

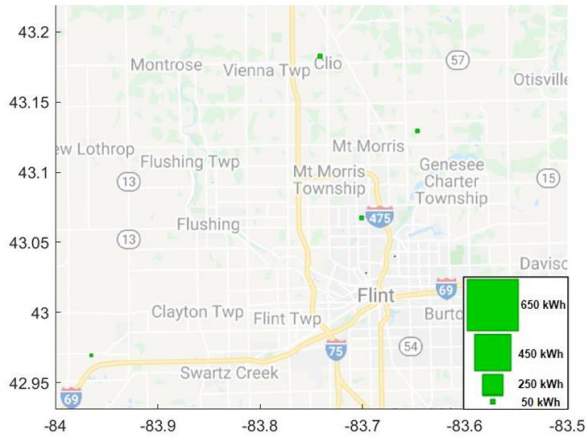

(ii) NB size (kWh)

a) EV load factor=1

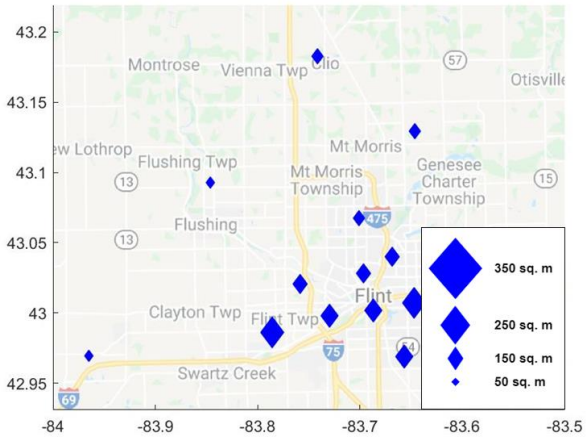

(i) Solar panel area (sq.m)

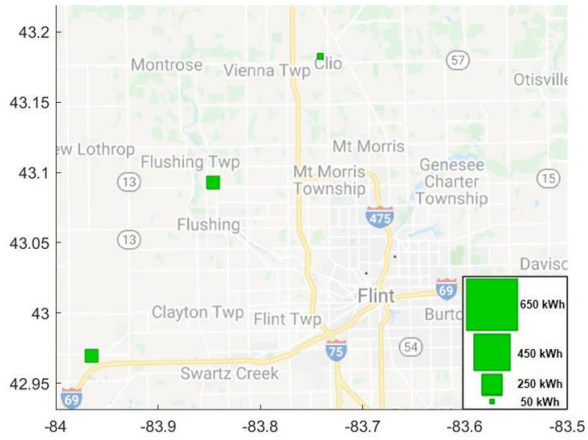

(ii) NB size (kWh)

b) EV load factor=1.5

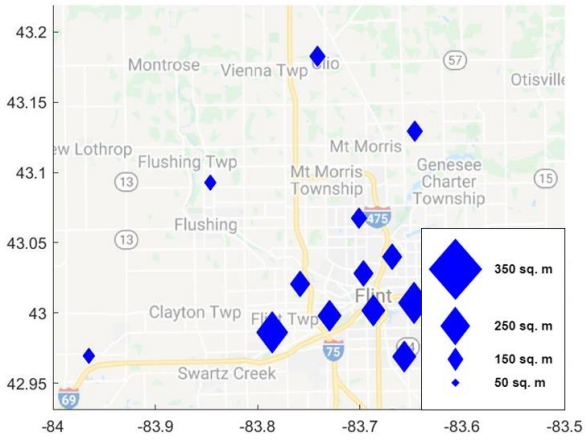

(i) Solar panel area (sq.m)

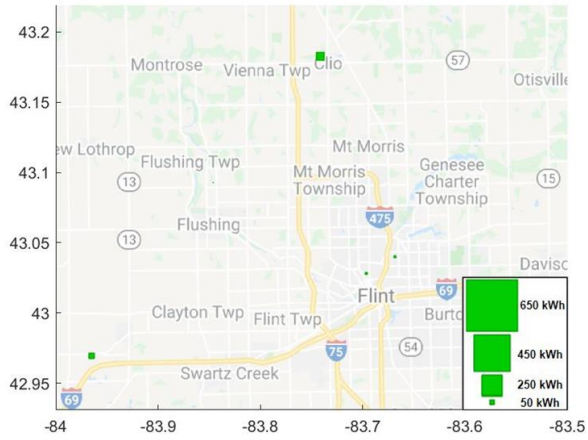

(ii) NB size (kWh)

c) EV load factor=2

Figure 5.16 Size of NB (4 hour storage duration) and solar panels for the city of Flint

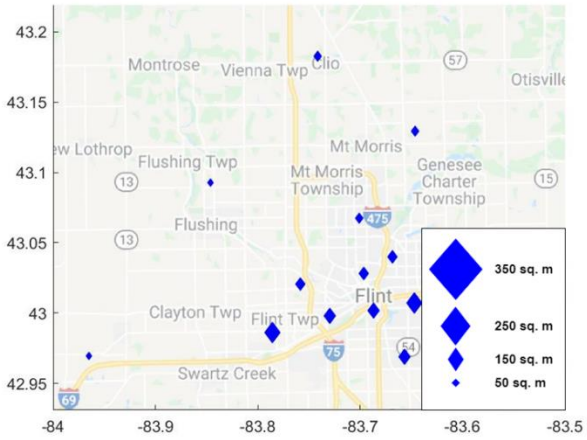

(i) Solar panel area (sq.m)

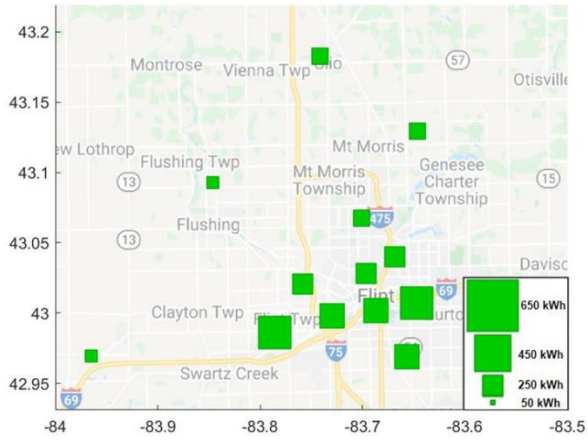

(ii) SLB size (kWh)

a) EV load factor=1

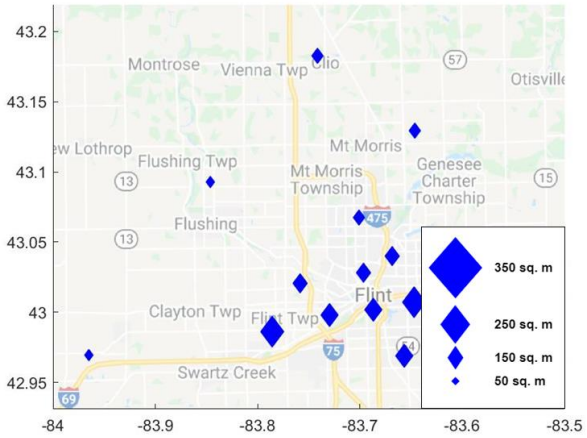

(i) Solar panel area (sq.m)

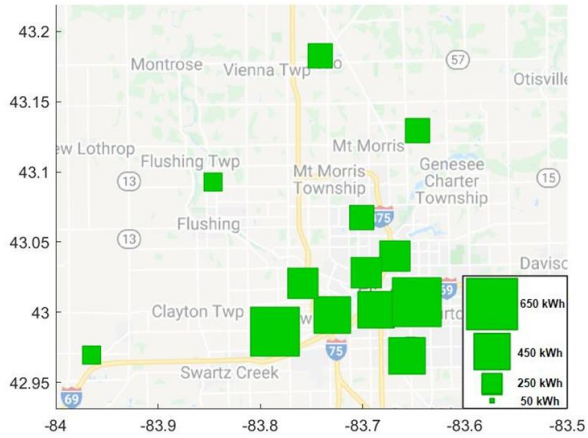

(ii) SLB size (kWh)

b) EV load factor=1.5

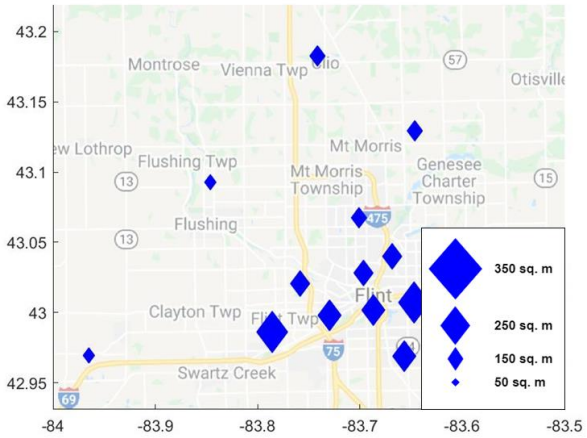

(i) Solar panel area (sq.m)

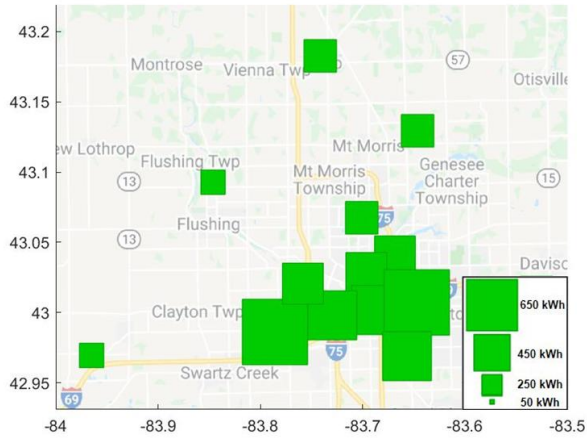

(ii) SLB size (kWh)

c) EV load factor=2

Figure 5.17 Size of SLB (4-hour storage duration) and solar panels for the city of Flint

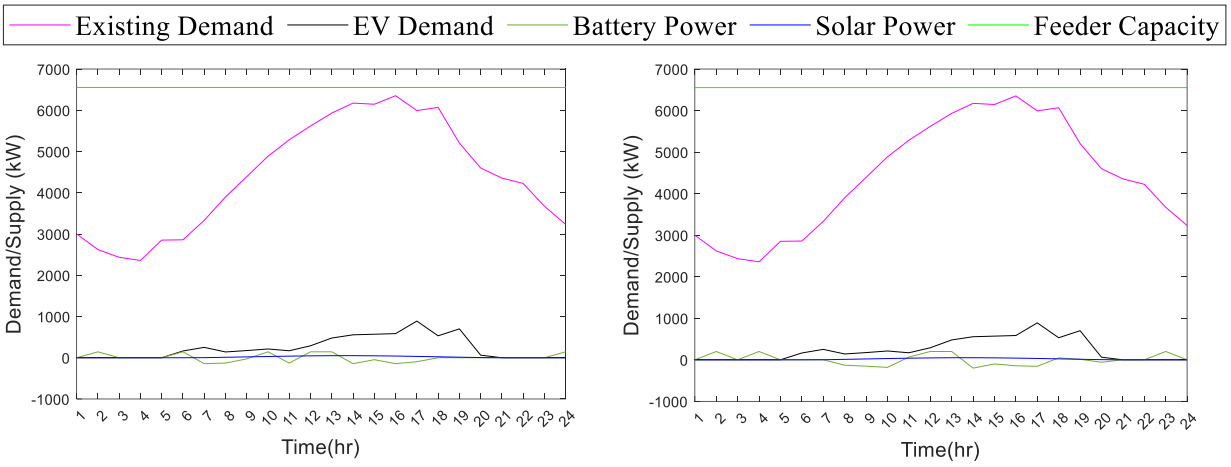

1. NB 2. SLB

Figure 5.18 Daily demand and supply variations at Grid level for the EV load factor of 2, during the summer season at a location in Saginaw, Michigan

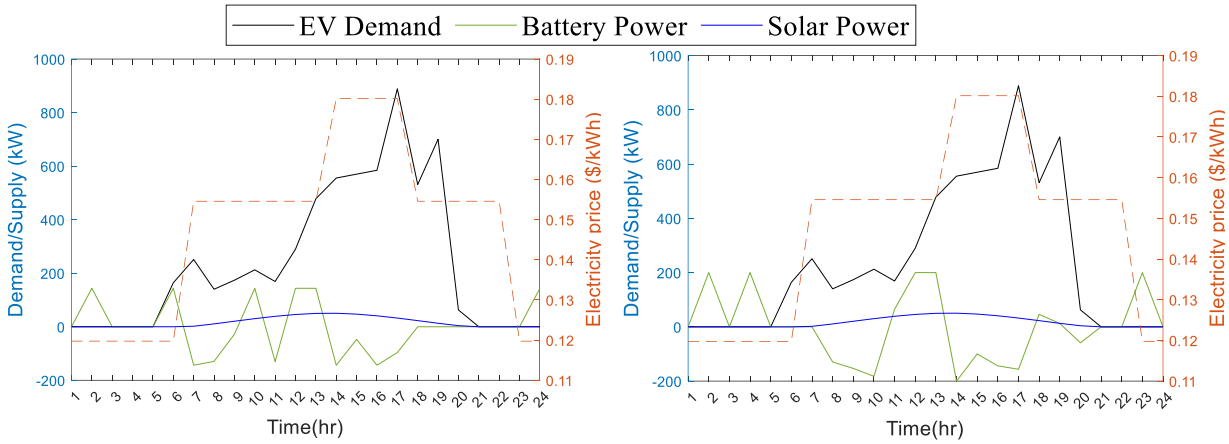

(a) NB (b) SLB

Figure 5.19 Daily demand and supply variations at DCFC station level for the EV load factor of 2, during the summer season at a location in Saginaw, Michigan

Table 5.5 Cost breakdown for the case of 4-hour SLB and the solar panels in Michigan

Saginaw								
EV Load Factor	Grid Cost ($k)	Battery Cost ($k)	Solar Panel Cost ($k)	Flywheel Cost ($k)	Electric Cost ($k/yr)	Total Cost ($k/yr)	Electricity Savings ($k/yr)	Total Savings ($k/yr)
1	498	469	207	0	1538	1595	95	63

Table 5.5 (cont'd)

1.5	755	713	310	0	2247	2334	142	87
2	894	937	414	0	2957	3068	189	111

Muskegon

EV Load Factor	Grid Cost ($k)	Battery Cost ($k)	Solar Panel Cost ($k)	Flywheel Cost ($k)	Electric Cost ($k/yr)	Total Cost ($k/yr)	Electricity Savings ($k/yr)	Total Savings ($k/yr)
1	273	252	108	0	862	893	50	29
1.5	281	378	163	0	1264	1305	75	44
2	316	504	217	0	1665	1719	100	57

Lansing

EV Load Factor	Grid Cost ($k)	Battery Cost ($k)	Solar Panel Cost ($k)	Flywheel Cost ($k)	Electric Cost ($k/yr)	Total Cost ($k/yr)	Electricity Savings ($k/yr)	Total Savings ($k/yr)
1	185	212	91	0	857	882	43	25
1.5	205	318	137	0	1259	1294	64	37
2	219	424	182	0	1662	1706	84	53

Kalamazoo

EV Load Factor	Grid Cost ($k)	Battery Cost ($k)	Solar Panel Cost ($k)	Flywheel Cost ($k)	Electric Cost ($k/yr)	Total Cost ($k/yr)	Electricity Savings ($k/yr)	Total Savings ($k/yr)
1	263	246	106	0	975	1005	49	29
1.5	289	370	159	0	1433	1474	73	45
2	314	493	212	0	1890	1943	99	64

Table 5.5 (cont'd)

Grand Rapids

EV Load Factor	Grid Cost ($k)	Battery Cost ($k)	Solar Panel Cost ($k)	Flywheel Cost ($k)	Electric Cost ($k/yr)	Total Cost ($k/yr)	Electricity Savings ($k/yr)	Total Savings ($k/yr)
1	397	711	306	0	2799	2873	141	81
1.5	455	1066	458	0	4141	4249	213	121
2	506	1421	611	0	5484	5624	284	165

Flint

EV Load Factor	Grid Cost ($k)	Battery Cost ($k)	Solar Panel Cost ($k)	Flywheel Cost ($k)	Electric Cost ($k/yr)	Total Cost ($k/yr)	Electricity Savings ($k/yr)	Total Savings ($k/yr)
1	286	407	175	0	1518	1563	81	47
1.5	326	610	262	0	2231	2294	121	70
2	368	814	350	0	2944	3026	162	93

Table 5.6 Cost breakdown for the case of 4 hour NB and the solar panels in Michigan

Saginaw

EV Load Factor	Grid Cost ($k)	Battery Cost ($k)	Solar Panel Cost ($k)	Flywheel Cost ($k)	Electric Cost ($k/yr)	Total Cost ($k/yr)	Electricity Savings ($k/yr)	Total Savings ($k/yr)
1	502	94	207	0	1572	1603	61	55
1.5	793	129	310	0	2299	2346	90	75
2	916	160	414	0	3027	3083	119	96

Table 5.6 (cont'd)

Muskegon

EV Load Factor	Grid Cost ($k)	Battery Cost ($k)	Solar Panel Cost ($k)	Flywheel Cost ($k)	Electric Cost ($k/yr)	Total Cost ($k/yr)	Electricity Savings ($k/yr)	Total Savings ($k/yr)
1	277	24	108	0	882	897	30	25
1.5	291	77	163	0	1291	1312	48	37
2	323	49	217	0	1705	1727	60	49

Lansing

EV Load Factor	Grid Cost ($k)	Battery Cost ($k)	Solar Panel Cost ($k)	Flywheel Cost ($k)	Electric Cost ($k/yr)	Total Cost ($k/yr)	Electricity Savings ($k/yr)	Total Savings ($k/yr)
1	185	36	91	0	873	885	27	22
1.5	219	17	137	0	1286	1299	37	32
2	226	143	182	0	1689	1713	57	46

Kalamazoo

EV Load Factor	Grid Cost ($k)	Battery Cost ($k)	Solar Panel Cost ($k)	Flywheel Cost ($k)	Electric Cost ($k/yr)	Total Cost ($k/yr)	Electricity Savings ($k/yr)	Total Savings ($k/yr)
1	267	30	106	0	994	1009	30	25
1.5	299	8	159	0	1464	1480	42	39
2	323	101	212	0	1926	1952	63	55

Grand Rapids

Table 5.6 (cont'd)

EV Load Factor	Grid Cost ($k)	Battery Cost ($k)	Solar Panel Cost ($k)	Flywheel Cost ($k)	Electric Cost ($k/yr)	Total Cost ($k/yr)	Electricity Savings ($k/yr)	Total Savings ($k/yr)
1	405	15	306	0	2859	2883	81	71
1.5	483	5	458	0	4233	4265	121	105
2	550	71	611	0	5602	5646	166	143

Flint

EV Load Factor	Grid Cost ($k)	Battery Cost ($k)	Solar Panel Cost ($k)	Flywheel Cost ($k)	Electric Cost ($k/yr)	Total Cost ($k/yr)	Electricity Savings ($k/yr)	Total Savings ($k/yr)
1	294	38	175	0	1551	1569	48	41
1.5	330	65	262	0	2279	2304	73	60
2	380	34	350	0	3011	3038	95	81

5.6 Summary

The rapid growth in EVs will necessitate the growth of EV fast-charging infrastructure. However, this will increase the electricity demand which might overload the electric grid. To counter this effect, electric grid upgrades or other DER might be required to support the rising EV demand. An optimization model has been developed to estimate the optimum investment technology to support EV charging demand at DCFC charging stations. The different investment technology includes installation and purchase of ESS (NBs, SLBs, flywheels), solar panels, cost of electric grid network upgrade, and cost of buying/selling electricity from/to the electric grid. A discrete time-dependent model is developed to capture the spatiotemporal demand (EV demand

and existing demand), electric grid distribution network, and capacity constraints, and seasonal impacts of solar radiation intensity, electricity rate, and electricity demand. The model is implemented to consider the expected EV charging in 6 major cities in Michigan by the year 2030. The study also did sensitivity analysis with varying EV demand, storage duration of the batteries, and cost of the ESS. The results indicate that maximizing the area of the solar panels considering site restrictions would maximize the benefits. Further, the Li-ion SLB are proved to be a cost-effective solution compared to other ESS (NB, flywheels, etc.). These SLBs make efficient use of the time of use of electricity rate, store the intermittent solar energy, charges during the night, and discharges during peak hours. The optimum charge/discharge schedule of SLBs proposed by the study should be adopted for maximum savings. Both solar panels and SLBs should be provided to substantially save total annual costs ($25000-$165,000 per city) and the annual electricity cost ($40,000-$300,000 per city). These savings can be further increased if more area is available to offer solar panels and the ESS.

CHAPTER 6 CONCLUSIONS

AVs and EVs technology claim to have numerous potential benefits such as improved safety, mobility, roadway capacity, efficient driving, efficient use of travel time, and reduced emissions. These technologies can also promote the adoption of each other due to synergies between them, such as enhanced battery performance and battery life by AV technology and reduced emissions operating cost of AVs by EV technology. However, these technologies might increase users' travel time, VMT, ownership cost, and electric load over the electric grid. The high cost of EVs' battery and AV technology will demote the adoption of these technologies as private modes, promoting the adoption of these technologies as a shared mobility system. Adopting these technologies as shared mobility systems can reduce ownership costs, but it will pose additional problems such as increased VMT, waiting time, and inconvenience to users. Another concern of EV technology is the limited range and high charging time, which can be overcome by deploying the DCFC charging station network. However, this network of DCFC stations would increase the electric load causing demand-supply imbalance, overloading the electric grid, and degradation of the electric grid distribution system. This challenge can be overcome by providing DER such as ESS solar panels at the DCFC charging stations. This study proposes frameworks to provide an optimal approach to promote the adoption of AV and EV technologies and reduce their effects on the transportation systems, environment, and the electric grid network. First, the study proposes a modeling framework for the optimum fleet configuration of PMVs, PAVs, and SAVs, to minimize the purchase and operating costs, time spent (travel time and waiting time), and emission production. Then this modeling framework is further extended to estimate optimum fleet configuration in private mobility and shared mobility systems of EVs and AVs. The study captures the trade-offs between all the competing factors that promote/demote the adoption of AVs and

EVs. The study also considers the adoption and implication of AV EV technologies for users with different VOTT attributed to their income levels. The metaheuristic algorithms are developed based on the genetic algorithm (GA) and simulated annealing algorithm to obtain the solution for the large-scale real-world NP-hard nonlinear optimization problem. Finally, the study estimates the optimal investment technology to support the electric grid hosting EV charging demand at DCFC stations. The different investment technology includes the installation of BESS (NB/SLB), FESS, solar panels, and electric grid upgrades. These models are implemented for hypothetical networks and real-world networks (Ann Arbor, Saginaw, Lansing, Flint, Kalamazoo, Grand Rapids, Muskegon).

The results suggest that EVs are optimal for the system due to low operating costs, and zero tailpipe emissions. Hence, policies should be adopted to promote EV by providing adequate charging infrastructure, rebates over the purchase of EVs, and imposing carbon taxes. Further, electrifying AVs would lower the operating cost and offset the high ownership cost. Hence, policies should be adopted to promote autonomous and electric vehicles together. SAEVs are recommended for users with low VOTT and long-distance trips of users with mid VOTT, due to low ownership costs, travel time savings, low waiting time cost, low crash cost, and no driver costs. Hence, these should be deployed in regions with a denser population of low VOTT/low-income groups. PMEVs are recommended for the short distance trips of users with mid VOTT and long distance trips of users with high VOTT. PAEVs adoption would be favorable if adopted by users with high VOTT and there are at least 20% savings in travel time, or the AV technology cost is reduced to at least one-third of the vehicle price. Hence, technology advancements are required to either reduce the AV technology cost or design these vehicles to provide amenities onboard that allow efficient use of travel time through meetings, reading books, novels, or recreational

activities. Targeting user-specific costs, the users with low VOTT or low incomes prefer SAVs. The users with high VOTT predominantly prefer PMEVs due to the low operating costs of EVs and no waiting time. Hence, EVs adoption should be promoted by eliminating uncaptured human factors, such as range anxiety and concerns for standing a long time at the charging stations.

Further, to support the rising EV charging demand and reduce the load on the electric grid, the Li-ion SLB and the solar panels should be provided at different locations. The solar panel area provided should be maximum to avail the maximum benefits considering the site restrictions. The 4-hour storage duration Li-ion SLB is the cost-effective solution compared to other BESS systems, NB, FESS, and other storage durations (2-hour, 6-hour). It efficiently utilizes the time of use of the electricity rate, stores the intermittent solar energy, charges at night, and discharges during peak hours. For maximum savings in total annual cost ($25000-$165,000 per city) and the annual electricity cost ($40,000-$300,000 per city), both the solar panels and SLBs should be provided, and the optimum charge/discharge schedule of SLBs proposed in this study should be adopted. These savings can be further increased if more area is available for solar panels and the ESS.

The study estimates various models, scenarios, and the range of different influential parameters that can be utilized by the car companies, policymakers, and utility companies to promote the adoption of these technologies and provide a sustainable system.

APPENDIX

APPENDIX

Cost breakdown for BESS with 6 hour storage duration and solar panels

Table A 1 Cost breakdown for the case of 6 hour NB and the solar panels in Michigan

Saginaw								
EV Load Factor	Grid Cost ($k)	Battery Cost ($k)	Solar Panel Cost ($k)	Flywheel Cost ($k)	Electric Cost ($k/yr)	Total Cost ($k/yr)	Electricity Savings ($k/yr)	Total Savings ($k/yr)
1	721	71	207	0	1574	1610	59	48
1.5	886	60	310	0	2304	2348	85	73
2	966	102	414	0	3031	3084	115	95
Muskegon								
EV Load Factor	Grid Cost ($k)	Battery Cost ($k)	Solar Panel Cost ($k)	Flywheel Cost ($k)	Electric Cost ($k/yr)	Total Cost ($k/yr)	Electricity Savings ($k/yr)	Total Savings ($k/yr)
1	277	34	108	0	882	897	30	25
1.5	303	50	163	0	1293	1312	46	37
2	323	67	217	0	1703	1727	62	49
Lansing								
EV Load Factor	Grid Cost ($k)	Battery Cost ($k)	Solar Panel Cost ($k)	Flywheel Cost ($k)	Electric Cost ($k/yr)	Total Cost ($k/yr)	Electricity Savings ($k/yr)	Total Savings ($k/yr)
1	185	50	91	0	872	885	28	22
1.5	219	24	137	0	1285	1299	38	32
2	256	172	182	0	1686	1714	60	45
Kalamazoo								
EV Load Factor	Grid Cost ($k)	Battery Cost ($k)	Solar Panel Cost ($k)	Flywheel Cost ($k)	Electric Cost ($k/yr)	Total Cost ($k/yr)	Electricity Savings ($k/yr)	Total Savings ($k/yr)
1	267	41	106	0	993	1009	31	25
1.5	299	12	159	0	1464	1480	42	39
2	314	180	212	0	1920	1952	69	55
Grand Rapids								

Table A 1 (cont'd)

EV Load Factor	Grid Cost ($k)	Battery Cost ($k)	Solar Panel Cost ($k)	Flywheel Cost ($k)	Eletric Cost ($k/yr)	Total Cost ($k/yr)	Electricity Savings ($k/yr)	Total Savings ($k/yr)
1	405	22	306	0	2858	2883	82	71
1.5	483	7	458	0	4233	4265	121	105
2	550	99	611	0	5600	5646	168	143
Flint								
EV Load Factor	Grid Cost ($k)	Battery Cost ($k)	Solar Panel Cost ($k)	Flywheel Cost ($k)	Electric Cost ($k/yr)	Total Cost ($k/yr)	Electricity Savings ($k/yr)	Total Savings ($k/yr)
1	294	56	175	0	1549	1569	50	41
1.5	342	40	262	0	2281	2304	71	60
2	380	54	350	0	3010	3038	96	81

Table A 2 Cost breakdown for the case of 6 hour SLB and the solar panels in Michigan

Saginaw								
EV Load Factor	Grid Cost ($k)	Battery Cost ($k)	Solar Panel Cost ($k)	Flywheel Cost ($k)	Electric Cost ($k/yr)	Total Cost ($k/yr)	Electricity Savings ($k/yr)	Total Savings ($k/yr)
1	717	439	207	0	1539	1602	94	56
1.5	861	674	310	0	2248	2336	141	85
2	951	879	414	0	2960	3068	186	111
Muskegon								
EV Load Factor	Grid Cost ($k)	Battery Cost ($k)	Solar Panel Cost ($k)	Flywheel Cost ($k)	Electric Cost ($k/yr)	Total Cost ($k/yr)	Electricity Savings ($k/yr)	Total Savings ($k/yr)
1	273	235	108	0	863	892	49	30
1.5	303	353	163	0	1264	1305	75	44
2	323	471	217	0	1666	1718	99	58
Lansing								
EV Load Factor	Grid Cost ($k)	Battery Cost ($k)	Solar Panel Cost ($k)	Flywheel Cost ($k)	Electric Cost ($k/yr)	Total Cost ($k/yr)	Electricity Savings ($k/yr)	Total Savings ($k/yr)
1	185	198	91	0	858	881	42	26

Table A 2 (cont'd)

1.5	219	297	137	0	1260	1293	63	38
2	256	396	182	0	1663	1706	83	53

Kalamazoo

EV Load Factor	Grid Cost ($k)	Battery Cost ($k)	Solar Panel Cost ($k)	Flywheel Cost ($k)	Electric Cost ($k/yr)	Total Cost ($k/yr)	Electricity Savings ($k/yr)	Total Savings ($k/yr)
1	263	230	106	0	976	1004	48	30
1.5	299	345	159	0	1433	1474	73	45
2	314	460	212	0	1891	1942	98	65

Grand Rapids

EV Load Factor	Grid Cost ($k)	Battery Cost ($k)	Solar Panel Cost ($k)	Flywheel Cost ($k)	Electric Cost ($k/yr)	Total Cost ($k/yr)	Electricity Savings ($k/yr)	Total Savings ($k/yr)
1	401	663	306	0	2800	2871	140	83
1.5	476	995	458	0	4144	4247	210	123
2	524	1327	611	0	5488	5621	280	168

Flint

EV Load Factor	Grid Cost ($k)	Battery Cost ($k)	Solar Panel Cost ($k)	Flywheel Cost ($k)	Electric Cost ($k/yr)	Total Cost ($k/yr)	Electricity Savings ($k/yr)	Total Savings ($k/yr)
1	286	380	175	0	1519	1562	80	48
1.5	338	570	262	0	2233	2294	119	70
2	368	760	350	0	2946	3024	160	95

Cost breakdown for BESS with 2 hour storage duration and solar panels

Table A 3 Cost breakdown for the case of 2 hour NB and the solar panels in Michigan

Saginaw								
EV Load Factor	Grid Cost ($k)	Battery Cost ($k)	Solar Panel Cost ($k)	Flywheel Cost ($k)	Electric Cost ($k/yr)	Total Cost ($k/yr)	Electricity Savings ($k/yr)	Total Savings ($k/yr)
1	427	82	207	0	1574	1601	59	57
1.5	503	182	310	0	2298	2339	91	82
2	845	145	414	0	3030	3083	116	96
Muskegon								
EV Load Factor	Grid Cost ($k)	Battery Cost ($k)	Solar Panel Cost ($k)	Flywheel Cost ($k)	Electric Cost ($k/yr)	Total Cost ($k/yr)	Electricity Savings ($k/yr)	Total Savings ($k/yr)
1	277	5	108	0	884	897	28	25
1.5	303	8	163	0	1296	1312	43	37
2	323	11	217	0	1708	1727	57	49
Lansing								
EV Load Factor	Grid Cost ($k)	Battery Cost ($k)	Solar Panel Cost ($k)	Flywheel Cost ($k)	Electric Cost ($k/yr)	Total Cost ($k/yr)	Electricity Savings ($k/yr)	Total Savings ($k/yr)
1	169	31	91	0	874	885	26	22
1.5	199	28	137	0	1285	1299	38	32
2	214	93	182	0	1693	1714	53	45
Kalamazoo								
EV Load Factor	Grid Cost ($k)	Battery Cost ($k)	Solar Panel Cost ($k)	Flywheel Cost ($k)	Electric Cost ($k/yr)	Total Cost ($k/yr)	Electricity Savings ($k/yr)	Total Savings ($k/yr)
1	267	18	106	0	995	1009	29	25
1.5	299	4	159	0	1464	1480	42	39
2	323	63	212	0	1929	1952	60	55
Grand Rapids								

Table A 3 (cont'd)

EV Load Factor	Grid Cost ($k)	Battery Cost ($k)	Solar Panel Cost ($k)	Flywheel Cost ($k)	Electric Cost ($k/yr)	Total Cost ($k/yr)	Electricity Savings ($k/yr)	Total Savings ($k/yr)
1	409	1	306	0	2860	2883	80	71
1.5	483	1	458	0	4233	4265	121	105
2	561	25	611	0	5605	5646	163	143
Flint								
EV Load Factor	Grid Cost ($k)	Battery Cost ($k)	Solar Panel Cost ($k)	Flywheel Cost ($k)	Electric Cost ($k/yr)	Total Cost ($k/yr)	Electricity Savings ($k/yr)	Total Savings ($k/yr)
1	294	23	175	0	1552	1569	47	41
1.5	342	10	262	0	2283	2304	69	60
2	380	20	350	0	3013	3039	93	80

Table A 4 Cost breakdown for the case of 2 hour SLB and the solar panels in Michigan

Saginaw								
EV Load Factor	Grid Cost ($k)	Battery Cost ($k)	Solar Panel Cost ($k)	Flywheel Cost ($k)	Electric Cost ($k/yr)	Total Cost ($k/yr)	Electricity Savings ($k/yr)	Total Savings ($k/yr)
1	411	126	207	0	1570	1599	63	59
1.5	445	340	310	0	2285	2334	104	87
2	733	303	414	0	3017	3077	129	102
Muskegon								
EV Load Factor	Grid Cost ($k)	Battery Cost ($k)	Solar Panel Cost ($k)	Flywheel Cost ($k)	Electric Cost ($k/yr)	Total Cost ($k/yr)	Electricity Savings ($k/yr)	Total Savings ($k/yr)
1	257	76	108	0	879	896	33	26
1.5	287	60	163	0	1292	1311	47	38
2	299	181	217	0	1696	1726	69	50
Lansing								
EV Load Factor	Grid Cost ($k)	Battery Cost ($k)	Solar Panel Cost ($k)	Flywheel Cost ($k)	Electric Cost ($k/yr)	Total Cost ($k/yr)	Electricity Savings ($k/yr)	Total Savings ($k/yr)
1	165	30	91	0	874	884	26	23

Table A 4 (cont'd)

1.5	185	82	137	0	1281	1298	42	33
2	193	134	182	0	1689	1711	57	48
Kalamazoo								
EV Load Factor	Grid Cost ($k)	Battery Cost ($k)	Solar Panel Cost ($k)	Flywheel Cost ($k)	Electric Cost ($k/yr)	Total Cost ($k/yr)	Electricity Savings ($k/yr)	Total Savings ($k/yr)
1	251	76	106	0	991	1008	33	26
1.5	283	74	159	0	1459	1479	47	40
2	308	97	212	0	1926	1951	63	56
Grand Rapids								
EV Load Factor	Grid Cost ($k)	Battery Cost ($k)	Solar Panel Cost ($k)	Flywheel Cost ($k)	Electric Cost ($k/yr)	Total Cost ($k/yr)	Electricity Savings ($k/yr)	Total Savings ($k/yr)
1	395	52	306	0	2856	2883	84	71
1.5	455	111	458	0	4226	4264	128	106
2	506	220	611	0	5592	5645	176	144
Flint								
EV Load Factor	Grid Cost ($k)	Battery Cost ($k)	Solar Panel Cost ($k)	Flywheel Cost ($k)	Electric Cost ($k/yr)	Total Cost ($k/yr)	Electricity Savings ($k/yr)	Total Savings ($k/yr)
1	286	36	175	0	1551	1569	48	41
1.5	308	162	262	0	2272	2303	80	61
2	356	105	350	0	3006	3037	100	82

REFERENCES

REFERENCES

AAA, 2017. Your Driving Costs | AAA NewsRoom [WWW Document]. URL http://newsroom.aaa.com/auto/your-driving-costs/ (accessed 12.14.17).

Andrews, M., Do˘ Gru, M.K., Hobby, J.D., Jin, Y., Tucci, G.H., 2012. Modeling and Optimization for Electric Vehicle Charging Infrastructure.

Annema, J.A., 2020. Policy implications of the potential carbon dioxide (CO2) emission and energy impacts of highly automated vehicles, in: Advances in Transport Policy and Planning. Elsevier B.V., pp. 149–162. https://doi.org/10.1016/bs.atpp.2020.03.001

Artelys, 2019. Knitro - Artelys [WWW Document]. URL https://www.artelys.com/solvers/knitro/ (accessed 7.14.19).

Avci, B., Girotra, K., Netessine, S., 2015. Electric vehicles with a battery switching station: Adoption and environmental impact. Manage. Sci. 61, 772–794. https://doi.org/10.1287/mnsc.2014.1916

Baatar, B., Heckmann, K., Hoang, T., Jarvis, R., Sakhiya, P., 2021. Preparing Rural America for the Electric Vehicle Revolution [WWW Document]. Washington, DC.

Beacon Power, 2021. Beacon Power Flywheel Energy Storage Systems.

Berman, B., 2016. Total Cost of Ownership of an Electric Car [WWW Document]. URL https://www.plugincars.com/eight-factors-determining-total-cost-ownership-electric-car-127528.html (accessed 7.17.19).

Bischoff, J., Maciejewski, M., 2016. Simulation of City-wide Replacement of Private Cars with Autonomous Taxis in Berlin. Procedia Comput. Sci. 83, 237–244. https://doi.org/10.1016/J.PROCS.2016.04.121

BloombergNEF, 2020. Battery Pack Prices Cited Below $100/kWh for the First Time in 2020, While Market Average Sits at $137/kWh [WWW Document]. URL https://about.bnef.com/blog/battery-pack-prices-cited-below-100-kwh-for-the-first-time-in-2020-while-market-average-sits-at-137-kwh/ (accessed 9.21.21).

BloombergNEF, 2019. A Behind the Scenes Take on Lithium-ion Battery Prices | BloombergNEF [WWW Document]. URL https://about.bnef.com/blog/behind-scenes-take-lithium-ion-battery-prices/ (accessed 7.15.19).

BLS, 2018a. San Francisco-Oakland-Hayward, CA - May 2017 OES Metropolitan and Nonmetropolitan Area Occupational Employment and Wage Estimates [WWW Document]. URL https://www.bls.gov/oes/2017/may/oes_41860.htm (accessed 8.21.20).

BLS, 2018b. Hammond, LA - May 2017 OES Metropolitan and Nonmetropolitan Area

Occupational Employment and Wage Estimates [WWW Document]. URL https://www.bls.gov/oes/2017/may/oes_25220.htm (accessed 8.21.20).

Bösch, P.M., Becker, F., Becker, H., Axhausen, K.W., 2018. Cost-based analysis of autonomous mobility services. Transp. Policy 64, 76–91. https://doi.org/10.1016/j.tranpol.2017.09.005

Bradley, W.G., Bradley, G., W., 1981. Electric vehicle battery charger-power line interface. ieee 430–434.

Brown, A., Gonder, J., Repac, B., 2014. An Analysis of Possible Energy Impacts of Automated Vehicle, in: Meyer G., Beiker S. (Eds) Road Vehicle Automation. Springer, Cham, pp. 137–153. https://doi.org/10.1007/978-3-319-05990-7

Brown, K.E., Dodder, R., 2019. Energy and emissions implications of automated vehicles in the U.S. energy system. Transp. Res. Part D Transp. Environ. 77, 132–147. https://doi.org/10.1016/j.trd.2019.09.003

Burns, L.D., Jordan, W.C., Scarborough, B.A., 2013. TRANSFORMING PERSONAL MOBILITY. Earth Institute, Columbia Univ. New York.

Byrd, R.H., Nocedal, J., Waltz, R.A., 2006. Knitro: An Integrated Package for Nonlinear Optimization. Springer, Boston, MA, pp. 35–59. https://doi.org/10.1007/0-387-30065-1_4

Carlisle, S., 2016. We traded carriages for cars – let's embrace the next disruption [WWW Document]. URL https://www.theglobeandmail.com/report-on-business/rob-commentary/we-traded-carriages-for-cars-lets-embrace-the-next-disruption/article29782316/ (accessed 4.8.21).

Center for Sustainable Systems, 2017. Autonomous Vehicles Factsheet. CSS16-18, Univ. Michigan.

Chakraborty, S., Vu, H.N., Hasan, M.M., Tran, D.D., El Baghdadi, M., Hegazy, O., 2019. DC-DC converter topologies for electric vehicles, plug-in hybrid electric vehicles and fast charging stations: State of the art and future trends. Energies 12, 1569. https://doi.org/10.3390/en12081569

Chehri, A., Mouftah, H.T., 2019. Autonomous vehicles in the sustainable cities, the beginning of a green adventure. Sustain. Cities Soc. 51, 101751. https://doi.org/10.1016/j.scs.2019.101751

Chen, R., Qian, X., Miao, L., Ukkusuri, S. V., 2020. Optimal charging facility location and capacity for electric vehicles considering route choice and charging time equilibrium. Comput. Oper. Res. https://doi.org/10.1016/j.cor.2019.104776

Chen, T.D., Kockelman, K.M., Hanna, J.P., 2016. Operations of a shared, autonomous, electric vehicle fleet: Implications of vehicle & charging infrastructure decisions. Transp. Res. Part A 94, 243–254. https://doi.org/10.1016/j.tra.2016.08.020

Chester, M., Horvath, A., 2008. Environmental Life-cycle Assessment of Passenger Transportation: A Detailed Methodology for Energy, Greenhouse Gas, and Criteria Pollutant Inventories of Automobiles, Buses, Light Rail, Heavy Rail and Air v.2. UC Berkeley Cent. Futur. Urban Transp. A Volvo Cent. Excell.

Childress, S., Nichols, B., Charlton, B., Coe, S., 2015. Using an Activity-Based Model to Explore the Potential Impacts of Automated Vehicles. Transp. Res. Rec. J. Transp. Res. Board 2493, 99–106. https://doi.org/10.3141/2493-11

ChooseEnergy, 2019. Electricity Rates by State [WWW Document]. URL https://www.chooseenergy.com/electricity-rates-by-state/ (accessed 7.17.19).

Cicchino, J.B., 2017. Effectiveness of forward collision warning and autonomous emergency braking systems in reducing front-to-rear crash rates. Accid. Anal. Prev. 99, 142–152. https://doi.org/10.1016/J.AAP.2016.11.009

Cokyasar, T., Auld, J., Javanmardi, M., Verbas, O., Souza, F. De, 2020. Analyzing Energy and Mobility Impacts of Privately-owned Autonomous Vehicles, in: 2020 IEEE 23rd International Conference on Intelligent Transportation Systems, ITSC 2020. Institute of Electrical and Electronics Engineers Inc. https://doi.org/10.1109/ITSC45102.2020.9294218

Cole, W., Frazier, A.W., Augustine, C., 2021. Cost Projections for Utility-Scale Battery Storage: 2021 Update. NREL TP-6A20-79236.

Correia, G.H. de A., van Arem, B., 2016. Solving the User Optimum Privately Owned Automated Vehicles Assignment Problem (UO-POAVAP): A model to explore the impacts of self-driving vehicles on urban mobility. Transp. Res. Part B Methodol. 87, 64–88. https://doi.org/10.1016/J.TRB.2016.03.002

Crist, P., 2012. Electric Vehicles Revisited: Costs, Subsidies and Prospects. Discuss. Pap. Int. Transp. Forum OECD 40. https://doi.org/https://doi.org/10.1787/5k8zvv7h9lq7-en

Das, T., Aliprantis, D.C., 2008. Small-signal stability analysis of power system integrated with PHEVs, in: 2008 IEEE Energy 2030 Conference, ENERGY 2008. https://doi.org/10.1109/ENERGY.2008.4781036

Dashora, Y., Barnes, J.W., Pillai, R.S., Combs, T.E., Hilliard, M., Chinthavali, M.S., 2010. The PHEV Charging Infrastructure Planning (PCIP) Problem. Int. J. Emerg. Electr. Power Syst. 11. https://doi.org/10.2202/1553-779X.2482

de Looff, E., Correia, G.H. de A., van Cranenburgh, S., Snelder, M., van Arem, B., 2018. Potential Changes in Value of Travel Time as a Result of Vehicle Automation: a Case Study in the Netherlands. Present. 97th Annu. Meet. Transp. Res. Board, Washington, D.C.

Deb, K., 2012. OPTIMIZATION FOR ENGINEERING DESIGN: Algorithms and Examples [WWW Document]. URL https://books.google.com/books?hl=en&lr=&id=cN_kjtySMhIC&oi=fnd&pg=PR1&ots=jEWsRUx2TM&sig=tUkhpRAITbVpOk5XXC6sG9Fp3zE#v=onepage&q&f=false (accessed

12.26.20).

Deb, K., 2001. Multi-Objective Optimization using Evolutionary Algorithms. Wiley.

Deb, K., 2000. An efficient constraint handling method for genetic algorithms. Comput. Methods Appl. Mech. Eng. 186, 311–338. https://doi.org/10.1016/S0045-7825(99)00389-8

Deb, K., Agrawal, R.B., 1995. Simulated Binary Crossover for Continuous Search Space. Complex Syst. 9.

Dias, F.F., Nair, G.S., Ruíz-Juri, N., Bhat, C.R., Mirzaei, A., 2020. Incorporating Autonomous Vehicles in the Traditional Four-Step Model. Transp. Res. Rec. J. Transp. Res. Board 2674, 348–360. https://doi.org/10.1177/0361198120922544

EASE, 2019. Energy Storage: A Key Enabler for the Decarbonisation of the Transport Sector [WWW Document]. URL https://ease-storage.eu/news/energy-storage-a-critical-link-in-the-chain-of-the-energy-transition-2/ (accessed 5.29.21).

EASE, (European Association for Energy Storage), 2022. Energy Storage Technologies [WWW Document]. URL https://ease-storage.eu/energy-storage/technologies/ (accessed 3.5.22).

Eberhard, M., Tarpenning, M., 2006. The 21 st Century Electric Car. Tesla Mot. Inc.

EERE, 2021. Maximizing Electric Cars' Range in Extreme Temperatures | Department of Energy [WWW Document]. Off. Energy Effic. Renew. Energy. URL https://www.energy.gov/eere/electricvehicles/maximizing-electric-cars-range-extreme-temperatures (accessed 5.22.21).

Ehnberg, J.S.G., Bollen, M.H.J., 2005. Simulation of global solar radiation based on cloud observations, in: Solar Energy. Pergamon, pp. 157–162. https://doi.org/10.1016/j.solener.2004.08.016

EIA, 2020a. San Francisco Gasoline and Diesel Retail Prices [WWW Document]. URL https://www.eia.gov/dnav/pet/pet_pri_gnd_dcus_y05sf_a.htm (accessed 8.21.20).

EIA, 2020b. Gulf Coast (PADD 3) Gasoline and Diesel Retail Prices [WWW Document]. URL https://www.eia.gov/dnav/pet/pet_pri_gnd_dcus_r30_a.htm (accessed 8.21.20).

EnergySage, 2019. How much do electric cars cost? [WWW Document]. URL https://www.energysage.com/electric-vehicles/costs-and-benefits-evs/electric-car-cost/ (accessed 7.17.19).

EPA, 1994. User's Guide to Mobile5 (Mobile Source Emission Factor Model). U.S. Environ. Prot. Agency Rep. EPA-AA-AQAB-94-01.

EPA, U., 2020. Fast Facts: U.S. Transportation Sector Greenhouse Gas Emissions.

Fagnant, D.J., Kockelman, K., 2015. Preparing a nation for autonomous vehicles: Opportunities,

barriers and policy recommendations. Transp. Res. Part A Policy Pract. 77, 167–181. https://doi.org/10.1016/j.tra.2015.04.003

Fagnant, D.J., Kockelman, K.M., 2018. Dynamic ride-sharing and fleet sizing for a system of shared autonomous vehicles in Austin, Texas. Transportation (Amst). 45, 143–158. https://doi.org/10.1007/s11116-016-9729-z

Fagnant, D.J., Kockelman, K.M., 2014. The travel and environmental implications of shared autonomous vehicles, using agent-based model scenarios. Transp. Res. Part C Emerg. Technol. 40, 1–13. https://doi.org/10.1016/j.trc.2013.12.001

Fagnant, D.J., Kockelman, K.M., Bansal, P., 2016. Operations of Shared Autonomous Vehicle Fleet for Austin, Texas, Market. Transp. Res. Rec. J. Transp. Res. Board 2563, 98–106. https://doi.org/10.3141/2536-12

Fakhrmoosavi, F., Kavianipour, M., Shojaei, M. (Sam), Zockaie, A., Ghamami, M., Wang, J., Jackson, R., 2021. Electric Vehicle Charger Placement Optimization in Michigan Considering Monthly Traffic Demand and Battery Performance Variations. Transp. Res. Rec. J. Transp. Res. Board 036119812098195. https://doi.org/10.1177/0361198120981958

FastCompany, 2014. Will You Ever Be Able To Afford A Self-Driving Car? [WWW Document]. URL https://www.fastcompany.com/3025722/will-you-ever-be-able-to-afford-a-self-driving-car (accessed 12.14.17).

Feldman, D., Ramasamy, V., Fu, R., Ramdas, A., Desai, J., Margolis, R., 2021. U.S. Solar Photovoltaic System and Energy Storage Cost Benchmark: Q1 2020.

FHWA, 2019. Table VM-1 - Highway Statistics 2017 - Policy | Federal Highway Administration [WWW Document]. URL https://www.fhwa.dot.gov/policyinformation/statistics/2017/vm1.cfm (accessed 8.13.20).

FHWA, 2017. Table VM-1 - Highway Statistics 2016 - Policy | Federal Highway Administration [WWW Document]. URL https://www.fhwa.dot.gov/policyinformation/statistics/2016/vm1.cfm (accessed 5.16.18).

Fletcher, T., 2019. The Price Paid For Automobile Accidents And Injuries [WWW Document]. URL http://www.tavss.com/library/va-nc-lawyer-economic-and-comprehensive-auto-accident-costs.cfm (accessed 7.16.19).

Folsom, T., 2012. Energy and Autonomous Urban Land Vehicles. IEEE Technol. Soc. Mag. 31, 28–38. https://doi.org/10.1109/MTS.2012.2196339

Frade, I., Ribeiro, A., Gonçalves, G., Antunes, A.P., 2011. Optimal Location of Charging Stations for Electric Vehicles in a Neighborhood in Lisbon, Portugal. Transp. Res. Rec. J. Transp. Res. Board 2252, 91–98. https://doi.org/10.3141/2252-12

Francfort, J., Garetson, T., Karner, D., Salisbury, S.D., Smart, J.G., 2017. Considerations for Corridor and Community DC Fast Charging Complex System Design. Idaho Falls, ID

(United States). https://doi.org/10.2172/1484708

Gai, Y., Wang, A., Pereira, L., Hatzopoulou, M., Posen, I.D., 2019. Marginal Greenhouse Gas Emissions of Ontario's Electricity System and the Implications of Electric Vehicle Charging. Environ. Sci. Technol. 53, 7903–7912. https://doi.org/10.1021/acs.est.9b01519

Gallinaro, S., 2020. Energy Storage Systems Boost Electric Vehicles' Fast Charger Infrastructure [WWW Document]. Analog Devices. URL https://www.analog.com/en/technical-articles/energy-storage-systems-boosting-the-electric-vehicles-fast-charger-infrastructure.html# (accessed 4.20.21).

Ghamami, M., Kavianipour, M., Zockaie, A., Hohnstadt, L.R., Ouyang, Y., 2020a. Refueling infrastructure planning in intercity networks considering route choice and travel time delay for mixed fleet of electric and conventional vehicles. Transp. Res. Part C Emerg. Technol. 120, 102802. https://doi.org/10.1016/j.trc.2020.102802

Ghamami, M., Zockaie, A., Miller, S., Kavianipour, M., Fakhrmoosavi, F., Singh, H., Jazlan, F., Shojaei, M., 2020b. Electric Vehicle Charger Placement Optimization in Michigan: Phase II-Urban.

Ghamami, M., Zockaie, A., Nie, Y. (Marco), 2016. A general corridor model for designing plug-in electric vehicle charging infrastructure to support intercity travel. Transp. Res. Part C Emerg. Technol. 68, 389–402. https://doi.org/10.1016/J.TRC.2016.04.016

Ghamami, M., Zockaie, A., Wang, J., Miller, S., Kavianipour, M., Shojaei, M. (Sam), Fakhrmoosavi Fatemeh, Hohnstadt, L., Singh, H., 2019. Electric Vehicle Charger Placement Optimization in Michigan: Phase I – Highways.

Gjelaj, M., Hashemi, S., Andersen, P.B., Traeholt, C., 2020. Optimal infrastructure planning for EV fast-charging stations based on prediction of user behaviour. IET Electr. Syst. Transp. 10, 1–12. https://doi.org/10.1049/IET-EST.2018.5080

Gjelaj, M., Traeholt, C., Hashemi, S., Andersen, P.B., 2017a. DC Fast-charging stations for EVs controlled by a local battery storage in low voltage grids, in: 2017 IEEE Manchester PowerTech, Powertech 2017. Institute of Electrical and Electronics Engineers Inc. https://doi.org/10.1109/PTC.2017.7980985

Gjelaj, M., Træholt, C., Hashemi, S., Andersen, P.B., 2017b. Optimal design of DC fast-charging stations for EVs in low voltage grids, in: 2017 IEEE Transportation and Electrification Conference and Expo, ITEC 2017. Institute of Electrical and Electronics Engineers Inc., pp. 684–689. https://doi.org/10.1109/ITEC.2017.7993352

Gjelaj, M., Traholt, C., Hashemi, S., Andersen, P.B., 2017c. Cost-benefit analysis of a novel DC fast-charging station with a local battery storage for EVs, in: 2017 52nd International Universities Power Engineering Conference, UPEC 2017. Institute of Electrical and Electronics Engineers Inc., pp. 1–6. https://doi.org/10.1109/UPEC.2017.8231973

Golbabaei, F., Yigitcanlar, T., Bunker, J., 2020. The role of shared autonomous vehicle systems

in delivering smart urban mobility: A systematic review of the literature. Int. J. Sustain. Transp. https://doi.org/10.1080/15568318.2020.1798571

Greenblatt, J.B., Saxena, S., 2015. Autonomous taxis could greatly reduce greenhouse-gas emissions of US light-duty vehicles. Nat. Clim. Chang. 5, 860–863. https://doi.org/10.1038/nclimate2685

Greenblatt, J.B., Shaheen, S., 2015. Automated Vehicles, On-Demand Mobility, and Environmental Impacts. Curr. Sustain. Energy Reports 2, 74–81. https://doi.org/10.1007/s40518-015-0038-5

Gruel, W., Stanford, J.M., 2016. Assessing the Long-Term Effects of Autonomous Vehicles: a speculative approach. Transp. Res. Procedia 13, 18–29. https://doi.org/10.1016/j.trpro.2016.05.003

Gucwa, M.A., 2014. Mobility and Energy Impacts of Automated Cars. Present. Autom. Veh. Symp. CA.

Harper, C.D., Hendrickson, C.T., Mangones, S., Samaras, C., 2016. Estimating potential increases in travel with autonomous vehicles for the non-driving, elderly and people with travel-restrictive medical conditions. Transp. Res. Part C Emerg. Technol. 72, 1–9. https://doi.org/10.1016/J.TRC.2016.09.003

Hawkins, A.J., 2019. Extreme weather is sucking the life from your electric car - The Verge [WWW Document]. URL https://www.theverge.com/2019/2/10/18217041/electric-car-ev-extreme-weather-polar-vortex (accessed 7.15.19).

Hayden, W., 2016. HISTORY: From horse to horsepower [WWW Document]. thenewsherald.com. URL https://www.thenewsherald.com/news/history-from-horse-to-horsepower/article_28d9c9fc-9a94-50c7-9363-9631e26697f5.html (accessed 4.8.21).

He, J., Yang, H., Tang, T.-Q., Huang, H.-J., 2018. An optimal charging station location model with the consideration of electric vehicle's driving range. Transp. Res. Part C Emerg. Technol. 86, 641–654. https://doi.org/10.1016/J.TRC.2017.11.026

He, X., Liu, H.X., Liu, X., 2015. Optimal vehicle speed trajectory on a signalized arterial with consideration of queue. Transp. Res. Part C Emerg. Technol. 61, 106–120. https://doi.org/10.1016/J.TRC.2015.11.001

Hidrue, M.K., Parsons, G.R., Kempton, W., Gardner, M.P., 2011. Willingness to pay for electric vehicles and their attributes. Resour. Energy Econ. 33, 686–705. https://doi.org/10.1016/J.RESENEECO.2011.02.002

Hilton, G., Kiaee, M., Bryden, T., Cruden, A., Mortimer, A., 2019. The case for energy storage installations at high rate EV chargers to enable solar energy integration in the UK – An optimised approach. J. Energy Storage 21, 435–444. https://doi.org/10.1016/j.est.2018.12.012

Hyland, M., Mahmassani, H.S., 2018. Dynamic autonomous vehicle fleet operations: Optimization-based strategies to assign AVs to immediate traveler demand requests. Transp. Res. Part C Emerg. Technol. 92, 278–297. https://doi.org/10.1016/J.TRC.2018.05.003

Iacobucci, R., McLellan, B., Tezuka, T., 2019. Optimization of shared autonomous electric vehicles operations with charge scheduling and vehicle-to-grid. Transp. Res. Part C Emerg. Technol. 100, 34–52. https://doi.org/10.1016/j.trc.2019.01.011

Iacobucci, R., McLellan, B., Tezuka, T., 2018. Modeling shared autonomous electric vehicles: Potential for transport and power grid integration. Energy 158, 148–163. https://doi.org/10.1016/j.energy.2018.06.024

IEA, 2020. Global EV Outlook 2020 [WWW Document]. URL https://www.iea.org/reports/global-ev-outlook-2020 (accessed 4.19.21).

IHS, 2014. Self-Driving Cars Moving into the Industry's Driver's Seat | IHS Online Newsroom [WWW Document]. URL http://news.ihsmarkit.com/press-release/automotive/self-driving-cars-moving-industrys-drivers-seat (accessed 12.14.17).

IHS Markit, 2016. Vehicles Getting Older: Average Age of Light Cars and Trucks in U.S. Rises Again in 2016 to 11.6 Years, IHS Markit Says | IHS Online Newsroom [WWW Document]. URL http://news.ihsmarkit.com/press-release/automotive/vehicles-getting-older-average-age-light-cars-and-trucks-us-rises-again-201 (accessed 5.24.18).

INL, 2015. What were the Cost Drivers for the Direct Current Fast Charging Installations?

Int Panis, L., Broekx, S., Liu, R., 2006. Modelling instantaneous traffic emission and the influence of traffic speed limits. Sci. Total Environ. 371, 270–285. https://doi.org/10.1016/j.scitotenv.2006.08.017

Jiang, Y., Zhang, J., Wang, Y., Wang, W., 2019. Capturing ownership behavior of autonomous vehicles in Japan based on a stated preference survey and a mixed logit model with repeated choices. Int. J. Sustain. Transp. 13, 788–801. https://doi.org/10.1080/15568318.2018.1517841

Jones, P.A., 1992. Cloud-Cover Distributions and Correlations. J. Appl. Meteorol. Climatol. 31.

Kamath, D., Arsenault, R., Kim, H.C., Anctil, A., 2020. Economic and Environmental Feasibility of Second-Life Lithium-Ion Batteries as Fast-Charging Energy Storage. Environ. Sci. Technol. 54, 6878–6887. https://doi.org/10.1021/ACS.EST.9B05883/SUPPL_FILE/ES9B05883_SI_001.PDF

Kandil, S.M., Farag, H.E.Z., Shaaban, M.F., El-Sharafy, M.Z., 2018. A combined resource allocation framework for PEVs charging stations, renewable energy resources and distributed energy storage systems. Energy 143, 961–972. https://doi.org/10.1016/j.energy.2017.11.005

Kane, M., 2021. CATL Unveils First-Generation Sodium-Ion Battery [WWW Document]. InsideEVs. URL https://insideevs.com/news/523413/catl-unveils-sodium-ion-battery/ (accessed 12.6.21).

Kang, J.E., Recker, W.W., 2009. An activity-based assessment of the potential impacts of plug-in hybrid electric vehicles on energy and emissions using 1-day travel data. Transp. Res. Part D Transp. Environ. 14, 541–556. https://doi.org/10.1016/j.trd.2009.07.012

Kars4Kids, 2017. Horse Pollution or Car Pollution? [WWW Document]. URL https://kars4kidsblog.com/horse-pollution-or-car-pollution/ (accessed 4.8.21).

Kavianipour, M., Fakhrmoosavi, F., Shojaei, M. (Sam), Zockaie, A., Ghamami, M., Wang, J., Jackson, R., 2021a. Impacts of technology advancements on electric vehicle charging infrastructure configuration: a Michigan case study. Int. J. Sustain. Transp. 1–14. https://doi.org/10.1080/15568318.2021.1914789

Kavianipour, M., Fakhrmoosavi, F., Singh, H., Ghamami, M., Zockaie, A., Ouyang, Y., Jackson, R., 2021b. Electric vehicle fast charging infrastructure planning in urban networks considering daily travel and charging behavior. Transp. Res. Part D Transp. Environ. 93, 102769. https://doi.org/10.1016/j.trd.2021.102769

Kavianipour, M., Mozafari, H., Ghamami, M., Zockaie, A., Jackson, R., 2020. Effects of Electric Vehicle Adoption for State-Wide Intercity Trips on the Emission Saving and Energy Consumption. arXiv.

Keim, B., 2013. Did Cars Save Our Cities From Horses? [WWW Document]. URL http://nautil.us/issue/7/waste/did-cars-save-our-cities-from-horses (accessed 4.8.21).

Khalid, M.R., Alam, M.S., Sarwar, A., Jamil Asghar, M.S., 2019. A Comprehensive review on electric vehicles charging infrastructures and their impacts on power-quality of the utility grid. eTransportation. https://doi.org/10.1016/j.etran.2019.100006

Khanghah, B.Y., Anvari-Moghaddam, A., Guerrero, J.M., Vasquez, J.C., 2017. Combined solar charging stations and energy storage units allocation for electric vehicles by considering uncertainties, in: Conference Proceedings - 2017 17th IEEE International Conference on Environment and Electrical Engineering and 2017 1st IEEE Industrial and Commercial Power Systems Europe, EEEIC / I and CPS Europe 2017. Institute of Electrical and Electronics Engineers Inc. https://doi.org/10.1109/EEEIC.2017.7977806

Knupfer, S., Noffsinger, J., Sahdev, S., 2018. How battery storage can help charge the electric-vehicle market [WWW Document]. McKinsey Co. URL https://www.mckinsey.com/business-functions/sustainability/our-insights/how-battery-storage-can-help-charge-the-electric-vehicle-market (accessed 4.20.21).

Koberstein, A., 2008. Progress in the dual simplex algorithm for solving large scale LP problems: techniques for a fast and stable implementation. Comput. Optim. Appl. 41, 185–204. https://doi.org/10.1007/s10589-008-9207-4

Kröger, L., Kuhnimhof, T., Trommer, S., 2019. Does context matter? A comparative study modelling autonomous vehicle impact on travel behaviour for Germany and the USA. Transp. Res. Part A Policy Pract. 122, 146–161. https://doi.org/10.1016/j.tra.2018.03.033

Krueger, R., Rashidi, T.H., Rose, J.M., 2016. Preferences for shared autonomous vehicles. Transp. Res. Part C Emerg. Technol. 69, 343–355. https://doi.org/10.1016/J.TRC.2016.06.015

Lam, A.Y.S., Yu, J.J.Q., Hou, Y., Li, V.O.K., 2016. Coordinated autonomous vehicle parking for vehicle-to-grid services, in: 2016 IEEE International Conference on Smart Grid Communications, SmartGridComm 2016. Institute of Electrical and Electronics Engineers Inc., pp. 284–289. https://doi.org/10.1109/SmartGridComm.2016.7778775

Levin, M.W., Boyles, S.D., 2015. Effects of Autonomous Vehicle Ownership on Trip, Mode, and Route Choice. Transp. Res. Rec. J. Transp. Res. Board 2493, 29–38. https://doi.org/10.3141/2493-04

LeVine Steve, 2017. Self-driving cars will cost more than $250,000 with today's available equipment — Quartz [WWW Document]. URL https://qz.com/924212/what-it-really-costs-to-turn-a-car-into-a-self-driving-vehicle/ (accessed 12.14.17).

Levitt, S.D., Dubner, S.J., 2009. SuperFreakonomics . William Morrow.

Li, S., Wu, H., Bai, X., Yang, S., 2019. Optimal Dispatch for PV-assisted Charging Station of Electric Vehicles. 2019 IEEE PES GTD Gd. Int. Conf. Expo. Asia, GTD Asia 2019 854–859. https://doi.org/10.1109/GTDASIA.2019.8715910

Lim, S., Kuby, M., 2010. Heuristic algorithms for siting alternative-fuel stations using the Flow-Refueling Location Model. Eur. J. Oper. Res. 204, 51–61. https://doi.org/10.1016/j.ejor.2009.09.032

Liu, J., Jones, S., Adanu, E.K., 2020. Challenging human driver taxis with shared autonomous vehicles: a case study of Chicago. Transp. Lett. 12, 701–705. https://doi.org/10.1080/19427867.2019.1694202

Loeb, B., Kockelman, K.M., Liu, J., 2018. Shared autonomous electric vehicle (SAEV) operations across the Austin, Texas network with charging infrastructure decisions. Transp. Res. Part C Emerg. Technol. 89, 222–233. https://doi.org/10.1016/J.TRC.2018.01.019

Lu, Q., Tettamanti, T., Hörcher, D., Varga, I., 2020. The impact of autonomous vehicles on urban traffic network capacity: an experimental analysis by microscopic traffic simulation. Transp. Lett. 12, 540–549. https://doi.org/10.1080/19427867.2019.1662561

Ma, C.-T., 2019. System Planning of Grid-Connected Electric Vehicle Charging Stations and Key Technologies: A Review. Energies 12, 4201. https://doi.org/10.3390/en12214201

Madsen, H., Spliid, H., Thyregod, P., 1985. Markov Models in Discrete and Continuous Time for Hourly Observations of Cloud Cover. J. Appl. Meteorol. Climatol. 24.

Mahalik, M., Poch, L., Botterud, A., Vyas, A., 2010. Impacts of plug-in hybrid electric vehicles on the electric power system in Illinois, in: 2010 IEEE Conference on Innovative Technologies for an Efficient and Reliable Electricity Supply, CITRES 2010. pp. 341–348. https://doi.org/10.1109/CITRES.2010.5619781

Masoum, A.S., Deilami, S., Moses, P.S., Abu-Siada, A., 2010. Impacts of battery charging rates of plug-in electric vehicle on smart grid distribution systems, in: IEEE PES Innovative Smart Grid Technologies Conference Europe, ISGT Europe. https://doi.org/10.1109/ISGTEUROPE.2010.5638981

McCarthy, D., Wolfs, P., 2010. The HV system impacts of large scale electric vehicle deployments in a metropolitan area , in: 2010 20th Australasian Universities Power Engineering Conference. Christchurch, New Zealand, pp. 1–6.

Mcguckin, N., Fucci, A., 2018. Summary of Travel Trends: 2017 National Household Travel Survey. FHWA-PL-18-019.

Menon, N., Barbour, N., Zhang, Y., Pinjari, A.R., Mannering, F., 2019. Shared autonomous vehicles and their potential impacts on household vehicle ownership: An exploratory empirical assessment. Int. J. Sustain. Transp. 13, 111–122. https://doi.org/10.1080/15568318.2018.1443178

Meyer, J., Becker, H., Bösch, P.M., Axhausen, K.W., 2017. Autonomous vehicles: The next jump in accessibilities? Res. Transp. Econ. 62, 80–91. https://doi.org/10.1016/j.retrec.2017.03.005

Milsom, P., 2019. Pollution - Why we replaced horses with automobiles [WWW Document]. GPM. URL https://www.blog.greenprojectmanagement.org/index.php/2019/05/13/pollution-why-we-replaced-horses-with-automobiles/ (accessed 4.8.21).

Molnar, C., 2019. Norway needs $1.6-billion power grid upgrade to support EVs by 2040: study [WWW Document]. Driving. URL https://driving.ca/auto-news/news/norway-needs-1-6-billion-power-grid-upgrade-to-support-evs-by-2040-study (accessed 5.29.21).

Mongird, K., Fotedar, V., Viswanathan, V., Koritarov, V., Balducci, P., Hadjerioua, B., Alam, J., 2019. Energy Storage Technology and Cost Characterization Report.

Moore, A.T., Staley, S.R., Poole, R.W., 2010. The role of VMT reduction in meeting climate change policy goals. Transp. Res. Part A Policy Pract. 44, 565–574. https://doi.org/10.1016/J.TRA.2010.03.012

Moore, M.A., Lavieri, P.S., Dias, F.F., Bhat, C.R., 2020. On investigating the potential effects of private autonomous vehicle use on home/work relocations and commute times. Transp. Res. Part C Emerg. Technol. 110, 166–185. https://doi.org/10.1016/j.trc.2019.11.013

Morrow, K., Darner, D., Francfort, J., 2008. U.S. Department of Energy Vehicle Technologies Program -- Advanced Vehicle Testing Activity -- Plug-in Hybrid Electric Vehicle Charging

Infrastructure Review. https://doi.org/10.2172/946853

Morrow, W.R., Greenblatt, J.B., Sturges, A., Saxena, S., Gopal, A., Millstein, D., Shah, N., Gilmore, E.A., 2014. Key Factors Influencing Autonomous Vehicles' Energy and Environmental Outcome, in: Meyer G., Beiker S. (Eds) Road Vehicle Automation. Springer, Cham, pp. 127–135. https://doi.org/10.1007/978-3-319-05990-7_12

NADA, 2012. Buying a New Car | Consumer Information [WWW Document]. URL https://www.consumer.ftc.gov/articles/0209-buying-new-car (accessed 12.14.17).

Negarestani, S., Fotuhi-Firuzabad, M., Rastegar, M., Rajabi-Ghahnavieh, A., 2016. Optimal sizing of storage system in a fast charging station for plug-in hybrid electric vehicles. IEEE Trans. Transp. Electrif. 2, 443–453. https://doi.org/10.1109/TTE.2016.2559165

Neubauer, J., Pesaran, A., Williams, B., Ferry, M., Eyer, J., 2012. A Techno-Economic Analysis of PEV Battery Second Use: Repurposed-Battery Selling Price and Commercial and Industrial End-User Value. SAE Int. NREL/CP-5400-53799.

NHTS, 2017. Local Area Transportation Characteristics for Households Data | Bureau of Transportation Statistics [WWW Document]. URL https://www.bts.gov/latch/latch-data (accessed 8.21.20).

NHTSA, 2016. Federal Automated Vehicles Policy. U.S. Dep. Transp.

Nicholas, M., Hall, D., 2018. Lessons learned on early electric vehicle fast-charging deployments . Int. Counc. Clean Transp.

Nie, Y. (Marco), Ghamami, M., 2013. A corridor-centric approach to planning electric vehicle charging infrastructure. Transp. Res. Part B Methodol. 57, 172–190. https://doi.org/10.1016/J.TRB.2013.08.010

Nie, Y. (Marco), Ghamami, M., Zockaie, A., Xiao, F., 2016. Optimization of incentive polices for plug-in electric vehicles. Transp. Res. Part B Methodol. 84, 103–123. https://doi.org/10.1016/J.TRB.2015.12.011

Nie, Y., Ghamami, M., Zockaie, A., Xiao, F., 2016. Optimization of incentive polices for plug-in electric vehicles. Transp. Res. Part B Methodol. https://doi.org/10.1016/j.trb.2015.12.011

Nielsen, L.B., Prahm, L.P., Berkowicz, R., Conradsen, K., 1981. Net incoming radiation estimated from hourly global radiation and/or cloud observations. J. Climatol. 1, 255–272. https://doi.org/10.1002/joc.3370010305

Nikiforuk, A., 2013. The Big Shift Last Time: From Horse Dung to Car Smog [WWW Document]. URL http://thetyee.ca/News/2013/03/06/Horse-Dung-Big-Shift/ (accessed 4.8.21).

Nizam, M., Wicaksono, F.X.R., 2019. Design and Optimization of Solar, Wind, and Distributed Energy Resource (DER) Hybrid Power Plant for Electric Vehicle (EV) Charging Station in

Rural Area. Proceeding - 2018 5th Int. Conf. Electr. Veh. Technol. ICEVT 2018 41–45. https://doi.org/10.1109/ICEVT.2018.8628341

Nocedal, J., Wright, S.J., 2006. Numerical Optimization, Springer Series in Operations Research and Financial Engineering. Springer New York. https://doi.org/10.1007/978-0-387-40065-5

NREL, 2021. Annual Technology Baseline-Commercial PV [WWW Document]. URL https://atb.nrel.gov/electricity/2021/commercial_pv (accessed 2.21.22).

Oh, S., Seshadri, R., Azevedo, C.L., Kumar, N., Basak, K., Ben-Akiva, M., 2020. Assessing the impacts of automated mobility-on-demand through agent-based simulation: A study of Singapore. Transp. Res. Part A Policy Pract. 138, 367–388. https://doi.org/10.1016/j.tra.2020.06.004

Onar, O.C., Khaligh, A., 2010. Grid interactions and stability analysis of distribution power network with high penetration of plug-in hybrid electric vehicles, in: Conference Proceedings - IEEE Applied Power Electronics Conference and Exposition - APEC. pp. 1755–1762. https://doi.org/10.1109/APEC.2010.5433471

Overtoom, I., Correia, G., Huang, Y., Verbraeck, A., 2020. Assessing the impacts of shared autonomous vehicles on congestion and curb use: A traffic simulation study in The Hague, Netherlands. Int. J. Transp. Sci. Technol. 9, 195–206. https://doi.org/10.1016/j.ijtst.2020.03.009

Padberg, M., 1999. Linear Optimization and Extensions, Algorithms and Combinatorics. Springer Berlin Heidelberg, Berlin, Heidelberg. https://doi.org/10.1007/978-3-662-12273-0

Patel, P., 2021. Sodium-Ion Batteries Poised to Pick Off Large-Scale Lithium-Ion Applications [WWW Document]. IEEE Spectr. URL https://spectrum.ieee.org/sodium-ion-battery (accessed 12.6.21).

PayScale, 2019. Taxi Driver Hourly Pay [WWW Document]. URL https://www.payscale.com/research/US/Job=Taxi_Driver/Hourly_Rate (accessed 7.16.19).

Pieltain Fernandez, L., Gomez San Roman, T., Cossent, R., Mateo Domingo, C., Frias, P., 2011. Assessment of the Impact of Plug-in Electric Vehicles on Distribution Networks. IEEE Trans. Power Syst. 26, 206–213. https://doi.org/10.1109/TPWRS.2010.2049133

Porter, J., 2020. Tesla raises price of 'Full Self-Driving' option to $10,000 [WWW Document]. The Verge. URL https://www.theverge.com/2020/10/30/21541571/tesla-full-self-driving-price-increase-10000-dollars-autopilot-beta (accessed 5.30.21).

Private Fleet, 2010. Pros And Cons Of The Horseless Carriage [WWW Document]. URL https://www.privatefleet.com.au/blog/home/pros-and-cons-of-the-horseless-carriage/ (accessed 4.8.21).

Putrus, G.A., Suwanapingkarl, P., Johnston, D., Bentley, E.C., Narayana, M., 2009. Impact of electric vehicles on power distribution networks, in: 5th IEEE Vehicle Power and

Propulsion Conference, VPPC ’09. pp. 827–831. https://doi.org/10.1109/VPPC.2009.5289760

Qi, Y. “Grace,” Teng, H. “Harry”, Yu, L., 2004. Microscale Emission Models Incorporating Acceleration and Deceleration. J. Transp. Eng. 130, 348–359. https://doi.org/10.1061/(ASCE)0733-947X(2004)130:3(348)

Rafi, M.A.H., Bauman, J., 2021. A Comprehensive Review of DC Fast-Charging Stations With Energy Storage: Architectures, Power Converters, and Analysis. IEEE Trans. Transp. Electrif. 7, 345–368. https://doi.org/10.1109/TTE.2020.3015743

Reiter, M.S., Kockelman, K.M., 2016. The problem of cold starts: A closer look at mobile source emissions levels. Transp. Res. Part D Transp. Environ. 43, 123–132. https://doi.org/10.1016/j.trd.2015.12.012

Richard, L., Petit, M., 2018a. Fast Charging Station with Battery Storage System for EV: Optimal Integration into the Grid. IEEE Power Energy Soc. Gen. Meet. 2018-Augus. https://doi.org/10.1109/PESGM.2018.8585856

Richard, L., Petit, M., 2018b. Fast charging station with battery storage system for EV: Grid services and battery degradation. 2018 IEEE Int. Energy Conf. ENERGYCON 2018 1–6. https://doi.org/10.1109/ENERGYCON.2018.8398744

Ritchie, E.J., 2019. Self-Driving Automobiles: How Soon And How Much? [WWW Document]. Forbes. URL https://www.forbes.com/sites/uhenergy/2019/05/21/self-driving-automobiles-how-soon-and-how-much/?sh=4f6f3d6938bd (accessed 2.23.21).

Rodier, C., 2018. Travel Effects and Associated Greenhouse Gas Emissions of Automated Vehicles.

Romm, J., 2006. The car and fuel of the future. Energy Policy 34, 2609–2614. https://doi.org/10.1016/J.ENPOL.2005.06.025

Salapic, V., Grzanic, M., Capuder, T., 2018. Optimal sizing of battery storage units integrated into fast charging EV stations. 2018 IEEE Int. Energy Conf. ENERGYCON 2018 1–6. https://doi.org/10.1109/ENERGYCON.2018.8398789

Saleh, M., Hatzopoulou, M., 2020. Greenhouse gas emissions attributed to empty kilometers in automated vehicles. Transp. Res. Part D Transp. Environ. 88, 102567. https://doi.org/10.1016/j.trd.2020.102567

Samaras, C., Meisterling, K., 2008. Life Cycle Assessment of Greenhouse Gas Emissions from Plug-in Hybrid Vehicles: Implications for Policy. Environ. Sci. Technol. 42, 3170–3176. https://doi.org/10.1021/es702178s

Santos, A., McGuckin, N., Nakamoto, H.Y., Gray, D., Liss, S., 2011. Summary of Travel Trends: 2009 National Household Travel Survey. FHWA-PL-11-022.

Schmitt, A., 2016. Parking Takes Up More Space Than You Think [WWW Document]. Streetsblog USA. URL https://usa.streetsblog.org/2016/07/05/parking-takes-up-more-space-than-you-think/ (accessed 9.2.21).

Shahraki, N., Cai, H., Turkay, M., Xu, M., 2015. Optimal locations of electric public charging stations using real world vehicle travel patterns. Transp. Res. Part D Transp. Environ. 41, 165–176. https://doi.org/10.1016/j.trd.2015.09.011

Sheela, P.V., Mannering, F., 2020. The effect of information on changing opinions toward autonomous vehicle adoption: An exploratory analysis. Int. J. Sustain. Transp. 14, 475–487. https://doi.org/10.1080/15568318.2019.1573389

Shindell, D.T., 2015. The social cost of atmospheric release. Clim. Change 130, 313–326. https://doi.org/10.1007/s10584-015-1343-0

Singh, H., Ghamami, M., Nouri, H., Gates, T., 2021. Multi-objective framework for optimum configuration of human-driven and shared or privately owned autonomous vehicles. Int. J. Sustain. Transp. 1–21. https://doi.org/10.1080/15568318.2021.1887415

Singh, H., Ghamami, M., Nouri, H., Gates, T., 2019. Developing Strategies for Optimum Fleet Assignment of Conventional, Autonomous and Shared Autonomous Vehicles in an Urban Setting. Present. 98th Annu. Meet. Transp. Res. Board, Washingt. D.C.

Soteropoulos, A., Berger, M., Ciari, F., 2019. Impacts of automated vehicles on travel behaviour and land use: an international review of modelling studies. Transp. Rev. 39, 29–49. https://doi.org/10.1080/01441647.2018.1523253

Spieser, K., Samaranayake, S., Gruel, W., Frazzoli, E., 2016. Shared-Vehicle Mobility-on-Demand Systems: A Fleet Operator's Guide to Rebalancing Empty Vehicles.

Stogios, C., Kasraian, D., Roorda, M.J., Hatzopoulou, M., 2019. Simulating impacts of automated driving behavior and traffic conditions on vehicle emissions. Transp. Res. Part D Transp. Environ. 76, 176–192. https://doi.org/10.1016/j.trd.2019.09.020

SunEarthTools, 2021. Calculation of sun's position in the sky for each location on the earth at any time of day [en] [WWW Document]. URL https://www.sunearthtools.com/dp/tools/pos_sun.php?lang=en#annual (accessed 1.28.21).

Sweda, T., Klabjan, D., 2011. An agent-based decision support system for electric vehicle charging infrastructure deployment. Present. 2011 IEEE Veh. Power Propuls. Conf. 1–5. https://doi.org/10.1109/VPPC.2011.6043201

Tate, E.D., Harpster, M.O., Savagian, P.J., 2008. The electrification of the automobile: From conventional hybrid, to plug-in hybrids, to extended-range electric vehicles. SAE Tech. Pap. https://doi.org/10.4271/2008-01-0458

Tefft, B., 2017. Rates of Motor Vehicle Crashes, Injuries, and Deaths in Relation to Driver Age, United States, 2014-2015. Washington, DC.

Thakur, P., Kinghorn, R., Grace, R., 2016. Urban form and function in the autonomous era. Proc. 38th Australas. Transp. Res. Forum.

Tomás, R.F., Fernandes, P., MacEdo, E., Bandeira, J.M., Coelho, M.C., 2020. Assessing the emission impacts of autonomous vehicles on metropolitan freeways, in: Transportation Research Procedia. Elsevier B.V., pp. 617–624. https://doi.org/10.1016/j.trpro.2020.03.139

Tradingeconomics.com, U.S.B. of L.S., 2020. United States Average Hourly Wages | 1964-2020 Data | 2021-2022 Forecast | Historical [WWW Document]. URL https://tradingeconomics.com/united-states/wages (accessed 8.21.20).

Tradingeconomics.com, U.S.B. of L.S., 2018. United States Average Hourly Wages [WWW Document]. URL https://tradingeconomics.com/united-states/wages (accessed 6.2.18).

Tu, W., Li, Q., Fang, Z., Shaw, S. lung, Zhou, B., Chang, X., 2016. Optimizing the locations of electric taxi charging stations: A spatial–temporal demand coverage approach. Transp. Res. Part C Emerg. Technol. 65, 172–189. https://doi.org/10.1016/j.trc.2015.10.004

Ugirumurera, J., Haas, Z.J., 2017. Optimal Capacity Sizing for Completely Green Charging Systems for Electric Vehicles. IEEE Trans. Transp. Electrif. 3, 565–577. https://doi.org/10.1109/TTE.2017.2713098

Union of Concerned Scientists, 2019. Electric Vehicle Battery: Materials, Cost, Lifespan [WWW Document]. URL https://www.ucsusa.org/clean-vehicles/electric-vehicles/electric-cars-battery-life-materials-cost#.W6AFsehKg2w (accessed 7.17.19).

US DOT, (US Department of Transportation), 2015. TIGER Benefit-Cost Analysis Resource Guide [WWW Document]. URL https://www.transportation.gov/sites/dot.gov/files/docs/Tiger_Benefit-Cost_Analysis_%28BCA%29_Resource_Guide_1.pdf (accessed 12.14.17).

van den Berg, V.A.C., Verhoef, E.T., 2016. Autonomous cars and dynamic bottleneck congestion: The effects on capacity, value of time and preference heterogeneity. Transp. Res. Part B Methodol. 94, 43–60. https://doi.org/10.1016/j.trb.2016.08.018

Vasebi, S., Hayeri, Y.M., 2020. Air emission impacts of low-level automated vehicle technologies in U.S. metropolitan areas. Transp. Res. Interdiscip. Perspect. 7, 100194. https://doi.org/10.1016/j.trip.2020.100194

Vosooghi, R., Puchinger, J., Bischoff, J., Jankovic, M., Vouillon, A., 2020. Shared autonomous electric vehicle service performance: Assessing the impact of charging infrastructure. Transp. Res. Part D Transp. Environ. 81, 102283. https://doi.org/10.1016/j.trd.2020.102283

Wadud, Z., MacKenzie, D., Leiby, P., 2016. Help or hindrance? The travel, energy and carbon impacts of highly automated vehicles. Transp. Res. Part A Policy Pract. 86, 1–18. https://doi.org/10.1016/j.tra.2015.12.001

Wang, A., Stogios, C., Gai, Y., Vaughan, J., Ozonder, G., Lee, S.J., Posen, I.D., Miller, E.J.,

Hatzopoulou, M., 2018. Automated, electric, or both? Investigating the effects of transportation and technology scenarios on metropolitan greenhouse gas emissions. Sustain. Cities Soc. 40, 524–533. https://doi.org/10.1016/j.scs.2018.05.004

Weather Spark, 2021. The Weather Year Round Anywhere on Earth [WWW Document]. Weather Spark. URL https://weatherspark.com/ (accessed 12.6.21).

Weiss, J., Hledik, R., Lueken, R., Lee, T., Gorman, W., 2017. The electrification accelerator: Understanding the implications of autonomous vehicles for electric utilities. Electr. J. 30, 50–57. https://doi.org/10.1016/j.tej.2017.11.009

Xie, S., Chen, X., Wang, Z., Ouyang, Y., Somani, K., Huang, J., 2016. Integrated planning for multiple types of locomotive work facilities under location, routing, and inventory considerations. Interfaces (Providence). 46, 391–408. https://doi.org/10.1287/inte.2016.0857

Yan, H., Kockelman, K.M., Gurumurthy, K.M., 2020. Shared autonomous vehicle fleet performance: Impacts of trip densities and parking limitations. Transp. Res. Part D Transp. Environ. 89, 102577. https://doi.org/10.1016/j.trd.2020.102577

Yang, J., Dong, J., Hu, L., 2017. A data-driven optimization-based approach for siting and sizing of electric taxi charging stations. Transp. Res. Part C Emerg. Technol. 77, 462–477. https://doi.org/10.1016/j.trc.2017.02.014

Yang, L., Ribberink, H., 2019. Investigation of the potential to improve DC fast charging station economics by integrating photovoltaic power generation and/or local battery energy storage system. Energy 167, 246–259. https://doi.org/10.1016/j.energy.2018.10.147

Yilmaz, M., Krein, P.T., 2013. Review of battery charger topologies, charging power levels, and infrastructure for plug-in electric and hybrid vehicles. IEEE Trans. Power Electron. https://doi.org/10.1109/TPEL.2012.2212917

Zhang, H., Sheppard, C.J.R., Lipman, T.E., Zeng, T., Moura, S.J., 2020. Charging infrastructure demands of shared-use autonomous electric vehicles in urban areas. Transp. Res. Part D Transp. Environ. 78, 102210. https://doi.org/10.1016/j.trd.2019.102210

Zhang, W., 2017. THE INTERACTION BETWEEN LAND USE AND TRANSPORTATION IN THE ERA OF SHARED AUTONOMOUS VEHICLES: A SIMULATION MODEL (Dissertation). Georgia Institute of Technology.

Zhang, W., Guhathakurta, S., Fang, J., Zhang, G., 2015. Exploring the impact of shared autonomous vehicles on urban parking demand: An agent-based simulation approach. Sustain. Cities Soc. 19, 34–45. https://doi.org/10.1016/j.scs.2015.07.006

Zhang, W., Guhathakurta, S., Khalil, E.B., 2018. The impact of private autonomous vehicles on vehicle ownership and unoccupied VMT generation. Transp. Res. Part C Emerg. Technol. 90, 156–165. https://doi.org/10.1016/J.TRC.2018.03.005

Zhong, H., Li, W., Burris, M.W., Talebpour, A., Sinha, K.C., 2020. Will autonomous vehicles change auto commuters' value of travel time? Transp. Res. Part D Transp. Environ. 83, 102303. https://doi.org/10.1016/j.trd.2020.102303

Zmud, J.P., Sener, I.N., 2017. Towards an Understanding of the Travel Behavior Impact of Autonomous Vehicles, in: Transportation Research Procedia. Elsevier B.V., pp. 2500–2519. https://doi.org/10.1016/j.trpro.2017.05.281

Zockaie, A., Aashtiani, H.Z., Ghamami, M., Marco Nie, Y., 2016. Solving Detour-Based Fuel Stations Location Problems. Comput. Civ. Infrastruct. Eng. 31, 132–144. https://doi.org/10.1111/mice.12170